Remembering What We've Seen:
The Hippocampus and Relational Memory

Seth Daniel König (Koenig)

A dissertation

submitted in partial fulfillment of the

requirements for the degree of

Doctor of Philosophy

University of Washington

2017

Reading Committee Members:

Elizabeth Buffalo, Chair

Greg Horwitz

Sheri Mizumori

Program Authorized to Offer Degree:

Neuroscience

University of Washington

Abstract

Remembering What We've Seen: The Hippocampus and Relational Memory

Seth Daniel Koenig

Chair of the Supervisory Committee: Professor Elizabeth Buffalo, Physiology and Biophysics

Relational memory is the ability to remember arbitrary associations between objects or events. These memories include things related by location, order, and context. Lesions of the medial temporal lobe (MTL) cause severe relational memory impairments suggesting that the MTL plays an important role in the formation of relational memories. Lesions to the hippocampus, the final output of the MTL, also causes relational memory impairments. Single unit recordings in rodents have identified place and time cells in the hippocampus that are hypothesized to support the spatial and temporal aspects of relational memories. Several studies have also identified neurons with spatial representations in the hippocampus of bats, monkeys, and humans, but it is unclear the extent to which spatial representations in non-rodent species may be sensitive to other parameters such as time and context, which are important components of relational memories. The goal of this thesis is to understand how the primate hippocampus could support the formation of relational memories during natural behavior. I first build the tools necessary to describe natural behavior, specifically focusing on behavior during the free viewing of complex images. I describe free viewing behavior using a foraging model and show that several factors including working memory, oculomotor constraints, and bottom-up salience influence viewing behavior. Additionally, scan paths are composed of short sequences of eye movements, and these sequences may aid in encoding relational memories. Furthermore, relational memory modulates these sequences: at first viewing behavior is well characterized by explorative-type behaviors, but then relational memory shifts viewing behavior towards exploitative-type behaviors. After understanding the behavioral correlates of relational memory, I recorded from neurons in the hippocampus of monkeys freely viewing images. Free viewing trials were interleaved with a directed eye movement task to understand how behavioral context modulates neurons in the hippocampus. Single unit recordings revealed representations of space, time, context, and stimulus novelty. In agreement with previous work, spatial representations were modulated by gaze position. Interestingly, each spatially modulated neuron fired at a consistent latency relative to fixation onset, and the response of the population of spatially modulated neurons fully tiled the duration of the fixation forming a spatiotemporal code that could link information across successive eye movements. Overall, my results highlight the importance of active sensing in organizing spatial representation in the hippocampus. Specifically, my results suggest that the hippocampus encodes information in spatiotemporal sequences reflecting the sequences of eye movements observed in the behavior. Certain patterns of eye movements may even help the hippocampus build relational memories. Finally, a review of the neuroanatomy suggests that there are many pathways in the prefrontal cortex that could explain the bi-directional relationship between relational memory and eye movements observed in this thesis.

TABLE OF CONTENTS

LIST OF FIGURES

LIST OF TABLES

ACKNOWLEDGEMENTS

I would like to thank my advisor, Elizabeth Buffalo, for all the support she has given me during my graduate career. Without her, I would not be where I am today. I am also grateful for the support I received from everyone in the lab. I would like to thank Mike Jutras for teaching me how to record and analyze neural data, I would like to thank Megan Jutras for keeping my projects organized and on track, and I would like to thank Kelly Morrisroe for teaching me how to train monkeys. I would like to thank Sepeadeh Radpour and Sierra Schleufer for helping me edit my thesis. Finally, I would like to thank all the lab techs and volunteers that have trained and run my monkeys. They have helped collect a tremendous amount of behavioral data that I have used in many of my analyses.

I would also like to thank the University of Washington for graciously accepting me into their graduate program when the Buffalo lab moved across the country from Atlanta to Seattle. Jane Sullivan and David Perkel, as well as administrative personnel, have treated me with nothing but kindness. I would like to thank the Biomedical engineering program at Georgia Tech and Emory for allowing me to continue my research with the Buffalo lab.

Funding for my research was provided by various NIH grants including two training grants. Each chapter lists funding for that specific project. Without this funding, none of the research published in this thesis would have been possible.

Chapter 1. INTRODUCTION

1.1 OVERVIEW

1.1.1 *Defining Hippocampal-Dependent Memory*

From remembering where we parked our car to learning how to play a sport, memory plays an essential role in our everyday lives. Decades of research have illustrated that different kinds of memory are critically dependent on different brain regions (Squire, 1992). For instance, the hippocampus and surrounding structures in the medial temporal lobe (MTL) are important for the formation of declarative memories (Squire, 1992; Eichenbaum, 2000; Moser et al., 2008b; Konkel and Cohen, 2009). Declarative memories enable us to consciously recollect our past experiences in order to optimize current and future behavior. For example, you can quickly find your keys in the kitchen if you remember that you came home with groceries.

Declarative memories are distinguished from nondeclarative memories which are learned but cannot be consciously accessed. Nondeclarative memories include learned skills, priming, and classical conditioning. For example, we cannot consciously access the "muscle memory" of throwing a ball. In fact, conscious scrutiny of learned skills can detrimentally interfere with the learned skill. MTL lesion studies suggest that the MTL is not important for the formation of nondeclarative memories (Squire, 1992). Humans with MTL damage can learn new skills, but they have no conscious recollection of the experience.

There are two types of declarative memories: episodic and semantic memories. Semantic memories contain factual-based content such as mathematical and scientific knowledge. Episodic memories contain personal, autobiographical information such as remembering your high school graduation. Several studies have shown that semantic and episodic memories are often retrieved

together (Bird and Burgess, 2008; Ryan et al., 2008), and as a result the specific role of the MTL in the formation of semantic memories is unclear. However, the formation of semantic memories is at least dependent on the integrity of the neocortex.

The literature uses several different terms to describe MTL-dependent memory. The human literature often calls declarative memory explicit memory, but the corresponding animal literature often calls episodic memory relational or configural memory. Human studies often use terms such as declarative and explicit memory as humans can verbally declare or explicitly illustrate what they do or do not remember. There exist subtle differences in the connotation of these terms, but for this thesis, I will consider the terms equivalent. Therefore, for the remainder of this thesis, I will use the term relational memory to describe MTL-dependent memory. Specifically, I define **relational memory** as the ability to remember arbitrary associations between objects or events. These memories include things related by location, order, and context.

1.1.2 *History and Function of the Hippocampus*

Patients with brain damage such as H.M. provided early insights into the function of the MTL (Scoville and Milner, 1957; Squire, 1992). Severe damage to the MTL in humans results in the inability to form new relational memories (i.e. anterograde amnesia). Subsequent lesion studies in animals later confirmed that MTL is indeed important for the formation of relational memories. Lesions to the MTL cause deficits in tasks that depend on spatial, temporal, and contextual cues. Thus, the MTL may serve the function of binding relevant information in space and time to a specific context. Lesions to the hippocampus, the final output of the MTL, also causes similar relational memory impairments

More recent studies conducting electrophysiological recordings from neurons in the MTL have largely focused on the spatial components of relational memories (O'Keefe and Dostrovsky,

1971; Moser et al., 2008b). The presence of place cells in the rodent hippocampus led to the suggestion that the hippocampus contains a "cognitive map" that supports the formation of relational memories (Okeefe and Nadel, 1979). The human and non-human primate hippocampus also contain spatial representations thought to serve a similar function (Rolls, 1999; Ekstrom et al., 2003). While a great deal of rodent literature has focused on the role of the hippocampus in spatial memory, the hippocampus is also important for the formation of relational memories in the absence of clear spatial cues (Squire, 1992; MacDonald et al., 2011).

In addition to playing a substantial role in memory, the hippocampus plays an important role in other cognitive functions (Rubin et al., 2014b). Specifically, the hippocampus plays an important role in flexible cognition. By utilizing our relational memories, we can optimize our current and future behavior based on previous knowledge. The role of the hippocampus in other cognitive functions is outside the scope of this thesis. Instead, I will focus on the role of the hippocampus in the formation of relational memories.

1.1.3 *Thesis Organization*

In the following sections, I will review in greater detail the current body of literature that explains the function of the hippocampus and how it differs from other structures in the MTL. In *Section 1.2* I will review the relevant electrophysiology and lesion literature, in *Section 1.3* I will review models of [spatial] memory, and in *Section 1.4* I will review the role of eye movements in cognition. In these sections, I will pay close attention to the role of active sensing. In particular, I will draw comparisons between sniffing and whisking in rodents to eye movements and vision in primates. These differences in active sensing modalities likely account for the differences in neural representations across species. Lastly, in *Section 1.5* I state my hypotheses and aims.

Studying the structure and function of the MTL is important for understanding and treating various neurological disorders because the MTL shows early signs of atrophy in Alzheimer's disease (Frisoni et al., 2010). Damage and dysfunction of the MTL are also observed in epilepsy, schizophrenia, and depression; and consequently these neurological disorders present with relational memory impairments. Developing a better understanding of the role of the MTL in memory could improve patient outcomes and lead to the development of better diagnostic tests and treatments.

The behavioral analysis tools described in *Chapters 2 and 3*, as well as those in the *Future Directions* section, may be useful for creating more sensitive behavioral measures of MTL-dependent memory. These chapters focus on understanding natural viewing behavior and the role that various forms of memory have in shaping viewing behavior.

Chapter 4 describes neural activity recorded in the hippocampus, the final output of the MTL, during the free viewing of images. *Chapter 4* provides insights into the how the primate hippocampus processes spatiotemporal and contextual information. In contrast to rodents, the neural activity in primates is largely modulated by eye movements. How could this eye movement-related activity reach the hippocampus? The anatomical pathways that support spatial representations based on physical movements in rodents also support eye movements in monkeys. In *Chapter 5* I review these pathways and I describe additional pathways by which memory can in return influence eye movements.

1.2 Review of Hippocampal Literature

1.2.1 *Spatial, Temporal, and Contextual Representations in the MTL*

The hippocampus is strongly interconnected with other structures within the MTL (see *Chapter 5*). Furthermore, the inputs to the hippocampus and other MTL structures are highly overlapping. Therefore, it should not be surprising that similar types of information are present throughout the whole MTL, albeit different regions represent this information in qualitatively different ways. In this section, I focus on electrophysiology data collected throughout the MTL but with specific a focus on the hippocampus and entorhinal cortex, the main input to the hippocampus. Substantially more is known about the neural representations in rodents than in other species. As a result, I use the rodent literature as a foundation for comparison to other species.

1.2.1.1 Rodent Electrophysiology

In rodents, the MEC (medial entorhinal cortex) and the subiculum contain grid cells and border cells (Eichenbaum et al., 1999; Hafting et al., 2005; Moser et al., 2008a; Boccara et al., 2010; Moser et al., 2015). Grid cells have multiple spatial fields organized in a periodic manner resembling a triangular grid while border cells fire along the border of an environment. Similarly, the subiculum contains boundary vector cells that encode the distance of the rat from a boundary (Lever et al., 2009). Head-direction and running speed also modulate many neurons in the MEC. On the other hand, neurons in the LEC (lateral entorhinal cortex) are modulated by object identity; LEC neurons encode spatial information to a lesser extent than neurons in the MEC (Deshmukh and Knierim, 2011).

Grid cells are anchored to the boundaries of the environment, and grid orientation rotates with the rotation of the boundaries of the environment and distal visual cues (Krupic et al., 2015).

Grid cells maintain their spatial firing patterns in darkness over long periods time suggesting that idiothetic cues (self-motion) but not visual cues are important for the spatial firing patterns of grid cells; however, visual cues improve the accuracy of the grid code (Hafting et al., 2005). Similarly, head-direction neurons rotate their direction tuning with the rotation of visual cues.

The hippocampus contains place cells that fire when the rat is in a single area of an environment (O'Keefe, 1976; Lee et al., 2004; Leutgeb et al., 2007; Colgin et al., 2010). A variety of sensory modalities including olfaction, somatosensation, and vision modulate place cell activity. For example, place fields rotate with the rotation of distal visual cues (Hetherington and Shapiro, 1997; Knierim et al., 1998). Place cells can also form in darkness suggesting that non-visual sensory cues are also important, but place selectivity degrades over time in the absence of both olfactory and visual cues (Quirk et al., 1990; Save et al., 2000). Tactile information also appears important for shaping hippocampal activity (Pereira et al., 2007; Bellistri et al., 2013). In the absence of other cues, place cells form in tactile-enriched environments (Gener et al., 2013). Not surprisingly, tactile deprivation, by inactivation of the whisker pad, leads to a reduction of place cell firing and an increase in field size. Like the rotation of visual cues, place fields rotate with the rotation of tactile cues. Lastly, sniffing and whisking play an important role in organizing hippocampal activity during active olfactory-based exploration (Grion et al., 2016; Kleinfeld et al., 2016). In sum, sensory cues play an important role in shaping place cells activity.

Place cells in the hippocampus encode more than just the position of the rat in space. Time and context are especially important components of the hippocampal [place] code.

First, behavioral and spatial context modulate place cell activity. Researchers believe that contextual modulation helps differentiate memories with highly overlapping content. Spatial context is dictated by the physical properties of the environment such as its geometry (Mizumori

et al., 1999). Many place cells remap after geometric manipulations of the environment (Colgin et al., 2008). Grid cells realign to environmental borders but do not undergo the same remapping that the hippocampus experiences. Many other experiments have illustrated that place cell activity depends on the behavioral context within the same environment (Smith and Mizumori, 2006a). In various spatial memory tasks, the firing rate of many place cells depends on the past, present, or future behavior of the animal (Wood et al., 2000; Smith and Mizumori, 2006b).

Secondly, place cells and grid cells fire in theta-sequences nested within theta-gamma cycles forming a spatiotemporal code (Skaggs et al., 1996; Dragoi and Buzsaki, 2006; Eichenbaum, 2014). In addition to representing time within a theta cycle, neurons in the hippocampus and entorhinal cortex fire at select times (i.e. time fields) during long delay periods in MTL-dependent tasks (Pastalkova et al., 2008; MacDonald et al., 2011). Time cells may link information across epochs allowing memories to form over delay periods. Time cells are important because events in our lives unfold before us over time rather of occurring all at once.

In summary, place cells in the hippocampus encode more than just space. Place cells conjunctively code space, time, and context with other forms of non-spatial information (e.g. object identity) (McKenzie et al., 2014). Space, time, and context may form a framework by which other forms of information can map onto. These three dimensions fit well with the putative role of place cells in the formation of relational memories (Konkel and Cohen, 2009; Howard and Eichenbaum, 2015; Ekstrom and Ranganath, 2017). Further, relevant sensory cues, including visual, tactile, and olfactory cues, modulate place cell activity suggesting that active sensing plays an important role in organizing hippocampal activity.

1.2.1.2 Non-Rodent Electrophysiology

The majority of our knowledge about the spatial firing properties of neurons in the entorhinal cortex and hippocampus come from rodent studies, but there is a growing body of research that now describes spatial representations in bats, humans, and monkeys. Researchers still do not fully understand the fundamental properties of spatial representations in non-rodent species. Additionally, many human studies have attempted to replicate rodent findings mostly ignoring the anatomical and behavioral differences between species. As each species actively explores their environment differently, each species may represent space differently.

Bats offer a unique opportunity to understand spatial representations in the MTL because bats explore their environment in a largely unique way using both vision and echolocation. Nachum Ulanovsky originally identified place cells, grid cells, and head-direction cells in crawling bats (Ulanovsky and Moss, 2007; Yartsev et al., 2011; Rubin et al., 2014a). In contrast to rodents, theta oscillations were intermittent occurring in bouts corresponding to times of echolocation, when the bat was stationary. Neurons showed phase locking to theta, but theta did not modulate spike trains. In subsequent experiments, Ulanovsky recorded from flying bats and found 3D head-direction and place cells (Yartsev and Ulanovsky, 2013; Finkelstein et al., 2015; Sarel et al., 2017). Again, in contrast to the rat, there was no evidence for theta modulation of the spike trains.

In one of the most interesting experiments to date, Ulanovsky's lab recorded place cells from echolocating bats in darkness and from the same place cells in light conditions when the bats used vision (Geva-Sagiv et al., 2016). Geva-Sagiv and colleagues found that place cells in CA1 remapped while place cells in the subiculum turned on and off depending on whether the bat used echolocation or vision to explore its environment. Place representations were more accurate in light conditions than in dark conditions, reflecting the acuity of each sensory system. These results

strongly suggest that the way the animal explores their environment dictates the type of spatial representations observed in the hippocampus.

Researchers are only beginning to understand spatial representations in the primate MTL. A few studies have identified place-like representations in the monkey hippocampus, but "place" responses concentrated at reward and object locations making it difficult to determine if these responses were truly spatial (Nishijo et al., 1997; Hori et al., 2005; Furuya et al., 2014). A more recent virtual reality experiment showed that neurons in the hippocampus conjunctively code spatial information (place, head-direction, and gaze location) with non-spatial information (e.g. task demands and reward) (Wirth et al., 2017).

Despite some evidence of place-like representations in monkeys, stronger evidence is pointing toward gaze-based representations of space. Rolls and colleagues identified view cells in the primate hippocampus that selectively respond when the monkey looks at particular locations of an environment, and these view-dependent responses are divorced from the physical position of the monkey (Rolls, 1999). Ringo and colleagues also showed gaze-based spatial responses in head-fixed animals (Nowicka and Ringo, 2000). Similarly, neurons in the monkey entorhinal cortex respond in a spatially periodic manner resembling grid cells in rodent but represent where the monkey looks while freely viewing images (Killian et al., 2012). The primate entorhinal cortex also encodes saccade direction (Killian et al., 2015). Saccade-related responses occur even in darkness (Ringo et al., 1994). Furthermore, eye movements modulate local field potentials (LFPs) throughout the MTL (Sobotka and Ringo, 1997), and in particular, saccades cause theta-phase resets, and the strength of this phase reset is correlated with subsequent stimulus memory (Hoffman et al., 2013a; Jutras et al., 2013a). Note as, in bats, theta-oscillations occur in bouts in the primate MTL.

In addition to spatial representations, the primate hippocampus encodes a variety of other types of information including new associations, stimulus novelty, time, object identity, and context (Wirth et al., 2003; Jutras and Buffalo, 2010a; Naya and Suzuki, 2011; Sakon et al., 2014). Like in rodents, non-spatial information may be bound to spatial, contextual, and temporal representations (Killian et al., 2012; Sakon et al., 2014).

Human spatial representations are very poorly understood. The human hippocampus and entorhinal cortex contain place-like and grid-like representations, respectively (Ekstrom et al., 2003; Jacobs et al., 2013). Researchers have also identified other types of spatial representations including path cells that encode holistic navigation patterns in clockwise or counterclockwise directions (Jacobs et al., 2010). As in bats and monkeys, human theta oscillations occur in bouts (Ekstrom et al., 2005; Aghajan et al., 2016; Bohbot et al., 2017). Moreover, greater theta power occurs during real-world movements as compared to virtual navigation or when patients sit still. Interestingly, theta bouts are three times more prevalent in a congenitally blind subject leading to the possibility that eye movements interrupt continuous theta because eye movements cause theta-phase resets in humans too (Hoffman et al., 2013a). Recordings of the human MTL have also identified neurons that represent context and stimulus novelty (Rutishauser et al., 2006; Miller et al., 2013).

In summary, researchers have found spatial representations in the MTL of several species. Compared to rodent spatial representations, researchers still have a poor understanding of fundamental properties of these spatial representations found in the human and primate MTL. Different types of spatial representations are found in each species reflecting the way that each species actively explores their environment. Neurons in the primate MTL represent the position of gaze, and neurons in flying bats represent 3D position. Gaze-based representations mirror how

primates use vision and eye movements to explore their environments from afar. Gaze-based spatial representations do not preclude spatial representations based on physical position. Instead, gaze-based spatial representations highlight the importance of active sensing in shaping neural activity throughout the brain. Lastly, in addition to encoding space, neurons in the MTL also encode context, time, and other forms of non-spatial information. Conjunctive encoding of various types of information may be important for the formation of relational memories.

1.2.2 *Lesions*

In this section, I briefly discuss the function of each region in the MTL using lesion studies. Our understanding of the human hippocampus began with the study of patient H.M who had his hippocampus surgically removed for the treatment of epilepsy. The lesion extended beyond the hippocampus and included the entorhinal cortex and amygdala (Annese et al., 2014). H.M had severe relational memory impairments, but the lesion spared semantic and nondeclarative memories (Corkin, 2002). MTL lesions studies in animals also support the role of MTL in the formation of relational memory, but the role of the hippocampus itself is not entirely clear.

In primates, perirhinal lesions produce impairments in long-term recognition memory (Buffalo et al., 1999; Buffalo et al., 2000; Huxlin et al., 2000; De Weerd et al., 2003; Buffalo et al., 2005). Additionally, the perirhinal cortex may be important for learning large sets of paired-associations (Eacott et al., 1994; Brown and Aggleton, 2001). Lesions to the parahippocampus cause impairments in [single-trial] object-place learning (Malkova and Mishkin, 2003); lesions to the hippocampus alone do not impair simple object-place learning. Lesions of the parahippocampus in humans lead to deficits in spatial learning and memory including deficits in route learning and object-place learning (Bohbot et al., 1998; Aguirre and D'Esposito, 1999; Bohbot et al., 2000; Ploner et al., 2000). Similarly, lesions of the postrhinal cortex (the rodent

analog of the parahippocampus) produce impairments in spatial memory (Rothblat et al., 1993). Sometimes conjunctive parahippocampal and perirhinal lesions cause non-spatial memory deficits even in the absence of spatial deficits. These deficits occur in tasks with temporal delays, contextual dependencies, and object discrimination (George et al., 1989; Rothblat et al., 1993; Bussey et al., 1999; Nemanic et al., 2004; Winters et al., 2004; Norman and Eacott, 2005).

Entorhinal lesions produce similar impairments to those observed in animals with combined perirhinal and parahippocampal lesions, but entorhinal lesions tend to produce less severe impairments (Squire, 1992; Meunier et al., 1993; Eacott et al., 1994; Buckmaster et al., 2004). Combined lesions of the entorhinal, parahippocampal, perirhinal cortices produce more severe impairments than lesions of individual areas. Overall, these results imply that the MTL functions in a hierarchical fashion and the more extensive the damage to the MTL, the more severe the memory impairment.

In primates, hippocampal lesions produce impairments in several tasks. These tasks include long delays (e.g. delayed-nonmatching-to-sample), contextual-dependent elements, inference, and learning of complex associations (Squire, 1992). Interestingly, hippocampal lesion effects are sometimes larger when tasks are learned postoperatively as compared to preoperatively. Hippocampal lesions produce less severe impairments than lesions of the rest of the MTL, but complete MTL lesions, including the hippocampus, produce the most severe impairments.

The primate MTL may only be necessary for the formation of relational memories after the amount of information exceeds the capacity of the neocortex. Relative expansion of the parahippocampus, perirhinal, and entorhinal cortices, as well as greater differentiation of the PFC, may produce a higher memory capacity in primates. The hippocampus itself may only be involved once other MTL structures have exceeded their capacity. Conversely, the limited capacity of the

neocortex in rodents may lead to the involvement of the MTL in many forms of memory. To support this idea, rodents with hippocampal lesions show spatial and path integration impairments in working memory tasks (Sapiurka et al., 2016). In direct contrast, humans do not need an MTL for navigation in a spatial working memory task (Kim et al., 2013; Urgolites et al., 2016). However, humans with MTL damage cannot remember doing the task.

Lastly, lesion and inactivation experiments are useful for understanding the flow of spatial information in the MTL. The serial and hierarchical models of the MTL do not match the anatomy (see *Chapter 5*). Instead, information flows through multiple pathways in and out of the MTL. Grid and time cells, but not place cells, degrade after medial septal inactivation (Winson, 1978; Brandon et al., 2011; Koenig et al., 2011; Brandon et al., 2014; Wang et al., 2015b). Correspondingly, inactivation of the hippocampus largely leaves the grid code intact (Hafting et al., 2008). Inactivation of the MEC impairs the temporal code of CA1 but does not impact the spatial or object code (Miao et al., 2015; Rueckemann et al., 2016; Robinson et al., 2017). MEC lesions do not completely abolish place activity in CA1 either (Hales et al., 2014). Lastly, inactivation of the anterior thalamic nuclei abolishes grid cells but not theta oscillations or place cells (Winter et al., 2015). Overall, these results suggest that the grid and place codes are somewhat independent, but their stability over long periods of time as well as their function during learning suggest these "independent" codes may be importantly intertwined especially in time. Developmental studies also support these results and show that various spatial representations develop at different times (Langston et al., 2010; Wills et al., 2010; Bjerknes et al., 2014; Bush et al., 2014; Tan et al., 2015).

In summary, lesion studies strongly support the role of the MTL in the formation of relational memories, but the MTL is not the final storage site of long-term memories (Teng and

Squire, 1999). Lesions of the MTL produce impairments in tasks with spatial, temporal, and contextual elements. Lesions of the perirhinal and parahippocampal cortices produce the most severe impairments while lesions of the hippocampus and entorhinal cortex alone produce less severe impairments. We do not fully understand the role of the primate hippocampus in relational memory, but in humans, the hippocampus is important for the conscious recollection of relational memories. Lastly, experiments combining electrophysiology, inactivation, as well as lesion experiments support some degree of independence between the spatial codes in the entorhinal cortex and hippocampus.

1.3 MODELS OF THE HIPPOCAMPUS

Complementary modeling studies have also described the function of the hippocampus and MTL. First, I describe models that explain how the brain forms egocentric (i.e. self-centered) representations of space. Afterwards, I describe how the brain forms allocentric (i.e. world-centered) representations from these egocentric representations. In particular, I focus on two classes of models: continuous attractor network models and oscillatory interference models. I will also describe two models that explain how eye movements and vision in primates could lead to the development of gaze modulated representations in the hippocampus. Lastly, most of these models ignore non-spatial representations. Therefore, I separately discuss non-spatial models.

1.3.1 *Egocentric Spatial Representations*

Egocentric spatial representations are ubiquitous in the nervous systems as sensory and motor representations are inherently egocentric (Andersen et al., 1993). However, transforming sensory information into a motor action is not that simple as egocentric representations contain several different reference frames: gaze, hand, head, or body. To produce a visually guided

reaching movement, visual information in gaze-centered coordinates must somehow interact with the motor command representing muscles in joint coordinates. The brain could transform information serially from gaze to head to body to joint or in a complex, parallel fashion.

The most basic models suggest that the brain computes the desired reaching movement by summing the vectors that represent the direction of the eyes, head, and body (Land, 2012). The brain computes these vectors from efference copies, proprioceptive feedback, optical flow and vestibular input. Vestibular input allows the brain to compute accurate egocentric representations in the absence of visual input. However, visually guided reaching is more accurate than reaching in darkness. While this is a cute mathematical model, this model does not explain how the brain actually computes these transformations.

Several studies propose that egocentric spatial representations reside within the posterior parietal cortex, premotor cortex, and basal ganglia (Colby and Goldberg, 1999; Pesaran et al., 2006); all these areas are important for planning motor actions based on sensory information. These areas are interesting because they contain what are known as "gain fields." Gain fields have mixed responses to various spatial reference frames. For example, a neuron may respond to visual stimuli presented in a specific retinotopic location, and the orbital position of the eye further modulates its response. Simple artificial networks made from gain fields allow a network to flexibly compute various egocentric transformations without explicitly choosing a particular reference frame. While each neuron has a fixed gain field, the population code dynamically changes depending on the inputs. Artificial neural networks trained to make visually-guided reaching movements can also learn gain field-like responses (Smith and Crawford, 2005; Blohm et al., 2009).

Interestingly, gaze-centered coordinates may dominate gain-fields though some have suggested that head-centered coordinates are also ideal (Batista et al., 1999; Crawford et al., 2011; Land, 2012). Because primates are visual creatures, having a more dominant gaze-centered representation may be well-suited for many types of sensory-motor behaviors. If gaze-centered representations dominate egocentric representations, then allocentric representations could also be modulated by eye movements. Additionally, when eye movements update egocentric representations, then allocentric representations should also update when eye movements occur.

1.3.2 *From Egocentric to Allocentric: Models of Grid Cells*

Why does the brain contain both allocentric and egocentric representations, and how does the brain form allocentric representations? One theory is that allocentric representations are built from egocentric representations (Burgess, 2006, 2008; Filimon, 2015). Egocentric representations are transient and important for sensory-motor transformations, but integrating egocentric representations over time accumulates large amounts of error. As a result, enduring memories and accurate navigation in large environments require allocentric information to reset the egocentric integrator. Further, for allocentric representations to impact behavior, the brain has to transform allocentric representations back into egocentric representations. Below, I discuss models of allocentric spatial representations with a focus on spatial representations in the entorhinal cortex and hippocampus.

Additional information is required to build an allocentric reference frame from egocentric information. To carry out path integration the brain needs to integrate velocity (heading and speed) relative to external landmarks (Redish, 1999; McNaughton et al., 2006). Without additional landmarks or others cues, path integration accumulates error over time. The perirhinal cortex, lateral entorhinal cortex, and hippocampus may provide landmark information. The posterior

parietal, retrosplenial, posterior cingulate, and parahippocampal cortices, as well as the anterior thalamic nuclei, may provide the necessary egocentric and velocity information (Byrne et al., 2007; Kravitz et al., 2011).

Before the discovery of grid cells in the MEC, researchers thought various areas in the MTL (e.g. subiculum complex) performed path integration (Redish, 1999); these areas are well-connected to the entorhinal cortex and head-direction networks. After the discovery of grid cells, most models have focused on the entorhinal cortex as contributing to path integration (McNaughton et al., 2006). The entorhinal cortex also contains border cells, speed cells, and head-direction cells, which may also play a direct role in path integration (McNaughton et al., 2006; Burgess, 2008; Moser et al., 2008b; Moser et al., 2014).

Unlike place cells, grid cells do not remap across environments thus creating a metric spatial code that is invariant across environments; the grid code is even present in novel environments. Such a spatial code is ideal for path integration. Models of path integration suggest that path integration is performed using a continuous attractor network. A simple two-layer model contains one layer made from a 1D attractor network representing head-direction and a second layer representing 2D position. The head-direction layer models head-direction tuning found in the anterior thalamic nuclei while the 2D positional layer models spatial representations in MEC. Vestibular input, optical flow, and efference copies update information in the 1D head-direction layer. The 2D positional layer is then updated by the 1D head-direction layer and is positively modulated by a speed signal. The network creates a periodic firing pattern similar to grid cells (McNaughton et al., 2006; Moser et al., 2008b). Modules with different speed gains create grid cells with different grid spacing. Spatial information also flows in both directions across the two layers. In many models, the path integrator also updates an egocentric spatial representation

(Burgess, 2008). Head-direction information is likely important for the transformation of allocentric information into a head-centered, egocentric reference frame.

In these models, the main output of the path integrator is the hippocampus. Some models assume the summation of multiple grid cells creates a single, dominant place field (Rolls et al., 2006; Solstad et al., 2006). Other models assume that the hippocampus itself is also an attractor network (Tsodyks, 1999; Wills et al., 2005; Burgess, 2008). In the path integration models, the hippocampus provides the path integrator with an error correcting signal to avoid error accumulation (Sreenivasan and Fiete, 2011). Consequently, the hippocampus may be useful for generating predictions about the environment through its ability to combine non-spatial (e.g. object) information with spatial information. Further, the hippocampal place code provides an easy readout for multiple brain areas.

Experimental evidence supports many of the ideas presented in these models. Evidence from hippocampal lesions suggests that the grid code is less accurate without the hippocampus (Bonnevie et al., 2013). Replay and pre-play in the hippocampus may be useful for making predictions (Carr et al., 2011). However, while the precision and stability of the place codes is partially dependent on the integrity of grid cells, the place code may require boundary vector cells or border cells to develop instead of grid cells.

Original place cell models theorized the existence of boundary vector cells that are summed to generate place cells (Byrne et al., 2007). This original hypothesis suggested that the parahippocampus contained these boundary vector cells, but recent evidence suggests boundary vector cells exist in the subiculum (Lever et al., 2009). Unlike border cells, boundary vector cells are modulated by the distance of the animal from the border of an environment. However, it is not clear what the relationship is between boundary vector cells and border cells. More recent models

combine grid cell, boundary vector cells/border cells, and landmarks to create a realistic place code that is only partially dependent on grid cells (Redish and Touretzky, 1998; Arleo and Gerstner, 2000; Widloski and Fiete, 2014).

In summary, the brain builds allocentric representations from egocentric representations. The brain integrates egocentric representations over time with speed and direction signals which are then anchored to external landmarks to perform various spatial computations including path integration. Continuous attractor networks can perform these computations and are stable in time and robust to noise. The entorhinal cortex and its connections are especially well-suited for performing path integration. The hippocampus may aid in path integration, but may not be necessary in familiar or small environments that do not require learning. Instead, the hippocampus may use the output of the path integrating circuit combined with additional non-spatial information to perform various memory-related computations, like making predictions or retrieving old memories. Lastly, allocentric representations feed back into egocentric representations to affect behavior. As with egocentric representations, gain-field like representations in intermediate regions (e.g. retrosplenial cortex) may aid in the transformation from allocentric to egocentric representations. Mixed selectivity may also aid in linear readouts as suggested by various gain-field models (Rigotti et al., 2013). In essence, similar computational principles may underlie spatial transformations throughout the brain.

1.3.3 *Alternative Models: Oscillatory Interference Models*

Attractor network models of spatial representations are becoming popular, but these models have several drawbacks (Zilli, 2012). First, these attractor models require very specific connection patterns that the brain may not be able to learn. Second, many attractor models ignore important timing principles ubiquitously found in the MTL. Specifically, theta oscillations play an

important role coordinating and organizing neural activity in time. Instead, a different class of models, called oscillatory interference models, describe how theta oscillations could generate grid cells and place cells. This class of models also has its drawbacks as I will explain shortly. Recently, researchers have combined features of both attractor and interference models to faithfully and realistically encode space with appropriate timing principles (Giocomo et al., 2011).

O'keefe and colleagues first proposed the oscillatory interference model for the formation of place cells but later expanded this model to explain grid cells (Okeefe and Recce, 1993; Lengyel et al., 2003; Burgess et al., 2007). In the place cell model, a dendritic input oscillates faster than the somatic oscillation, creating a constructive wave at certain phases dictated by the position and speed of the animal. The somatic oscillation never changes. The gain of the speed-dependent dendritic input dictates the size of the place field. Outside the place field, the somatic and dendritic oscillations are equal in amplitude and frequency and of anti-phase thus causing destructive interference. As the animal approaches the place field, the dendritic oscillation increases in frequency and then constructively interferes with the somatic oscillation. If constructive interference exceeds a certain threshold, the neuron will then spike. When the animal leaves the field, the dendritic and somatic oscillations once again destructively interfere. The model faithfully reproduces spike phase relationships (e.g. precession). Note that pure attractor network models can also produce phase precession (Tsodyks, 1999).

The oscillatory interference model of grid cells is similar but has a greater number of dendritic inputs. Specifically, at least three dendritic oscillations with separate phases offset by 60 degrees constructively interfere to produce a grid-like firing pattern. A different preferred head-direction drives each dendrite. In the grid cell model, the gain of the speed-dependent input modulates the grid spacing. As with the path integration models, the oscillatory interference model

of grid cells is susceptible to error accumulation. Burgess and colleagues propose that place cells or border cells could produce a theta-phase reset to help realign grid cells to landmarks.

The major drawback of the oscillatory interference models is that the oscillatory interference model is biologically implausible. The soma and dendrites cannot simultaneously oscillate independently and integrate (Remme et al., 2010). Burgess and colleagues also suggested that the oscillatory interference could occur across a small group of neurons instead of within the dendrites of a single neuron. However, grid cells in bats and monkeys in the absence of continuous theta suggest that grid cell formation does not require continuous theta (Yartsev et al., 2011; Killian et al., 2012).

1.3.4 *Models of View Cells*

Models of spatial representations in the MTL focus primarily on those found in rodents, but a handful of papers have described how view cells may develop in primates. These papers argue that the difference in spatial representations across rodent and primate species may arise from differences in the way each animal explores their environment.

Rolls and colleagues suggest that high acuity vision in primates (encompassing 30 degrees of visual angle) leads to a different pattern of activation of visually responsive neurons than low acuity vision in rodents (encompassing 270 degrees of visual angle) (de Araujo et al., 2001). In this model, visually responsive neurons are activated when the observer simulataneously sees a combination of visual cues. High acuity vision in primates leads to the activation of visually responsive neurons only when primates look directly towards the neuron's preferred visual cues creating view cells which are largely divorced from the position of the animal. Low acuity vision in rodents leads to the activation of visually responsive neurons only when the rat is in one location

creating place cells because the rodent has to be far enough away from the preferred stimuli to see all preferred stimuli at once.

An alternative explanation is that view cells arise because primates use eye movements to explore their environment (Franzius et al., 2007). Franzius and colleagues used Slow Feature Analysis and unsupervised learning in a multi-layered model to extract the optimal sparse code for representing an animal's position in a visual environment. The first two layers of the model are analogous to the visual system. These layers simply extract and process visual information. The third layer of the model then mixes this visual information with information about the movement of the animal. Then a fourth layer extracts a sparse code. A model animal only producing head and body movements creates a spatial code containing place-like cells and head-direction cells. However, the addition of fixational eye movements produces view cell-like properties. This model suggests that the brain builds spatial representations governed by how the animal moves about its environment.

1.3.5 *Non-Spatial Models of the Hippocampus*

Models of the hippocampus encompass a much wider body of literature that is not focused solely on spatial navigation and memory. The same models discussed in the section above could also perform associations between spatial and non-spatial information, but many models describe the spatial and non-spatial functions of the hippocampus separately (Buzsaki and Moser, 2013). In fact, Hopfield originally proposed a discrete attractor network that encoded associated information (Hopfield, 1982). Hopfield's work has inspired many other types of attractor models including those above (Gluck et al., 2003).

In many models, each region within the MTL and hippocampus serve a distinct function (Lisman, 1999a; Yassa and Stark, 2011; Schapiro et al., 2017). The entorhinal cortex could be

useful for extracting regularities from the environment; this information broadly includes contextual information as it does not change within an environment. Additionally, the Dentate Gyrus has been implicated in pattern separation while CA3 acts like an attractor network and performs pattern completion. Pattern separation transforms similar inputs and maps them to distinct, non-overlapping outputs, whereas pattern completion transforms partial inputs and into a complete representation. CA1 performs several functions: 1) CA1 transforms information back into a cortical code so that information can effectively leave the hippocampus, and 2) CA1 performs an error prediction function by comparing information computed by CA3 with information in the entorhinal cortex (e.g. match/mismatch).

Lisman has generalized the ideas above and suggested that the hippocampus is important for sequence learning (Lisman, 1999b). Lisman's predicts that the Dentate Gyrus forms auto-associations and CA3 forms hetero-associations. Auto-associations create associations within the same event while hetero-associations create associations across events. Auto-associations tolerate noise and will not easily degrade over time, but hetero-associations could underlie the formation of relational memories as many events unfold in time. Thus, Lisman's model allows the hippocampus to form sequences of information within and across events.

1.4 Eye Movements and the Brain

In this section, I briefly detail my motivation for using eye movements to study memory. The stimulus in front of us, as well as our ongoing thought processes, dictate the way we move our eyes. The way we move our eyes provides a noninvasive measure of cognitive functions such as arousal, attention, memory, and perception. As such, eye tracking is becoming a popular way to understand how diseases alter our state of mind. There are many types of eye movements, but in

this thesis, I focus on fixations and saccades as I use static stimuli to understand memory-related changes in eye movements.

Understanding the cognitive underpinnings of eye movements began with the influential work of Yarbus in the 1960's (Yarbus, 1967; Martinez-Conde and Macknik, 2015). Subsequent work by many others has described how bottom-up and top-down factors influence viewing behavior. Bottom-up factors are stimulus features (e.g. a red balloon or a face) that rapidly draw our attention. Top-down factors are task demands and cognitive processes that influence how observers allocate attention to the bottom-up features in order to achieve one's goal. Top-down factors allow observers to ignore distractors and enhance attention towards relevant targets.

Especially in recent years, there has been a push to develop eye tracking methods for diagnosing neurodegenerative diseases and assessing treatment outcome. As highly visual creatures, oculomotor areas have strong connections to many regions involved in various cognitive processes. As such, dysfunction of specific brain regions can lead to altered eye movements. For example, hypokinetic disorders like Parkinson's disease lead to altered saccade statistics such as smaller amplitude saccades (Tseng et al., 2013a). Similarly, damage to the cerebellum leads to inaccurate saccade production (Robinson and Fuchs, 2001). Outside of motor disorders, Autism Spectrum Disorder (ASD) and Attention Deficit Hyperactivity Disorder (ADHD) also present with altered scan patterns. Children with ADHD show altered attentional drive and are easily distracted (Tseng et al., 2013a; Mueller et al., 2017). Children with ASD also have altered bottom-up drive accompanied by changes in attention toward social (e.g. face) stimuli (Chawarska and Shic, 2009; Wang et al., 2015a). Eye tracking in infants can even be used to predict those who will later develop ASD (Chawarska et al., 2013).

Other studies have used eye tracking to assess MTL-dependent memory. In general, there is a strong relationship between eye movements and memory (Meister and Buffalo, 2016; Voss et al., 2017). Several behavioral studies have shown that scan patterns during novel stimulus viewing subsequently predict recognition memory strength (Kafkas and Montaldi, 2011; Olsen et al., 2016). Subsequent eye movement effects are even correlated with MTL activation in fMRI studies (Hannula and Ranganath, 2009; Liu et al., 2017). Additional evidence for the relationship between eye movements and memory comes from studies of patients with MTL damage. During repeated stimuli presentations with altered content, patients with hippocampal damage fail to recognize that something in the image has changed (Smith et al., 2006b; Smith and Squire, 2008b); there is no change in their viewing behavior either to suggest that they subconsciously noticed the change. Conversely, healthy control subjects show a significant increase in fixations in the altered region but only when they recognize that something has changed. These results strongly illustrate how hippocampal-dependent memory correlates with eye movements in image viewing tasks. Reflecting conscious memory for a stimulus, several studies in humans have observed changes in eye movements between novel and repeated stimulus viewing. For example, fixation durations become longer, and saccade amplitudes become shorter during repeated viewing (Smith et al., 2006b; Kaspar and Konig, 2011). Published data in monkeys is lacking, but our studies (see *Chapter 4* and *Future Directions*) largely show similar results. Lastly, eye-tracking studies show impaired novelty preference in individuals with mild cognitive impairments who will later develop Alzheimer's disease (Crutcher et al., 2009; Lagun et al., 2011). Similar tasks in monkeys also suggest that the hippocampus is necessary for this novelty preference (Zola et al., 2000). Moreover, LFPs and neurons in the monkey hippocampus differentiate between novel and repeated stimuli (Jutras and Buffalo, 2010a).

There is a convincing relationship in humans between eye movements and memory. Certain scanning strategies affect encoding. Further, eye movements change during repeated stimulus presentations suggesting that memory, in turn, influences eye movements. More work needs to be done to establish this relationship in monkeys, but a small number of studies support a similar relationship in monkeys. The work presented in this thesis also supports this bi-directional relationship. In *Chapter 3,* I use a foraging model to show that bottom-up salience and working memory strongly influence eye movements during novel image presentations. In *Chapter 4* and the *Future Directions* section, I show long-term stimulus memory (i.e. relational memory) during repeated presentations leads to changes in fixations and saccade statistics. Moreover, these changes in eye movement statistics correlate with changes in neural activity found in the hippocampus.

1.5 Hypothesis and Aims

Damage to the hippocampus in humans is associated with impairments in relational memory. However, very little is known about the neural substrates of relational memory in primates. Therefore, **the objective of my thesis is to test the central hypothesis that the hippocampus contributes to the formation of relational memories.** I will investigate the role of the hippocampus in the formation of relational memory by first building the tools needed to understand the behavioral correlates of relational memory in monkeys. Second, I will conduct electrophysiological recordings in the monkey hippocampus to understand the neural substrates of relational memory. My thesis was conducted in conjunction with other studies that address the causal role of the hippocampus in the formation of relational memories.

Aim #1: Develop quantitative methods for analyzing and modeling relational memory as assessed through viewing behavior. Viewing behavior has been well characterized in humans across a large number of paradigms and is known to depend on task parameters. However, in non-humans primates, the vast majority of viewing behavior has been studied under well-controlled conditions. The objective of this aim is to develop tools for analyzing viewing behavior in primates under controlled and unrestrained viewing of visual stimuli. First, I will develop a saccade detection algorithm so that I can accurately describe viewing behavior. Second, I will determine quantitative descriptors of viewing behavior including how stimulus features and working memory influence viewing behavior during a novel stimulus presentation. I will then examine how viewing behavior changes when monkeys view a familiar stimulus to assess memory for that stimulus. I *expect* that viewing behavior can be quantified and modeled with a small number of parameters and that behavior changes in a stereotyped manner when monkeys view a familiar stimulus.

Aim #2: Determine whether single units and local field potentials in the hippocampus encode information that may be used for the formation of relational memories. I will conduct electrophysiological recordings in the hippocampus from two monkeys freely viewing natural images and performing a directed eye movement task. I hypothesize that neurons in the hippocampus encode learned relational associations. Moreover, I hypothesize that neurons will respond differently to well-remembered stimuli compared to forgotten stimuli. Specifically, I will determine how the variability in neural activity correlates with behavioral variability, particularly behavior associated with learning and memory. I *expect* to identify individual neurons in the hippocampus that encode information about space, time, context, and the monkey's familiarity with a visual stimulus.

Chapter 2. DETECTING FIXATIONS AND SACCADES[1]

2.1 ABSTRACT

Eye tracking is an important component of many human and non-human primate behavioral experiments. As behavioral paradigms have become more complex, including unconstrained viewing of natural images, eye movements measured in these paradigms have become more variable and complex as well. Accordingly, the common practice of using acceleration, dispersion, or velocity thresholds to segment viewing behavior into periods of fixations and saccades may be insufficient. Here we propose a novel algorithm, called Cluster Fix, which uses *k*-means cluster analysis to take advantage of the qualitative differences between fixations and saccades. The algorithm finds natural divisions in 4 state space parameters—distance, velocity, acceleration, and angular velocity—to separate scan paths into periods of fixations and saccades. The number and size of clusters adjusts to the variability of individual scan paths. Cluster Fix can detect small saccades that were often indistinguishable from noisy fixations. Local analysis of fixations helped determine the transition times between fixations and saccades. Because Cluster Fix detects natural divisions in the data, predefined thresholds are not needed. A major advantage of Cluster Fix is the ability to precisely identify the beginning and end of saccades, which is essential for studying neural activity that is modulated by or time-locked to saccades. Our data suggest that Cluster Fix is more sensitive than threshold-based algorithms but comes at the cost of an increase in computational time.

[1] Adapted from König, Seth D., and Elizabeth A. Buffalo. "A nonparametric method for detecting fixations and saccades using cluster analysis: Removing the need for arbitrary thresholds." Journal of neuroscience methods 227 (2014): 121-131.

2.2 INTRODUCTION

Rigorous analysis of eye movements dates back to the seminal work of Alfred Yarbus (Yarbus, 1967). Today, eye tracking is used to determine the location of visual attention (Duchowski, 2002; McAlonan et al., 2008; Lee et al., 2011), measure memory (Smith et al., 2006a; Smith and Squire, 2008a; Hannula and Ranganath, 2009; Jutras et al., 2009; Richmond and Nelson, 2009; Hannula et al., 2010; Jutras and Buffalo, 2010a; Hannula et al., 2012; Killian et al., 2012), detect cognitive impairments (Crutcher MD, 2009; Lagun et al., 2011; Zola et al., 2013), and evaluate visual search strategies (Najemnik and Geisler, 2005; Dewhurst R, 2012). The development of non-invasive infrared eye-tracking technologies has further enhanced the value and feasibility of collecting viewing behavior across a large range of experimental tasks.

Commonly, viewing behavior, represented as a scan path, is parsed into periods of fixations and saccades using a variety of algorithms. The most widely used algorithms employ velocity and acceleration thresholds to detect the occurrences of saccades because the velocity and acceleration of the eye are much greater during a saccade than during a fixation (Otero-Millan et al., 2008; Nystrom and Holmqvist, 2010; Kimmel et al., 2012). Threshold-based algorithms have the benefit of being intuitive, quick, and easy to implement. Other popular algorithms use density or dispersion and areas of interest (Tatler BW, 2005; Ito et al., 2011). Variants and combinations of these algorithms include mechanisms to correct for errors in eye tracking such as blinks and other temporary losses of signal (Wass et al., 2013).

Despite a significant increase in the use of eye movements in neuroscience, there have been very few advances in the algorithms used to detect fixations and saccades (Salvucci and Goldberg, 2000). We could only find a few instances of algorithms that deviated significantly from the most widely used algorithms. Unfortunately, many of these alternative algorithms still

employ a velocity threshold to detect potential saccades, followed by additional techniques including principal component analysis to distinguish between smooth pursuit, saccades, and noise (Berg et al., 2009; Liston et al., 2012). One exception is (Urruty et al., 2007) which used dispersion and projection clustering into arbitrary subspace to detect fixations. To the best of our knowledge, these algorithms have not been adopted in subsequent studies.

Algorithms employing velocity and acceleration thresholds for saccade detection may be sufficient for simple tasks in which subjects make predictable saccades towards a stationary target; however, more complex oculomotor tasks such as unconstrained viewing of natural scenes or dynamic stimuli may produce more variable eye movements (Andrews and Coppola, 1999; Hayhoe and Ballard, 2005b; Berg et al., 2009; Rayner, 2009). A major source of this variability arises from the variability in saccade amplitude which is strongly correlated with the peak velocity of the saccade (Otero-Millan et al., 2008; Martinez-Conde et al., 2009; Martinez-Conde et al., 2013). Velocity thresholds may not accurately parse highly variable scan paths into periods of fixations and saccades since saccade amplitudes and thus their peak velocity are not constrained in free viewing. Further, many algorithms employ arbitrary thresholds based on qualitative human observations which can vary across research laboratories and even from one experiment to the next within a laboratory. Finally, computed viewing behavior statistics including saccade rate, fixation duration, saccade duration, and saccade amplitude vary not only according to experimental variables but also by the method used to calculate them (Duchowski, 2007; Shic et al., 2008; Nystrom and Holmqvist, 2010). Therefore, there exists a need for a more accurate, sensitive, non-arbitrary, and completely automated saccade detection algorithm. Such an algorithm could constitute a “gold standard” for detecting fixations and saccades from scan

paths so that viewing behavior could be accurately compared across experiments, laboratories, and algorithms.

Here we present a novel algorithm, called Cluster Fix, which applies *k*-means cluster analysis to parse scan paths into fixations and saccades. There are several clear qualitative differences between fixations and saccades—saccades are temporally short with a high velocity whereas fixations are longer in duration with a slower velocity. These qualitative differences translate into quantitative differences and the occupation of different regions in state space. Cluster Fix makes no assumptions about the arrangement of scan paths in state space, requires no human inputs, and includes only duration thresholds as free parameters.

2.3 METHODS

2.3.1 *Eye Tracking*

Scan paths were obtained at 200 Hz using an infrared eye tracker (ISCAN) from rhesus macaques freely viewing 288 images of natural scenes. Eye tracking data were collected from 4 adult male macaques seated head-fixed in a dimly illuminated room 60 cm away from a 19" CRT monitor with a refresh rate of 120 Hz. Images of natural scenes were 600 by 800 pixels large and subtended 25 by 33 degrees of visual angle (dva). Experimental control software (CORTEX http://dally.nimh.nih.gov/) displayed images for 10 seconds each. Initial calibration of the infrared eye tracking system consisted of a 9 point calibration task. Drift was tracked throughout the experiment by presenting additional calibration trials between image viewing trials. We excluded from further analysis any eye tracking data more than 50 pixels (2 dva) outside of the image. Blinks were rarely observed in our data so we did not make any corrections other than the exclusion of data outside of the image. Standard blink correction techniques should work with Cluster Fix if scan paths are evaluated in a piece-wise manner ignoring blinks and as long as at

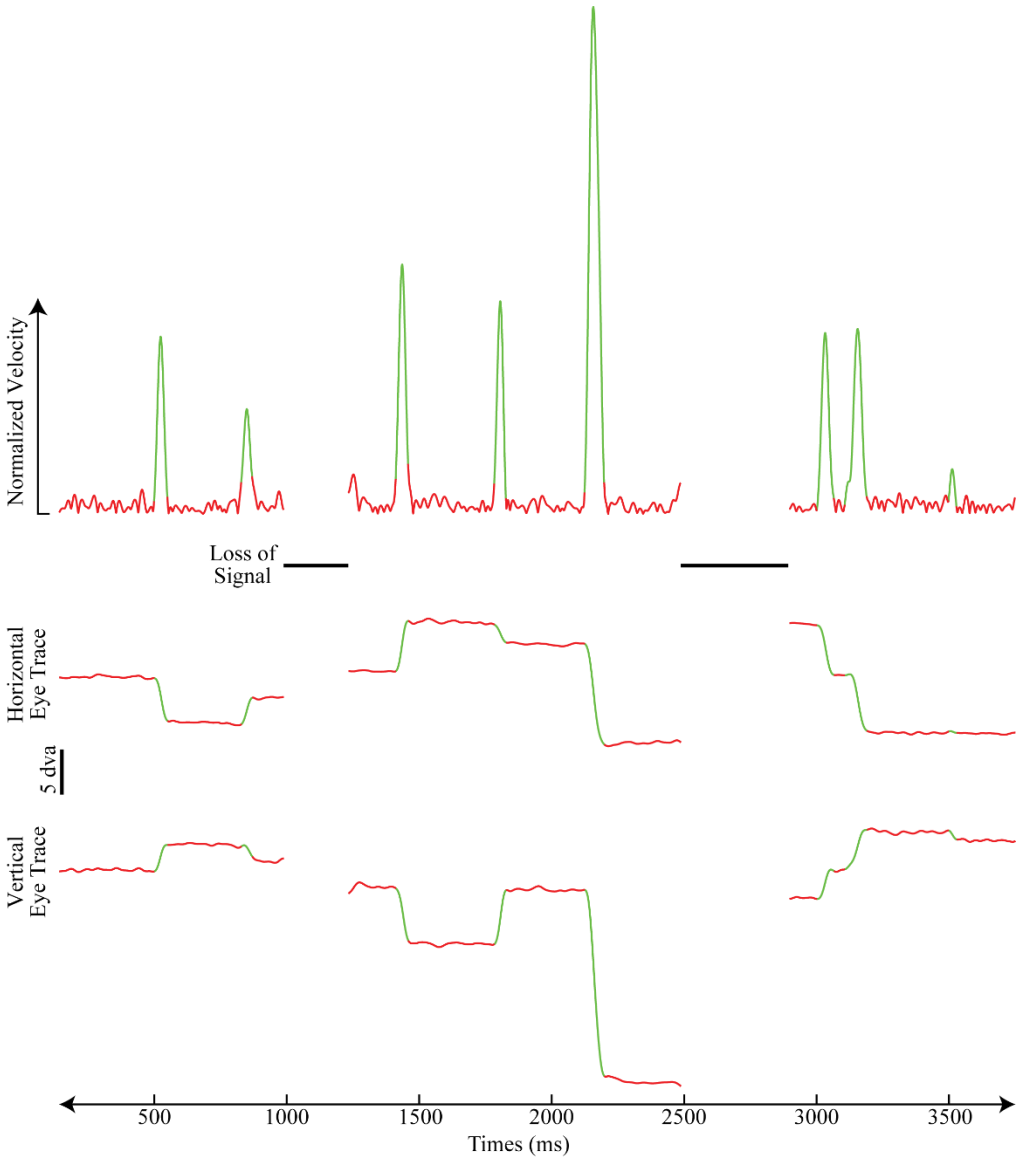

Figure 2-1 Cluster Fix applied to Human Data with Signal Loss
We applied Cluster Fix to human data acquired at 120 Hz using a Toby T120 eye tracker. Humans were allowed to freely move during the experiment thus, unlike the scan paths from monkeys, we frequently lost the ability to track eye position either due to blinking or head movements. Abrupt losses in signal shorter than 25 ms were linearly interpolated while segments of the eye trace containing less than 333 ms of signal were eliminated altogether. After up-sampling using linear interpolation and then applying a 30 Hz low pass filter, we used Cluster Fix to analyze the interrupted scan paths in a piece-wise manner ignoring signal loss. Visual inspection of the up-sampled and filtered scan path as well as the velocity profiles indicate that Cluster Fix can accurately classify fixations (red) and saccades (green) when applied to scan paths with signal loss in a piece-wise manner.

least one fixation is present in each evaluated portion of the scan path (**Figure 2.1**). All experiments were carried out in accordance with the National Institutes of Health guidelines and were approved by the Emory University Institutional Animal Care and Use Committee and Emory Institutional Review Board.

2.3.2 *Cluster Fix Algorithm*

The Cluster Fix algorithm was written in MATLAB and is available as supplementary material. **Table 2.1** contains the procedural outline detailing the major processes achieved by the algorithm. To avoid filtering artifacts, eye traces were buffered prior to filtering, filtered, and then the buffers were removed. First, horizontal and vertical eye traces from the viewing of each image were individually pre-processed using a polyphase implementation (MATLAB function RESAMPLE) to up-sample the data from 200 Hz to 1000 Hz and then filtered using a 60^{th} order low pass filter with a cutoff frequency of 30 Hz. These pre-processing steps were used to remove noise from the scan path while retaining prominent features of saccades. These pre-processing steps followed the method used previously in our laboratory to remove noise for saccade detection with a velocity threshold. However, these pre-processing steps could be replaced by any pre-processing steps that sufficiently increase the signal-to-noise ratio.

Next, the absolute value of 4 state space parameters—distance, velocity, acceleration, and angular velocity—were calculated for every time point. Velocity and acceleration were computed as the first and second derivative of position, respectively. Distance was measured as the Euclidian distance between the position of the scan path at a time point to the position of the scan path two time points later. Angular velocity was calculated as the difference in the angle of scan path from one time point to the next. Angular velocity was subtracted from 360 degrees so that lower values were associated with fixations. For each state space parameter, any values

Table 2-1 Cluster Fix Procedural Outline

1. Pre-process and Filter
    a. Up-sample horizontal and vertical eye traces from 200 Hz to 1000 Hz
    b. Low pass filter with a cutoff frequency of 30 Hz
2. Calculate distance, velocity, acceleration, and angular velocity for every time point
3. Move Outliers and Normalize
    a. Move outliers greater than the mean + 3*std to the mean + 3*std
    b. Individually normalize the 4 state space parameters to be from 0 to 1
4. Global Clustering
    a. Determine the number of clusters
    b. Cluster using k-means
    c. Determine fixation clusters and saccades clusters
    d. Reclassify fixations with durations less than 25 ms as saccades
5. Local Re-clustering
    a. Compare detected fixations to adjacent portions of the scan path
    b. Determine the number of clusters
    c. Cluster using k-means
    d. Determine fixation clusters and saccade clusters
6. Reclassify global fixation time points that were locally determined to be saccades
7. Consolidate using duration thresholds
    a. Classify fixations with durations less than 5 ms as saccades
    b. Reclassify saccades with durations less than 10 ms as fixations
    c. Reclassify fixations with durations less than 25 ms as saccades
8. Post-processing
        a. Down-sample to acquisition frequency of 200 Hz

greater than 3 standard deviations above the mean were set to 3 standard deviations above the mean, and all values were then normalized from 0 to 1.

Cluster Fix globally clustered every time point in state space into *k* number of clusters. We determined the appropriate number of clusters using the average silhouette width (MATLAB function SILHOUETTE). The silhouette width measures the average ratio of inter- and intra-cluster distances to determine the appropriate number of clusters. Higher ratio values indicate that points within clusters were closer to each other than points outside of their respective clusters. We chose the number of possible clusters to be from 2 to 5 clusters because in a typical scan path there is at least 1 fixation and 1 saccade, and in the most complex scan path we can divide fixations into 2 separate clusters and saccades into 3 separate clusters. Fixations can be subdivided into 2 clusters: one with low angular velocity and one with high angular velocity. Saccades can be subdivided into 3 clusters: low velocity but high acceleration, low acceleration but high velocity, and high velocity and high acceleration.

To reduce the number of computations, SILHOUETTE was used iteratively on 10% of the time points to determine the *k*, between 2 and 5, that produced the highest ratio or within 90% of the highest ratio. We found no difference between using only 10% of the time points or all the time points except a reduction in the number of computations. In the case where the ratio was high for several *k*, the largest *k* was used. Once the appropriate number of clusters was identified, clusters were determined using *k*-means cluster analysis on all the time points (**Figure 2.2 A**-**B**). Five replicates were performed for determining the appropriate number of clusters and for clustering of all the time points. The cluster with the lowest sum of the mean velocity and acceleration was classified as a cluster consisting of fixation time points. Because fixations were often divided into 2 clusters, one with high angular velocity and one with low angular velocity

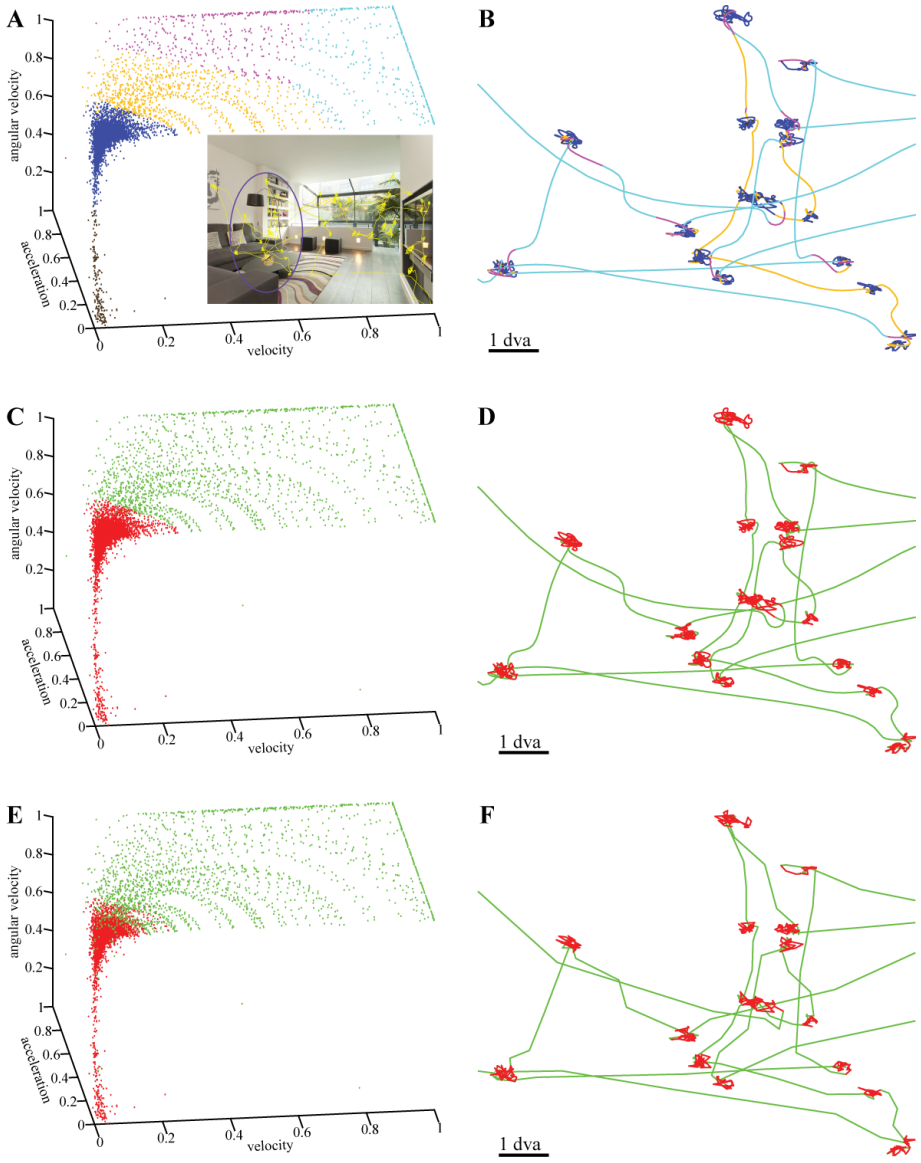

Figure 2-2 Global Clustering in Scan Path State Space

A) Global clustering identified the appropriate number of clusters in 4 state space parameters—distance (not shown), velocity, acceleration, and angular velocity—normalized from 0 to 1. Each dot represents a single time point (1 ms) from a representative scan path (yellow lines overlaying image in inset) with each color representing a different cluster. Blue and brown clusters represent time points with low acceleration and velocity. These two clusters represent the two states of fixation (high and low angular velocity). Pink, gold, and turquoise clusters represent clusters with higher velocity and acceleration. These three clusters represent the three states of saccades. **B)** Representative section of the up-sampled scan path globally clustered in A (indicated by purple circle in inset image). Each cluster represents a different portion of the scan path across multiple fixations or saccades. **C)** Fixation clusters (red) were determined as the clusters with the lowest velocity and acceleration. All other clusters were classified as saccades (green). **D)** The same portion of the scan path now parsed into fixations and saccades. **E)** Following local re-clustering many of the fixation time points were reclassified as the beginning and end of saccades. Additionally, re-classification reduced the size of the fixation cluster and resulted in some fixation and saccade time points overlapping in state space. **F)** Representative section of the final raw scan path parsed into fixations and saccades.

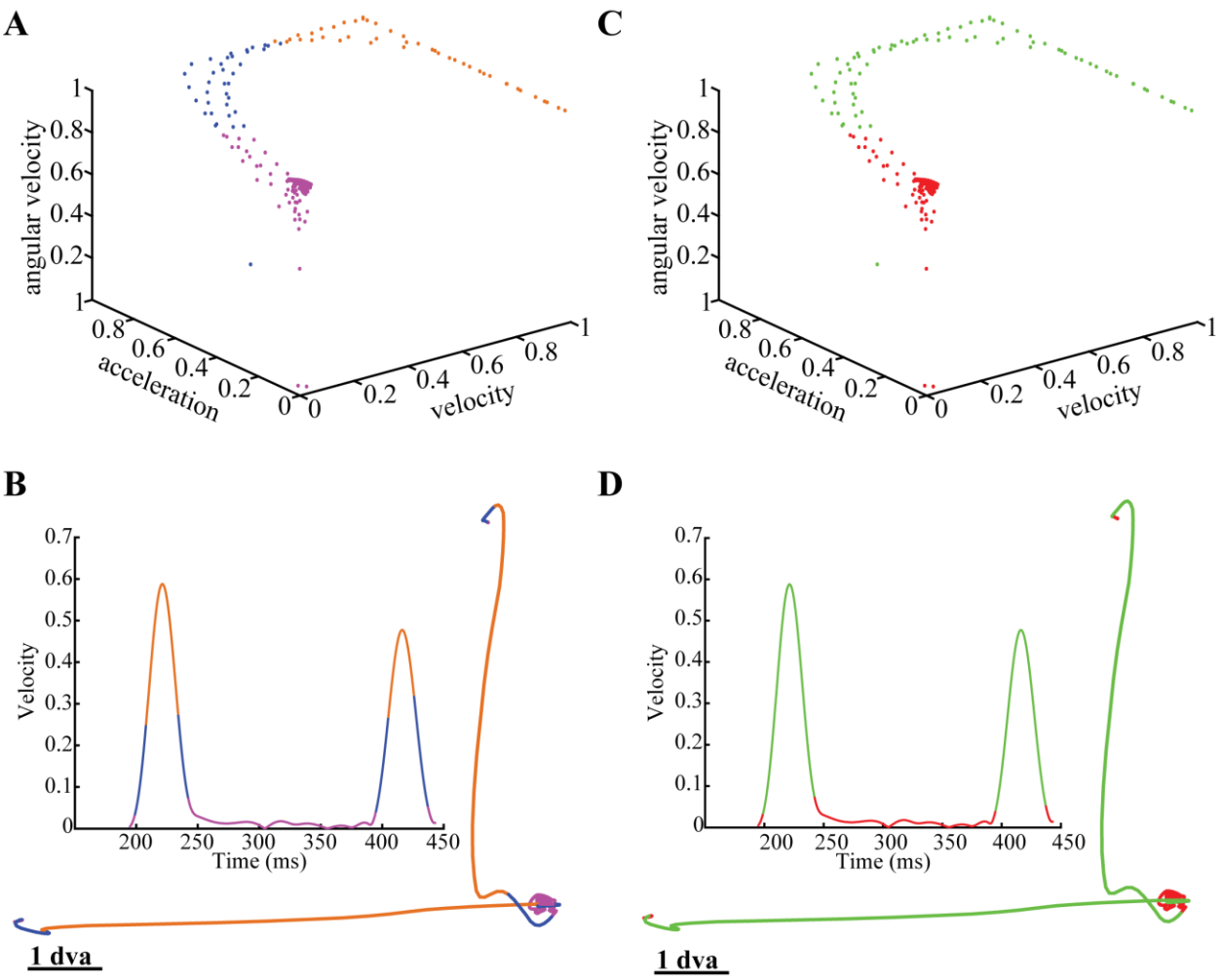

Figure 2-3 Local Re-clustering of a Detected Fixation in State Space
A) Initially, local re-clustering identified the appropriate number of clusters between a fixation and surrounding portions of the scan path typically including 2 saccades. **B)** The velocity profile from the same portion of scan path. **(Inset)** Each cluster represented a different portion of the up-sampled scan path. **C-D** show the clusters, scan path, and velocity profile now classified as fixations (red) or saccades (green). Cluster Fix classified the clusters with the lowest velocity and acceleration as fixations. All other clusters were classified as saccades.

angular velocity, additional fixation clusters were determined by finding clusters whose mean velocity and acceleration were within 3 standard deviations of the mean of the first fixation cluster. All other clusters were classified as saccade clusters (**Figure 2.2 C-D**). Fixation periods shorter than 25 ms in duration were also reclassified as saccades.

To increase the sensitivity of the algorithm to smaller amplitude saccades, the algorithm reevaluated each fixation locally using the same method applied in global clustering (**Figure 2.3**). The concept of local re-clustering is to analyze data at the appropriate scale (i.e. in between 2 "large" saccades detected by global clustering) to remove the over shadowing effects of the larger variability in the whole data. In local re-clustering, time points 50 ms (approximately the average saccade duration) prior to and following a detected fixation were re-clustered with the detected fixation. SILHOUETTE was used iteratively on 20% of the time points to determine the *k*, between 1 and 5. The median of the best *k* was chosen for the final number of clusters. The additional possibly of only finding 1 optimal cluster was added in case the evaluated portion of the scan path only contained a single fixation and no saccades. For each cluster, the median velocity and median acceleration were identified. Then, the cluster with the lowest sum of these two values was considered to consist of fixation time points. Because the number of time points in each cluster was relatively small, measures of the mean and standard deviation of each cluster were more sensitive to outliers. Therefore, additional fixation clusters were determined by finding clusters whose median velocity and acceleration overlapped with the first fixation cluster in velocity and acceleration state space.

Time points that fell within saccade clusters identified using local re-clustering were classified as saccade time points in the global clusters. Any fixations shorter than 5 ms in duration were also temporarily classified as saccades. This duration criterion should not be

considered a free parameter but simply accounted for incorrectly detected fixations that occurred at velocity or acceleration peaks and troughs where acceleration or velocity was near 0, respectively. Next, Cluster Fix flagged saccades less than 10 ms in duration as classification errors and reclassified them as fixations. Then, Cluster Fix flagged fixations that were less than 25 ms in duration as classification errors and reclassified them as saccades. These duration criteria operate independently, but infrequently these criteria were used together when a very short "fixation" (i.e. less than 25 ms) was adjacent to another very short "fixation" to create a fixation with a duration greater than 25 ms. Finally, fixation and saccade time periods were down-sampled to the acquisition frequency of 200 Hz.

2.4 RESULTS

Local re-clustering was performed after global clustering because the variability in each state space parameter within a single fixation or saccade was much smaller than the variability across all fixations or saccades. As shown in **Figure 2.4**, previously detected fixations were reevaluated via local re-clustering to ensure that the algorithm was more sensitive to smaller saccades and to increase the specificity for determining the transition time between fixations and saccades. For this representative scan path, global clustering and even liberal thresholds could not distinguish three smaller saccades from the noisy fixation.

Surprisingly, local re-clustering revealed some overlap between saccades and fixations in global state space (**Figure 2.2E-F**). The overlap in state spaces is due to the detection of smaller saccades whose velocity and acceleration profiles were similar to that of a noisy fixation. A reduction in the size of the fixation cluster was also observed due to an increase in specificity of the transition time between fixations and saccades.

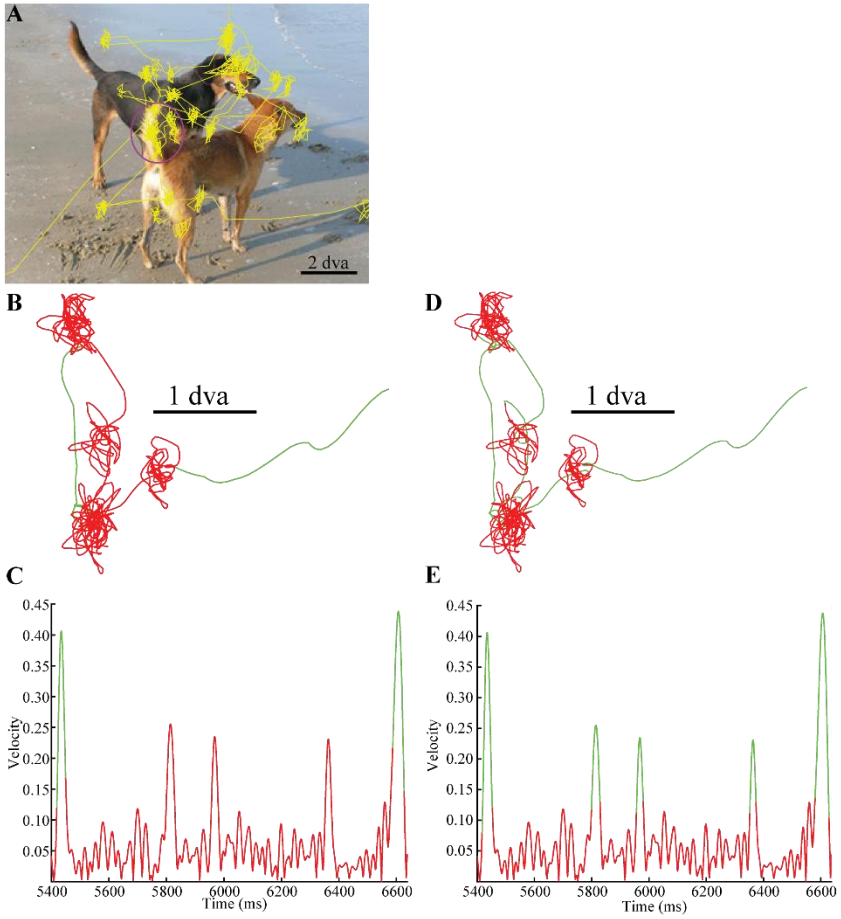

Figure 2-4 Local Re-clustering Detects Smaller Saccades Hidden by Global Variability. **A)** A representative scan path (yellow) overlaying the viewed image. **B)** In a portion of the scan path (purple circle in A), global clustering only identified a single fixation (red) surrounded by 2 larger saccades (green). **C)** The velocity profile during this portion of the scan path revealed that the fixation detected by global clustering was highly variable with several potential saccades having velocities just above this variance. **D-E)** Local re-clustering of the fixation identified 3 additional saccades, which separated the single fixation detected by global clustering into 4 distinct fixations. Local re-clustering also reclassified some of the fixation time points near the two larger saccades—initially detected by global clustering—as saccades.

Velocity and acceleration thresholds appear to often miss smaller saccades that are similar to noisy fixations. While it is problematic to compare methods for detecting fixations because every method will produce different results and no gold standard currently exists, it is possible to demonstrate the utility of this novel method by showing that arbitrary thresholds in velocity and acceleration state space cannot achieve the same sensitivity as Cluster Fix. On the same set of scan paths, we implemented a basic velocity and acceleration threshold algorithm which detected saccades above various velocity thresholds with the additional constraint that each saccade had to contain a maximum acceleration above a specific threshold. The same pre-processing of scan paths for Cluster Fix was performed prior to the implementation of each threshold algorithm. Additionally, the threshold algorithms included a local re-classification in which fixation time points juxtaposed to saccades with an acceleration greater than the acceleration threshold became reclassified as saccade time points. Finally, the threshold algorithm applied a saccade and a fixation duration threshold of 10 ms and 25 ms, respectively. As seen in **Table 2.2** the values selected for the thresholds included both arbitrary thresholds and thresholds dependent on the variability of the scan path (i.e. mean + std). Importantly, the choice of thresholds dramatically altered the computed behavioral statistics. Compared to Cluster Fix, the threshold algorithms appeared to omit smaller amplitude saccades as indicated by larger average saccade arc length and increased distances between fixations. Because threshold algorithms omitted potential small amplitude saccades, the number of detected fixations and saccades decreased.

Visual inspection of velocity profiles and the arrangement of scan paths in state space also revealed that velocity and acceleration thresholds often omitted potential smaller saccades and classified them as fixations **(Figure 2.5)**. The omission of potential smaller saccades occurred either when the velocity during a saccade did not reach the threshold or when the

Table 2-2 Computed Behavioral Statistics by Algorithm and Threshold

Algorithm	Threshold	Fixation Duration (ms)	Saccade Duration (ms)	Saccade Arc Length (dva)	Distance Between Fixations (dva)	Fixations per Image	Instantaneous Saccade Rate (Hz)
Cluster Fix	N/A	177.0 ± 97.0	52.4 ± 12.8	7.5 ± 4.6	6.0 ± 4.6	35.8 ± 7.6	4.6 ± 1.8
Velocity and Acceleration	mean + std (global*)	296.9 ± 185.7	48.5 ± 7.0	9.1 ± 4.6	8.0 ± 4.5	24.3 ± 5.4	3.4 ± 1.4
	30 °/s 8,000 °/s²	280.8 ± 179.3	54.5 ± 9.4	9.7 ± 4.7	8.0 ± 4.5	24.5 ± 6.3	3.5 ± 1.5
	75 °/s 5,000 °/s²	247.3 ± 144.5	50.7 ± 7.9	8.5 ± 4.5	7.2 ± 4.4	28.6 ± 6.3	3.8 ± 1.4
	100 °/s 8,500 °/s²	315.1 ± 201.8	46.8 ± 7.5	9.7 ± 4.7	8.5 ± 4.4	22.3 ± 6.0	3.3 ± 1.4
Dispersion	0.5 dva	137.2 ± 80.4	37.6 ± 18.3	5.9 ± 4.6	5.0 ± 4.6	44.5 ± 9.3	6.1 ± 3.8
	0.75 dva	183.5 ± 94.2	32.6 ± 13.0	6.1 ± 4.5	5.8 ± 4.5	37.9 ± 7.5	4.9 ± 2.5
	1 dva	215.7 ± 107.3	29.2 ± 10.7	6.3 ± 4.5	6.4 ± 4.5	33.9 ± 6.6	4.3 ± 1.7
	1.25 dva	242.3 ± 121.2	26.6 ± 9.2	6.4 ± 4.6	6.8 ± 4.6	31.1 ± 6.5	4.1 ± 1.5
Minimum Spanning Tree	mean + std (local†)	112.18 ± 48.2	27.1 ± 6.6	3.3 ± 3.1	3.5 ± 4.4	65.3 ± 8.2	7.6 ± 2.5
	0.5 dva	122.2 ± 70.9	52.1 ± 23.5	6.3 ± 4.9	4.7 ± 4.6	47.4 ± 8.8	6.2 ± 3.2
	0.75 dva	154.9 ± 82.7	45.0 ± 15.2	6.5 ± 4.6	5.4 ± 4.6	41.1 ± 7.8	5.2 ± 2.4
	1 dva	183.3 ± 93.0	42.3 ± 12.2	6.8 ± 4.4	6.1 ± 4.5	35.8 ± 7.0	4.5 ± 1.7
	1.25 dva	207.6 ± 106.3	39.8 ± 10.0	6.9 ± 4.4	6.3 ± 4.5	34.5 ± 6.6	4.4 ± 1.6

Values are mean ± std

*Global refers to calculating threshold based on the entire scan path.

†Local refers to calculating the threshold for the window being analyzed. The window was 100 ms long. A larger window size (e.g. 200 ms) will produce results similar to a threshold of 0.75 dva.

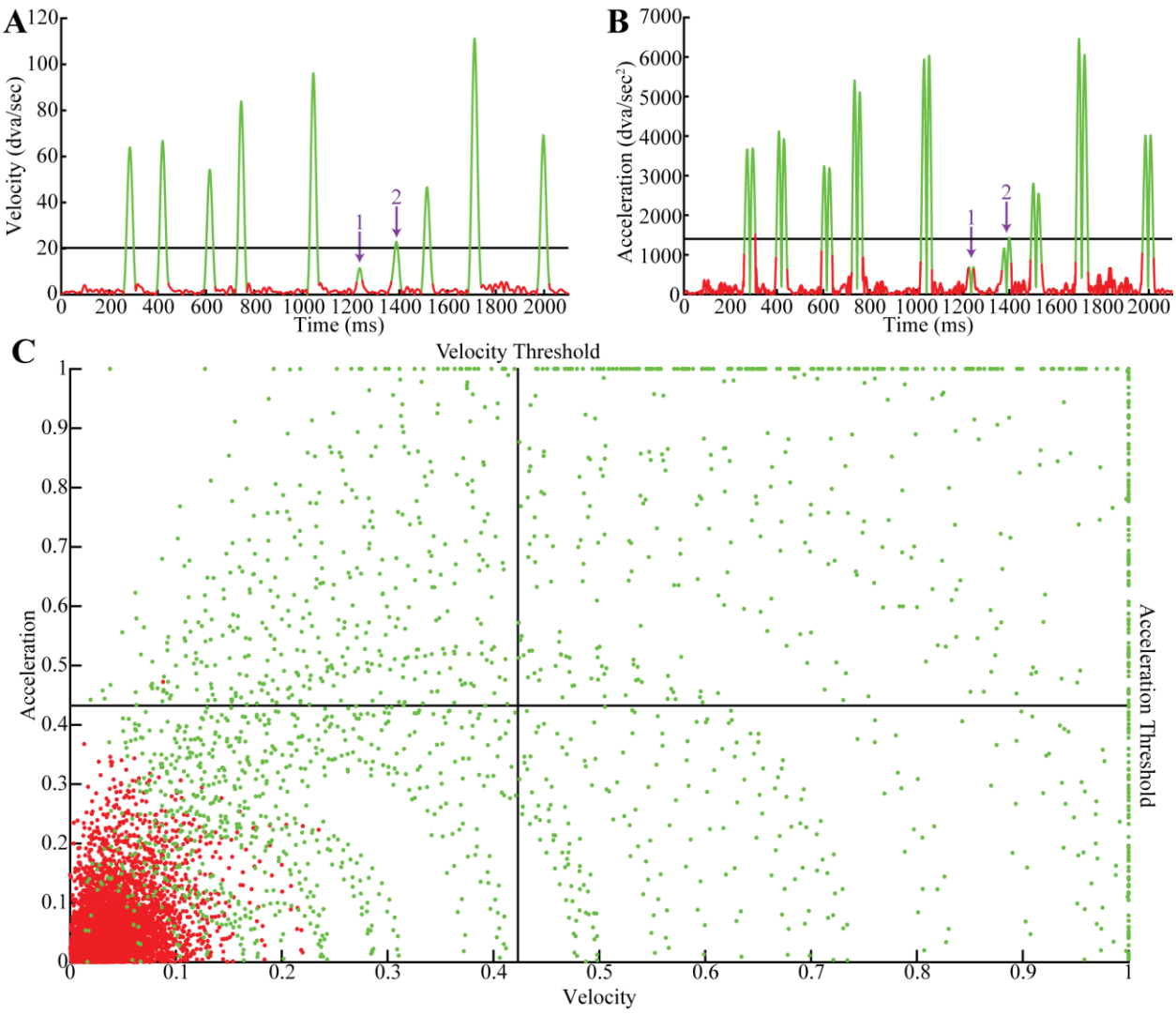

Figure 2-5 Thresholds vs. Cluster Fix

Fixations (red) and saccades (green) determined through Cluster Fix for an example segment of a scan path. Velocity (**A**) and acceleration (**B**) thresholds (black lines, mean + std) appear to miss smaller amplitude saccades either due to velocity or acceleration values not exceeding the threshold (purple ↓ #1) or values did not exceeded the threshold for a sufficient duration (purple ↓ #2) . **C)** A 2D state space plot indicates that single-value thresholds may misclassify fixation and saccade time points which may be critical to properly identify the onset and offset of saccades. Note that because velocity and acceleration values were normalized to the mean plus 3 times the standard deviation many saccade time points are located on the edge of the plot. Also, note that up-sampling and low pass filtering creates an appearance of arc-like patterns in state space.

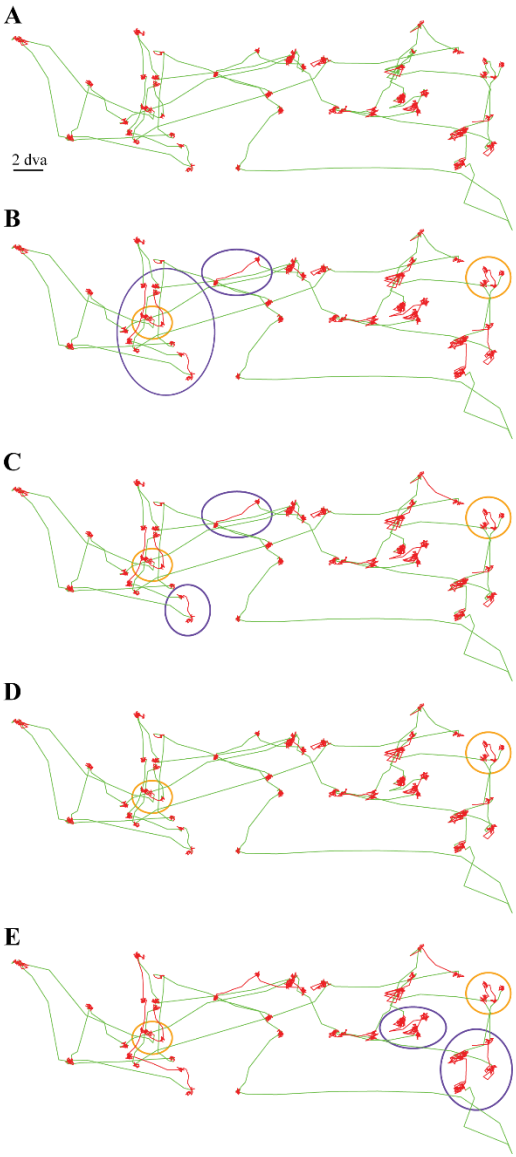

Figure 2-6 Visual Comparison of Detected Fixations and Saccades by Algorithm Compared to Cluster Fix (**A**), velocity and acceleration threshold algorithms (**B-E**) appeared unable to detect smaller saccades (red: fixations, green: saccades). The velocity and acceleration algorithms are as follows: B) mean + standard deviation, C) 30º/s & 8000º/s^2, D) 75º/s & 5000º/s^2, and E) 100º/s & 8500º/s^2. Purple circles highlight some of the key discrepancies between Cluster Fix and the threshold-based algorithms, and orange circles indicate potential saccades commonly missed across multiple threshold-based algorithms.

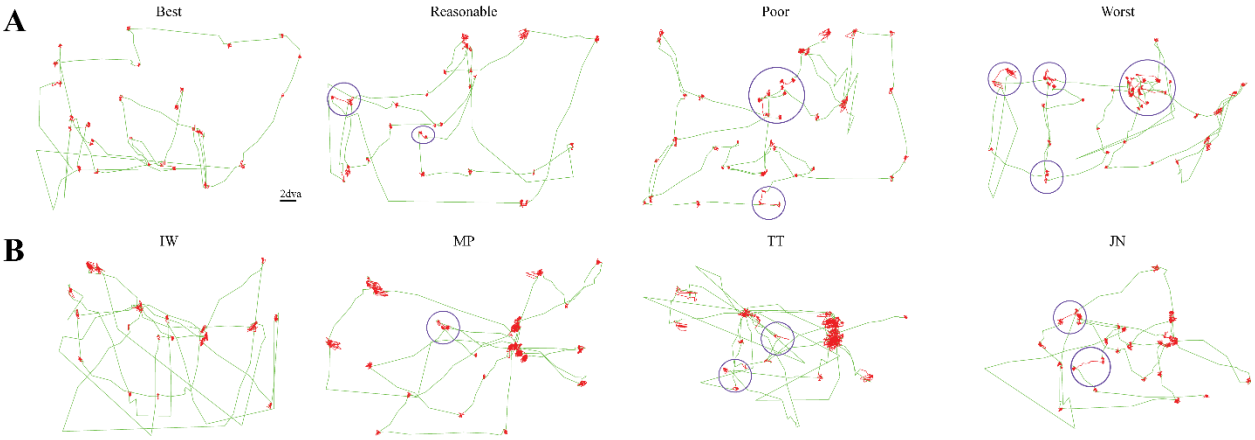

Figure 2-7 Accuracy of Threshold-based Algorithms across Monkeys and Scan Paths. Cluster Fix adapts to individual scan paths, but single-valued thresholds do not. Comparison of scan paths from the same monkey MP **(A)** and across monkeys who viewed the same image **(B)** show that while certain thresholds appear to work better for some monkeys and scan paths, these thresholds may not work well for other scan paths or subjects. All scan paths shown here were analyzed using a velocity threshold of 75º/s and an acceleration threshold of 5000º/s^2. Purple circles indicate where saccades (green) were clearly mislabeled as fixations (red). Most of the misclassification errors occurred during small saccades. Thresholds typically did not misclassify fixations as saccades. Accuracy of scan path analysis is arranged from best to worst, left to right.

saccade's velocity did not exceed the threshold for a sufficient duration. Further, thresholds appeared to be insufficient for precisely identifying the onset and offset of saccades. This is particularly evident when visualized in 2D state space (**Figure 2.5C**). There exist an infinite number of combinations of thresholds, but no combination of these types of thresholds could identify saccades and fixations that overlap in state space. From the 2D state space plot, we observed that an optimal velocity and acceleration threshold would be a nonlinear function of both velocity and acceleration instead of singular threshold values.

A key advantage of Cluster Fix was that the algorithm impartially identified saccade start and end times based on the 4 state space parameters. Similar to the threshold algorithm that we implemented, additional computation could be added to threshold-based algorithms, such as determining when the saccade reaches a minimum velocity or acceleration. However, this may require additional arbitrary thresholds.

Visual inspection of the scan paths supported the same conclusions as above in which it appeared that Cluster Fix correctly identified saccades of various amplitudes not identified by the threshold-based algorithms (**Figure 2.6**). Various thresholds omitted different probable saccades (purple circles), and several of the probable smaller saccades were consistently omitted across different thresholds (orange circles); however, none of the algorithms appeared to misclassify fixations. Visual inspection across multiple scan paths from the same monkey and scan paths from different monkeys indicated that while some thresholds may appear to be sufficient for one scan path, that same threshold may not be sufficient for another scan path or subject (**Figure 2.7**).

In addition to the velocity and acceleration threshold-based algorithms, we implemented two common dispersion-based algorithms: a simple dispersion threshold algorithm and a

minimum spanning tree algorithm (MATLAB code from (Komogortsev et al., 2010; Komogortsev and Karpov, 2013)). In the dispersion threshold algorithm, we used a window of 25 ms comparable to the minimum expected fixation duration. In the minimum spanning tree algorithm, we used a 100 ms window comparable to the longest expected saccade duration. Unlike the dispersion threshold algorithm, the minimum spanning tree algorithm required fixation (25 ms) and saccade duration (10 ms) thresholds to accurately analyze scan paths. Similar to the velocity and acceleration threshold algorithms, the threshold values drastically altered computed behavioral statistics (**Table 2.2)** and the accuracy of these algorithms (**Figure 2.8).** In general, dispersion-based algorithms had difficulty detecting the onset and offset of saccades. As indicated by the behavioral statistics in **Table 2.2**, the dispersion-based algorithms also detected a larger number of fixations and saccades. Visual inspection of the scan paths revealed that the lower dispersion threshold values caused the algorithms to detect noisy portions of fixations as saccades inappropriately dividing fixations into multiple "fixations" with shorter durations.

The *k*-means clustering algorithm employed by Cluster Fix is an optimization algorithm attempting to find a global minimum in the distances between points in a cluster and the clusters' centroids. The *k*-means algorithm initiates randomly and then iteratively computes clusters. Replications of this iterative process are used to increase the chance of finding the best clusters. Because this process is random and an optimal solution is not guaranteed to be found, the results produced by Cluster Fix may have some inconsistencies across multiple applications to the same scan path. We have developed a bootstrapping method to determine the consistency of the results produced by Cluster Fix (**Figure 2.9**). We found that Cluster Fix consistently detects saccades with amplitudes greater than 1.5 dva. However, saccades with smaller amplitudes were less

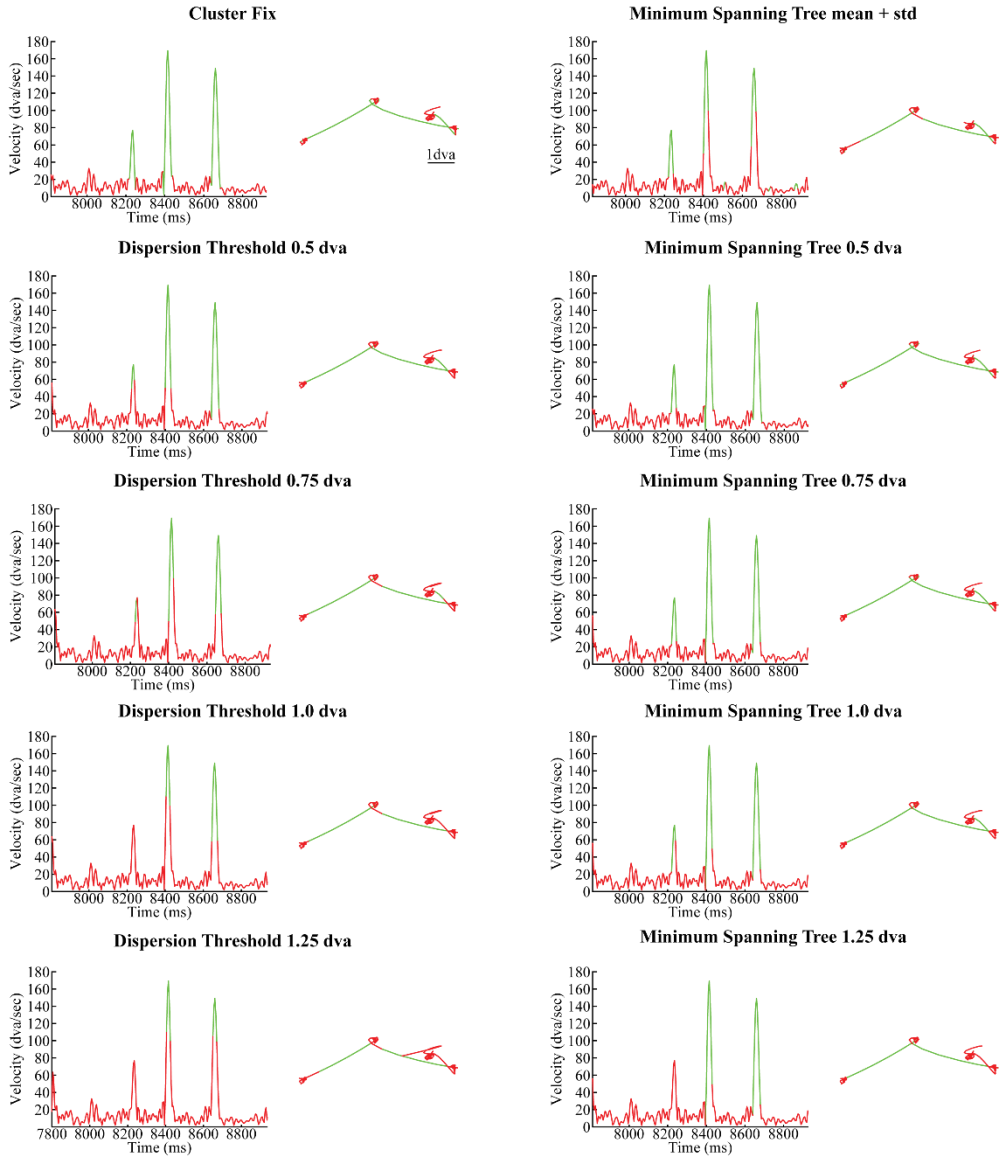

Figure 2-8 Accuracy of Dispersion-based Algorithms

Dispersion-based algorithms appeared to accurately detect the presence of fixations (red) but these algorithms had difficulty detecting the onset and offset of saccades (green). Varying the threshold drastically changed the detection of the offset and onset of saccades. Because some thresholds missed probable smaller saccades or inaccurately determined the transition time between fixations and saccades, different amounts of time are plotted for each algorithm.

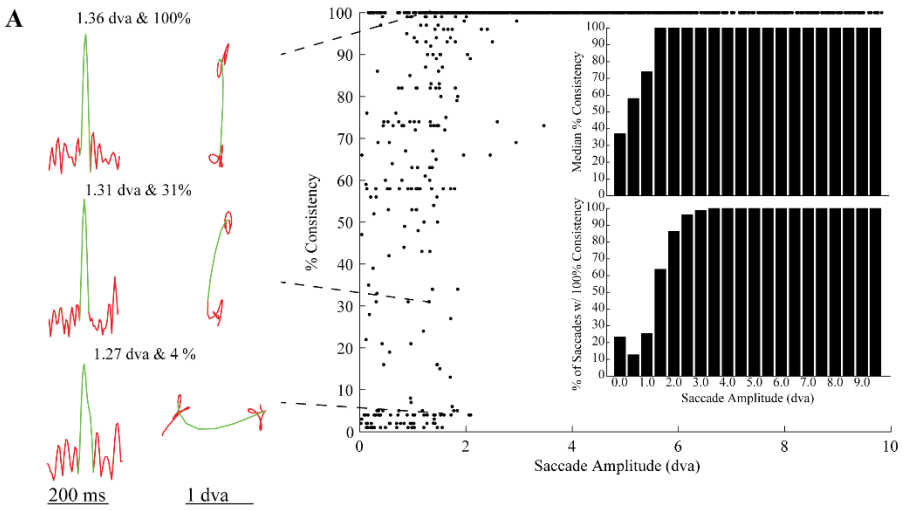

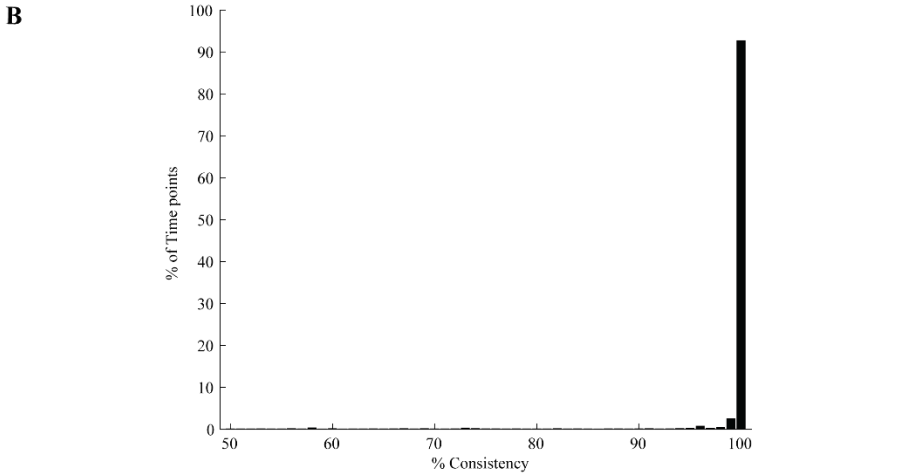

Algorithm	Number of Scan Paths	Run time / scan path	% of time points ≥ 90% consistency	% of time points ≥ 95% consistency	% of time points ≥ 99% consistency	% of time points 100% consistency
k-means 5 replicates	36	3.33 seconds	97.03	96.57	95.11	92.66
k-means 10 replicates	36	5.85 seconds	97.29	97.07	96.12	95.63
k-means 25 replicates	36	12.66 seconds	98.26	97.90	97.24	97.02

Figure 2-9 Consistency of Cluster Fix Results

Cluster Fix relies on a *k*-means clustering algorithm to determine the natural divisions in scan path state space. The initialization or seeding process in the *k*-means clustering algorithm is stochastic and thus the results from Cluster Fix may be inconsistent across multiple applications to the same scan path. Therefore, we developed a bootstrapping method by applying Cluster Fix to a scan path (n = 36) 100 times to determine the consistency of the results produced by Cluster Fix. **A)** Here, we define "% consistency" as the percent of applications in which Cluster Fix detected those time points as a saccade. Cluster Fix detected saccades with greater than 4 dva in amplitude with a perfect 100% consistency, but saccades with amplitudes less than 4 dva were detected at various consistencies. The consistency of detection appeared to be related to the local variability in the scan path (low pass filtered scan paths and normalized velocity traces; saccades in green with 200 ms of surrounding fixations in red). To better quantify these results, we grouped saccades into 0.5 dva bins and then examined the median percent consistency and the percent of saccades detected with a 100% consistency (inset). Saccades of 1.5 dva and greater were detected with a median consistency of 100%. **B)** Next, we examined the consistency of all time points. Here "% consistency" is defined as the percent of applications in which a time point was classified as a saccade or a fixation; a time point detected as a fixation during 50% of the applications and a saccade during the other 50% of the applications has a consistency of 50%. The vast majority of time points were classified as a fixation or a saccade with a 100% consistency. The table shows the percentage of time points classified with consistencies greater than or equal to 90%. Additionally, we found as we increased the number of replications in the k-means clustering algorithm the percent of times points classified with a 100% consistency increased but at a cost of computational time.

consistently detected, and the consistency of their detection appeared to be related to the noisiness of the surrounding scan path. Smaller saccades may be detected more consistently with a higher acquisition frequency. Further, approximately 92% of all time points were always classified as a fixation or a saccade across multiple applications, and 97% of time points were consistently classified as a fixation or a saccade across at least 90% of applications.

Lastly, we calculated average parameter values across multiple images for individual monkeys. Although the average parameter values changed substantially for saccades, these values changed less for fixations (**Figure 2.10**), which could be useful for real-time fixation detection. The average parameter values for fixations and saccades occupied completely separate regions of state space. In fact, a support vector machine classified which regions of state space belonged to fixations versus saccades with greater than 99% accuracy for each monkey individually (n = 4) trained on as little as 5% of the data.

2.5 DISCUSSION

Here, we have described a novel algorithm using cluster analysis to detect periods of fixations and saccades to improve the analysis of highly variable scan paths. Both global and local cluster analysis were necessary to detect small saccades that were often indistinguishable from noisy fixations or hidden by the large variability in saccade amplitudes. Global clustering offers an initial pass on classifying scan paths into fixations and saccades while local re-clustering refines these results, allowing for the detection of smaller saccades and a determination of the transition times between fixations and saccades. Cluster Fix removed the need for determining thresholds and removed the need for any assumptions regarding the arrangement of parameters in state space. The algorithm assumed that individual clusters are of Gaussian distributions since *k*-means was used, but we did not make any assumptions about the

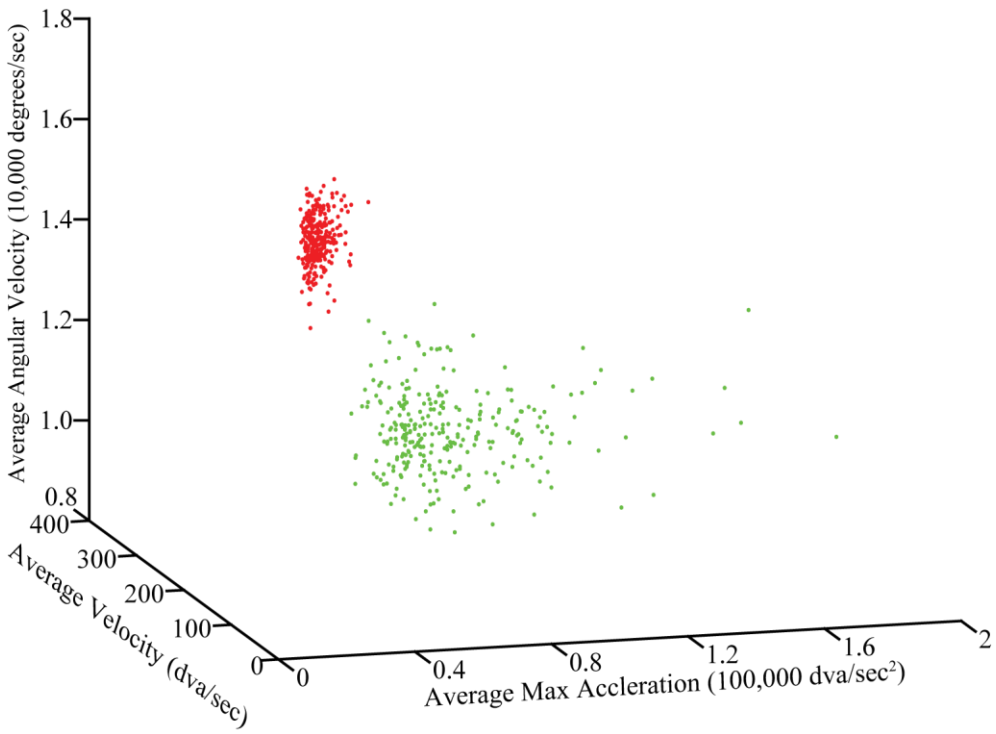

Figure 2-10 Single Subject Cluster Means were Consistent across Scan Paths
The average velocity, peak acceleration, and angular velocity during fixations (red) across multiple scan paths from a monkey viewing 288 different images remained consistent, but values for these parameters during saccades (green) were more variable. Each dot represents the average value for all fixations or saccades from one scan path.

arrangement or size of these clusters in state space. Moreover, clusters changed with the amount of noise and variability found in the scan path allowing the algorithm to adapt to individual scan paths. One caveat is that Cluster Fix still requires fixation and saccade duration thresholds as free parameters. In theory, additional classifiers could distinguish between fixations and saccades without the need for duration thresholds.

We are confident that Cluster Fix can correctly identify smaller saccades because these smaller saccades were identified by finding natural divisions in scan paths, and these smaller saccades occupied different regions of state space than fixations. Visual inspection of the scan paths supports this conclusion as well. Identification of smaller saccades was more difficult when the smaller saccades were surrounded by highly variable fixations in comparison to smaller saccades surrounded by less noisy fixations. Further, identification of these smaller saccades often served to break up longer "fixations," detected by global clustering, into more appropriate length fixations.

A common practice in the analysis of human eye movement data is to operationally define saccades that are smaller than 1 dva in amplitude as microsaccades (Engbert and Kliegl, 2003; Otero-Millan et al., 2008; Martinez-Conde et al., 2013). Here we did not distinguish between microsaccades and saccades albeit approximately 4% of the observed saccades had amplitudes of less than 1 dva (not equivalent to saccade arc length in Table 2). We observed that a large portion of these saccades were detected during "complex fixations" in which the eye covered a substantially larger area of the image for longer durations than most fixations. Often these "complex fixations" were observed when monkeys looked at complex objects such as faces and may have included rapid eye movements not clearly distinguishable at a sampling rate of 200 Hz. Therefore, we do not know if Cluster Fix is sufficient for detecting microsaccades or

other fixational eye movements often observed at higher sampling frequencies (Martinez-Conde et al., 2009).

Future work could improve Cluster Fix by adding parameters or adaptations to detect eye movements that are neither fixations nor saccades such as smooth pursuit. The largest challenge in detecting smooth pursuit would be determining the best way to consolidate clusters. With Cluster Fix each cluster represents tangible aspects of the scan path. Typically, in our binary classification, we find a saccade cluster with high velocity and low acceleration, and this cluster often represents periods of consecutive time points in the scan path. With the right selection of clusters and duration thresholds, we see no reason why one could not identify periods of smooth pursuit with Cluster Fix.

For a given subject, parameter values across multiple images were consistent for fixations, and fixation clusters did not overlap in state space with saccade clusters. This consistency suggests the plausibility of analyzing viewing behavior across multiple images using a single scan path as a template. During a practice trial, fixation and saccade clusters could quickly be determined as well as which areas of state space belong to each cluster using a classification algorithm such as a support vector machine. For subsequent experimental trials, for each time point, the position in state space could be classified as a fixation or saccade. With the addition of a duration threshold, these classifications could be used to determine when fixations and saccades occur in near real-time. Real-time detection of eye movements is essential for gaze-contingent experiments in which trial parameters depend on the subject's viewing behavior. Other applications of Cluster Fix could include using the algorithm to determine proper velocity and acceleration thresholds for novel or complex tasks instead of trying to determine these thresholds empirically.

Determining the number of parameters to use is an important aspect of parameter selection. We found that the removal of distance from Cluster Fix drastically decreased the specificity and sensitivity of the algorithm for small saccades and made the algorithm more susceptible to noise. Likewise, the removal of angular velocity from the algorithm produced similar results despite mostly distinguishing between periods of fixation with high angular velocity and periods of fixation with low angular velocity. We postulate that the addition of these parameters may help classify time points properly when the other parameters cannot. Alternatively, these additional parameters may help determine the appropriate number and size of clusters in state space. There is no constraint on the number of parameters used in Cluster Fix though a minimum of 2 parameters, namely velocity and acceleration, would be highly recommended.

When choosing state space parameters, we took what we qualitatively observed as differences between fixations and saccades and turned these into quantifiable parameters. Distance was selected because, during a fixation, data points are compact and close to each other while data points are more dispersed during a saccade. Density-dispersion algorithms explicitly take advantage of this parameter. Velocity and acceleration parameters were chosen because the eye moves faster during a saccade than during a fixation. The angular velocity parameter accounts for the smooth linear-like movements of saccades while fixations appear irregular (at 200 Hz) with position fluctuating around an attended location.

A great deal of effort has been expended on determining or developing methods for determining the proper thresholds for threshold-based algorithms. Even if one threshold is found to be optimal for a scan path for one subject in one experiment, that threshold is not guaranteed to be appropriate for another subject, experiment, or even the same subject on another trial. Our

data support the idea that thresholds are suboptimal for detecting fixations and saccades. Velocity and acceleration thresholds are relatively fast and easy to implement but suffer from detection errors. Dispersion-based algorithms can be implemented relatively quickly in real-time and appear to detect the presence of fixations with relatively high accuracy. However, dispersion-based algorithms fail to accurately measure the transition times between fixations and saccades which are extremely important in understanding potential neural correlates of eye movements.

A primary goal of this work was to create an algorithm that would be easy to implement across laboratories for a variety of behavioral tasks. For this reason, the algorithm was devised in MATLAB using commonly available functions. However, this algorithm may be enhanced through the use of better clustering algorithms as well as alternative ways of determining the appropriate number of clusters such as statistical measures (e.g. explanation of variance), visual inspection, the separation of clusters, and stability of clusters with resampling (Ben-Hur et al., 2002; Dudoit and Fridlyand, 2002; Pham et al., 2005). Cluster Fix requires approximately 240 seconds to analyze 720 seconds of eye data sampled at 200 Hz (MATLAB 2012b, Intel Core Xeon Processor 2.80 GHz with 16 GB RAM). This is significantly slower than an algorithm using velocity and acceleration thresholds which requires only a few seconds to analyze the same amount of data. The two dispersion-based algorithms analyzed scan paths substantially slower than Cluster Fix, but optimization of these algorithms could substantially increase the speed of analysis. In Cluster Fix nearly 80% of the computation time is devoted to determining the number of clusters of which nearly 90% is devoted to local re-clustering. Cluster Fix sacrifices time for a significant increase in sensitivity and specificity. Cluster Fix may run faster by

parallelizing local re-clustering or compiling Cluster Fix in a different programing language optimized for cluster analysis.

One limitation of the *k*-means clustering algorithm is that the clusters are determined by the distance between the points in the clusters and the clusters' centroids. *K*-means initiates with random points and iteratively computes clusters until the distance between points in the clusters to the centroid of the clusters converges. The convergence most often occurs at a local minimum. To increase the probability that a better minimum is found, *k*-means can be replicated several times. We used 5 replicates for determining the appropriate number of clusters and for performing *k*-means to cluster all the time points. Occasionally, only poor local minima are found or convergence does not occur in a reasonable number of computations thus producing less than optimal clustering. This produces some variability in the results and affects the detection of smaller saccades since these are less distinguishable from noise. For this reason, each time Cluster Fix is applied to the same scan path the results may vary slightly. If one wanted to be absolutely certain that they detected all of the smaller amplitude saccades, Cluster Fix results could be averaged over several applications. Additionally, more replications could be performed to increase the consistency of the results but at the cost of computational time. Other clustering algorithms may solve some of the limitations of k-means clustering, but previous attempts to use hierarchical clustering were unsuccessful.

2.6 CONCLUSION

A primary advantage of Cluster Fix is the ability to properly detect the onset and offset of saccades. Several neural mechanisms are aligned in time to saccades including saccadic suppression in the LGN (Ross et al., 2001), modulation in firing rates of neurons outside of the early visual areas (Krekelberg et al., 2003; Crapse and Sommer, 2012), and phase reset of theta-

oscillations (Rajkai et al., 2008; Jutras and Buffalo, 2010a; Hoffman et al., 2013b; Jutras and Buffalo, 2013; Jutras et al., 2013b). More accurate scan path analysis may help improve the detection of these neural phenomena as well as reduce variability in data possibly attributable to improper saccade detection. Finally, the general concepts behind Cluster Fix could be extended to the tracking of animal positions, complex dynamical systems, and the motion of body parts.

2.7 ACKNOWLEDGMENTS

The authors would like to thank Michael Jutras and Nathan Killian for the basic MATLAB code used to analyze eye tracking data; Esther Tonea and William Li for the creation of image sets; and Megan Jutras for helping with collecting, organizing, and analyzing the behavioral data. We would also like to thank Niklas Wilming for his helpful comments on the manuscript. Funding for this work was provided by the National Institute of Mental Health Grants MH080007 (to E.A.B.) and MH093807 (to E.A.B.); National Center for Research Resources Grant P51RR165 (currently the Office of Research Infrastructure Programs/OD P51OD11132); and the National Institute of Health 5T90DA032466-02 and 5T90DA032436-03 (S.D.K).

Chapter 3. MODELING FREE VIEWING BEHAVIOR IN MONKEYS[2]

Abbreviations
AUROC: Area Under the Receiver Operating Characteristic Curve
BCRW: Biased Correlated Random Walk
CRW: Correlated Random Walk
dva: degrees of visual angle
KL divergence: Kullback–Leibler divergence
ks-test: Kolmogorov-Smirnov test
IOR: Inhibition of Return
PDF: Probability Distribution Function

3.1 ABSTRACT

There is a growing interest in studying biological systems in natural settings, in which experimental stimuli are less artificial and behavior is less controlled. In primate vision research, free viewing of complex images has elucidated novel neural responses, and free viewing in humans has helped discover attentional and behavioral impairments in patients with neurological disorders. In order to fully interpret data collected from free viewing of complex scenes, it is critical to better understand what aspects of the stimuli guide viewing behavior. To this end, we have developed a novel viewing behavior model called a Biased Correlated Random Walk (BCRW) to describe free viewing behavior during the exploration of complex scenes in monkeys. The BCRW can predict fixation locations better than bottom-up salience. Additionally, we show that the BCRW can be used to test hypotheses regarding specific attentional mechanisms. For example, we used the BCRW to examine the source of the central bias in fixation locations. Our analyses suggest that the central bias may be caused by a natural tendency to reorient the eyes towards the center of the stimulus, rather than a photographer's bias to center

[2] Adapted from König, Seth D., and Elizabeth A. Buffalo. "Modeling Visual Exploration in Rhesus Macaques with Bottom-Up Salience and Oculomotor Statistics." Frontiers in integrative neuroscience 10 (2016).

salient items in a scene. Taken together these data suggest that the BCRW can be used to further our understanding of viewing behavior and attention, and could be useful in optimizing stimulus and task design.

3.2 INTRODUCTION

Recently, there has been a growing interest in studying biological systems in natural settings, in which experimental stimuli are less artificial and behavior is less controlled (Felsen and Dan, 2005; Hayhoe and Ballard, 2005a; Meister and Buffalo, 2015). Behavioral paradigms using free viewing in primates have uncovered novel signals in the hippocampal formation related to recognition memory, spatial representations, visual exploration, and saccadic eye movements (Killian et al., 2012; Hoffman et al., 2013a; Jutras et al., 2013a). Additionally, several recent studies in humans have illustrated the utility of complex scenes and movies in studying changes in attention and behavior in patients with neurological disorders (Smith et al., 2006b; Crutcher et al., 2009; Mannan et al., 2009; Tseng et al., 2013b; Zola et al., 2013; Wang et al., 2015a). In order to fully interpret these data, it is critical to better understand what aspects of the stimuli guide viewing behavior. To this end, we have developed a novel foraging model to describe free viewing behavior during the exploration of complex scenes in monkeys. This model allows us to predict where the monkeys will fixate.

A variety of viewing behavior models exist which can be broadly classified as "top-down" or "bottom-up" (see (Kimura et al., 2013; Bylinskii et al., 2015) for recent reviews on human models of attention). Top-down models predominately focus on search-based tasks in which participants attempt to find a target among distractors in a complex environment (Wolfe, 1994). Conversely, bottom-up models predominately utilize salience in pop-out search tasks and in free viewing of complex scenes (Itti et al., 1998; Parkhurst et al., 2002; Bruce and Tsotsos,

2005; Elazary and Itti, 2008; Judd et al., 2011; Wilming et al., 2011; Zhao and Koch, 2011). The success of individual models appears to depend on various experimental factors including task demands and the types of stimuli used (Turano et al., 2003; Henderson et al., 2007; Shic and Scassellati, 2007). It is becoming increasingly popular to incorporate aspects of both bottom-up and top-down mechanisms to create hybrid models that can predict behavior better than either mechanism separately (Lee et al., 2005; Walther and Koch, 2006; Zhang et al., 2008; Kollmorgen et al., 2010; Nordfang et al., 2013). While the majority of these models were designed to predict human behavior, several studies have shown that these models sufficiently predict behavior in non-human primates as well (Einhauser et al., 2006; Berg et al., 2009).

Most attention models are deterministic and often employ a winner-take-all algorithm to interpret attention maps. However, viewing behavior is inherently stochastic and can vary within and across observers. Several stochastic models of viewing behavior have been proposed, including a few which model realistic eye movements (Verghese, 2001; Boccignone and Ferraro, 2004; Harel et al., 2006; Rutishauser and Koch, 2007; Barthelmé et al., 2012; Boccignone and Ferraro, 2013; Zehetleitner et al., 2013). While these models address the variability found in natural behavior, it is difficult to directly apply some of these models to the free viewing of complex scenes. Further, some of these models do not include realistic models of eye movement statistics making it difficult to test hypotheses regarding changes in attention and viewing behavior.

To address these limitations, we propose a novel model of viewing behavior for complex scenes called a Biased Correlated Random Walk (BCRW). We build the BCRW model under the hypothesis that the constraints of the oculomotor system interact with the arrangement of the salient regions of the image to guide behavior. To this end, we use a simple random walk process

to construct a foraging model of viewing behavior in which observers forage for salience as a simple surrogate of visual information. The BCRW is essentially a model of eye movements and provides a method for interpreting salience maps or other forms of attention maps.

To demonstrate the utility of the BCRW, we show that the BCRW can help adjudicate between competing hypotheses regarding the central bias in fixation locations commonly observed during the viewing of complex scenes. A large number of studies have observed a central bias in fixation locations with humans typically producing a stronger central bias than monkeys (Parkhurst et al., 2002; Berg et al., 2009; Wilming et al., 2011; Wang et al., 2015a). The central bias has been hypothesized to be driven by a variety of factors including a photographer's bias (the tendency of photographers to center objects of interest in a picture), the use of a central fixation target to initiate trials, the centering of stimuli relative to subjects, a natural tendency for subjects to re-center the eyes, and the fact that subjects typically make small amplitude saccades resulting in the location of gaze remaining near the center of the image (Tatler, 2007; Tseng et al., 2009; Bindemann, 2010).

Here, we hypothesized that the central bias in fixation locations is caused by the interaction between the arrangement of salient regions in complex scenes (i.e. photographer's bias) and the statistics of the oculomotor system. We offer empirical and modeling evidence using the BCRW which suggest that the photographer's bias and statistics of the oculomotor system are not sufficient to explain the central bias.

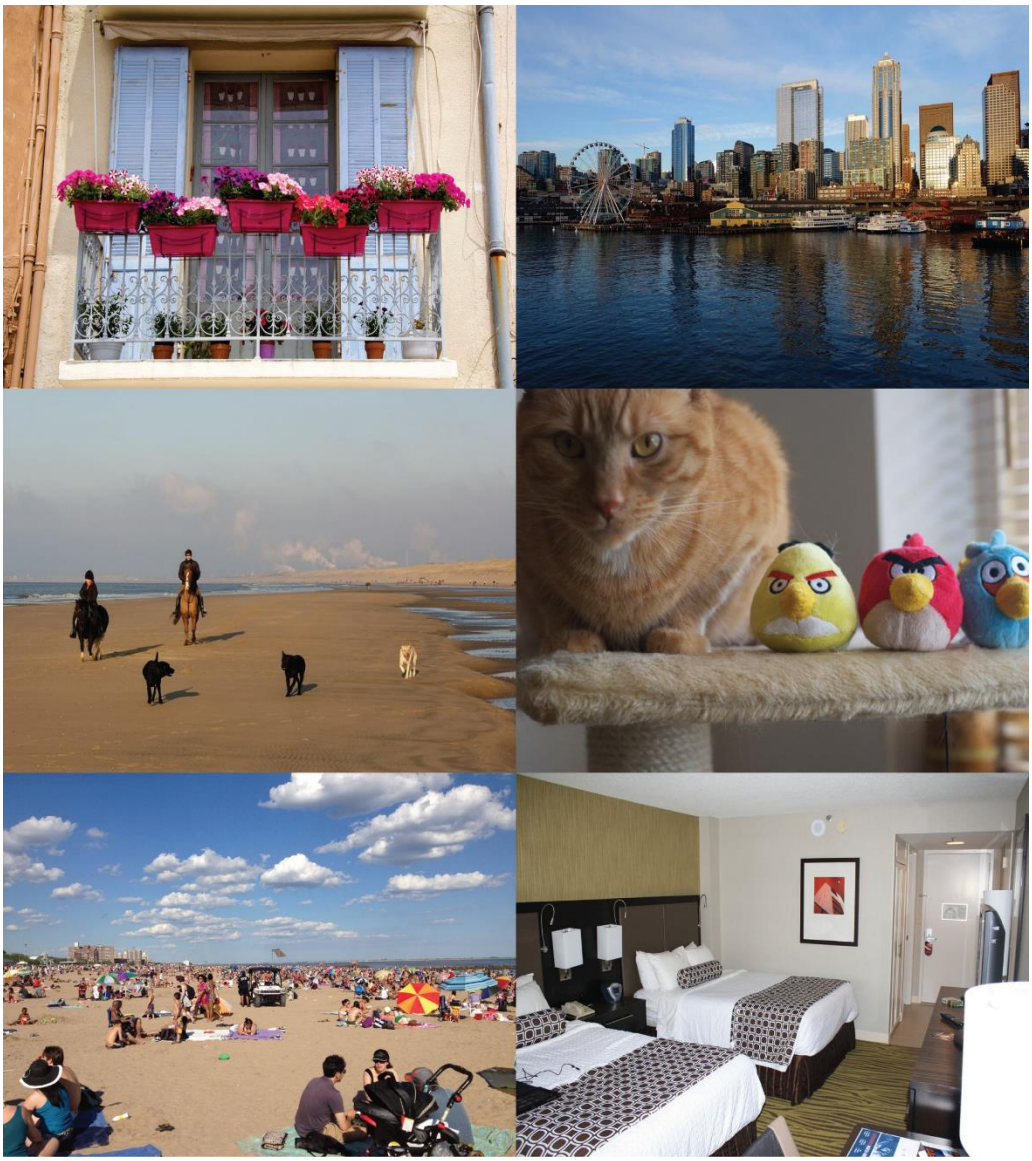

Figure 3-1 Example Images

These images range in complexity and may include images of humans, non-human primates, animals, urban scenes, outdoor scenes, or indoor scenes from a variety of vantage points. All images were taken from Flickr. Images were captured by (from top to bottom and left to right): Amanda, Sean Munson, Marcel Oosterwijk, Melinda Seckington, Luna Park NYC, Richard Franklin. These images are reproduced under creative commons licenses.

3.3 METHODS

3.3.1 *Behavioral Task and Eye Tracking*

Scan paths were obtained at 200 Hz using an infrared eye tracker (ISCAN) from 4 male rhesus macaques who freely viewed complex images. Monkeys were head-fixed in a dimly illuminated room and positioned 60 cm away from a 19 in. CRT monitor with a refresh rate of 120 Hz. Monkeys were presented a total of 8 image sets with each image set containing 36 novel images. Images were 600 by 800 pixels large and subtended 25 by 33 degrees of visual angle (dva). Images were taken from Flickr. These images ranged in complexity and included animals, humans, architecture, outdoor scenes, indoor scenes, and manmade objects (**Figure 3.1)**.

Each trial began with the presentation of a 0.5 dva cross in the center of the screen. The monkey was required to fixate the cross, within a fixation window with a width of 4 dva, for 1 second. Immediately following a successful fixation, an image was displayed and the monkey was allowed to freely view the image for 10 seconds of cumulative looking time. We analyzed the first 10 seconds of viewing behavior, regardless of the length of the image presentation. Because viewing behavior data were collected for a separate experiment, a second image presentation followed the novel image presentation. Data for these trials were not analyzed as part of the current study; only novel image trials were used for analysis. Pairs of image presentations were interleaved with calibration trials.

Initial calibration of the infrared eye tracking system consisted of a 9-point manual calibration task (Jutras et al., 2013a). Post-hoc calibration was achieved by presenting additional calibration trials between image viewing trials. Monkeys were rewarded for successful calibration trials but were not rewarded during the image viewing periods. We excluded from further analysis any eye tracking data more than 25 pixels (1 dva) outside of the image. To

account for small calibration errors at the edge of images, any fixations occurring within 25 pixels of the image were moved to the closest point on the image.

A k-means cluster analysis based algorithm, called Cluster Fix, detected fixations and saccades from scan paths in state space (König and Buffalo, 2014). Briefly, Cluster Fix determined the distance, velocity, acceleration, and angular velocity of the scan path. Cluster Fix found natural divisions in these 4 parameters using k-means clustering to separate time points into fixations and saccades and required minimum fixation and saccade durations of 25 ms and 10 ms, respectively.

All experiments were carried out in accordance with the National Institutes of Health guidelines and were approved by the Emory University Institutional Animal Care and Use Committee and by the University of Washington Institutional Animal Care and Use Committee.

3.3.2 *Viewing Behavior Statistics and Time Warping*

The eye tracking data contained approximately 40,000 fixations and saccades. We simulated the BCRW separately for each monkey using individual parameters for fixation durations, saccade durations, angles of saccades leaving fixations, the eye velocity over time, and relative weight of the salience bias (**Figure 3.2**). The average fixation duration and saccade duration across all monkeys was 215 ms and 56 ms, respectively; fixations occupied 79% of the scan path. Several eye movement statistics varied systematically by ordinal fixation or saccade number, but these phenomena were not incorporated into the BCRW.

Viewing behavior statistics were calculated directly from the raw scan paths. Cluster Fix detected the start and end of fixations and saccades. To combine fixations and saccades of different durations, we used a process called time warping (Sober et al., 2008). In particular fixation durations were not normally distributed and varied over a large range. To calculate

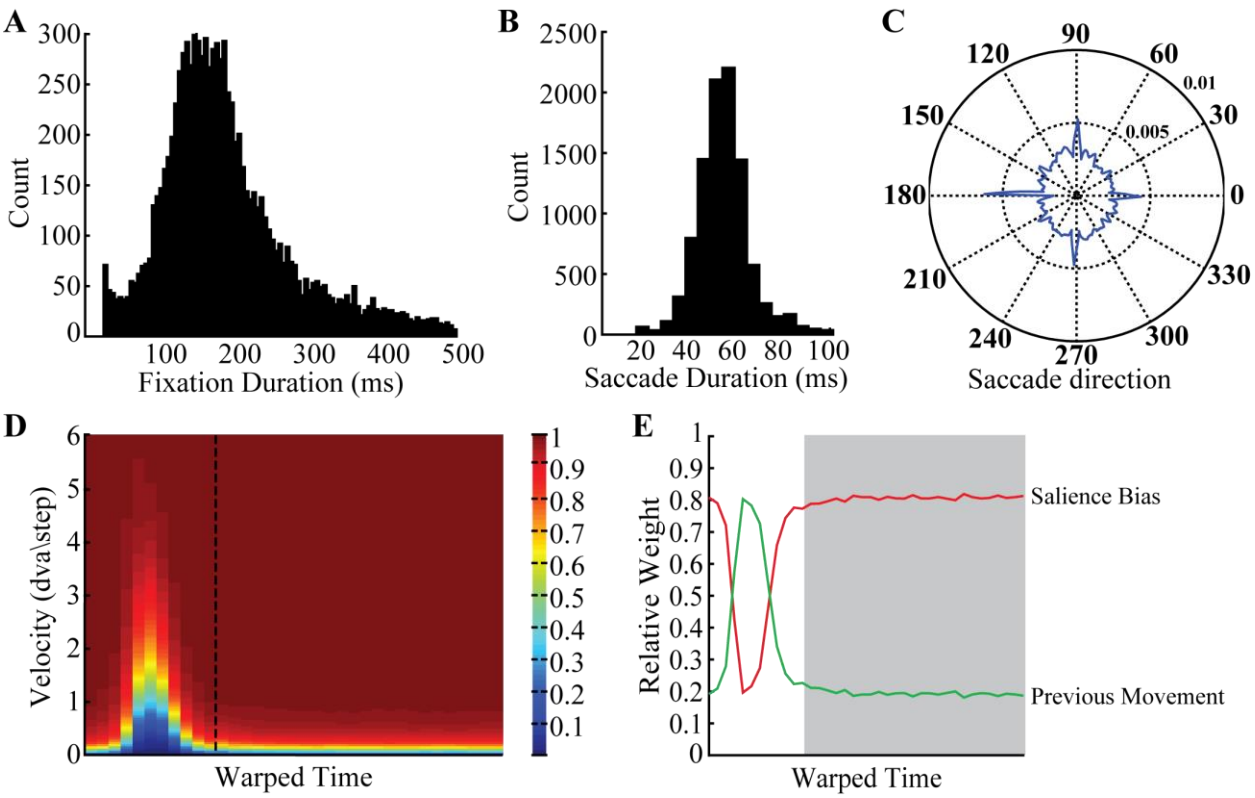

Figure 3-2 Observed Behavioral Statistics

Viewing behavior statistics incorporated into the BCRW included (**A**) fixation durations, (**B**) saccade durations, (**C**) the saccade angle leaving a fixation, (**D**) the eye movement velocity over time (dashed line is transition time from saccade to fixation), and (**E**) the relative weight of the salience bias and direction of previous movement (white background: saccade period, gray background: fixation period). The color axis for Figure 2D is cumulative probability. Examples shown here are from monkey MP, but these statistics were similar across monkeys. Histograms are plotted over a limited range to illustrate the distribution; raw data were incorporated directly into the BCRW.

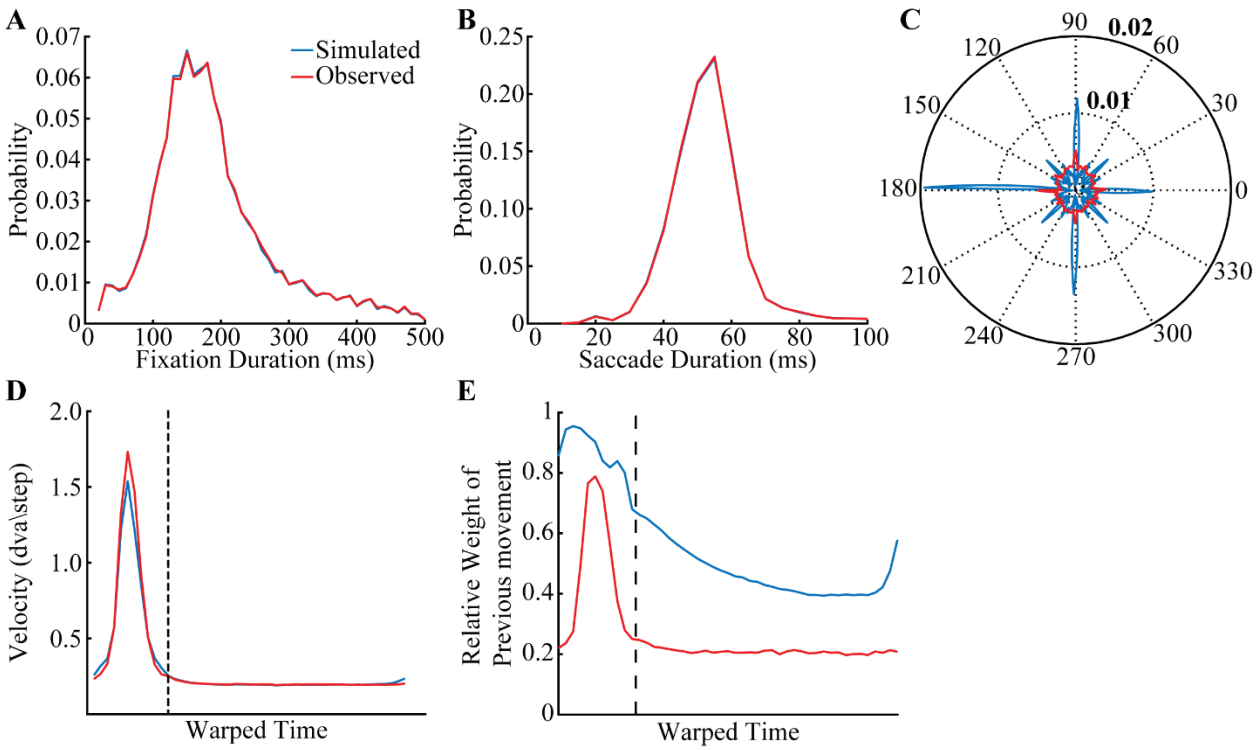

Figure 3-3 Behavioral Statistics Generated by the BCRW

The following viewing behavior statistics were incorporated into the BCRW: (**A**) fixation durations, (**B**) saccade durations, (**C**) the saccade angle leaving a fixation, (**D**) the [mean] eye movement velocity over time (dashed line is transition time from saccade to fixation), and (**E**) the relative weight of the previous movement (i.e. persistence). Blue lines represent behavioral statistics derived from the BCRW's scan paths and red lines represent behavioral statistics from monkey MP's scan paths. The probability distributions for fixation durations and saccade amplitudes were virtually identical. Due to rounding simulated scan paths to the nearest pixel in the BCRW, the BCRW's behavior diverged slightly from the observed behavior for saccade angles leaving a fixation and the velocity of eye movements over time.

parameter values such as persistence it was important to determine these values across all fixations and saccades. Therefore, we warped each fixation or saccade using linear spaced sampling to rescale all fixations and saccades to their respective medians. During the simulation, parameter values were warped to fit fixation durations and saccade durations selected by the BCRW. Viewing behavior statistics generated by the BCRW are shown in **Figure 3.3**.

3.3.3 *Calculating Salience Maps and Image Intensity*

Salience is a bottom-up property of visual stimuli and is defined as stimulus features distinct from the background that immediately attract attention. Mathematically, we computed salience by summing color, orientation, and intensity contrast over multiple spatial scales (Itti et al., 1998). We then normalized the salience map from 0 to 1 within each image. Image intensity was also normalized from 0 to 1 within each image and was defined as the gray scale value of each pixel. Salience and image intensity chance levels were calculated as the 95% confidence intervals of randomly selected locations. The selection of the Itti, Koch, and Niebur salience model was based on the simplicity of the model as well as the inclusion of biologically inspired contrast filters.

3.3.4 *Biased Correlated Random Walk (BCRW)*

The BCRW consisted of a salience map and a random walk process informed by viewing behavior statistics. See **Figure 3.4** for a summary of rules that dictated movement in the BCRW, and see **Table 3.1** for pseudo code. In the BCRW, a bias term and the direction of the previous movement competed to influence the walk (Crone and Schultz, 2008). The bias term caused the walk to move towards the most salient regions of the image. The direction of the previous movement was used to emulate saccadic eye movements in which the eyes move in the same

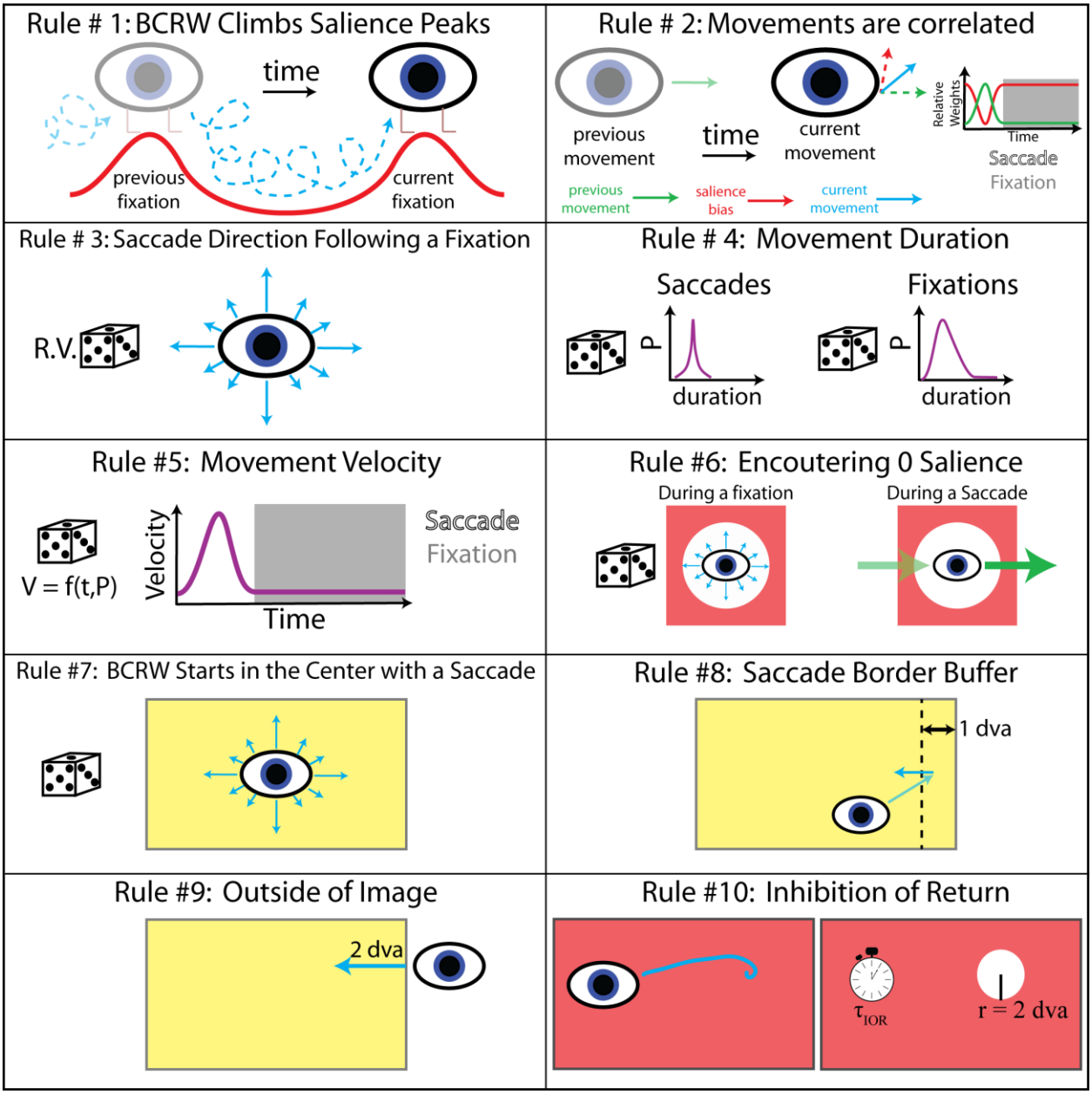

Figure 3-4 BCRW Rules

10 rules dictated the velocity, direction, and duration of movement. The values for rules 8-10 were determined by a parameter sweep. *R.V.* random variable, *P* probability, *f* function, *t* time, *V* velocity, τ_{IOR} time constant of IOR, and *r* radius.

Table 3-1 BCRW pseudo-code

1. Smooth salience map with Gaussian filter
2. Calculate gradient of salience map to get direction of salience bias
3. Start eye at the center of the image
4. **Do**
    a. Simulate Saccade()
    b. Simulate Fixation()

While simulated time < 10 seconds

Simulate Saccade()

a. Randomly select a saccade duration from the observed distribution
b. Warp observed eye velocity distribution and persistence to selected saccade duration
c. **For** each time step during the saccade
    i. **If** this is the first time step in the saccade
        1. Randomly select a velocity from the eye velocity distribution
        2. Randomly select a saccade angle leaving a fixation from observed distribution
        3. Move selected velocity and direction
    ii. **Else**
        1. Randomly select a velocity from the eye velocity distribution
        2. **If** salience at current locations is 0
            a. Current direction = previous movement direction
        3. **Else**
            a. Direction of current movement = persistence*previous movement direction+ (1-persistence)*direction of salience bias
        4. Move selected velocity and calculated direction
    iii. **If** saccade approaches within 1 dva of the border of the image
        1. Move in direction away from the border of the image
    iv. **Else If** the saccade leaves the image
        1. Move 2 dva back into the image

Simulate Fixation()

a. Randomly select a fixation duration from the observed distribution
b. Warp observed eye velocity distribution and persistence to selected fixation duration
c. **For** each time step during the fixation
    i. **If** salience at current locations is 0
        1. Set salience bias to random direction
        2. Randomly select a velocity from the eye velocity distribution
        3. Direction of current movement = persistence*previous movement direction+ (1-persistence)*direction of salience bias
        4. Move selected velocity and calculated direction
    ii. **If** this is the last time step in the fixation
        1. Estimate fixation location as average position over the last 5 time steps (25 ms)
        2. Set salience at fixation location and surrounding area (IOR_{radius} = 2 dva) to 0
        3. Recover salience at prior fixation locations if locations were fixated 17 fixations ago (i.e. $1/\tau_{IOR}$)

direction until the eyes approach a fixation target. A weighted average of the previous movement angle and the gradient of the salience map determined the direction of movement. We estimated the weighting term, which we call persistence, from the probability that the scan paths did not change direction by more than 45 degrees; persistence was greater during a saccade than during a fixation.

The direction of movement dictated by the salience map always pointed in the direction of the highest salience so that the BCRW climbed salience peaks. To assist the BCRW, the salience maps were smoothed by a Gaussian filter with a standard deviation of 1/2 dva. In the case where the walk encountered 0 salience, walks producing saccades continued in the previous direction while walks producing fixations moved in a random direction dictated by the probability distribution function (PDF) of saccade angles leaving a fixation.

All distributions of durations, directions, and velocity of movements in the BCRW were determined directly from the observed scan paths for each monkey individually. A PDF of saccade angles leaving a fixation dictated the saccade direction at the start of the BCRW and following a fixation. Parallel to the monkey experiments, the BCRW started at the center of the image. PDFs of fixation and saccade durations as well as PDFs of fixation and saccade velocity, which were functions of time and velocity, determined the duration and velocity of movement in the BCRW. The persistence term and PDFs of fixation and saccade amplitudes were time-warped to the median length of all fixations and saccades, respectively. Since the duration of fixations and saccades changed randomly within the BCRW these movement distributions were then warped to the length of the fixation or saccade determined during the BCRW.

The BCRW produced a saccade followed by a fixation for a predetermined duration based on PDFs of saccade and fixation durations, respectively. At the end of the fixation period,

the fixation location was defined as the mean location of the simulated scan path for the last 25 ms of the fixation. Averaging over the last 25 ms accounted for any positional jitter as well as the fact that the BCRW could systematically drift towards local salient peaks (**Figure 3.5**). The salience surrounding the fixation location within the area of inhibition of return (IOR) was then set to 0 (see below). The BCRW then "reset" and produced the next fixation and saccade pair until the scan path had been simulated for a total of 10 seconds. The BCRW had a temporal resolution of 5 ms similar to the acquisition rate of the eye tracker (200 Hz). For each monkey and each image, we simulated the BCRW 100 times using that monkey's behavioral statistics to obtain a prediction of fixation locations.

The BCRW contained 4 additional parameters not derived from viewing behavior statistics: a border buffer rule, border saccade distance rule, the time constant of IOR, and the area effected by IOR. A parameter sweep estimated these parameters (**Table 3.2**). These parameters were fit across all monkeys and did not vary individually. For the parameter sweep, we used Kullback–Leibler divergence (KL divergence) to compare observed fixations to predicted fixation locations from 10 simulations of the BCRW for each image and monkey. The border buffer rule stated that whenever a saccade approaches within 1 dva of the image border then the saccade must move in the direction opposite to the border. The border saccade distance rule stated that whenever the BCRW left the image and crossed the image border, the BCRW must move in the direction opposite to the border with a distance that is at least 2 dva. The radius for the area of IOR was found to be 2 dva and the optimal time constant for IOR was found to be 1/17. The time constant of IOR required a certain number of fixations, the reciprocal of this value, to occur before the salience returned to its original value at a previous fixation location. IOR models the consumption and recovery of visual information at fixation locations.

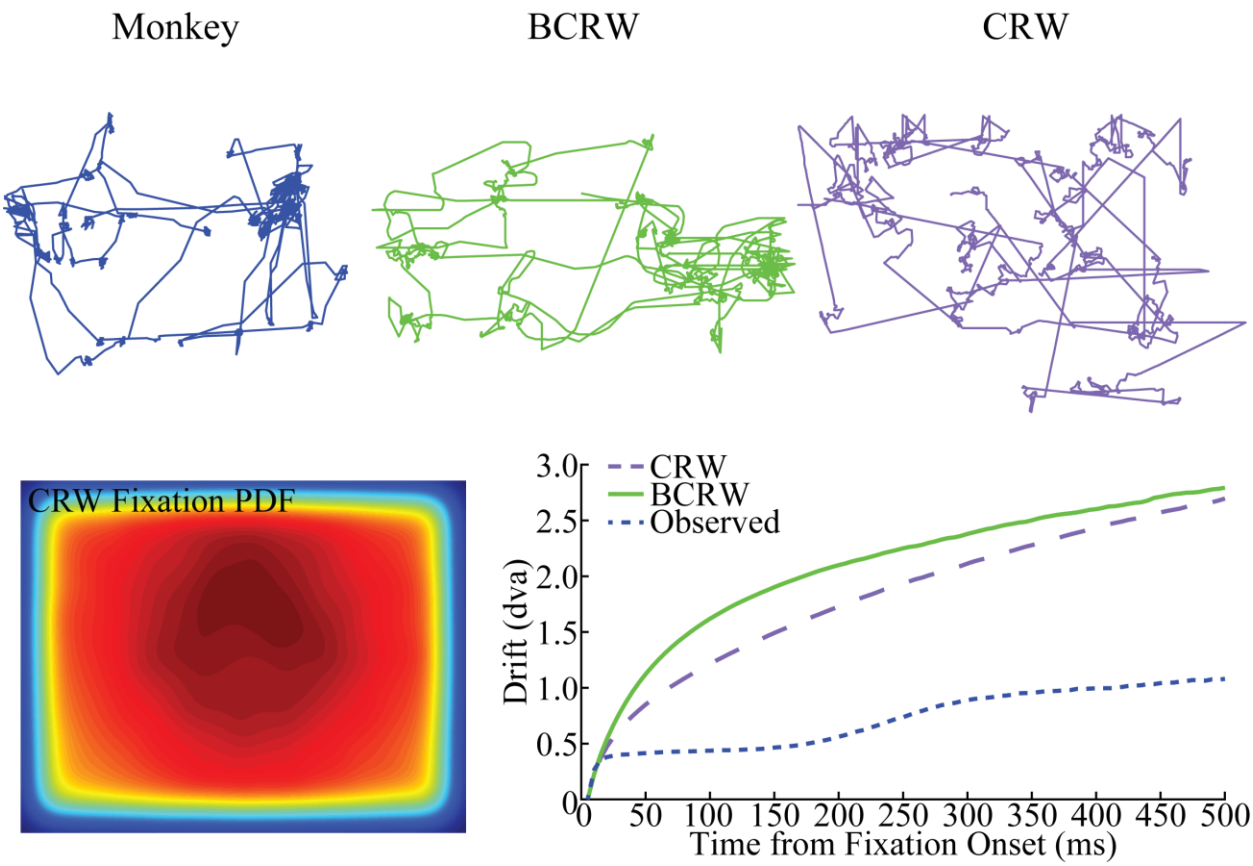

Figure 3-5 Comparison of the Scan Paths Simulated by the BCRW and CRW
Top row: example scan paths from monkey IW, BCRW, and CRW for the same image. Fixation patterns appeared similar for the observed scan path and the BCRW. However, the CRW made fixations in random locations. Bottom row: as expected the average fixation PDF for the CRW appears relatively uniform except along the border of the image and did not reflect the observed fixation PDF well. BCRW scan paths continued to drift towards local salient peaks after fixation onset. The BCRW drifted slightly more than the CRW which did not contain a salience bias. Both the BCRW and CRW drifted more than the observed data. There was a small bump (~0.5 dva) in the observed data around 200 ms likely reflecting undetected microsaccades interrupting longer fixations.

Table 3-2 Parameter Sweep values.

Parameter Name	Tested Values	Value of Best Fit
Border Buffer (dva)	0.04, 0.4, 1, 2, 4	1 dva
Border Saccade Distance (dva)	0.4, 1, 2, 4, 8	2 dva
Time Constant of IOR (1/# of fixations)	0, 1/50, 1/35, 1/25, 1/17, 1/12, 1/7, 1/3, 1	1/17
Area of IOR (radius in dva)	0, 1, 2, 4	2 dva

3.3.5 *Correlated Random Walk (CRW)*

To determine how important the salience bias was for predicting viewing behavior, we created a correlated random walk (CRW) model without a salience bias. Because we use IOR to model the consumption of information with salience being a proxy for information, the CRW does not contain IOR. In the CRW persistence determined the relative weight of the direction of the previous movement and a random direction.

3.3.6 *KL divergence and ROC Analysis*

KL divergence was used to compare the PDFs of observed fixation locations to the PDFs of the predicted fixation locations. The observed and predicted fixation PDFs were calculated by combining the fixation locations for all 4 monkeys who viewed the same image into a single fixation matrix of the same size as the image. The fixation matrix was marked with a 1 where fixations occurred and then smoothed by a 2D Gaussian filter with a standard deviation of 1 dva. The smoothing accounted for small errors in the eye tracking system and natural variability in fixation location (Wilming, Betz, Kietzmann, & Konig, 2011); the standard deviation of the eye tracking error was typically less than ¼ dva. Binning the fixation matrix into 1 x 1 dva bins created a new matrix containing 24 x 32 bins. In the case where a bin contained no fixations, the bin's value was replaced with the lowest value defined in MATLAB, eps (2^{-52}). Finally, the fixation PDF was estimated by dividing the binned fixation matrix by the sum of the entire matrix. The predicted fixation PDF for the salience map and image intensity map were derived directly from these maps by binning the maps and then dividing the maps by their resulting sum.

KL divergence was calculated from the binned PDFs using the following equation:

$$D_{KL} = D_{KL}(P||Q) + D_{KL}(Q||P) = \sum_{i,j} \ln\left(\frac{P(i,j)}{Q(i,j)}\right) P(i,j) + \sum_{i,j} \ln\left(\frac{Q(i,j)}{P(i,j)}\right) Q(i,j)$$

where D_{KL} is the symmetric form of KL divergence, P is the first fixation PDF, Q is the second fixation PDF, *i* is the bin row, and *j* is the bin column.

A Receiver Operating Characteristic (ROC) analysis allowed us to determine whether the models could discriminate between fixated and non-fixated locations. We used ROC analysis to compare the distribution of BCRW, salience map, or image intensity map values at fixated locations to the distribution of values at random locations. We then calculated the AUROC (Area Under the Receiver Operating Characteristic Curve) from the ROC curves. AUROC values close to 1.0 suggest that these models are good at discriminating between fixated and non-fixated locations while an AUROC value of 0.5 suggests these models discriminate between fixated and non-fixated locations at chance levels.

There exist a variety of methods for determining model fitness and in particular for visual salience models (Wilming et al., 2011). Compared to a ROC analysis, KL divergence better examines how well models predict the probability of fixation in certain locations because KL divergence weighs higher fixation probabilities heavier than low fixation probabilities. This notion is important because certain areas (theoretically the most salient regions) are repeatedly fixated as compared to other areas which are less likely to be fixated even once. In contrast to KL divergence, a ROC analysis weighs each location equally regardless of the probability of fixation. Thus ROC analysis is better at assessing models' abilities to predict fixation locations regardless of the fixation probability. Another benefit of a ROC analysis is that ROC analysis does not require corrections for locations with 0 fixation probability and thus smaller sample size affects ROC measures less. Because both methods have their advantages and disadvantages, we used both to test the model's goodness of fit.

3.3.7 *Shift Task*

To test the central bias hypothesis, we used data from 2 monkeys performing a free viewing task as part of a separate experiment. Data for this experiment were obtained separately from one monkey used in the previous experiment and an additional fifth monkey. In this task, the image position was shifted left or right of the center of the monitor by 2 dva. Importantly, the initial fixation cross was presented at 9 different points, located along the border of the image in the 8 cardinal and intermediate directions and one at the center of the image. Compared to the central fixation cross condition, the fixation cross was shifted vertically approximately 7 dva and horizontally approximately 15 dva.

For the examination of the central bias hypothesis, only the viewing behavior statistics from this task were incorporated into the BCRW. We simulated the BCRW 100 times for a total of 360 images for each monkey. Three or four image sets were used for each monkey with image sets containing 120 or 90 novel images, respectively. Images were 378 by 756 pixels large and subtended 16 by 32 dva.

3.4 RESULTS

3.4.1 *Fitness of Salience and BCRW Models*

Because the BCRW relies heavily on salience, we first determined whether observed fixation locations occurred at more salient locations than expected by chance (**Figure 3.6**). Not surprisingly, fixations occurred at locations with salience values higher than expected by chance, while fixations occurred at locations with image intensity values lower than expected by chance (z-test, all p's < 0.001). The mean salience at all fixation locations was 0.3806, and the mean image intensity was 0.4533. The salience and image intensity chance levels were 0.2579 and

0.5238, respectively. Salience at fixation locations was higher during the first few fixations compared to later on in the viewing period, and salience at later fixations appeared to approach an asymptote. Similarly, fixations occurred at brighter locations later in the viewing period compared to earlier in the viewing period.

Individual scan paths revealed that fixations occurred in many but not all of the salient regions of the image **(Figure 3.7)**. Accordingly, we built the BCRW to simulate the variability in scan paths. We used KL Divergence and ROC analysis to compare the ability of the BCRW, salience, and image intensity maps to predict fixation locations.

The KL divergence analysis showed that the distance between the BCRW's predicted fixation PDF and observed fixation PDF was significantly shorter than the distance between the fixation PDF predicted by the salience map and the observed fixation PDF (t-test, $p < 0.001$), and was significantly shorter than the distance between the fixation PDF predicted by the image intensity map and the observed fixation PDF (t-test, $p < 0.001$) (**Figure 3.8**). Additionally, the fixation PDF predicted by the salience map was significantly closer to the observed fixation PDF than the fixation PDF predicted by the image intensity map (t-test, $p < 0.001$). The mean distance between observed fixations and fixations predicted by the BCRW, salience, and image intensity maps was 3.63 bits, 4.47 bits, and 5.63 bits, respectively. These results indicated that the BCRW performed better than salience or image intensity maps.

Similar results were obtained from a ROC analysis: the BCRW discriminated between fixated and random locations better than salience (ks-test, $p = 0.02$) and better than image intensity (ks-test, $p < 0.001$). Additionally, salience discriminated between fixated and random locations better than image intensity (ks-test, $p < 0.001$) (**Figure 3.8**). The mean AUROC for the

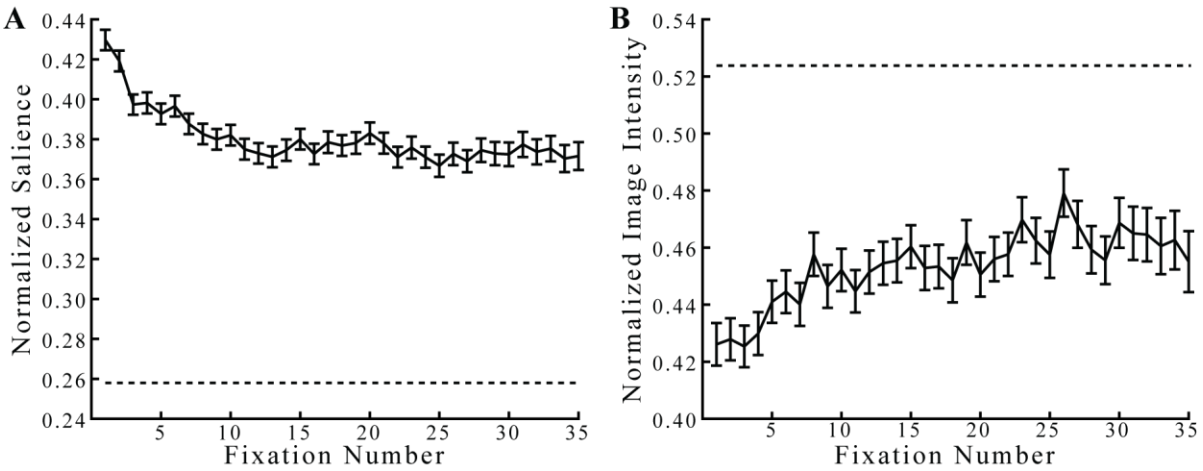

Figure 3-6 Salience and Image Intensity at Observed Fixation Locations

A) Observed fixations occurred at locations with salience values higher than would be expected by chance (dashed lines represent chance levels), and **B**) fixations occurred at locations with image intensity values lower than expected by chance. Error bars represent mean ± *SEM.*

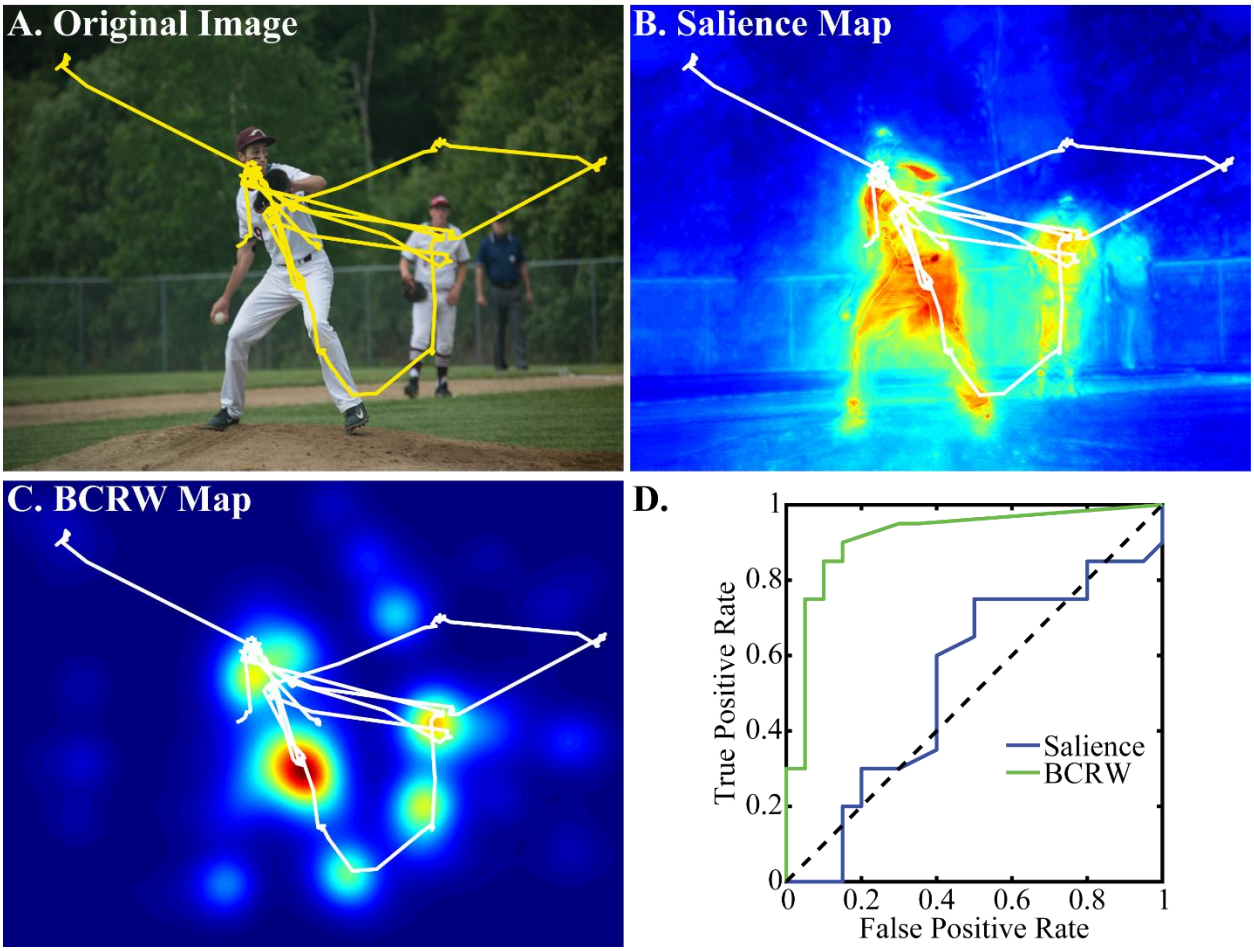

Figure 3-7 Examples of Observed Scan Path, Salience Map, and BCRW Map
The observed scan path (yellow/white) overlaying the viewed image shows that the monkey attends to many of the objects in the scene. The observed scan path overlaying the salience map shows that fixations occurred in many, but not all of the salient regions of the image. The BCRW was able to predict many of these fixations.

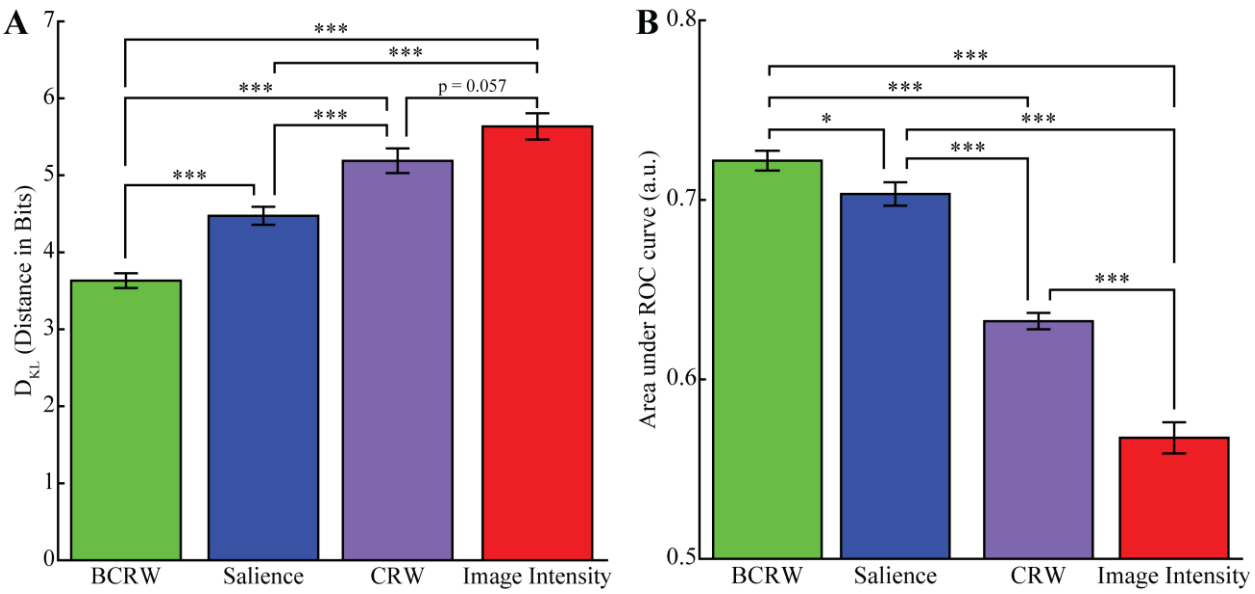

Figure 3-8 Comparing Models for Predicting Fixation Locations

A) KL Divergence analysis showed that the BCRW predicted fixation locations better than salience and image intensity, and salience predicted fixation locations better than image intensity. The CRW was worse at predicting fixation locations than the BCRW and salience but not image intensity. **B**) The mean AUROC was significantly higher for the BCRW than for salience or image intensity, and the AUROC for salience was higher than for image intensity. The CRW was worse at predicting fixations than the BCRW and salience but better than image intensity. The CRW, BCRW, salience, and image intensity can all be useful for discriminating between fixated and non-fixated locations because the AUROC for all maps were significantly greater than chance. Error bars represent mean ± *SEM.* (* $p < 0.05$ & *** $p < 0.001$).

BCRW, salience, and image intensity was 0.722, 0.704, and 0.567, respectively. All AUROCs were significantly greater than chance (z-test, all *p*'s < 0.001).

To determine whether the salience bias was important for predicting fixation locations we generated scan paths using a CRW. The CRW predicted a uniform distribution of fixation locations except near the edge of the image and did not represent the observed fixation data (**Figure 3.5**). KL divergence analysis showed that the CRW (mean of 5.19 bits) was significantly worse at predicting fixation locations than the BCRW or salience (t-test, $p < 0.001$), but the CRW was marginally better than image intensity (t-test, $p = 0.057$). A ROC analysis showed the similar results. The AUROC for the CRW (mean of 0.632) was significantly worse than the BCRW and salience (ks-test, $p < 0.001$) but significantly better than image intensity (ks-test, $p < 0.001$).

3.4.2 *How well can a Central Bias and Interobserver Consistency Predict Fixations?*

Interobserver consistency in humans is very high and is often considered the upper limit on model performance. To calculate interobserver consistency, we compared fixation locations of an individual monkey to the remaining group of monkeys using a ROC analysis. We did this for every combination of individuals and groups. The average AUROC was 0.748 which was significantly better than chance (z-test, $p < 0.001$). Interestingly, AUROC values ranged from 0.467 to 0.929 suggesting that some images were viewed consistently while others were viewed dissimilarly. Interobserver consistency was significantly better at predicting fixation location than image intensity, salience, and the BCRW (t-test, all *p*'s < 0.001) although this difference was modest for the BCRW (approximately a 4% change).

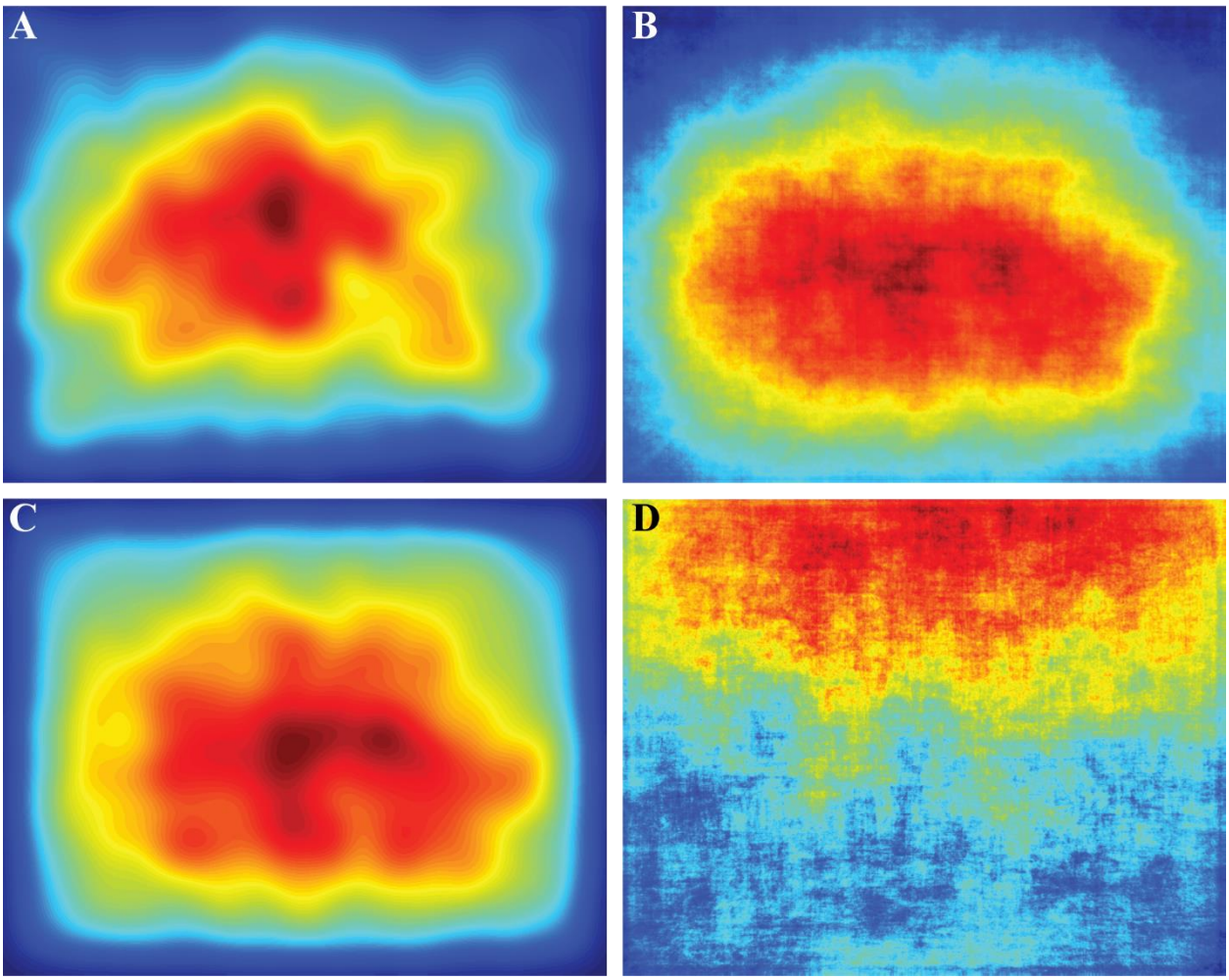

Figure 3-9 Average Probability Density Functions (PDFs) across all Images
A) The average observed fixation PDF contained an evident central bias. The initial fixation to start the trial was not included in this PDF. **B)** The salience map contained a central bias that appeared similar to the observed fixation PDF. **C)** The average BCRW map also contained a strong bias towards the center. **D)** The average image intensity map did not contain a central bias and did not represent the fixation PDF well. Averaging across all images revealed that the top of the image was brighter than the bottom of the image. Many images contained the horizon in the upper portion of the images which contributed to this phenomenon.

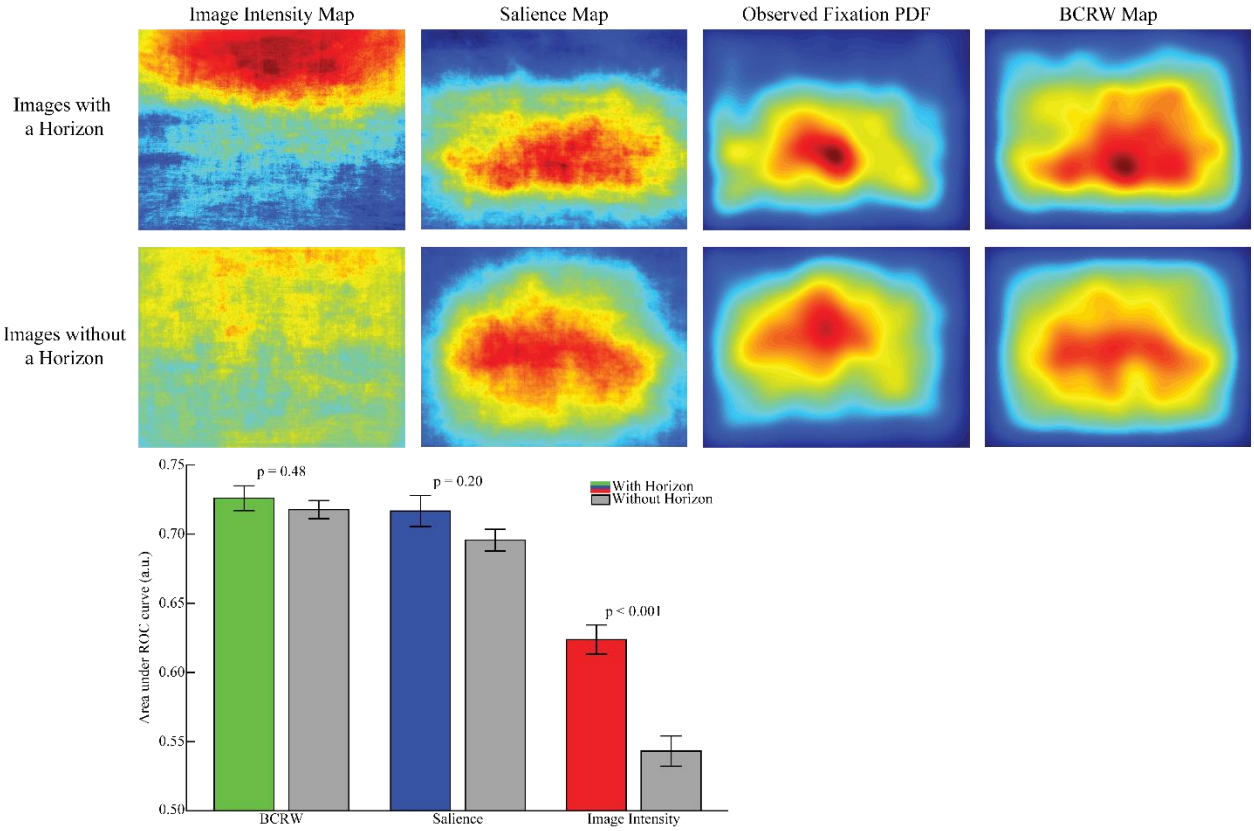

Figure 3-10 Model Fits for Images with and without a Horizon

On average images that had a horizon (n = 84) had higher image intensity values towards the top of the image. No evident image intensity pattern was observed for images without a horizon (n = 204). The average salience map for images with a horizon had a bias towards the bottom of the screen while images that did not contain a horizon showed a strong central bias. The observed fixation PDF and BCRW map followed this downward shift in the salience map for images with a horizon. Image intensity was a better predictor of the observed fixation locations for images that had a horizon while the BCRW and salience maps predicted fixations for images with and without a horizon equally. Heat maps are scaled the same for images with and without a horizon. Error bars represent mean ± *SEM*.

To calculate the influence of the central bias on fixation location we compared observed fixation locations to the average observed fixation PDF, salience PDF, or BCRW PDF (**Figure 3.9**) using KL divergence and a ROC analysis. There was no central bias in the average image intensity map, and therefore, we did not pursue any further analysis with image intensity. Even when we removed images containing a horizon below the upper third of the image, we still could not find evidence of a central bias in image intensity maps (**Figure 3.10**). In fact image intensity was a better predictor of the observed fixation locations for images with a horizon than images without a horizon.

Using KL divergence we found that there was no difference in the predictive ability of the central bias in observed fixations and the salience map (ks-test, $p = 0.477$), but the BCRW predicted fixations better than the central bias in fixation locations (ks-test, $p < 0.001$). Central biases in the BCRW and salience maps were significantly worse (ks-test, both *p*'s < 0.001) at predicting fixation location than the BCRW or salience, respectively.

A ROC analysis showed slightly different results. Central biases in the BCRW and salience maps could be used to discriminate between fixation locations and random locations better than chance (z-test, both *p*'s < 0.001), but the observed central bias in fixated locations was worse at discrimination than the BCRW or salience (ks-test, both *p's* < 0.001). The mean AUROC values using the average salience map, the average BCRW map, and the average observed fixation PDF biases as predictors of fixation locations were 0.640, 0.649, and 0.6591, respectively.

3.4.3 *Determining Factors Influencing the Central Bias in Fixation Locations*

We hypothesized that a central bias in fixation locations is caused by the interaction between the arrangement of salient objects in complex scenes (i.e. photographer's bias) and the

statistics of the eye movements. The BCRW is well-positioned to test this hypothesis because it allows for an isolation of factors influencing the central bias, such as a natural tendency to reorient the eyes towards the center of the stimulus, from the other statistics of eye movements. Further, data from the Shift Task can be used to determine whether the initial starting fixation position influences the central bias.

To measure the central bias, we calculated the centroid (center of mass) of the fixation PDF for each scan path on each image separately. In the observed data, we found there was no significant (1-way ANOVA, $p > 0.11$) displacement in the fixation centroid among the trials with different initial fixation cross positions (**Figure 3.11**). Further, changes in the position of the image relative to screen center did not influence the central bias (1-way ANOVA, $p > 0.10$).

Interestingly, horizontal shifts in the initial starting position of the BCRW resulted in significant (1-way ANOVA, $p < 0.05$) displacements in horizontal position of the fixation centroid as compared to the central starting position condition. Vertical shifts in the initial starting position of the BCRW resulted in smaller, non-significant (ANOVA, $p > 0.05$) displacements in the vertical position of the fixation centroid as compared to the central starting position condition. Northern shifts in the initial starting position of the BCRW were significantly displaced north as compared to Southern shifts in the initial starting position of the BCRW in fewer than half of all comparisons (1-way ANOVA corrected for multiple comparisons using the Tukey-Kramer method, $p < 0.05$).

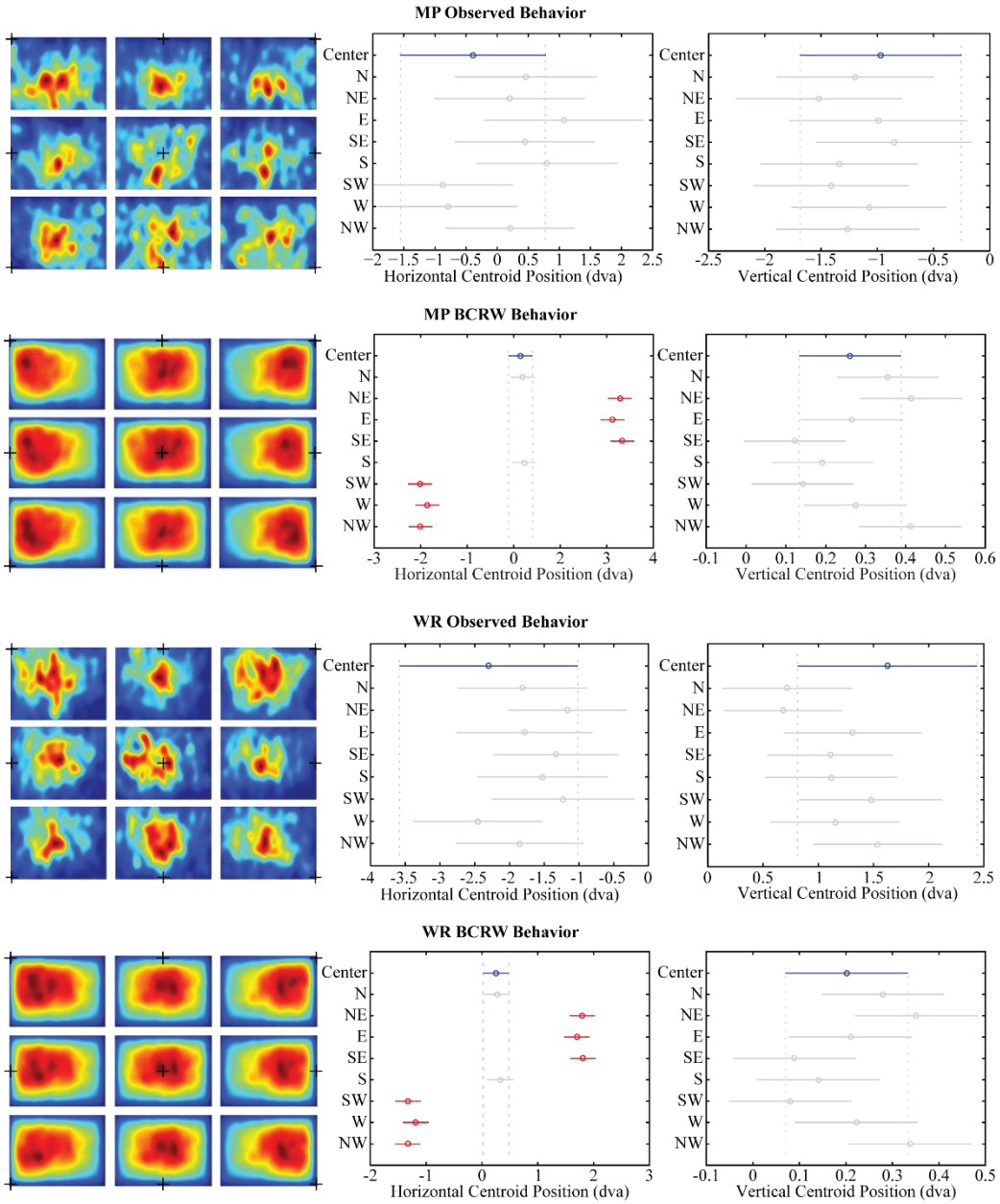

Figure 3-11 Modeling a Central Bias in Fixation Locations

Shifts in the position of the initial fixation cross (black + in all left panels) did not significantly displace the observed position of fixations (ANOVA, both *p's* > 0.11) for either monkey MP or monkey WR. However, when simulating viewing behavior with the BCRW, shifts in the position of the initial fixation cross resulted in significant displacements in the horizontal position of fixations (Middle panels, ANOVA corrected for multiple comparisons). Highlighted in blue is the centroid for the center fixation cross condition. Centroids significantly different than the centroid for the center fixation cross condition are highlighted in red. Significant displacements relative to the center fixation cross condition were not observed in the vertical shift conditions (Right panels). Error bars represent mean ± 95% confidence interval.

3.5 DISCUSSION

The use of natural stimuli along with natural viewing behavior is becoming widespread in neuroscience. Several recent studies provide evidence that complex scenes are useful for studying and diagnosing neurological disorders (Smith et al., 2006b; Crutcher et al., 2009; Mannan et al., 2009; Tseng et al., 2013b; Zola et al., 2013; Wang et al., 2015a). Additional studies have elucidated novel neural responses in macaques freely viewing complex scenes (Killian et al., 2012; Hoffman et al., 2013a; Jutras et al., 2013a). Unfortunately, complex scenes are difficult to describe quantitatively and to parameterize. Further, complex stimuli are likely to elicit complex behavior that requires new analysis techniques. In order to fully interpret free viewing behavior, it is critical to understand what aspects of the stimuli guide this behavior.

We built the BCRW model to advance understanding of natural viewing behavior. The BCRW can aid in stimulus parameterization and can capture the complex behavior associated with viewing more complex stimuli. Here, we demonstrated that the BCRW could predict monkey viewing behavior for complex visual images better than chance. Additionally, the BCRW was able to predict viewing behavior better than maps based on image salience or image intensity. Interestingly, the CRW, which did not contain a salience bias, was unable to predict viewing behavior as well as the BCRW. This suggests that *both* the statistics of eye movements and salience are important factors influencing fixation locations. We then demonstrated that the BCRW could be extended beyond the prediction of fixation locations. We showed that a central fixation bias could not be explained by the interaction of the statistics of eye movements and the arrangement of salient objects in scenes.

The BCRW uses data derived from eye tracking in monkeys and combines these statistics with a salience map in a piece-wise fashion. The BCRW model incorporates statistics from

individuals to account for interobserver and intraobserver variability. A shortcoming of many deterministic attention models is the use of a winner-take-all algorithm to predict the next fixation, which assumes that the next fixation will always be in the same location regardless of the individual. However, there exists a great deal of individual variability in viewing behavior, and each individual may view the same image differently across repeated presentations. The BCRW addresses this issue by directly predicting the probability of fixation at all locations. Regions with higher probabilities of a fixation will be fixated more often than regions with lower probabilities.

The mechanisms and circuits underlying attention and the control of eye movements are complex and not fully understood (Desimone and Duncan, 1995; Miller and Buschman, 2013). Instead of describing the mechanisms by which the brain executes attentional control, here, we built a more simplistic model of eye movements. The BCRW model is an appetitive foraging model in which the eyes are attracted to salience. Once the eyes fixate a location in the image, salience at that specific location becomes "consumed" until it recovers a specific time later at a rate dictated by the time constant of IOR. This consumption of salience may parallel extraction of visual information from fixated locations. The goal of the BCRW model is to parameterize viewing behavior during the viewing of complex scene stimuli at a phenomenological level. Future extensions of the BCRW could help us understand how certain mechanisms, such as IOR, are important for attention and how disease affects these mechanisms.

3.5.1 *The Origin of the Central Bias in Fixation Locations*

Whereas other models of viewing behavior often must incorporate additional measures to create a bias for fixations close to the center of an image (Parkhurst et al., 2002), the BCRW creates this bias without any additional influences. The average central biases in fixation

locations were able to predict fixation locations better than chance. However, these average central biases were significantly worse at predicting fixation locations than salience or the BCRW model. Observation of individual scan paths supports the same conclusion. Individual scan paths did not strongly demonstrate a central bias but rather a strong bias towards salient regions. An apparent central bias in fixation locations was only revealed after averaging over a large number of scan paths.

Our last experiment aimed to understand which factors influence the central bias. The behavioral data showed that the position of the initial starting fixation and the position of the stimuli relative to the monkey and monitor are factors that do not strongly influence the central bias in fixation locations.

The BCRW was well-positioned to test the central bias hypothesis because parameters such as the initial starting position of the model could be easily manipulated. The BCRW could not reproduce the results found in the observed data suggesting that the central bias in fixation locations may not be caused solely by the interaction of oculomotor statistics with a central bias for salient regions of the image. Taken together with the behavioral results, these data suggest that the central bias is most strongly influenced by a natural tendency of the monkeys to re-orient their eyes towards the center of the stimulus.

Recent human studies exploring the nature of the central fixation bias have suggested that photographer's bias contributed prominently, and that the central bias was stronger during the beginning of a viewing period, with fixations distributed outside of the central area later in the viewing period (Tseng et al., 2009). In contrast, other studies have identified image and screen position as strongly influencing the central bias, particularly for early fixations (Bindemann, 2010). Further, Tatler suggested that observers demonstrate a central fixation bias because the

center of the screen and stimulus offer a convenient reorienting location in that the eyes naturally relax to a forward position and observers are typically centered to the stimuli (Tatler, 2007). Our results are consistent with this later view and suggest that while the photographer's bias and eye movement statistics likely contribute to the central bias, monkeys have a general tendency to re-orient their eyes towards the center of the stimulus. Future experiments are necessary to fully understand the central bias of fixations. Additional modeling work offers a potential avenue for explaining some of these factors.

3.5.2 *Limitations of the BCRW model*

Because the monkeys in our experiments viewed images for a cumulative looking time of 10 seconds, the apparent ability of the BCRW model and salience to predict fixations is less than some previous findings with shorter viewing periods (Judd et al., 2011; Wilming et al., 2011; Zhao and Koch, 2011). Here, we grouped viewing behavior statistics across the entire viewing period, but statistics including fixation duration and saccade amplitude change systematically over the viewing period. We also did not include higher-order relationships between preceding and subsequent fixation durations and saccade amplitudes (Tatler and Vincent, 2008). Incorporating these changes into the BCRW model may increase the predictive power of the BCRW. In addition, future investigations of the time-course of prediction by the BCRW could be useful in identifying periods of viewing behavior that are guided predominantly by bottom-up salience, as compared to other aspects of attentional control, including stimulus memory.

We used data from four monkeys to test the BCRW model and two monkeys to test the central bias hypothesis. While this sample size is small, it is of a size typical of many non-human primate studies. To alleviate statistical errors due to a small number of subjects we repeated the experiments over a large number of images and combined data across monkeys. Nonetheless,

future studies with larger sample sizes will be useful in confirming the BCRW's interpretation of the salience maps.

Finally, a major limitation of the BCRW may derive from that fact that the model is an agent-based model in which the agent both diffuses randomly and is also heavily biased towards salient regions of the image. In short "saccades" in the BCRW do not always appear completely realistic and curve towards salient regions of the image. Ideally, the persistence term would maintain smooth saccade movements, but additional constraints may be necessary in order to create a more realistic model with increased predictive power. By averaging the results of the BCRW over 100 repetitions, we may be removing the effects of this abnormality from the model.

3.6 Conclusion

Bottom-up stimulus features such as salience predict free viewing behavior in monkeys. We can further increase the ability of bottom-up salience to predict behavior by interpreting the salience maps with a BCRW informed by viewing behavior statistics. We developed the BCRW to interpret salience maps, but the BCRW should be compatible with any algorithm used to calculate salience or other forms of attentional maps. Salience maps predict free viewing of complex scenes but may be insufficient for predicting viewing behavior in search-based tasks or viewing of familiar scenes where top-down mechanisms likely also influence viewing behavior. A potential solution to this limitation is the creation of hybrid models employing both bottom-up and top-down components of attention. Hybrid models could incorporate the BCRW as an eye movement model. Additional parameters, constraints, or layers could be added to the BCRW to increase the predictive power of the BCRW model.

The BCRW model can help in the creation and testing of novel behavioral tasks. The BCRW can be used to predict fixation locations, and in the case where there is a target or object of interest in a scene, the BCRW can predict the probability that a subject will look at the target or object of interest. Predictions like these can parameterize the non-intuitive aspects of behavioral tasks thus enabling the design of free-viewing tasks with consistent or incremental levels of difficulty.

3.7 ACKNOWLEDGMENTS

The authors would like to thank Esther Tonea and William Li for the creation of image sets and Megan Jutras for helping with collecting, organizing, and analyzing the behavioral data. We would also like to thank Miriam Meister for designing the shift task and Kiril Staikov for collecting data from the shift task. Funding for this work was provided by the National Institute of Mental Health Grants MH080007 (to E.A.B.) and MH093807 (to E.A.B.); National Center for Research Resources Grant P51RR165 (currently the Office of Research Infrastructure Programs/OD P51OD11132); and the National Institute of Health 1T90DA032466 (to S.D.K) and 5T90DA032436 (to S.D.K).

Chapter 4. EYE MOVEMENT-RELATED NEURAL ACTIVITY IN THE PRIMATE HIPPOCAMPUS[3]

Place cells in the rodent hippocampus create a 2D representation of the animal's environment (O'Keefe, 1976). Spatial representations have also been found in the hippocampus of bats (Ulanovsky and Yartsev, 2013) and monkeys (Rolls, 1999; Killian et al., 2012). Importantly, neurons in non-rodent species represent ethologically relevant spatial variables such as gaze location in monkeys and 3D position in flying bats. It is, however, unclear the extent to which spatial representations in non-rodent species may be sensitive to other parameters such as time (Pastalkova et al., 2008; MacDonald et al., 2011) and context (Smith and Mizumori, 2006a; Colgin et al., 2008), which have been shown to be important components of the rodent hippocampal code. Further, because primates use eye movements and vision to actively explore their environment, eye movements may provide an important timing signal representing the pace at which the brain acquires new visual information. Here we investigate the functional properties of neurons in the primate hippocampus in head-fixed monkeys during the free viewing of images. In agreement with previous work, we found view cells modulated by gaze position. Interestingly, these place cells demonstrated temporal tuning relative to fixation onset, with the neuronal population fully tiling the fixation duration. View cells also demonstrated rate remapping across behavioral contexts, which may be useful for the formation of relational memories. Taken together, our results highlight the importance of active sensing in organizing spatial and contextual representations in the hippocampus. Specifically, eye movements in primates may sequentially organize place cell representations in time which may allow information to be linked across successive eye movements.

[3] Adapted from König, Seth D., and Elizabeth A. Buffalo. "Eye Movements Temporally Organize Spatial Representations in the Primate Hippocampus." *To be Submitted*.

Active sensing plays an important role in how animals perceive their environment (Schroeder et al., 2010). Rodents primarily use sniffing and whisking to explore their environment up-close while primates use eye movements and vision to explore their environments from afar. Interestingly, sniffing and whisking in rodents (Grion et al., 2016) and eye movements in primates (Hoffman et al., 2013a; Jutras et al., 2013a) have been shown to modulate the hippocampal local field potential. While sensorimotor information is inherently egocentric, allocentric representations in the hippocampus must update with new sensorimotor information to accurately reflect the current state of the animal and its environment. In particular, active sensing plays an important role in dictating the rate of incoming sensory information and enhances sensory information at attended locations (Lakatos et al., 2007; Rajkai et al., 2008). Accordingly, we examined the extent to which eye movements modulate spatial, temporal, and contextual representations in the primate hippocampus.

Here, we recorded from 347 hippocampal neurons while monkeys freely viewed complex images on a computer monitor (**Figure 4.1A**). We evaluated the spatial modulation using Spearman's rank correlation (ρ) between firing rate maps for the first and second half of the recording session as well as Skagg's information score (Skaggs et al., 1993) across the whole session; observed values were then compared to 1,000 time-shifted permutations of spikes trains to determine significance. We found that 109 (31%) neurons were spatially modulated (**Figure 4.1B**). We refer to these spatially-modulated neurons as view cells as they resemble place cells found in the rodent hippocampus but are modulated by viewing location. View cells were highly stable over time, and across the population, view cells had a significantly higher ($p < 0.001$, t-test) spatial stability (median of $\rho_{1/2} = 0.68$) than the non-view cells (median of $\rho_{/12}$

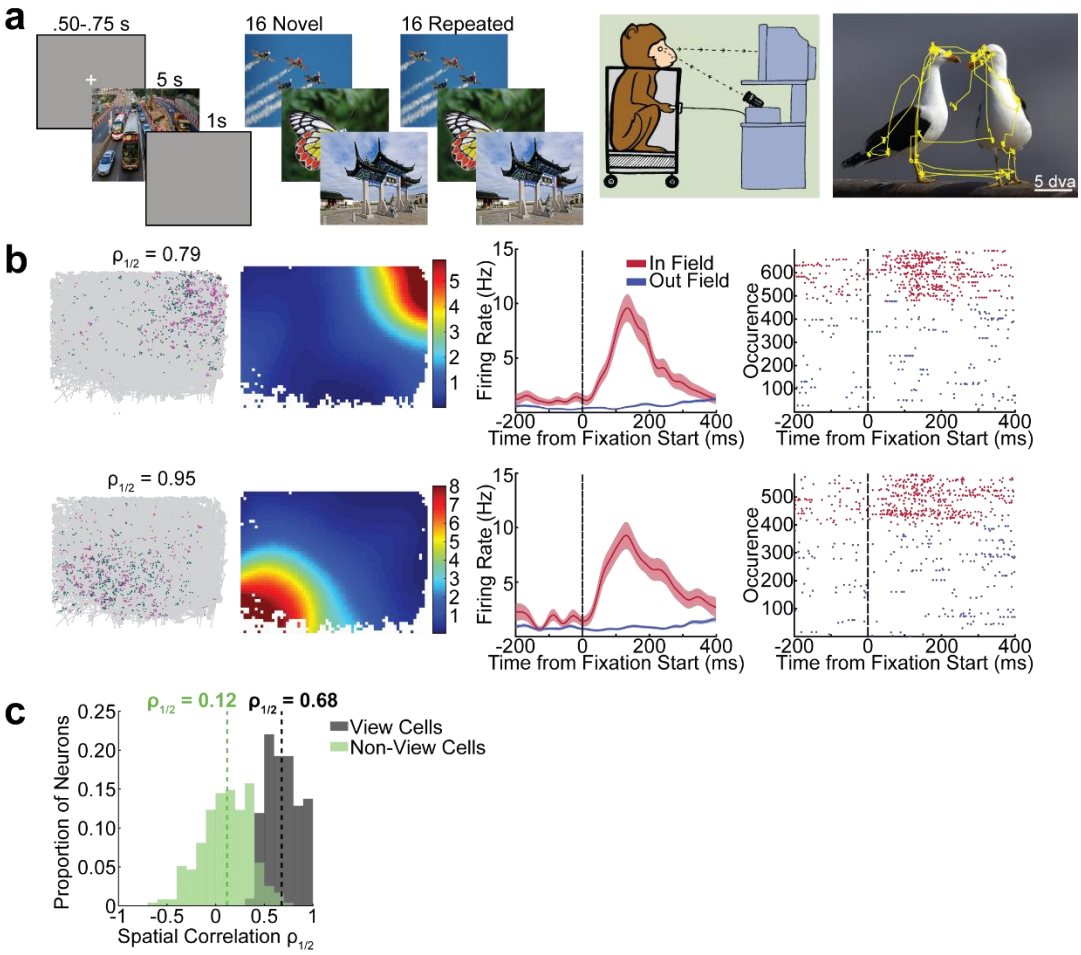

Figure 4-1 Spatial Representations in the Primate Hippocampus

A) Recordings were conducted while monkeys freely viewed complex images on a computer monitor. Images were presented twice, once novel then repeated, in blocks of 16 images. Gaze location was tracked with an infrared camera while monkeys sat still in a chair. An example scan path (yellow) overlaying the viewed image suggests that monkeys attend to image features. **B)** Two example view cells that were simultaneously recorded on different electrodes. *First column*: raw spike locations (green dots 1st half of recording session, magenta dots 2nd half of recording session) overlaying eye position (gray) across all viewed images during the recording session reveals stable, concentrated spatial selectivity. Spearman's ($\rho_{1/2}$) spatial correlation between the firing rate maps for the first and second half of the recording session is indicated at the top. *Second column*: firing rate maps indicating where the neuron fired the fastest in red and the slowest in blue. *Third column*: peri-fixation firing rate curves (mean ± s.e.m.) for fixations in the view field preceded by an out of field fixation (*OUT2IN*) and out of the field fixations preceded by out of field fixations (*OUT2OUT*) indicate that the neurons fired significantly faster for fixations in the view field than outside of the view field. *Fourth column*: peri-fixation rasters showing the reliability of firing rate patterns across many fixations. For clarity, only a random subset of *OUT2OUT* fixations are shown due to the large number of *OUT2OUT* fixations. **C)** Spatial correlations for the 109 view cells were significantly higher (t-test, $p < 0.05$) than the 238 non-view cells.

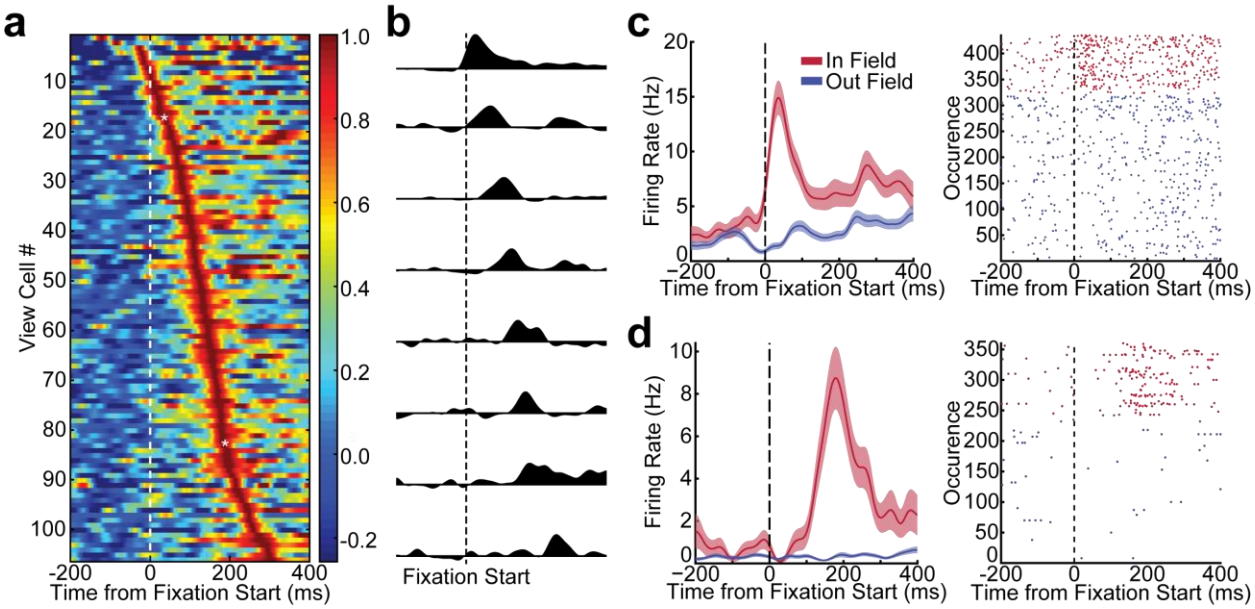

Figure 4-2 Eye Movements Temporally Organize View cells

A) A pseudo population plot of all view cells shows that each view cell reached its maximum firing rate at a different latency relative to the start of a fixation in the field (*OUT2IN*). Each row shows the normalized activity of one neuron. For each neuron, firing rate was normalized between its average firing rate outside of the field and its peak firing rate in the field. As some neurons were briefly inhibited when the monkey fixated outside the field, the normalized firing rate can be negative. White asterisks indicate example neurons in C and D. **B)** Normalized responses of 8 example view cells showing different response latencies. Some view cells fired maximally towards the beginning of the fixation period while others fired maximally towards the end of the fixation period. **C** and **D** show the peri-fixation firing rate curves (mean ± s.e.m.) and rasters for two additional view cells.

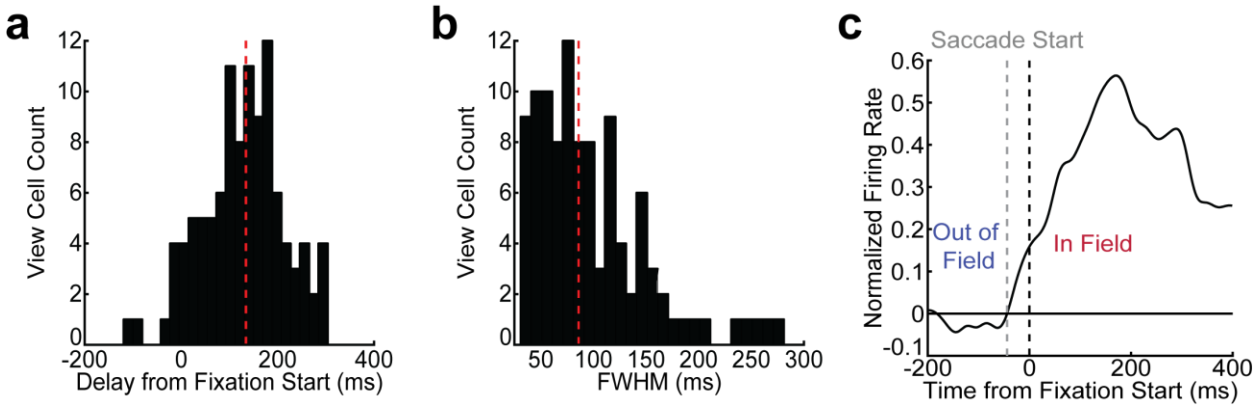

Figure 4-3 Extended Figure 4.2: Temporal Tuning Properties of View cells

A) Distribution of peak latencies relative to the start of the fixation period with a median delay of 135 ms, represented by the red dashed line. **B)** Distribution of full width at half max (FWHM) with median FWHM of 86 ms, represented by the red dashed line. **C)** Normalized, average peri-fixation firing rate curve across the population of view cells showing that the population firing rate begins to increase at the start of the saccade but reaches its maximum firing rate later in the fixation period.

= 0.12) (**Figure 4.1C**). Further, all view cells showed a significantly higher firing rate for fixations within the firing field compared to fixations outside of the field ($p < 0.05$, permutated resampling (Fujisawa et al., 2008; Prerau et al., 2014)).

Across the population, we observed that view cells demonstrated considerable variability in response latency relative to fixation onset. To quantify this, we restricted our analysis to fixations made into the field that were preceded by an out of field fixation (*OUT2IN*), and then we identified the latency of the peak response. Interestingly, across the population of view cells, each neuron appeared to reach its maximum firing rate at a different time relative to the start of the fixation (**Figure 4.2A**). Some neurons reached their maximum firing rate towards the beginning of the fixation period (**Figure 4.2C**) while others reached their maximum firing rate towards the end of the fixation period (**Figure 4.2D**). This pattern suggests that eye movements sequentially organize view cells in time. While each view cell fired with a different latency, the population average firing rate began to increase at the start of the saccade preceding the fixation (**Figure 4.3C**) further suggesting that eye movements modulate view cells.

There was a systematic bias in saccade direction by viewing location. For example, fixations along the right edge of an image were likely preceded by a rightward saccade. Accordingly, we investigated whether view fields along the edge of the image could spuriously arise due to saccade direction tuning. Overall, 26% (52/197) of neurons were significantly modulated (10,000 resampled mean resultant length (MRL), $p < 0.05$) by saccade direction (**Figure 4.4**). Moreover, 36% (29/81) of view cells showed significant saccade direction modulation compared to a smaller proportion (20%, 23/116) of non-view cells. For most (72%, 21/29) of the directionally modulated view cells, direction modulation was also observed for eye movements outside

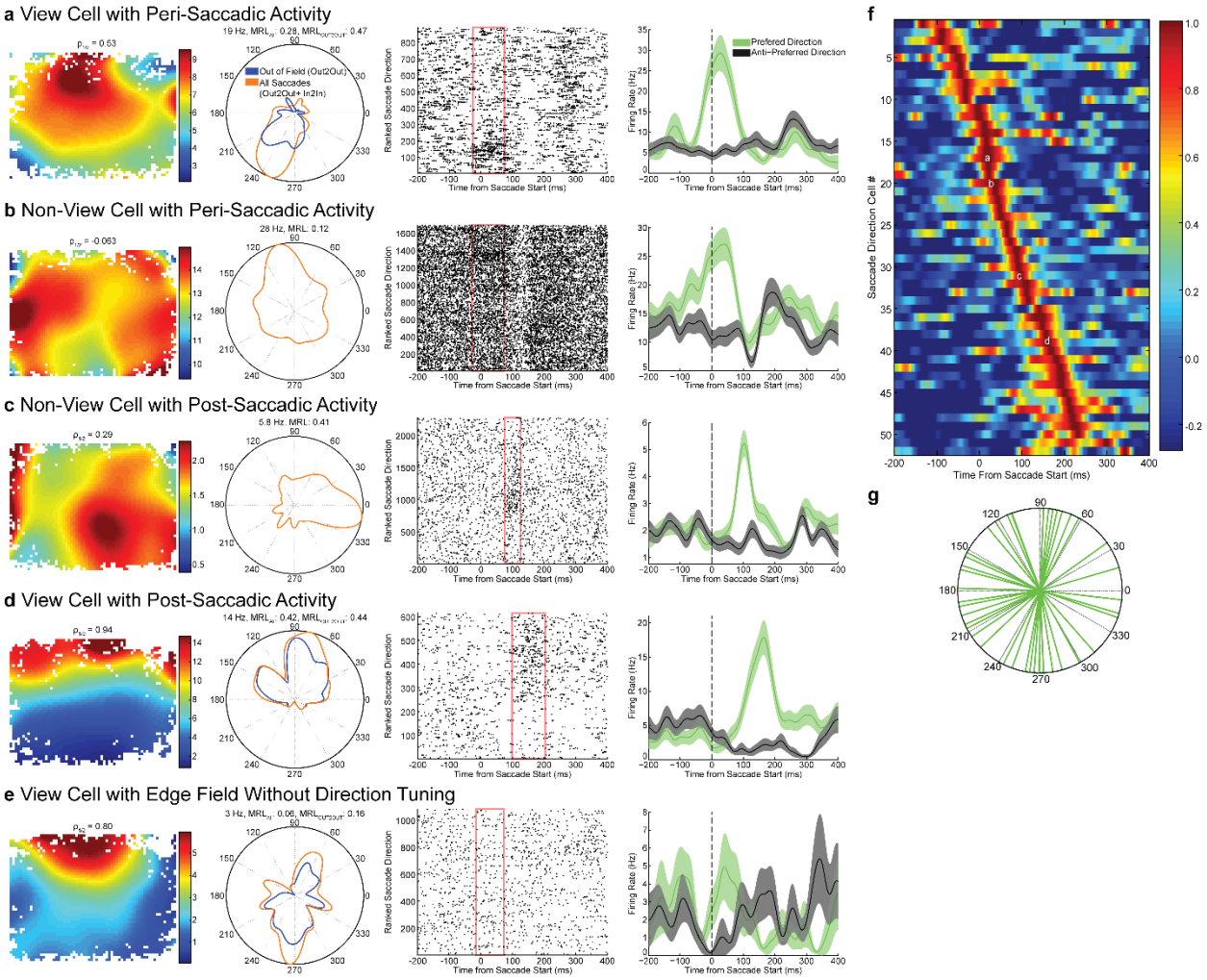
a View Cell with Peri-Saccadic Activity
b Non-View Cell with Peri-Saccadic Activity
c Non-View Cell with Post-Saccadic Activity
d View Cell with Post-Saccadic Activity
e View Cell with Edge Field Without Direction Tuning
Out of Field (Out2Out)
All Saccades
(Out2Out+ In2In)
Prefered Direction
Anti-Preferred Direction
Ranked Saccade Direction
Firing Rate (Hz)
Time from Saccade Start (ms)
f
Saccade Direction Cell #
Time From Saccade Start (ms)
g

Figure 4-4 Temporally Organized Representations of Saccade Direction

Overall, 26% (52/197) of neurons were significantly modulated (10,000 resampled MRL, $p < 0.05$) by saccade direction including 36% (29/81) of view cells and 20% (23/116) of non-view cells. For most (72%, 21/29) of the directionally modulated view cells, direction modulation was also observed for saccades outside of the field (*OUT2OUT* fixations) suggesting that the field location was not solely due to saccade direction. Some neurons (**A/B**) showed increases in firing rate before saccade onset, while other neurons (**C/D**) showed post-saccadic modulation during the subsequent fixation period. **E**) Not all view cells with fields along the edge of the image space showed direction tuning. **F)** The population of saccade direction modulated neurons tiled the full duration of the saccade and subsequent fixation period. The white letters indicate example neurons in A-D. Each row shows the normalized activity of one neuron. Normalized activity was calculated by subtracting the anti-preferred tuning curve from the preferred tuning curve and then dividing the resultant curve by its maximum firing rate. **G**) Distribution of preferred saccade directions across the population.

A-E) *First column*) Firing rate maps with Spearman's ($\rho_{1/2}$) spatial correlation between the first and second half of the recording session indicated at the top. *Second column*) smoothed polar plots showing direction tuning properties of the neuron for all saccades in orange and *OUT2OOUT* saccades in blue. In order to reduce directional biases in the view cells caused by large changes in firing rate across field boundaries, only *IN2IN* and *OUT2OUT* saccades were analyzed; most saccades were *OUT2OUT*. Peak firing rate and MRL (mean resultant length) are indicated at the top. *Third column*) peri-saccade rasters ranked by the saccade direction. The pink box indicates the time window in which the greatest direction tuning was observed. *Fourth column*) Peri-saccade firing rate curves for saccades in the preferred direction in green and anti-preferred direction in black.

MRLs were calculated without binning or smoothing. For visualization purposes only, polar plots were computed by calculating the average firing rate of saccade angles in 3º bins and further smoothed with a standard deviation of 9º. Peri-saccade firing rate curves were smoothed with a Gaussian kernel with a standard deviation of 15 ms.

of the field (*OUT2OUT* fixations) suggesting that the field location was not solely due to saccade direction. These results suggest that some view cells show conjunctive place and direction selectivity, consistent with place cells found in the bat (Rubin et al., 2014a) and rodent (Wiener et al., 1989) hippocampus. Consistent with our finding in view cells, a sequential-like representation of time was also observed across the population of saccade direction modulated neurons (**Figure 4.4G**). Strong evidence for purely pre-saccadic activity was missing though some (35%, 18/52) neurons increased their firing rate before saccade onset.

Previous studies using free-viewing tasks in monkeys have demonstrated recognition memory signals in hippocampal neurons (Jutras and Buffalo, 2010a; Jutras et al., 2013a). Here, we examined whether view cells show differential responses to novel and repeated images. Monkeys demonstrated increased fixation durations and changes in saccade amplitudes during repeated images compared to novel images suggesting that the monkeys were able to remember viewed images (**Figure 4.5**). A majority of view cells (78/109, 72%) were stimulus responsive, showing significant changes in firing rate aligned to the onset of the image presentation, while only 38% (91/238) of non-view cells were stimulus responsive (**Figure 4.6**). Further, 49% (82/168) of stimulus-responsive neurons showed significant differences in firing rate during novel compared to repeated images: 51% (40/78) of view cells and 46% (42/91) of non-view cells (**Figure 4.7**). These findings suggest that both view cells and non-view cells in the primate hippocampus participate in non-spatial forms of recognition memory.

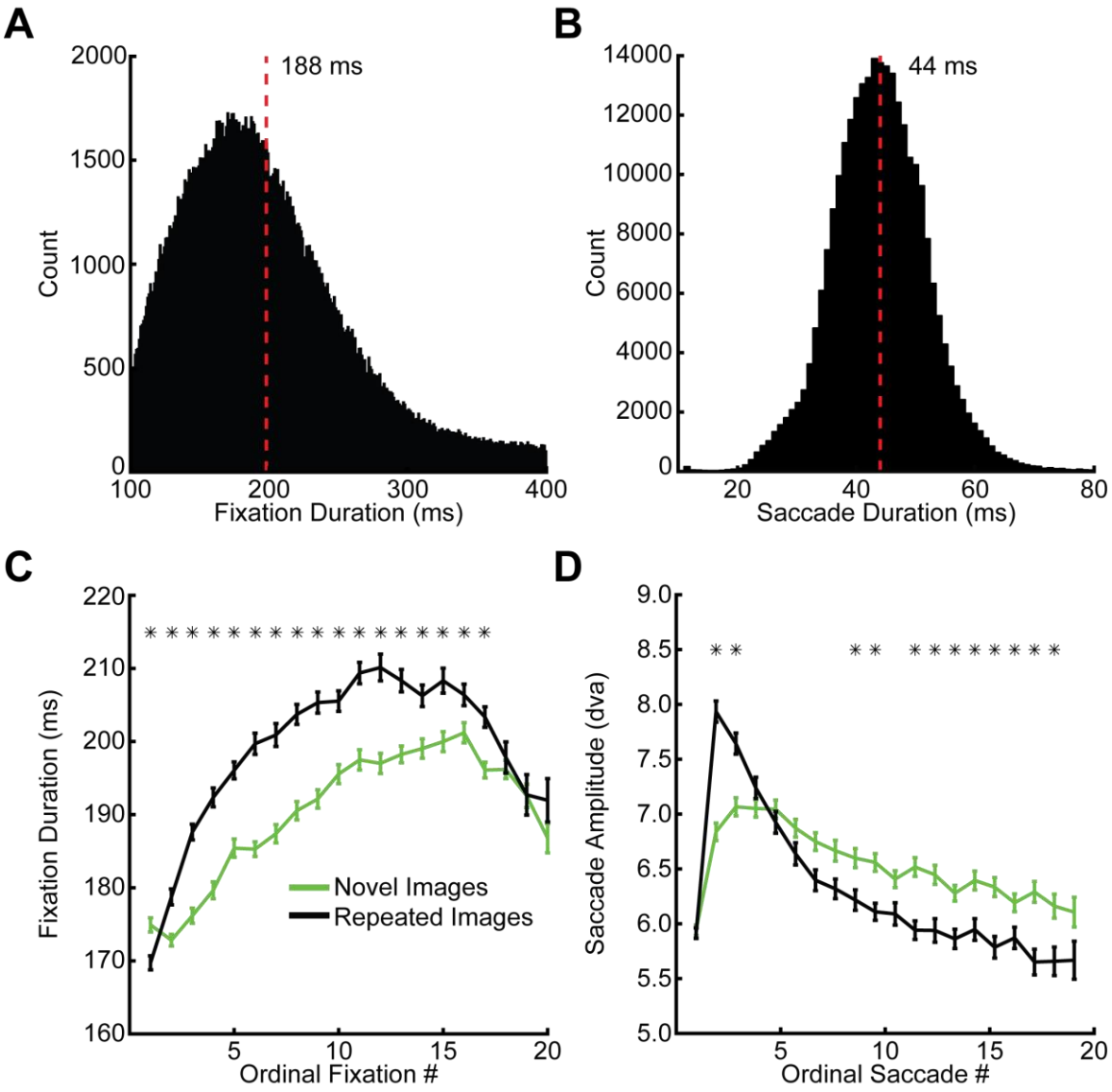

Figure 4-5 Eye Movements Statistics from 84 Recording Sessions

Fixations (**A**) varied greatly in duration while saccades were more narrowly distributed in duration (**B**). Mean fixation duration was 198 ms and a median fixation duration was 188 ms (red dashed line). The mean and median saccade duration was 44 ms. **C)** Monkeys produced fixations with longer durations during repeated image presentations than during novel image presentations ($p < 0.001$, signed-rank test). By ordinal fixation number, fixation durations were most often significantly longer during repeated image presentations than during novel image presentations (*, $p < 0.05$, paired t-test, Bonferroni corrected). **D)** On average, monkeys produced larger amplitude saccades during novel image presentations than during repeated image presentations ($p < 0.01$, signed-rank test). However, some of the early saccades were significantly larger in amplitude during repeated image presentations than during novel image presentations (*, $p < 0.05$, paired t-test, Bonferroni corrected). Error bars represent median ± s.e.m.

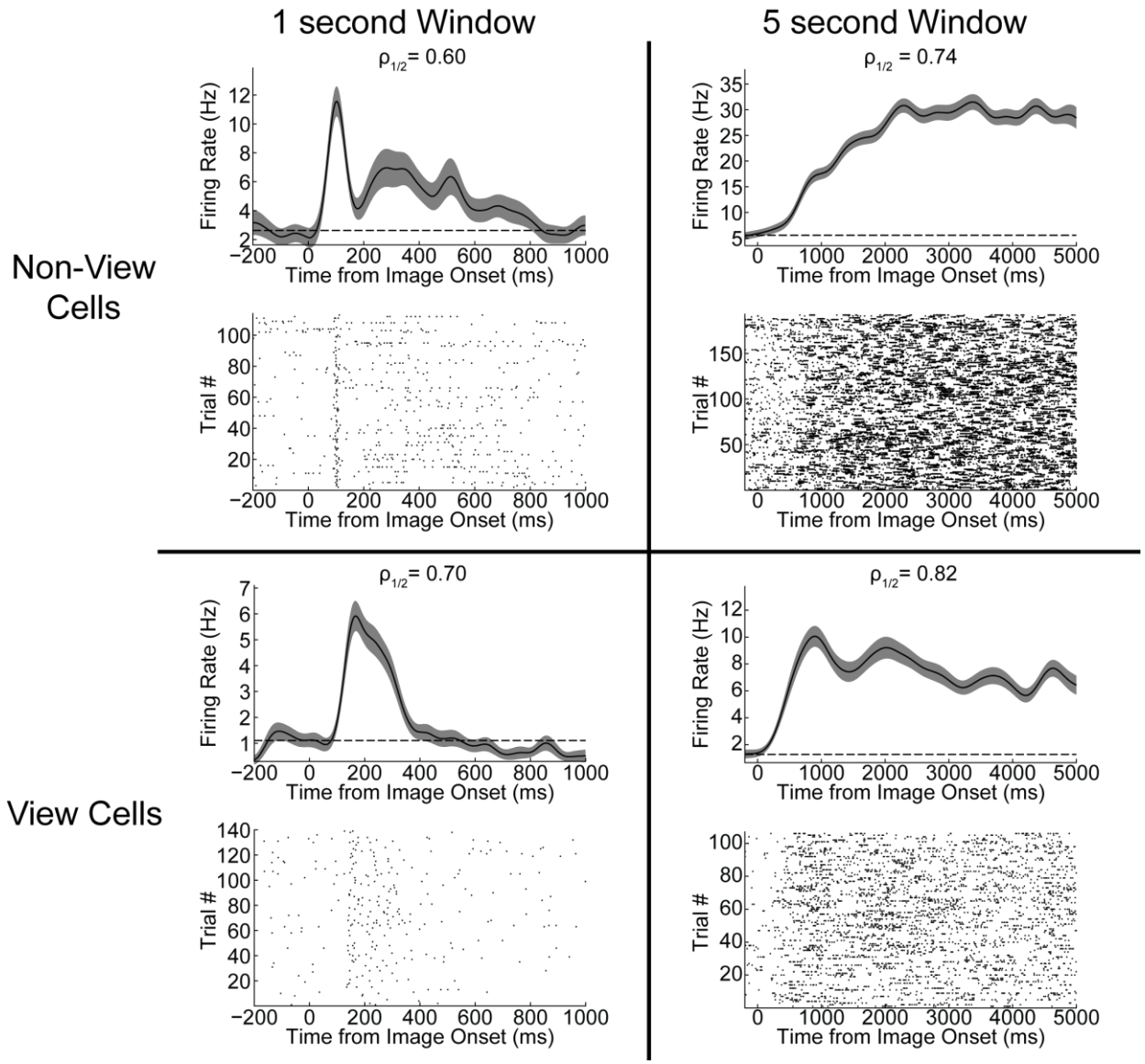

Figure 4-6 Stimulus Responsive Neurons

View cells (78/109, 72%) and non-view cells (91/238, 38%), showed consistent changes in firing rate (mean ± s.e.m.) following the start of the image presentation. Most neurons showed rapid changes in firing rate contained within the first 1 second of the image presentation period (*left column*). However, some neurons showed consistent changes in firing rate that were maintained or occurred later in the 5 second viewing period (*right column*). The black dashed line indicates the average firing rate during the 200 ms "baseline" period prior to the image appearing. Spearman's ($\rho_{1/2}$) temporal correlation between the first and second half of the recording session is indicated above the firing rate curves for each neuron.

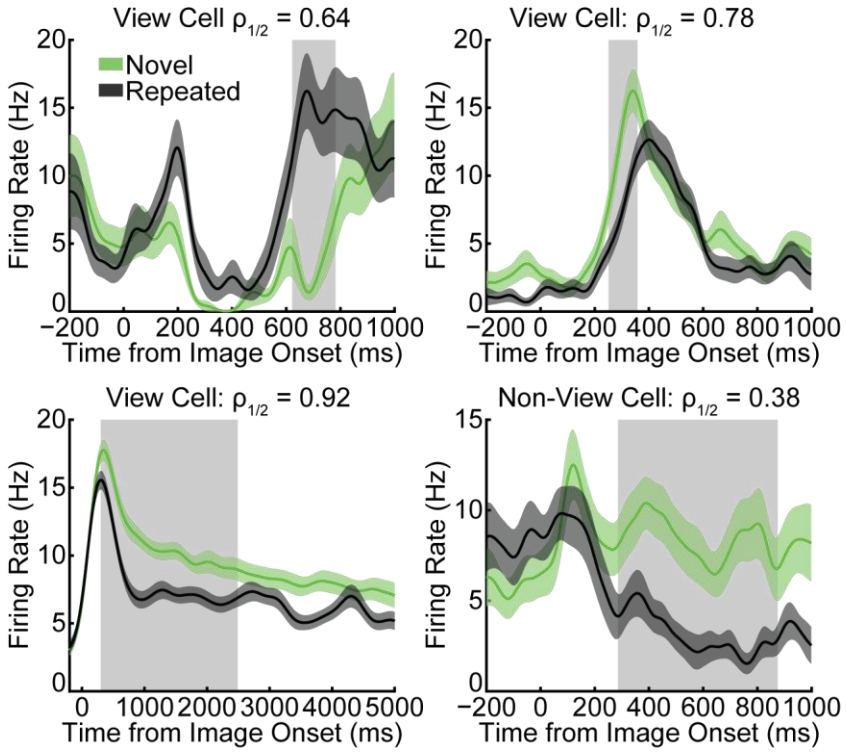

Figure 4-7 Conjunctive Spatial and Stimulus Memory Responses
Similar proportions of stimulus-responsive view cells (40/78, 51%) and non-view cells (42/91, 46%) showed significant differences (gray shading, $p < 0.05$) in firing rate dependent on whether the stimulus presented was novel (green) or repeated (black). Firing rate curves represent mean ± s.e.m. Spearman's ($\rho_{1/2}$) temporal correlation between the first and second half of the recording session for the stimulus response analysis is indicated at the top.

Contextual modulation is thought to enable the hippocampus to distinguish between memories with overlapping content. Therefore, we asked if view cells were modulated by behavioral context. Interleaved with the free viewing of images, monkeys performed a directed eye movement task in which monkeys received a reward for fixating a series of 4 simple shapes (**Figure 4.8a**). During the directed eye movement task, 75% (79/109) of view cells contained at least 1 shape in the field and 1 shape outside of the field. Of these 79 view cells, 48 (61%) view cells showed consistent spatial tuning across tasks with significantly higher firing rates when the monkey fixated shapes in the field compared to shapes outside the field (**Figure 4.9**). Further, 21 (27%) view cells showed no spatial tuning, and 10 (13%) view cells showed the opposite spatial tuning. In the directed eye movement task, view cells that showed consistent spatial tuning had a median peak firing rate of 7.9 Hz while view cells showing no spatial tuning had a median peak firing rate of 0.85 Hz ($p < 0.001$, *ks-test*). In comparison, view cells with the opposite spatial tuning had a similar firing rate (9.3 Hz vs. 7.9 Hz, $p > 0.31$, *ks-test)*. These results suggest that the view cells without spatial tuning in the directed eye movement task were silent. The 10 view cells with presumably opposite spatial tuning may have arisen from view cells with sensitivity to other task variables such as reward expectation. Alternatively, field shape and size may change across contexts. Overall, many of the view cells showed contextual modulation by changing their firing rate across different behavioral tasks, and on average view cells fired 2.0 times faster for their preferred task (**Figure 4.8b**).

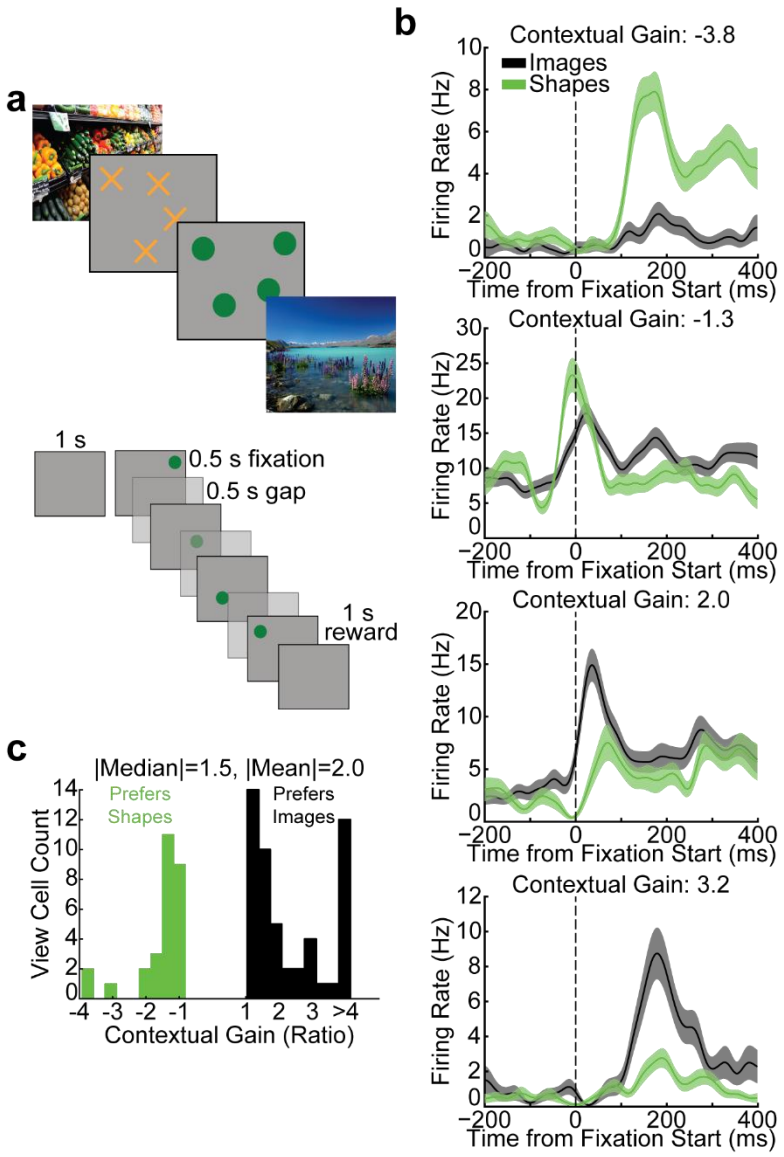

Figure 4-8 View cells are Contextually Modulated

A) In between the free viewing of images, the monkeys performed a directed eye movement task in which they fixated a series of 4 shapes as the shapes appeared on the screen. Many (48/79, 61%) view cells identified during the free viewing of images also demonstrated consistent spatial tuning during the directed eye movement task. **B**) Additionally, most view cells showed contextual modulation in that view cells fired faster during the directed eye movement task than during the free viewing of images (*top two view cells*) or fired faster during the free viewing of images than the directed eye movement task (*bottom two view cells*). Firing rate curves (mean ± s.e.m.) for in field fixations (*OUT2IN*) during the free viewing of images are in black while fixations on in field shapes during the directed eye movement task are in green. The bottom two view cells are the neurons in Figure 4.2b and 4.2c. **C**) Across this population of 79 view cells with at least 1 shape in the field and 1 shape outside the field, the median contextual gain was 1.5 and the mean contextual gain was 2.0.

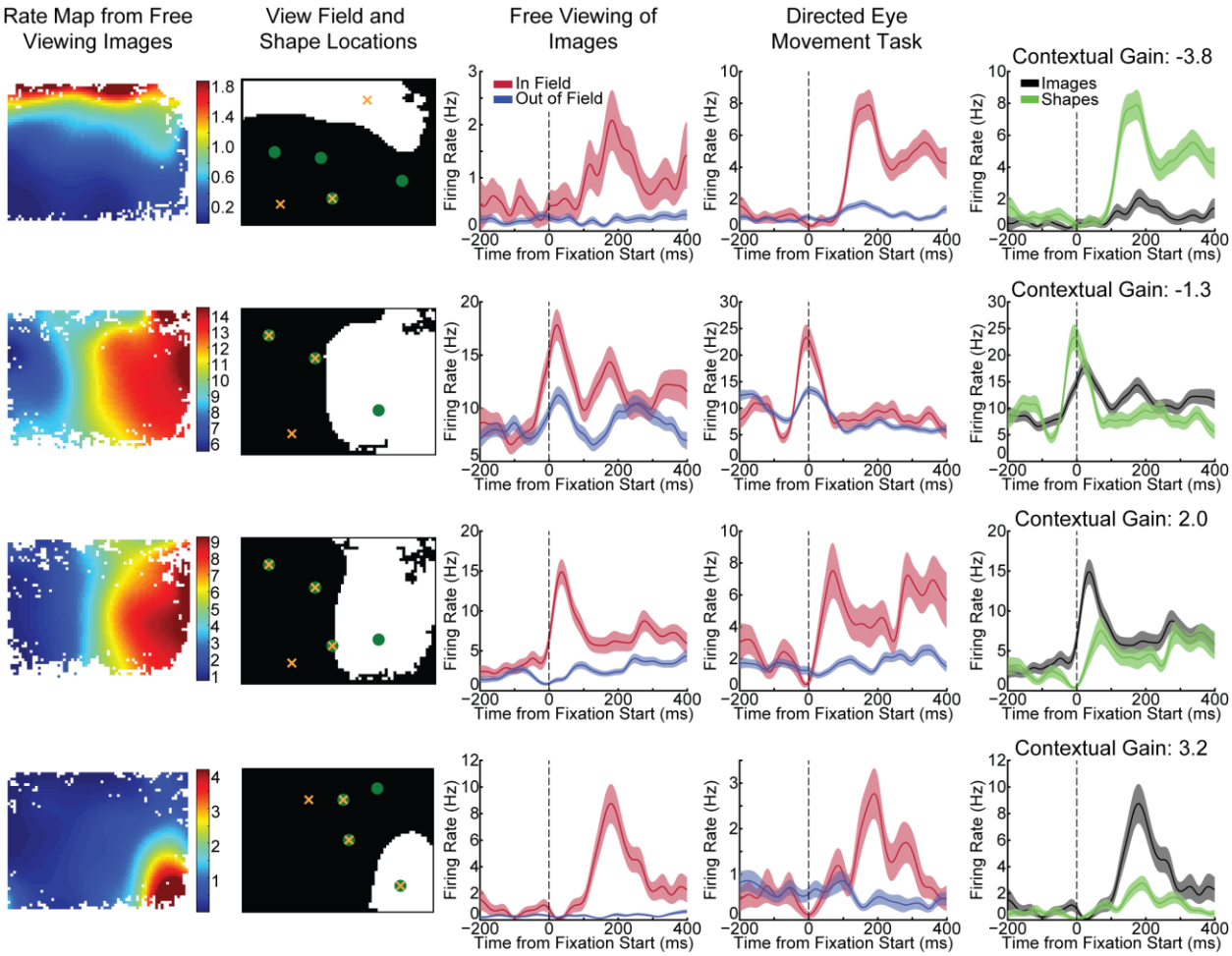

Figure 4-9 Extended Figure 4.8: View cells are Contextually Modulated

View cells organized by row in the same manner as in Figure 4.8b. **Column 1**) Firing rate maps calculated during the free viewing of images. **Column 2**) View field location in white and out of field locations in black overplayed with the shapes from the directed eye movement task (orange X's series 1, green O's series 2). **Column 3**) Peri-fixation firing rate curves for in field (*OUT2IN*) and out of field (*OUT2OUT*) fixations during the free viewing of images. **Column 4)** Peri-fixation firing rate curves for fixations on shapes in the field and outside of the field during the directed eye movement task. **Column 5**) Peri-fixation firing rate curves for in field fixations during the free viewing of images and the directed eye movement task plotted to the same scale. Note, the 2nd and 3rd view cells were simultaneously recorded on different electrodes; despite showing similar spatiotemporal properties, the 2nd view cell shows a weak preference for the directed eye movement task while the 3rd view cell shows a strong preference for the free viewing of images.

In summary, our results demonstrate that eye movements temporally organize spatial and contextual representations in the primate hippocampus. Specifically, each spatially modulated neuron fired at a consistent latency relative to the start of an eye movement with the neuronal population forming a sequential-like representation of time across the extent of the saccade and fixation. We hypothesize that the sequential organization of spatial representations is an important mechanism for forming spatial relationships between viewed items across consecutive eye movements. View cells also responded to the stimulus presentation and differentiated between novel and repeated stimuli. The combination of spatial, temporal, contextual, and stimulus information within a single neuron may be important for the formation of relational memories. Overall, our results highlight the importance of active sensing in shaping neural representations in the hippocampus. Further supporting the importance of active sensing, place codes in the bat hippocampus differ for echolocation and vision even in the same environment (Geva-Sagiv et al., 2016).

The structure and function of the medial temporal lobe are largely conserved across species. However, the cortical connections of the medial temporal lobe are overwhelmingly visual in primates (Suzuki and Amaral, 1994a) compared to rodents in which olfaction dominates (Burwell and Amaral, 1998b). The hippocampus in every species processes similar information (e.g. spatial), but we also find that eye movements signals in the primate hippocampus which can largely be explained by the differences in cortical connections. Several higher-order thalamic nuclei may also play an important role in providing the medial temporal lobe with eye movement-related signals (Schlag-Rey and Schlag, 1984; Aggleton et al., 2011). These nuclei may contain an efference copy of the eye movement signal allowing the hippocampus to update spatial representations in real time.

At first, our results appear to contradict studies in humans finding that the hippocampus and entorhinal cortex represent the physical location of the person in virtual reality (Ekstrom et al., 2003; Jacobs et al., 2013). However, gaze-contingent responses are rarely reported in human studies. Importantly, view cells do not preclude a physical place code in the primate hippocampus. In fact, a recent virtual reality experiment showed that the primate hippocampus contains representations of both gaze and location (Wirth et al., 2017).

4.1 Methods Summary

Neurons in the hippocampus were acutely recorded while monkeys freely viewed full-screen images on a computer monitor that subtended 33 by 25 degrees of visual angle. In between the free viewing of images, monkeys performed a directed eye movement task in which monkeys fixated a series of 4 simple shapes to receive a food-based reward; monkeys learned two novel series during each recording session. Monkeys were head-fixed in a dimly illuminated room and positioned 60 cm away from a 19 inch CRT monitor. Eye movements were recorded at 240 Hz using a noninvasive infrared eye-tracking system (ISCAN). Fixations and saccades were detected using Cluster Fix (Konig and Buffalo, 2014). Spikes were recorded (filtered from 250 Hz to 8 kHz) using 4 independently movable tungsten microelectrodes (FHC). For each neuron, firing rate maps were computed with a Gaussian smoothing procedure (Killian et al., 2012). Spearman's rank correlation ($\rho_{1/2}$) between firing rate maps for the first and second half of the recording session as well as Skagg's information score (Skaggs et al., 1993) across the whole session were used to evaluate spatial modulation of neurons; the observed values were then compared to 1,000 time-shifted permutations of spikes trains to determine significance. Stimulus responses to the appearance of the image and eye movement aligned responses were evaluated in the same manner using peri-event firing rate curves. Reliability of spatial responses across eye movements,

consistency of spatial response across behavioral contexts, recognition memory signals, saccade direction modulation, and saccade amplitude modulation was evaluated using 10,000 resampled permutations and when appropriate corrected for multiple comparisons using cluster-level statistics (Maris and Oostenveld, 2007). All procedures were carried out in accordance with the National Institutes of Health guidelines and were approved by the University of Washington Institutional Animal Care and Use Committee.

4.2 Full Methods

4.2.1 *Electrophysiological Recording and Behavioral Tasks*

All procedures were carried out in accordance with the National Institutes of Health guidelines and were approved by the University of Washington Institutional Animal Care and Use Committee. Electrophysiological recordings were conducted in two rhesus monkeys (Macaca mulatta): 1 male (4.6 yo, 10.7 kg) and 1 female (4.3 yo, 10.3 kg). Before implantation of recording hardware, monkeys were scanned with an MRI to localize the hippocampus and to guide placement of the recording chamber. Then we surgically implanted a cilux plastic chamber (Crist Instrument Co.) for recording neural activity and a titanium post for holding the head. We performed a postsurgical MRI to determine recording locations.

Monkeys were head-fixed in a dimly illuminated room and positioned 60 cm away from a 19 inch CRT monitor with a refresh rate of 120 Hz. The monitor was 600 by 800 pixels large and subtended 25 degrees by 33 degrees of visual angle (dva). Eye movements were recorded at 240 Hz using a noninvasive infrared eye-tracking system (ISCAN). Stimuli were presented using experimental control software (CORTEX, www.cortex.salk.edu). Initial calibration of the infrared eye tracking system consisted of a nine-point manual calibration task. *Post-hoc* calibration was

achieved by presenting additional calibration trials before starting the electrophysiological recording.

We used Cluster Fix to detect fixations and saccades (Konig and Buffalo, 2014). Briefly, Cluster Fix determined the distance, velocity, acceleration, and angular velocity components of the scan path. Cluster Fix found natural divisions in these four parameters using *k*-means clustering to separate scan paths into fixations and saccades; Cluster Fix required a minimum fixation and saccade durations of 25 ms and 10 ms, respectively. To improve the reliability of scan path segmentation, Cluster Fix used 25 replications of the *k*-means algorithm.

Monkeys performed the calibration task, a delayed-match-to-sample task, or watched videos while we lowered electrodes down into the hippocampus. The recording apparatus consisted of a multichannel microdrive (FHC Inc.) holding a manifold consisting of a 23-gauge guide tube containing four independently movable tungsten microelectrodes (FHC Inc.), with each electrode inside an individual polyamide tube. Electrode tips were separated horizontally by 190 μm. Electrode impedance at 1000 Hz ranged from 1 to 3 MΩ. For each recording, the guide tube was slowly lowered through the intact dura mater and advanced to ~1-2 mm dorsal to the hippocampus (often the caudate) with the use of coordinates derived from the MRI scans. The electrodes were then slowly advanced out of the guide tube into the hippocampus. In addition to the MRI, we used physiological markers such as firing rate to more accurately locate the hippocampus. Once we isolated neurons in the hippocampus, electrodes were allowed to settle for at least 15 minutes before starting the recording. No attempt was made to select neurons based on firing pattern. Instead, we lowered electrodes down until we found units, let the electrodes settle, and then we started the recording often finding different units were active in different tasks. At the end of each recording session, the microelectrodes and guide tube were retracted. Recordings took

place in the left anterior portion of the hippocampus in one monkey and in the right posterior portion of the hippocampus in the other monkey. We did not discriminate between hippocampal subfields, and we putatively recorded from CA1-4, the dentate gyrus, and the prosubiculum.

Data amplification, filtering, and acquisition were performed with a Multichannel Acquisition Processor system from Plexon, Inc. The neural signal was split separately to extract the spike and the LFP components. For spike recordings, the signals were filtered from 250 Hz to 8 kHz, further amplified, and digitized at 40 kHz. LFPs were filtered from 0.7 Hz to 170 Hz, further amplified, and digitized at 1000 Hz. A spike threshold was set interactively, to separate spikes from noise, and spike waveforms were stored in a time window from 200 μs before to 600 μs after threshold crossing. Recordings typically yielded between two and six units. Units were later sorted manually using Offline Sorter (Plexon, Inc.).

Recordings were conducted while monkeys freely viewed images and performed a directed eye movement task. Images were downloaded from Flickr, and image content was not filtered. The recording session started with the directed eye movement task in which monkeys fixated a series of simple shapes as they appeared on a screen to receive a reward. On each trial, either one of 2 series consisting of 4 simple shapes were presented. Each shape in the series appeared one at a time. Monkeys were required to fixate each shape in the series for 500 ms within a square fixation window with a width of 5 dva. Following the successful fixation of each shape, the shape then disappeared. There was then a 500 ms inter-shape-interval in which nothing appeared on the screen. Following the successful fixation of all 4 shapes in the series, the monkey received several food rewards evenly spaced over a 1000 ms period; a sound beep was played at the time of each reward pulse.

Each day, a series of 4 shapes were randomly generated from 4 different colors (green, yellow, cyan, and magenta) and 6 different shapes (circles, ellipses, rectangles, X's, O's, and triangles). Shapes were as small as possible and either 0.38 dva by 0.38 dva, 0.75 by 0.38 dva, or 0.75 by 0.75. Shapes could be presented at various rotations. Shape locations were generated on a 1 by 1 dva grid and subtended a maximum of 24 by 18 dva. Shape characteristics were determined before the recording and did not change throughout the recording session. Finally, across the two series, 1 random shape or the first 3 shapes overlapped in location and order.

At the beginning of each recording session, the monkeys performed 10 familiarization trials of the first series followed by 10 familiarization trials of the second series. Thereafter, trial order was pseudorandomized across the remaining recording session. In total, the monkeys performed up to 404 directed eye movement trials. Following each directed eye movement trial, a 1000 ms inter-trial-interval occurred in which only a dark gray background was displayed. Following the familiarization trials, monkeys freely viewed complex images in between every two directed eye movement trials.

Images were full screen and subtended 25 degrees by 33 dva. Each image trial began with the presentation of a 0.5 dva light gray cross in the center of the screen against a dark gray background. The monkey was required to fixate the cross, within a fixation window of 7 dva, for 500 to 750 ms. Following a successful fixation, an image was displayed and the monkey was allowed to freely view the image for 5 seconds of cumulative looking time. We only analyzed the first 7.5 seconds of the image trial, regardless of the length of the image presentation. Image presentations were organized into 6 blocks with each block consisting of 16 novel images followed by the repeated presentation of these same 16 images in the same order. In total each recording session consisted of up to 96 novel images and 96 repeated images.

4.2.2 *Data Analysis*

Data analysis was implemented in MATLAB (Mathworks, Inc.) using custom-written code. We recorded from 347 hippocampal units in two monkeys (123 units in monkey PW and 224 units in monkey TO). Well isolated single units were manually isolated when possible based on cluster quality in Plexon Inc.'s Offline Sorter; otherwise, 19 units were designated as possible multiunits but still used in all analyses. Waveforms and spike times were then imported into MATLAB. Gross firing rate stability was assessed by calculating the average trial-by-trial firing rate across the recording session. Trials in which a neuron's firing rate consistently drifted by more than 1 standard deviation away from the mean trial-by-trial average were removed. Only neurons whose firing rate was stable for at least 64 image presentations (at least 128 directed eye movement trials) were used for further analysis. Firing rate stability was also confirmed by visually assessing rasters aligned to the start of image trials, start of the directed eye movement trials, reward periods, eye movements, and inter-trial-intervals to ensure that the trial-by-trial average firing rate accurately reflected neural activity, especially for the low firing rate neurons. Neurons were never excluded based on particular firing patterns. We further removed neurons whose firing rate likely drifted due to mechanical instability in which the waveform amplitude likely affected threshold crossings. Neurons with fewer than 100 sorted spikes were removed as well.

4.2.3 *View Cell Spatial Analysis*

Firing rate maps were computed with a Gaussian smoothing procedure (Killian et al., 2012). Eye position data from the image presentation periods were concatenated across trials. The first 500 ms of data after the image appeared was removed in order to negate strong stimulus responses combined with a strong central bias. Spikes (sampled at 1000 Hz) and eye position (up-

sampled to 1000 Hz) were independently binned into 0.5 dva square bins over the image space. The resulting values were then smoothed by convolving with a 2D Gaussian filter with a standard deviation of 3 dva. Finally, the smoothed spike counts and eye position were divided to estimate the firing rate map. Bins without any eye coverage were removed from the rate maps. For visualization purposes only, rate maps were scaled to the 97.5^{th} percentile of the firing rate values to ensure that outliers did not affect visualization.

For each neuron, significant spatial modulation was determined by calculating the spatial correlation (Spearman's $\rho_{1/2}$) between firing rate maps for the first and second half of the recording session in addition to calculating Skagg's information score for the whole recording session (Skaggs et al., 1993). The observed values were compared to bootstrapped rate maps calculated from 1,000 time-shifted permutations of the spike trains. Skagg's information score alone was found to produce unreliable results (see next section), while we found Spearman's rank correlation coefficient ($\rho_{1/2}$) produced more reliable results. To assess spatial stability using Spearman's correlation coefficient ($\rho_{1/2}$), spike trains and eye position data were first divided in half across the recording session before bootstrapping firing rate maps. Spike trains were shifted by at least 10 seconds. View cells were determined to be neurons that possessed observed spatial correlation and Skagg's information score that exceeded the 95^{th} percentile of the bootstrapped data.

View field location was determined by dividing the firing rate distribution of the rate maps into high firing rates (in the field) and low firing rate (out of the field) regions. First, firing rates above the 95^{th} percentile were set to the 95^{th} percentile so that we could better fit low firing rate values. We then used *k*-means to categorize the firing rates into 2 to 3 clusters; the appropriate number of clusters was determined using silhouette width. The cluster containing the highest firing rate values was defined as in field pixels, and the remaining cluster(s) were defined as

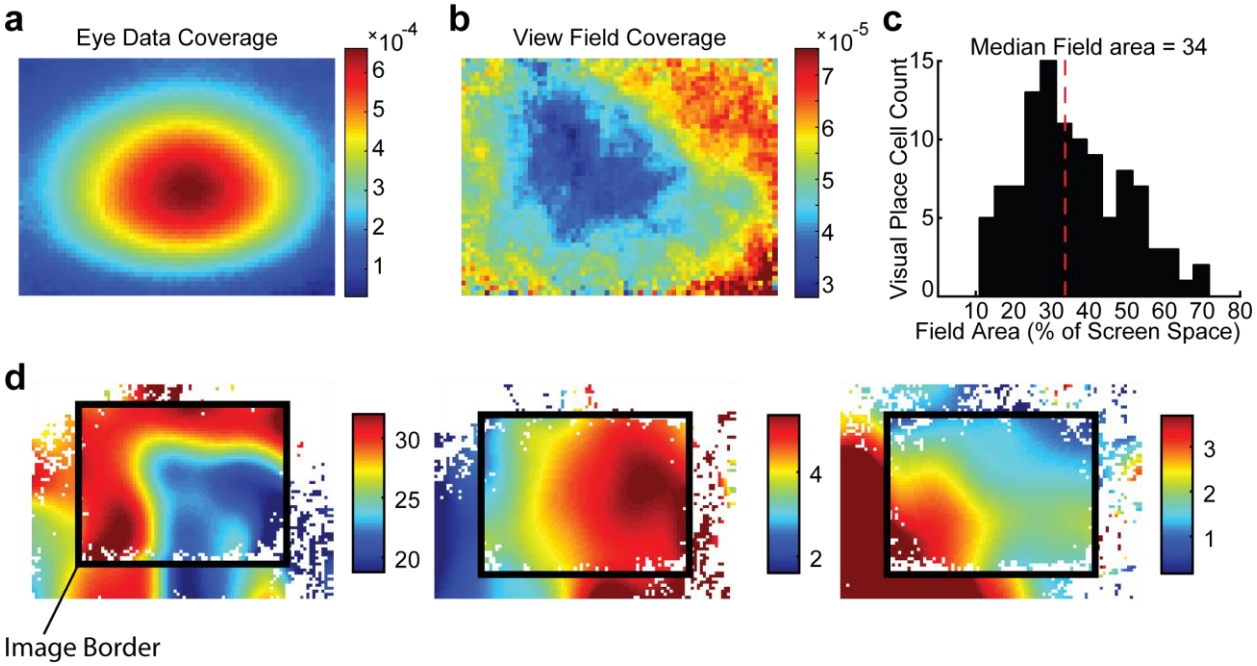

Figure 4-10 Eye and View Field Coverage

A) Eye data (binned and smoothed) used to calculate firing rate maps for the view cells showed a clear central bias where the monkeys gazed more often at the center of images than the edges. The first 500 ms of the image presentation period was removed. **B)** View fields, on the other hand, were observed more often along the edge of the image than in the center of the image. **C)** On average, view fields occupied 34% of the image space. **D)** Three example view cells in which the data suggest that the place fields extended past the border of the image. Since coverage was limited, data outside of the image boundary were obtained from the whole recording session; most of the off-screen data was obtained from the inter-trial-interval when nothing was presented on the screen. Firing rate maps outside the image boundary were scaled to the firing rate maps obtained during the free viewing of images. These results suggest that view cells could be anchored to the image border. Alternatively, view fields may have rather large fields, and we could be sampling only a small portion of the field.

as out of field pixels. This method is analogous to fitting Gaussian distributions to the firing rate values. View field size was estimated by the percentage of the image covered by in field pixels. In nearly all view cells, only 1 contiguous field was identified.

4.2.4 *Reliability of Spatial Representations Across Fixations*

Interestingly, many of the view fields appeared along the edge of the monitor (**Figure 4.10B**), and on average fields were rather large, occupying approximately 34% of the image space (**Figure 4.10C**). Additionally, many view fields appeared to extend their spatial tuning past the border of the image (**Figure 4.10D**). Given that many fields appeared along the border of the image where eye coverage was more limited (**Figure 4.10A**), we asked whether view cells showed reliably higher firing rates across fixations in the field compared to fixations out of the field. We divided fixations into in field and out of field fixations based on fixation location. Peri-fixation firing rate curves were then calculated for in field and out of field fixations by aligning spike trains to these fixations and smoothing them with a Gaussian kernel with a standard deviation of 15 ms. We calculated the firing rate curve for 200 ms before (~1 fixation) the start of the fixation until 400 ms after (~2 fixation periods) the fixation started. The observed difference in smoothed firing rate curves was compared to the shuffled difference of 10,000 resampled permutations in which in field and out of field assignments were randomly assigned to fixations (Fujisawa et al., 2008; Prerau et al., 2014). Time points in which the observed difference was greater than the 95^{th} percentile of the shuffled difference were determined to be significant. Further, view cell responses were deemed reliable if neurons displayed at least 30 ms (2 standard deviations) of contiguous significant differences between in field and out of field firing rates when corrected for multiple comparisons using cluster-based statistics (Maris and Oostenveld, 2007). This analysis is

analogous to a sliding window analysis using a 1-tailed t-test but can be used on nonparametric distributions and can account for sampling biases.

Firing rates aligned to fixation were normalized for peak detection as well as for the pseudo-population plot in **Figure 4.2**. For each neuron, we estimated the "baseline" firing rate by taking the average firing rate 200 ms before the in field fixation. The "baseline" firing rate was then subtracted from the firing rate curve. Finally, the firing rate curve was then divided by the peak firing rate. Peaks were detected using *findpeaks* in MATLAB using a minimum width of 30 ms (2 standard deviations). Three view cells showed ramp-like responses without a definable peak and were removed from the subsequent temporal analyses. Peaks which were less than two-thirds the maximum firing rate were ignored. Further, peaks detected at times that were not significantly different between in field and out of field fixations were also ignored. In the case that multiple peaks were still detected, the first peak was used.

4.2.5 *Eye Movement Modulation, Saccade Direction, and Saccade Amplitude Analysis*

Peri-fixation firing rate curves were calculated for each neuron during image presentation trials. Fixations during the first 500 ms after the image appeared were removed in order to avoid the influences of strong stimulus responses. Peri-fixation firing rate curves were calculated by aligning spike trains to all fixations and smoothing them with a Gaussian kernel with a standard deviation of 15 ms. We calculated the firing rate curve for 200 ms before (~1 fixation) the start of the fixation until 400 ms after (~2 fixation periods) the start of the fixation. Significant eye movement modulation was determined by calculating the temporal correlation ($\rho_{1/2}$) between firing rate curves for the first and second half of the recording session in addition to calculating Skagg's information score for the whole recording session. The observed values were compared to bootstrapped firing rate curves calculated from 1,000 time-shifted permutations of the spike trains.

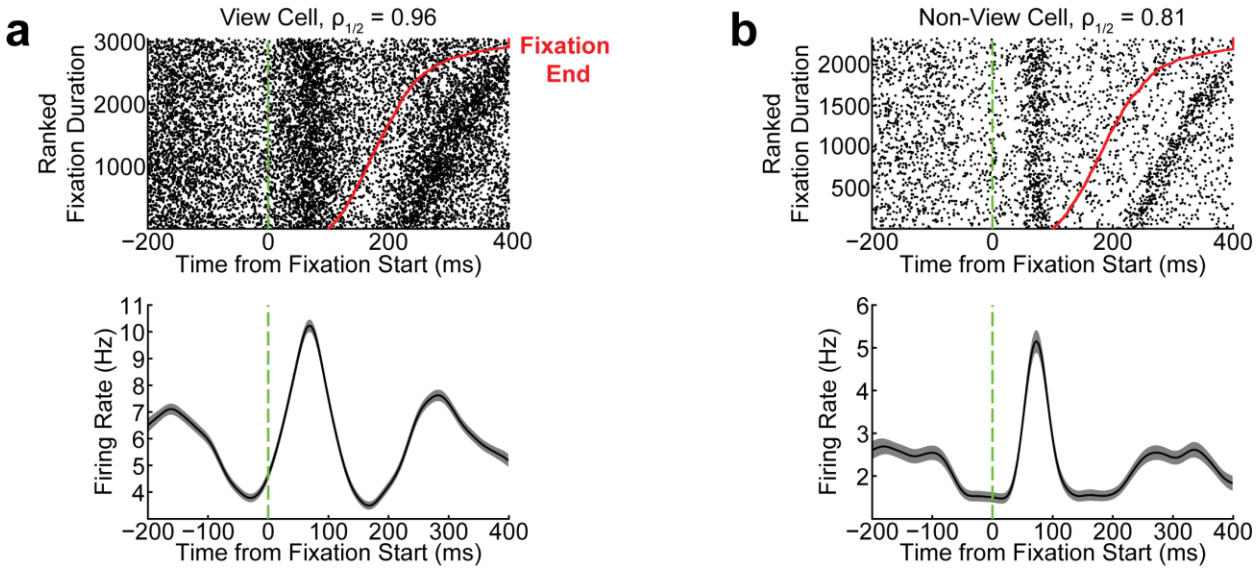

Figure 4-11 Eye Movement Modulated Neurons

A) 46/109 (43%) view cells showed consistent changes in firing rate across all eye movements. *Top*: Rasters ranked by fixation duration show consistent neural activity across 1000s of fixations of different durations. Consistent neural activity can be observed for the following fixation period as well. Fixation onset is at time 0 (green dashed line) and fixations end at the solid red line. We did not rank fixations preceding or following the fixations that started at time 0. Spearman's ($\rho_{1/2}$) temporal correlation between the first and second half of the recording session is indicated above each raster. *Bottom*: the average peri-fixation firing rate curve calculated from the raster above. **B)** Of the remaining neurons that were non-spatial, non-directional, non-amplitude modulated, (21/202, 10%) neurons showed consistent changes in firing rate across all eye movements.

Spike trains were randomly time-shifted relative to the start of fixation. Neurons were considered to be significantly modulated by eye movements if both observed values exceeded the 95th percentile of the bootstrapped values.

When considering the neural activity across *all* eye movements regardless of fixation location, 43% (46/109) of view cells showed significant firing rate modulation across *all* fixations (**Figure 4.11A**). A small number (21/202, 10%) of non-spatial, non-direction, non-amplitude modulated neurons, showed significant eye movement modulation as well (**Figure 4.11B**). These neurons may be similar to theta modulated neurons in rodents, and these neurons may aid in sequentially organizing view cells. Alternatively, these neurons may be spatially modulated but not evidently so during the free viewing of images.

Due to a large number of view cells with view fields along the border of the image, it is possible that view cells are really directionally modulated cells due to the strong direction biases caused by the image geometry. We determined neurons to be modulated by saccade direction if the observed mean resultant length (MRL) was greater than the 95th percentile of 10,000 resampled permutations in which saccade directions were randomly assigned to saccades. First, we crudely estimated direction tuning by calculating peri-saccade firing rate curves for 8 different directions--the cardinal and intermediate directions. Using these peri-saccade firing rate curves, we identified the time window in which there was the greatest difference in firing rate in the 8 different directions. Second, we more accurately estimated this time window by finding the full-width-half-max of the greatest change in firing rate between preferred direction and anti-preferred direction. The minimum window width was set to 50 ms. The preferred saccade direction was defined as the saccade direction that corresponded to the largest firing rate while the anti-preferred saccade direction was defined as the saccade direction that corresponded to the smallest firing rate.

Preferred saccades were determined to be saccade directions within a certain range, 15 to 45 degrees, of the absolute preferred direction; the range was defined as the full-width-half-max of the direction tuning curve. Third, we used this time window to calculate the observed and bootstrapped MRLs across all saccade directions. If the neuron was classified as a view cell, then saccades entering (*OUT2IN*) or leaving (*IN2OUT*) the field were removed as these saccades could bias the preferred and anti-preferred saccade directions. Out of field (*OUT2OUT*) saccades were also analyzed separately for view cells using the same time window.

Because it was important to remove *OUT2IN* and *IN2OUT* saccades from the analysis of view cells, fixations preceding and following the saccade were removed if they started or ended before the time window. If the end of the time window was greater than the median fixation duration, then the time window was truncated to the median fixation duration. Unfortunately, this will be detrimental for analyzing neurons with longer response latencies and results in the window to be no more than approximately 232 ms (median fixation duration plus median saccade duration) from the start of the saccade. As a result, a large portion of the data for some neurons were removed to fit the criteria above. Therefore, we removed neurons that fired a spike on less than 5% of saccades in the time window of interest (approximately an average firing rate of 0.5 Hz or less). The same methodology was also applied to non-view cells.

Analysis of saccade amplitude modulation was conducted in a similar manner. We determined neurons to be modulated by saccade amplitude if the magnitude of the observed Spearman's rank correlation (ρ) between saccade amplitude and firing rate, was greater than the 95^{th} percentile of 10,000 resampled permutations in which saccade amplitudes were randomly assigned to saccades. The magnitude of the correlation was used as we found significant positive and negative correlations. Firing rate curves were calculated across saccade amplitudes in 2 dva

bins. Saccades with amplitudes less than 2 dva and greater than 16 dva (95th percentile of saccade amplitudes) were removed from this analysis. Only a marginal proportion (*chi-square test*, $p = 0.07$) of neurons (10.0%, 18/180) showed significant saccade amplitude modulation suggesting that amplitude information is not present to the same extent as direction information in the primate hippocampus.

4.2.6 *Stimulus Responses and Recognition Memory*

Significant stimulus responses to the presentation of images were determined by first comparing the "baseline" firing rate of each neuron 200 ms before the image appeared to 200 ms periods after the image appeared (Jutras and Buffalo, 2010b). To compare firing rates, we used a sliding window with a step size of 25 ms to test whether the firing rate had changed significantly ($p < 0.01$) using a ks-test. However, many neurons appeared to respond during the fixation on the central crosshair (500-750 ms in duration) which made baseline firing rate estimates difficult. Therefore, we used temporal correlation (Spearman's $\rho_{1/2}$) and Skagg's information score to find stimulus responsive neurons. Peri-image onset firing rate curves were calculated by aligning spike trains to the appearance of images from 200 ms before image onset to 1000 ms after image onset. Firing rate curves were then smoothed with a Gaussian kernel with a standard deviation of 30 ms. Then the observed temporal correlation between the first and second half of the recording session as well as Skagg's information across the whole recording session score were compared to 1,000 time-shifted permutations of the spike trains. For each image trial, spike trains were randomly time-shifted relative to image onset. Neurons were considered to show significant stimulus responses if both observed values exceeded the 95th percentile of the bootstrapped values. Most neurons showed significant stimulus responses using the method described in Jutras and Buffalo (Jutras and Buffalo, 2010b) and the method described here.

Further, some neurons also appeared to respond later in the image viewing period or maintain higher than "baseline" firing rates throughout the whole viewing period. Unlike Jutras and Buffalo, (Jutras and Buffalo, 2010b) here image viewing periods were much longer and lasted at least 5 seconds. Stimulus responses that occurred later in the viewing period were assessed in a similar manner but up to 5 seconds after the image appeared. For this analysis, spike trains were smoothed with a wider Gaussian kernel of 150 ms to remove low-frequency firing rate modulations.

To assess recognition memory responses, we asked whether neurons showed differential responses to novel and repeated images. Peri-image onset firing rate curves were calculated for pairs of novel and repeat image presentations separately. Only pairs of the novel and repeated images were compared in case neurons responded to particular image content. Further, this analysis was only conducted on stimulus responsive neurons (analysis above), for short time periods after image onset (1000 ms) or long time periods (5000 ms). The observed difference in firing rate curves for novel and repeated image presentations was compared to the shuffled difference of 10,000 resampled permutations in which novel and repeat assignments were randomly assigned to trials (Fujisawa et al., 2008; Prerau et al., 2014). Time points in which the observed difference was greater than or less than the 95^{th} percentile of the shuffled difference were determined to be significant. Further, recognition memory responses were deemed reliably different if neurons displayed at least 60 ms (2 standard deviations) of contiguous significant differences in firing rate between the novel and repeated images when corrected for multiple comparisons using cluster-based statistics (Maris and Oostenveld, 2007). For longer time period analyses, clusters of contiguously significant time points less than 300 ms (2 standard deviations)

in duration were ignored. This analysis is analogous to a sliding window analysis using a 2-tailed t-test ($p < 0.05$) but can be used for nonparametric distributions.

Due to several factors--such as stimulus presentation length, the addition of the directed eye movement task, and stability of single unit isolation--we did not have enough image presentations to replicate previous recognition memory studies (Jutras and Buffalo, 2010a). In particular, post-hoc analysis of behavior (e.g. fixation durations) suggested we would need all 96 novel and repeat presentations to correlate behavior with memory responses. Unfortunately, most view cells were not well isolated for the whole 70-minute recording session; as mentioned above we only analyzed trials while units were well isolated.

4.2.7 *Contextual Modulation*

To determine if view cells were modulated by behavioral context, we compared the firing rates of view cells identified during image trials to their activity during the directed eye movement trials. First, in the directed eye movement task, we asked if the firing rate of view cells was higher during fixations on shapes in the field compared to firing rates during fixations on shapes outside of the field. Shapes on the border (within 0.5 dva) of the view field were first removed. We divided fixations into in field and out of field fixations based on shape location. Peri-fixation firing rate curves were then calculated for in field and out of field fixations by aligning spike trains to these fixations and smoothing them with a Gaussian kernel with a standard deviation of 15 ms. We calculated the firing rate curve 200 ms before the start of the fixation until 400 ms after the start of the fixation. The observed difference in firing rate curves was then compared to the shuffled difference of 10,000 resampled permutations in which in field and out of field assignments were randomly assigned to fixations. Time points in which the observed difference was greater than or less than the 95^{th} percentile of the shuffled difference were determined to be significant. Further,

spatial consistency across tasks was deemed reliable if neurons displayed at least 30 ms (2 standard deviations) of contiguous significant differences in firing rate between in field and out of field fixations when corrected for multiple comparisons using cluster-based statistics (Maris and Oostenveld, 2007). This analysis is analogous to a sliding window analysis using a 2-tailed t-test ($p < 0.05$) but can be used on nonparametric distributions and can account for sampling biases.

In the directed eye movement task, peak response latencies for in field fixations were calculated in the same manner as during the free viewing task. However, the majority of neurons showed ramp-like responses without a definable peak; in this case, the maximum firing rate was defined as the peak firing rate. Contextual gain was calculated as the ratio of peak firing rates between the free viewing of images and the directed eye movement task.

Chapter 5. ANATOMICAL AND FUNCTIONAL PATHWAYS TO AND FROM THE HIPPOCAMPUS: THE INTERACTION BETWEEN EYE MOVEMENTS AND MEMORY

Abbreviations

ACC: anterior cingulate cortex (BA 24/25/32)
ATN: anterior thalamic nuclei
BA: Brodmann Area
CA1-4: Cornu Ammonis areas 1-4
cIPL: caudal inferior parietal lobule (BA 7a)
DG: Dentate Gyrus
DLPFC: dorsolateral prefrontal cortex (BA 9/46)
FEF: frontal eye fields (BA 8/45)
IML: intralaminar nuclei of the thalamus
IT: inferior temporal cortex
LD: lateral dorsal nucleus of the thalamus
LEC: lateral entorhinal cortex
LIP: lateral intraparietal cortex (BA 7)
LP: lateral posterior nucleus of the thalamus
MEC: medial entorhinal cortex
MD: medial dorsal nucleus of the thalamus
mPFC: medial prefrontal cortex
MST: medial superior temporal area
MTL: medial temporal lobe
MT: middle temporal area
OFC: orbital frontal cortex
PCC: posterior cingulate cortex (BA 23/31)
PFC: prefrontal cortex
Re/Rh: reuniens & rhomboid thalamic nuclei
RSC: retrosplenial cortex (BA 29/30)
SC: superior colliculus
SEF: supplementary eye fields (BA 6)
SNpr: substantia nigra pars reticulata
STG: superior temporal gyrus
STS: superior temporal sulcus
TE/TEO: areas of the inferior temporal cortex
TF/TH: parahippocampus
vmPFC: ventromedial prefrontal cortex
V4: visual area 4

5.1 INTRODUCTION

In recent years there has been a growing interest in the interaction between eye movements and memory (Meister and Buffalo, 2016; Voss et al., 2017). Many studies have identified a reciprocal interaction between eye movements and memory (Smith and Squire, 2008b; Olsen et al., 2016). Recent electrophysiology studies have also identified eye movement-related neural signals in the primate MTL (Ringo et al., 1994; Jutras et al., 2013a; Killian et al., 2015). Despite these findings, the anatomical pathways supporting the interaction between eye movements and memory are still a mystery. An extensive body of literature explains how spatial signals reach the MTL in rodents, but it is unknown whether these same pathways also carry eye movement-related information to the primate MTL.

Here I will focus on the cortical and subcortical pathways that may mediate the interaction between oculomotor and memory networks. Several studies have already summarized many of the relevant connections within each network (Felleman and Van Essen, 1991; Young, 1993; Suzuki and Amaral, 1994a; Lynch and Tian, 2006a; Kravitz et al., 2011; Yeterian et al., 2012). However, very few studies have attempted to understand the connections between networks (Meister and Buffalo, 2016; Shen et al., 2016). Moreover, those who have discussed the connections between these networks have focused only on how memory influences eye movements, yet there is a reciprocal interaction between eye movements and memory.

In the first two sections, I separately describe the anatomical connections within the oculomotor and memory networks. In addition to the anatomical connections, I will briefly discuss the function of certain areas. The functional descriptions will aid in understanding the potential role of each brain region in eye movements and memory. After describing each network separately,

I then discuss the connections between the oculomotor and memory networks. Here, I propose three pathways by which eye movement-related information reaches the MTL: a parieto–medial temporal pathway, a thalamo-medial temporal pathway, and an indirect visuo-medial temporal pathway.

Many of these pathways contain reciprocal connections, and therefore these pathways may also describe how memories exert top-down control over eye movements. In addition to these pathways, there are several other areas, mostly within the PFC, which also have strong connections to both networks. Thus the PFC may act as a relay between networks.

In primates, the same pathways that support eye movements also support body movements. As I will describe, these same pathways help form spatial representations in rodents which are modulated by physical body movements. The additional support of eye movements by these pathways in primates should not be surprising as primates are highly visual creatures. In fact, visual processing occupies 52%, 27%, and 18% of the neocortex in primates, humans, and rodents, respectively (Burwell, 1996; Van Essen and Drury, 1997; Van Essen, 2004; Krubitzer, 2007). Combined the other senses occupy only 16% and 14% of the neocortex in humans and primates, respectively. Note that in humans 51% of the neocortex is devoted to cognition, emotion, and language. Conversely, somatosensation, audition, and olfaction occupy 26%, 4%, and 14% of the neocortex in rodents, respectively. The differences in the distribution of cortical areas devoted to each sense across species has strong implications in what types of information reach the MTL (Brown and Aggleton, 2001). Thus as highly visual creatures, signals in the primate MTL are likely to include eye movement-related and visual information.

Before I describe these networks in detail, I wish to highlight several caveats. First, attention, eye movements, and vision are well studied in primates. In contrast, the anatomy and

function of the MTL are well understood in rodents. Second, the function and anatomy of the higher-order thalamic nuclei (e.g. lateral dorsal thalamus) are less studied than the sensory thalamic nuclei and are thus poorly understood. The anatomy and function of the thalamus will be summarized from findings of cats, rats, and monkeys. Third, it is important to note that many connections are often dependent on subregions within key brain areas (e.g. AP organization or retinotopic maps). I will mostly ignore these differences unless it is necessary to specify because complete knowledge of these subdivisions is often lacking. Lastly, I will focus on brain regions involved in the production of fixations and saccades.

5.2 MTL NETWORKS

5.2.1 *Overview*

The function and anatomy of brain regions involved in relational memory are well studied in rodents. These areas are circumscribed within the MTL and include the postrhinal cortex (the parahippocampal cortex in primates), perirhinal cortex, entorhinal cortex, hippocampus, and subiculum [complex]. Further, several subcortical areas including the higher-order thalamus are also important for the formation of relational memories. Below, I will discuss the anatomy and function of these areas in rodents and primates. A review of the literature shows that inputs into the primate MTL are different than those in rodents, yet the anatomy within the MTL is largely conserved. These findings explain why the neural activity found in the MTL is different across species, but the conservation of anatomy within the MTL suggests that the MTL is processing information in a fundamentally similar manner across species.

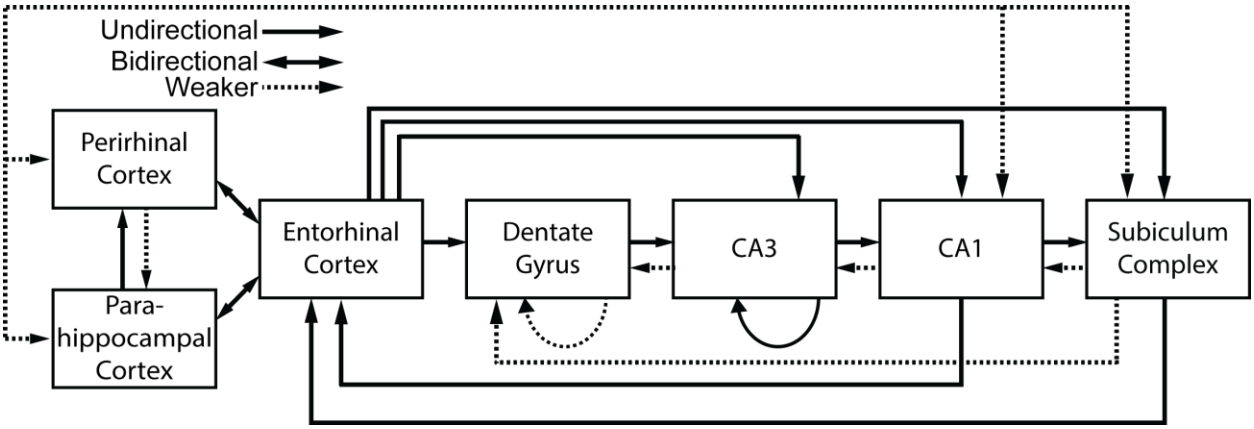

Figure 5-1 Intrinsic Connections of the Medial Temporal Lobe

The perirhinal and parahippocampal cortices receive the majority of sensory and polysensory information coming into the MTL (see Figure 5.2). The parahippocampus provides modest input into the perirhinal cortex while the perirhinal cortex only provides a small amount of input back to the parahippocampus. The perirhinal and parahippocampal cortices have strong, reciprocal connections with the entorhinal cortex. The entorhinal cortex provides the vast majority of input into the Dentate Gyrus. The entorhinal cortex also provides input to CA3, CA1, and the subiculum complex though these connections are mostly on the distal dendrites in contrast to the internal hippocampal connections which primarily synapse onto the proximal dendrites. The Dentate Gyrus also receives some input from the subiculum complex. Connections in the hippocampal proper from Dentate Gyrus to CA3 to CA1 to the Subiculum complex are mostly feedforward. Further, CA3 has strong recurrent connections. A small number of recurrent (mostly inhibitory) connections are also present within the Dentate Gyrus. Recently, a small of number (~2-3% of connections) of back projections have been discovered within the hippocampal proper that may be important for timing. Additionally, the perirhinal and parahippocampal cortices have a small amount of direct, reciprocal connections with CA1 as well as a modest amount of reciprocal connections with the subiculum complex. Lastly, the subiculum complex and to a lesser extent CA1 also project back to the entorhinal cortex. Note that topographical organization along the anterior-posterior and transverse axes is not shown.

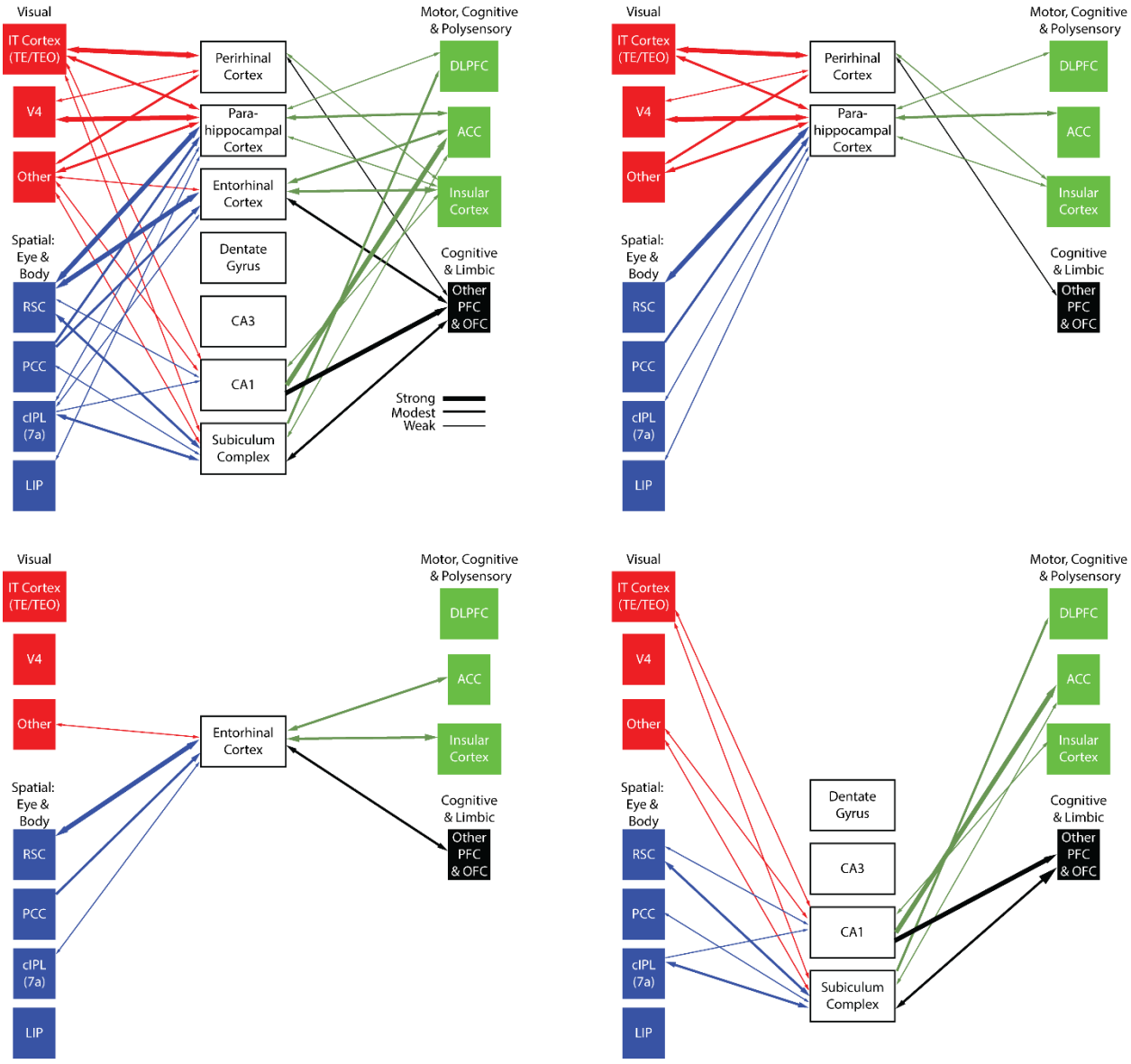

Figure 5-2 Extrinsic Cortical Connections of the Medial Temporal Lobe

The MTL has connections with much of the cortex. In primates, the perirhinal and parahippocampal cortices receive a large amount of visual and visuospatial inputs. Polymodal sensory information primarily reaches the MTL through ACC and insular cortex. In rodents, sensory input is much less visual and is balanced by olfaction, somatosensation, and audition (not shown). Most connections are reciprocal, but inputs and outputs are not always balanced. Overall, RSC, PFC, and OFC receive more projections from the MTL than they send in return. Further, the subiculum complex projects modestly to DLPFC but DLPFC provide very few inputs to the MTL. In comparison to RSC, PCC's connections to the MTL are modest and mostly unidirectional. The first figure depicts all connections while the remaining figures more clearly illustrate connections to specific subregions.

5.2.2 *Anatomy*

Classical models of the MTL illustrate a serial and hierarchical processing of information. The perirhinal (BA 35/36), and parahippocampal (TH/TF) cortices receive the majority of cortical projections into the MTL (Suzuki and Amaral, 1994a). In turn, the perirhinal and parahippocampal cortices project to the entorhinal cortex, which then projects to the hippocampus. The anatomy of the hippocampus itself is usually described as a trisynaptic pathway from entorhinal cortex to DG to CA3 to CA1.

The notion of serial and hierarchical processing vastly oversimplifies the circuits within the MTL. Rather, there is a large number of reciprocal and longer range loops within the MTL which may have important implications for learning (**Figures 5.1 and 5.2**). While many connections within the MTL are reciprocal, the strength of these connections are certainly not balanced. Further, cortical structures in the MTL receive the largest amount of cortical input, but there certainly are other [cortical and subcortical] inputs throughout the MTL. Of particular interest here are the direct connections to the subiculum. Below, I will separately go through each MTL subregion in detail.

The anatomy of the perirhinal and parahippocampal cortices is best understood by comparing the two. Perirhinal cortex is well connected to areas involved in sensory processing whereas the parahippocampus is well connected to areas involved in spatial processing. In primates, the main inputs into the perirhinal cortex are IT, the parahippocampus, and STS (polymodal areas); a small number of connections arise from other cortical areas including V4, the insula, and OFC (Suzuki and Amaral, 1994a; Buffalo et al., 2006). On the other hand, the parahippocampal receives strong inputs from V4, RSC, PCC, ACC, and STS; a small number of

connections arise from IT, STG (auditory), perirhinal cortex, posterior parietal cortex (LIP and cIPL), DLPFC, and the insula. Note the connectivity pattern of TF and TH are quite different.

The portion of V4 connected to parahippocampus is mainly concerned with peripheral vision, and unlike the rest of the V4, these peripheral areas are heavily connected with the posterior parietal cortex suggesting that this part of V4 is involved in visuospatial processing (Ungerleider et al., 2008). The portion of ACC (BA 24) connected to the parahippocampus may correspond to the "cingulate eye fields" (Lynch and Tian, 2006b). RSC input to parahippocampus seems to be at least two times stronger than PCC or ACC. Projections back to the cortex from the parahippocampus and perirhinal cortex differ only slightly from their inputs suggesting many connections are reciprocal (Lavenex et al., 2002). One important exception is RSC which receives more projections from the MTL than RSC sends in return.

The connections to the perirhinal and postrhinal cortices in rodents are qualitatively different. In primates, the perirhinal and parahippocampus receive somatosensory and polysensory information through the insula, STS, STG, and posterior parietal areas (Brown and Aggleton, 2001). Rodent perirhinal cortex receives much less visual input which is balanced by strong inputs from auditory, somatosensory, olfactory cortices; perirhinal cortex receives inputs from all these sensory cortices while postrhinal cortex primarily receives visual and somatosensory input (Burwell et al., 1995; Burwell, 1996; Burwell, 2000; Brown and Aggleton, 2001).

The perirhinal and parahippocampal cortices also have many subcortical connections. The parahippocampus is strongly connected with the striatum (nucleus accumbens, putamen, and caudate) and claustrum (Burwell et al., 1995; Kondo et al., 2005). Similarly, the perirhinal cortex is strongly connected with the amygdala, claustrum, and striatum (Kondo et al., 2005). Other

subcortical connections include the hypothalamus and basal forebrain nuclei including the septal nuclei (Agster et al., 2016).

Amaral and colleagues suggested that the thalamic inputs are similar in rodents and primates (Burwell et al., 1995). Thalamic input to the perirhinal cortex arises from the midline nuclei (e.g. Re), IML, medial pulvinar, posterior nuclei, and MDmc while the parahippocampal cortex is strongly connected to the ATN, LD, LP, medial pulvinar, and to a lesser extent the midline nuclei (Russchen et al., 1987; Yeterian and Pandya, 1988; Burwell et al., 1995; Agster et al., 2016). LP may provide the strongest thalamic input to the parahippocampus, but in general, there is a substantial amount of thalamic input from multiple nuclei. The connections from the parahippocampal and perirhinal cortices to the medial pulvinar overlap with connections from RSC, PCC, and to a less extent posterior parietal (7a), STS, and PFC (Baleydier and Mauguiere, 1985).

In both rat and primate, parahippocampus and perirhinal cortex provide a major input into the entorhinal cortex. However, there are a small number of direct connections from the perirhinal and parahippocampal cortices to CA1 and the subiculum (Suzuki and Amaral, 1990; Blatt and Rosene, 1998; Yukie, 2000; Agster and Burwell, 2013). These direct connections may be functionally important for learning and plasticity (Liu and Bilkey, 1996).

The entorhinal cortex is strongly interconnected with the perirhinal and parahippocampal cortices (Suzuki and Amaral, 1994b; Insausti and Amaral, 2008). In primates, the perirhinal and parahippocampal cortices represent approximately 60% of cortical inputs to the entorhinal cortex (Insausti and Amaral, 2008). Other cortical inputs come from RSC (20%), OFC, mPFC, insula, STS, 7a, ACC, and PCC. Subcortical connections in monkey include the amygdala, claustrum, basal forebrain, hypothalamus, and brainstem (e.g. raphe, locus coeruleus, VTA) (Amaral and

Price, 1984; Insausti and Amaral, 2008). Thalamic connections include the Re, IML, medial pulvinar, and very light connections with LD. The main output of the entorhinal cortex is the DG, CA subfields, and the subiculum (Witter and Amaral, 1991). In turn, the entorhinal cortex receives inputs from CA1 and the subiculum.

The connection patterns in rodents are different and more topographically organized. Perirhinal and postrhinal cortices constitute major inputs into the entorhinal cortex particularly into LEC and MEC, respectively (Burwell and Amaral, 1998a). Note MEC and LEC are well interconnected. The entorhinal cortex also receives strong inputs from mPFC, OFC, insula, TEv, RSC, ACC, piriform cortex (smell), and posterior parietal cortex. In particular, the piriform cortex constitutes 33% of cortical input into entorhinal cortex while the perirhinal and postrhinal cortices contribute 25% of the input. The insula also provides substantial input into LEC (21%) and MEC (6%). Thus, the inputs into the rodent entorhinal cortex contain more auditory, olfactory, and polysensory information than in primates. Specifically, in rodents, the piriform cortex constitutes the largest input into the entorhinal cortex. Thalamic inputs into the entorhinal cortex are similar across species include the Re and an analogous IML connection (Wyss et al., 1979; Dolleman-Van Der Weel and Witter, 1996).

The entorhinal cortex directly projects to the DG, all CA subfields, and the subiculum. The hippocampus proper contains primarily feedforward connections from DG to CA3 to CA1. The subiculum offers an extension to this pathway. Finally, CA1 and the subiculum project back to the entorhinal cortex. Interestingly, the DG and CA3 have virtually no cortical outputs and minimal subcortical outputs. Essentially, CA1 and the subiculum are the only outputs of the hippocampus. I will progressively discuss each subregion separately. The pathways within the hippocampus are

mostly conserved across species. There are a few minor differences mainly that the connections within primate hippocampus are less topographically organized.

The main input (~85%) into the DG is the entorhinal cortex. Other inputs arise from the presubiculum and parasubiculum (Kohler, 1985); these presubiculum connections provide a disynaptic route for thalamic input into the DG. The basal forebrain also shows modest connections to the DG providing cholinergic and GABAergic modulation. Other subcortical inputs include the suprammamillary bodies, locus coeruleus, VTA, and raphe nuclei.

Less is known about the anatomy of CA2 and CA4 (i.e. the hilus). The anatomy of CA4 appears similar to that of CA3. CA2 has special anatomy. The main inputs to CA2 come from CA3 and the entorhinal cortex (Amaral and Witter, 1989; Ishizuka et al., 1990; Yoshida and Oka, 1995; Bartesaghi and Gessi, 2004). The granule cells in the DG do not project to CA2. CA2 also receives input from the basal forebrain, amygdala, supramammillary bodies, and hypothalamus. Like CA3, CA2 diffusely projects to CA1 and the septum.

CA3 mainly receives projections from the DG granule cells and the entorhinal cortex, and the main output of CA3 is CA1 (Witter and Amaral, 1991; van Groen et al., 2003) In rat, 2.5% of CA3 axon terminals back project to the DG, 27.5% stay within CA3, and 70% project to CA1 (Wittner et al., 2007). Most inputs from the entorhinal cortex innervate distal dendrites while the DG granule cells innervate the proximal portions of the dendrites. CA3 also has bidirectional connections with the basal forebrain (Swanson et al., 1981). Other small connections include the amygdala and endopiriform cortex (in rat only) (Witter, 2007). CA3 does not have appreciable thalamic input.

Compared to the DG and CA3, CA1 has substantially different connections. The main inputs into CA1 are from CA3 onto proximal dendrites and from the entorhinal cortex onto distal

dendrites. CA1 projects back to the deep layers of the entorhinal cortex, but to a lesser extent than the subiculum (Amaral and Witter, 1989; Witter et al., 2000). CA1 also back projects to CA3 (van Strien et al., 2009). Further, CA1 has strong connections with the subiculum including some bidirectional connections (Ding, 2013). In both species, CA1 also receives thalamic input but to a lesser extent than the subiculum. Re and other midline nuclei provide the main thalamic input to CA1 (Herkenham, 1978; Su and Bentivoglio, 1990; DollemanVanderWeel and Witter, 1996; Van der Werf et al., 2002).

CA1 and the subiculum are the major outputs of the hippocampus. CA1 projections tend to be more limbic and subcortical than subiculum. In rodents, the dorsal one-third of CA1 strongly projects to the subiculum, RSC, perirhinal cortex, entorhinal cortex, and basal forebrain (Strange et al., 2014); Vangroen and Wyss, 1990; Cenquizca and Swanson, 2006). The ventral one-third projects to the subiculum, entorhinal cortex, ACC, olfactory nucleus and bulb, lateral septum, nucleus accumbens, amygdala, hypothalamus, supramammillary nucleus, and midline thalamic nuclei. Note that CA1 projections to the mammillary nuclei in turn project to the ATN (Blair et al., 1998). The temporal two-thirds contains neurons that project to the medial and lateral parts of PFC (Verwer et al., 1997). Thus the ventral portion of CA1 appears to regulate motivation and goal-directed behaviors while the dorsal portion appears to be more strongly related to space and cognition.

Similar outputs are observed in primates, but there are some differences that parallel the inputs in the MTL (Saunders et al., 1988; Barbas and Blatt, 1995; Insausti and Munoz, 2001). Further, in rodents, the dorsal-ventral long axis is analogous to the posterior-anterior axis in primates. In addition to connections mentioned above, primate anterior CA1 modestly projects to [v]mPFC, ACC, OFC, and perirhinal cortex. There is a similar topographical organization across

the long-axis. For example, projections to OFC, ACC, and mPFC arise from anterior CA1. Lastly, CA1 in primates only sends light projections to RSC and PCC.

In primates, CA1 also receives direct projections from TE, perirhinal, parahippocampus, posterior parietal cortex (7a and 7b), insula, STS, and RSC (Suzuki and Amaral, 1990; Blatt and Rosene, 1998; Rockland and Van Hoesen, 1999; Ding et al., 2000; Insausti and Munoz, 2001; Zhong and Rockland, 2004); most of these connections are reciprocal and preferably connect with the posterior portions of CA1. LIP does not project directly to CA1 (Clower et al., 2001). In rodents, CA1 also receives direct projections from perirhinal and postrhinal cortex (Kosel et al., 1983; Witter et al., 2000).

The subiculum complex is often referred to as just the subiculum. The subiculum complex includes the Subiculum proper, the Prosubiculum, the Presubiclum, the Parasubilculum, and Postsubiculum. Many of these subdivisions are well interconnected, but each subdivision also has its own distinct connections (Ding, 2013). Overall, the subiculum complex has strong connections with LEC, MEC, perirhinal and parahippocampal cortices, RSC, 7a, ACC, PCC, DLPFC, vmPFC, OFC, and septal nuclei. Other connections include CA3, piriform (rodent), amygdala, hypothalamus, BNST, mammillary bodies, V1/V2, TEO, and claustrum. Interestingly, 7a densely projects to the presubiculum and these same neurons seem to send collaterals to TF, perirhinal, and entorhinal cortices.

In general, the Subiculum proper is an output structure with fewer reciprocal connections. The Pro-, Pre-, Post-, and Para-subiculum have strong reciprocal connections. The medial septum and other neuromodulatory inputs more or less project to all subdivisions except the Parasubiculum. Further, the midline thalamic nuclei including Re are modestly connected with all of the subiculum complex. Bidirectional connections with midline nuclei are observed for the

ProSubiculum, Subiculum, and PostSubiculum while midline nuclei have unidirectional projections to the PreSubiculum and ParaSubiculum projects into the midline nuclei. Further, ProSubiculum and Subiculum have connections to the IML while the PostSubiculum and Presubiculum have modest to strong connections with LD. The ATN has strongly bidirectional connects with all but the Prosubiculum.

5.2.3 *Summary*

In summary, the MTL does not simply process information in a serial and hierarchical fashion (**Figure 5.1**). The MTL is connected to a large number of brain regions (**Figure 5.2**). Many of these areas are provide inputs into the MTL through the perirhinal, parahippocampus, and entorhinal cortices. Some areas even provide direct input into CA1 and the subiculum. In primates, a large portion of inputs contain visual and visuospatial signals while in rodents visual input is balanced by olfactory, auditory, and somatosensory inputs. Further, the long axis of the hippocampus in rodents has distinct connections where the dorsal portion has particularly strong connections to brain areas involved in spatial processing and cognition while the ventral portion has strong connections to areas involved in the regulation of motivation and goal-directed behaviors (Strange et al., 2014). The connections of the entorhinal cortex are also organized in a complementary fashion. There is also evidence that this topographical organization across the long-axis (the posterior-anterior axis) is also present in primates though the connection patterns are less distinct.

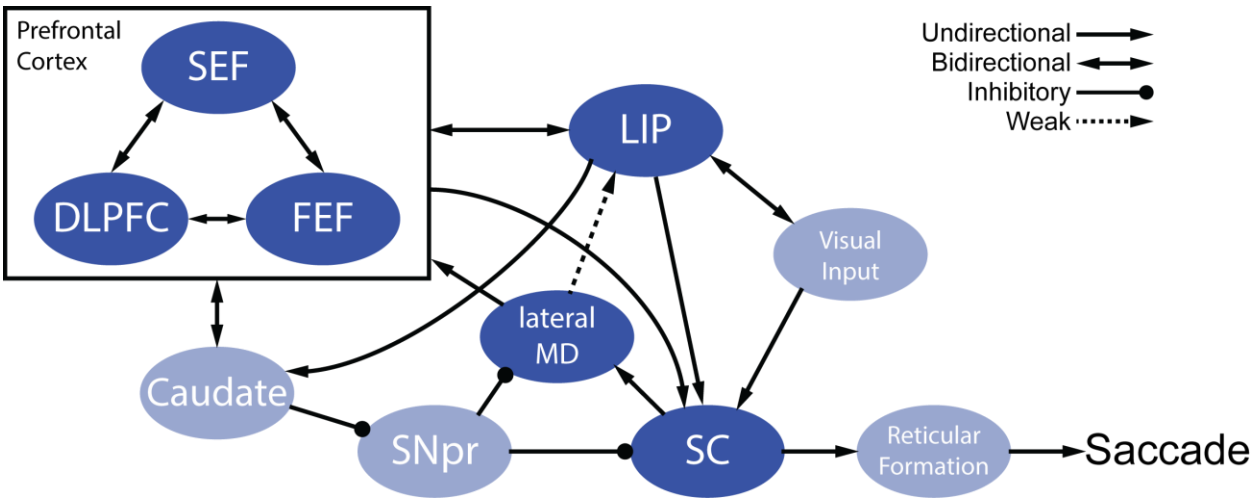

Figure 5-3 The Cognitive Oculomotor Network

The prefrontal cortex and LIP exert top-down control over eye movements. The superior colliculus integrates these top-down signals and sends this information to premotor neurons in the reticular formation that generate saccades. The prefrontal cortex and LIP also have direct connections to the reticular formation, but these connections are generally considered too weak to produce saccades under normal conditions. Also, the prefrontal cortex and LIP strongly project to the caudate and pontine nuclei (cerebellar route, not shown). Corollary discharge signals from the superior colliculus reach the prefrontal cortex through the lateral portions of MD. LIP receives light projects from MD but stronger connections from the pulvinar (not shown).

5.3 OCULOMOTOR NETWORKS

5.3.1 *Overview*

In primates, the function and anatomy of brain regions involved in the production of eye movements are reasonably well understood. These areas include the premotor neurons in the reticular formation, superior colliculus, cerebellum, basal ganglia, thalamus, and posterior parietal cortex including LIP, SEF, FEF, and DLPFC (**Figure 5.3**). The premotor neurons in the reticular formation generate the motor command, and the superior colliculus integrates cortical signals and relays them to the premotor neurons in the reticular formation. The cerebellum processes eye movement signals from the majority of these cortical areas and sends projections directly to the reticular formation. Further, most of these areas send strong projections to the basal ganglia. The main effect of the basal ganglia is inhibition of eye movements via the inhibitory output of the SNpr to the thalamus and superior colliculus. While the basal ganglia, cerebellum, and reticular formation play important roles in the control of eye movements (Hikosaka et al., 2000; Robinson and Fuchs, 2001; Patel and Zee, 2015), I will not discuss these areas in further detail.

Below, I will focus on the top-down control of eye movements by DLPFC, LIP, FEF, and SEF. In addition to playing a role in generating eye movements, these areas are also involved in attention and working memory. I will discuss their anatomy and function using lesion and electrophysiology studies. The functional analysis of each area will help in determining the appropriate pathways for the interaction between eye movements and memory. I will first discuss subcortical areas and then cortical areas. The organization of this section is different from the section describing the memory network as the areas involved in the production of eye movements are highly interconnected and perform similar functions. Therefore, the easiest way to describe their individual functions is by direct comparison.

5.3.2 *Subcortical Areas*

Saccade burst generators in the reticular formation project to the oculomotor nuclei to produce eye movements (Girard and Berthoz, 2005). The function of the reticular formation is to produce the eye movement commands received from other brain structures. The reticular formation is reciprocally connected to the superior colliculus and FEF. FEF alone is not normally sufficient to generate saccades, but plasticity within FEF to the reticular formation pathway may occur after damage to the superior colliculus which allows for normal saccade production (Hanes and Wurtz, 2001).

A major role of the superior colliculus appears to integrate higher order signals (e.g. from PFC) in order to generate eye movements. Further, the superior colliculus also receives many subcortical connections from the thalamus, SNpr, inferior colliculus, monoaminergic inputs (locus coeruleus and raphe nucleus), hypothalamus and cerebellum (Edwards et al., 1979; Taylor et al., 1986). These subcortical inputs may be useful inhibiting, initiating, modulating, or correcting eye movements. Many of the superior colliculus connections are reciprocal. However, of particular interest here are the ascending connections which include projections to the pulvinar, MD, and LD. These thalamic connections are thought to relay eye movement information to the cortex (Sommer and Wurtz, 2002, 2004; Berman and Wurtz, 2010). In particular, these thalamic nuclei carry a corollary discharge signal to the cortex.

Stimulation of the superior colliculus causes eye, body, and neck movements, and lesions to the superior colliculus lead to deficits in orienting behaviors mediated by eye, neck, and body movements (Sprague and Meikle, 1965; Wurtz and Goldberg, 1972a); bilateral lesions essentially cause blindness. Neurons in the superior colliculus fire before each eye movement and encode eye movements in a retinotopic reference frame (Wurtz and Goldberg, 1972b). Additionally, neurons,

particularly in the superficial superior colliculus, also show visual responses with receptive fields resembling inputs from early visual areas (Sprague and Meikle, 1965; Wang et al., 2010). Furthermore, neurons also respond to auditory and somatosensory stimuli reflecting the general role of the superior colliculus in orienting behavior towards salient stimuli (Jay and Sparks, 1984; White et al., 2017).

MD is of particular interest as it carries a corollary discharge signal from the superior colliculus to the PFC (Sommer and Wurtz, 2002). MD can be subdivided into at least five different sub-nuclei. These divisions are as follows: magnocellular (MDmc), the parvocellular (MDpc), densocellular (MDdc), pars multiforms (MDmf), and lateral (MDl). The subdivisions of MD are isolated from each other and form different networks (Russchen et al., 1987; Ray and Price, 1993; Jones, 2007; Mitchell and Chakraborty, 2013). In particular, the lateral portions of MD (MDl, MDdc, MDmf) receive input from the superior colliculus and SNpr (Jones, 2007). In turn, these lateral subdivisions project to various cortical areas including SEF, FEF, ACC, and DLPFC. MDpc and MDmc do not receive inputs from the SNpr or superior colliculus. MDpc and MDmc are well connected with memory and learning systems such as the amygdala, entorhinal cortex, perirhinal cortex, DLPFC, vmPFC, ACC, and OFC (Mitchell and Chakraborty, 2013; Pergola and Suchan, 2013; Saalmann, 2014); most but not all connections are reciprocal. Nearly all subdivisions of MD receive neuromodulatory inputs from the locus coeruleus, VTA, and raphe nuclei.

Lesions to MD cause various deficits but most notably deficits in memory, conditioning, and reward associations. However, MDpc and MDmc are the largest nuclei, and it has been difficult to target the smaller lateral nuclei. Single unit recordings in lateral MD suggest that lateral MD is involved in eye movements and working memory (Sommer and Wurtz, 2002; Watanabe and Funahashi, 2012). Overall, MD is an important component of the memory system with strong

connections throughout the brain including the MTL and prefrontal cortex. Notably, the lateral subdivisions of MD, which do not connect with the MTL, play a role in relaying eye movement information to the cortex. In sum, from an anatomical standpoint, the eye movement and memory functions of MD are physically separate.

5.3.3 *Cortical Areas*

DLPFC, FEF, SEF, and LIP play an important role in the control of eye movements. All these areas show pre-saccadic, peri-saccadic, and visual activity. These areas are best understood by comparing and contrasting their functions as they are interconnected and appear to carry similar information. SEF and DLPFC appear to be more cognitive, FEF is more visual and motor, and LIP is more visual. All these areas carry "top-down" information to other areas, but from a hierarchical standpoint, SEF and DLPFC appear to sit at the top of this hierarchy. Below, I compare the functional and anatomical properties of these areas to support the hierarchical organization of the oculomotor network.

First, electrical stimulation offers an interesting avenue to understand the role each of these areas. Low-threshold stimulation of FEF evokes saccades in retinotopic coordinates with some head-centered biases (Caruso et al., 2017). Microstimulation of FEF can also cause pupillary changes, attentional enhancement, and shifts in extrastriate receptive fields (Clark et al., 2011; Wang et al., 2012; Lehmann and Corneil, 2016; Ebitz and Moore, 2017). Low-threshold stimulation of SEF evokes neck, forelimb, and eye movements indicating SEF may be involved in body and eye movement coordination (Abzug and Sommer, 2017). Further, these saccades are evoked to fixed points in space rather than retinotopic locations suggesting SEF may code information in allocentric coordinates (Olson and Gettner, 1995). Microstimulation of SEF can also reorder learned eye movement sequences suggesting SEF is involved in the planning and

learning of eye movement sequences (Chen and Wise, 1997; Histed and Miller, 2006). Stronger stimulation of parietal cortex can evoke eye movements too (Kurylo and Skavenski, 1991); these saccades are evoked in retinotopic, head-centered, or a combination of coordinates (Caruso et al., 2017). Electrical stimulation of DLFPC can cause eye movements; however, the electrical current required to evoke saccades is likely much higher (Wagman et al., 1961). Rather, recent evidence suggests that DLPFC is involved in goal-oriented eye movements and suppression of inappropriate saccades.

Second, response properties during bottom-up and top-down tasks can be useful for understanding the role of each area in the visual "hierarchy." For example, activity in FEF precedes LIP activity in top-down tasks while LIP activity precedes FEF in bottom-up tasks (Buschman and Miller, 2007). However, response latencies alone do not disambiguate hierarchical control of eye movement as neurons in the DLFPC can fire as soon as or sooner than LIP during a task with a combination of working-memory and pop-out elements. These results suggest that multiple pathways exist between these areas (Katsuki and Constantinidis, 2012). Further illustrating a hierarchical organization, LIP neurons are susceptible to distractors while DLPFC neurons can suppress responses to distractors (Suzuki and Gottlieb, 2013).

Third, performance on the anti-saccade task also illustrates a potential hierarchical organization (Schlag-Rey et al., 1997; Gottlieb and Goldberg, 1999; Everling and Munoz, 2000; Munoz and Everling, 2004). Performance on this task cannot be predicted by LIP activity as LIP activity indicates the presence of the saccade, target, and distractors. FEF activity is reduced during anti-saccades in comparison to pro-saccades but does correlate with behavioral performance. Instead, SEF and DLPFC represent the intended saccade during pro- and anti-saccades suggesting that these areas are the predominant source of top-down signals.

Fourth, lesions and inactivation of FEF, LIP, or superior colliculus initially causes severe deficits in eye movement generation. However, only combined lesions of FEF, LIP, or superior colliculus appear to cause long-term eye movement disorders. These results suggest independently modifiable pathways for the control of eye movements by FEF and the superior colliculus. Inactivation and lesions of SEF cause minimal changes in eye movement statistics suggesting SEF is not important for generating single eye movements (Abzug and Sommer, 2017). Stimulating SEF in animals with FEF lesions will still produce eye movements indicating a pathway to the superior colliculus and reticular formation independent of FEF. Inactivation of the parietal cortex causes spatial neglect, perceptual defects, and can affect hand-eye coordination (Andersen, 1989; Shimozaki et al., 2003; Suzuki and Gottlieb, 2013; Yttri et al., 2013).

DLPFC lesions cause deficits in attention, inhibitory control, [rule]-learning, task-switching, spatial working memory but have no effects on eye movement generation (Petrides, 1985; Funahashi et al., 1993; Dias et al., 1997). However, DLPFC lesions impair performance on the anti-saccade task and decrease anticipatory saccades in a predictive task (Pierrot-Deseilligny et al., 2003). Overall, DLPFC lesions suggest that DLPFC is involved in several higher-order cognitive processes which is also supported by single unit recordings (Funahashi et al., 1989; Curtis and D'Esposito, 2003; Funahashi et al., 2004; Heekeren et al., 2006; Averbeck and Lee, 2007; Suzuki and Gottlieb, 2013; Mendoza-Halliday et al., 2014; Donahue and Lee, 2015; de la Vega et al., 2016). Moreover, saccade related-activity in DLPFC spans from pre-saccadic to post-saccadic, and this saccade-related activity is directionally modulated (Funahashi et al., 1991). In general, DLPFC appears to integrate many types of information in order to regulate behavior through other brain areas.

Fifth, the connection patterns among these areas share a degree of similarity, but the overall connection strength is different. There is also a large degree of dissimilarity reflecting the differences in their functions.

FEF connects strongly to much of the visual system including MT, V4, and IT which supports the attentional role of FEF (Felleman and Van Essen, 1991). Also, FEF receives inputs from the lateral portions of MD and sends projections back to the superior colliculus and many of the brainstem nuclei including the reticular formation (Huerta et al., 1986, 1987). The above connections illustrate FEF's role in eye movements and attention. Further, FEF has strong connections with a variety of other areas such as SEF, posterior parietal cortex including LIP, DLPFC, cerebellum, medial pulvinar, and the caudate. Note the connections between FEF and ACC are extremely weak suggesting that information from ACC reaches FEF mainly through SEF (Schall et al., 2002).

SEF lies within the supplementary and premotor cortices. SEF has strong connections with FEF, ACC, PCC, superior colliculus, reticular formation, claustrum, basal ganglia (caudate), cerebellum (through the pons), DLPFC, inferior prefrontal cortex, OFC, posterior parietal cortex including LIP, various thalamic nuclei including MD and pulvinar, locus coeruleus, and other regions of the premotor cortex (Shook et al., 1988; Huerta and Kaas, 1990; Shook et al., 1990, 1991; Cavada et al., 2000; Schall et al., 2002; Lynch and Tian, 2006a). Interestingly, SEF has reciprocal connections to nearly all subdivisions of MD including MDmc and MDpc suggesting it may have a disynaptic thalamic connection with the learning and memory systems. Additionally, SEF has particularly strong connections with Olszewski's Area X of the thalamus and the ventral anterior nuclei which are strongly connected with the cerebellum and basal ganglia, respectively.

LIP is strongly connected to the superior colliculus, cerebellum (through the pons), and basal ganglia (caudate and putamen) (Andersen et al., 1990; Lynch and Tian, 2006a). LIP is also strongly connected to FEF, DLPFC, SEF, MT/MST, early visual areas (V2, V3, and V4), IT cortex, parahippocampal cortex, and other parietal subregions. Interestingly, while LIP mostly projects to the intermediate layers of superior colliculus which are involved in generating eye movements, projections back to LIP come through the medial and lateral pulvinar from the superficial layers of the superior colliculus which are more visual (Lynch and Tian, 2006a). LIP also connects strongly with LD but only sparsely with MD.

DLPFC has connections with the pulvinar, MD, ventral anterior thalamic nuclei, superior colliculus, FEF, SEF, parietal cortex (7a, 7b, LIP, and 7m), caudate, and cerebellum (through the pons)(Barbas et al., 1991; Petrides and Pandya, 1999; Nakano et al., 2000; Lynch and Tian, 2006a, b). These connections underlie the role of DLPFC in eye movements. However, DLPFC contains many other reciprocal connections which support its role in various cognitive functions. These connections include ACC, RSC, PCC, parahippocampal cortex, perirhinal cortex, subiculum, visual areas (V2-V4, MT/MST), IT, and PO. DLPFC also has light connections with Re (Petrides and Pandya, 1999; Lynch and Tian, 2006b). Overall, DLPFC and posterior parietal cortex share many common connections allowing visuospatial and cognitive signals to be integrated across most of the cortex (Selemon and Goldmanrakic, 1988).

5.3.4 *Summary*

In summary, LIP and other parietal areas likely signal salient stimuli as well as signal covert attention towards those stimuli. Further, parietal areas are involved in coordinate transformation across several references frames including retinotopy and body-centered coordinates. FEF, on the other hand, exerts top-down control over eye movements by integrating information from higher-

order brain areas including DLPFC, ACC, and SEF. ACC has weak direct connections to FEF, but the information in ACC passes through the SEF on its way to the FEF. DLFPC plays multiple roles in higher-order cognition potentially integrating information over the whole prefrontal cortex as well as other brain areas. DLPFC plays a larger role in inhibiting and modulating eye movements rather than generating them. Like DPLFC, the SEF appears to be involved in higher-order cognition. Specifically, the SEF plays a role in generating sequences of eye movements as well as learning and memory. Together, anatomy, electrophysiology, and lesion studies support a hierarchical organization in the control of eye movements.

5.4 Anatomical interface between Eye Movements and Memory

5.4.1 *Direct Pathway #1: Parieto-Medial Temporal Pathway*

The parieto-medial temporal pathway is likely the major source of spatial signals within the MTL (**Figure 5.4**). The parieto-medial temporal pathway has already been described in detail by others (Kravitz et al., 2011). Researchers postulate that egocentric and allocentric information are processed and transformed in the parietal, cingulate, and retrosplenial cortices which then provide the MTL with allocentric information. Several areas within the parietal lobe have direct connections to the MTL, albeit these connections are weaker than the connections from RSC and PCC. All these areas process body movements and eye movements in primates. A similar pathway exists in rodents.

While LIP has been extensively studied in relation to its role in eye movements, other parietal areas are more important to the MTL, in particular, cIPL (BA 7a) which contains areas OPT and PG (Kravitz et al., 2011). As mentioned above, cIPL projects to nearly all levels of the MTL including the parahippocampus, entorhinal cortex, CA1, and subiculum (Rockland and Van

Hoesen, 1999; Ding et al., 2000). LIP only directly projects to the parahippocampus. Instead, LIP and other posterior parietal areas strongly project to cIPL. cIPL itself contains strong projections to PCC and RSC which in-turn project to the MTL. Direct feedback from the MTL to cIPL is also relatively weak (Clower et al., 2001). However, this pathway receives more input from the MTL than it sends in return.

cIPL also has connections to other brain regions involved in vision and the production of eye movements. These connections include ACC, SEF, DLPFC, 7m, MT/MST, LD, ATN, and the insula as well as lighter connections to the superior colliculus, FEF, pulvinar, and early visual areas (Vogt and Pandya, 1987; Schmahmann and Pandya, 1990; Augustine, 1996; Lynch and Tian, 2006b). Importantly, cIPL receives vestibular inputs from vestibular thalamic nuclei (Ventre and Faugier-Grimaud, 1988; Schmahmann and Pandya, 1990; Hitier et al., 2014; Ventre-Dominey, 2014; Wijesinghe et al., 2015). MST, which is a major input into cIPL, also receives strong vestibular inputs.

cIPL neurons respond to gaze shifts towards allocentric and object-centered targets suggesting that cIPL may be involved in landmark-based navigation (Chafee et al., 2005; Crowe et al., 2008; Rozzi et al., 2008). As with other oculomotor areas, activity precedes movement. Interestingly, electrical stimulation of cIPL does not evoke eye movements (Thier and Andersen, 1998). cIPL neurons are also sensitive to optic flow and direction of motion further supporting its role in navigation (Phinney and Siegel, 2000; Crowe et al., 2004). Lesions to parietal lobe including cIPL, produce egocentric disorientation and some loss of landmark-based memories relative to one’s self (Aguirre and D'Esposito, 1999).

Another component of the Parieto-Medial Temporal Pathway includes 7m (PGm). 7m shares similar connections to cIPL and also contains eye movement and reaching signals (Cavada

and Goldman-Rakic, 1989; Lynch and Tian, 2006b, a; Kravitz et al., 2011). 7m has strong connections to cIPL, superior colliculus, caudate, brainstem premotor nuclei, pulvinar, ventrolateral thalamus, IML, LIP, SEF, FEF, DLPFC, MT/MST, PCC, V2, parietal-occipital area PO, supplementary motor cortex, and premotor cortex.

The main pathway from cIPL to the MTL is through PCC and RSC. RSC and PCC are strongly interconnected with cIPL and each other.

PCC is well connected to parietal areas including LIP, DP, and 7m (Vogt and Pandya, 1987; Kobayashi and Amaral, 2003, 2007). PCC is also strongly connected to the SEF, ACC, and DLPFC, insula, OFC, RSC, and striatum. PCC is connected to several thalamic nuclei including ATN, LD, ventral complex, IML, and Re (Vogt and Pandya, 1987; Yeterian and Pandya, 1988; Huerta and Kaas, 1990; Olson and Musil, 1992). PCC has additional connections to the entorhinal cortex and parahippocampus (TF/TH) as well as light connections with the Pre- and Post-subiculum. Feedback from the MTL to the PCC is extremely weak. However, PCC inputs into the MTL are modest in strength.

Compared to PCC, RSC has much stronger connections to the MTL and other limbic areas, but RSC has weaker connections to motor areas. RSC has strong connections to the parahippocampal, perirhinal, entorhinal cortices as well as CA1 and the majority of the subiculum complex. Connections to posterior parietal areas are weaker than those to PCC. RSC's connection to the MTL, LD, and ATN define its important role in the head-direction network (Vann et al., 2009). Additionally, RSC is connected to DLPFC, OFC, Re, medial pulvinar, PCC, and the caudate (Vangroen and Wyss, 1992; Wyss and Vangroen, 1992; Morris et al., 1999; Kobayashi and Amaral, 2003, 2007). The strongest inputs into RSC are from the MTL. RSC also receive

vestibular input from the vestibular cortex (PVIC). Reciprocal connections between ACC, RSC, cIPL, and PCC may also lead to PCC processing vestibular information (Wijesinghe et al., 2015).

In rodents, there is no anatomically defined PCC. Instead, RSC is analogous to both PCC and RSC in primates. The dysgranular RSC may be analogous to PCC and contains strong connections to motor areas including M2, while granular RSC may be analogous to the primate RSC and has stronger connections to limbic structures involved in navigation and memory (Yamawaki et al., 2016). Similar to primates, the subdivisions of RSC are modestly interconnected in rodents.

In primates, only a handful of studies have recorded neurons in PCC. Interestingly, PCC contains mostly peri- and post-saccadic responses (Olson et al., 1996; Dean et al., 2004; Dean and Platt, 2006). Further, some PCC neurons encode eye movements in allocentric space. Not surprisingly, these neurons have gain-fields that are modulated by saccade direction and amplitude. Therefore, PCC may be involved in the translation of egocentric to allocentric coordinates (Small et al., 2003; Bledowski et al., 2009). PCC also contains representations of spatial attention, motivation, and navigation-related signals (Vogt et al., 1992; McCoy et al., 2003). PCC, 7m and possibly RSC show navigation-selective (including place-like) responses (Sato et al., 2006, 2010). Not surprisingly, inactivation of PCC results in deficits following learned routes (Whishaw et al., 2001; Leech and Sharp, 2014).

There are no papers explicitly describing single unit recordings in primate RSC, but given what we know about the connections of PCC and RSC, RSC likely contains similar eye movement-related signals. In rodents, RSC conjunctively encodes place, route, and head-direction (Alexander and Nitz, 2015). RSC lesions reduce head-direction tuning in the ATN relative to landmarks (Clark et al., 2010). Interestingly, in learning a new spatial task, hippocampal place activity develops

sooner than in RSC. Furthermore, the hippocampal code is more contextually rich than the spatial code in RSC. Since task-relevant responses are also observed in RSC, RSC is likely involved in learning spatial contexts thought the specific role of RSC is likely different than the hippocampus (Smith et al., 2012).

In summary, the Parieto-Medial Temporal Pathway provides the MTL with allocentric spatial information. The Parieto-Medial Temporal Pathway first transforms egocentric spatial information in the posterior parietal cortex to allocentric information via RSC and PCC. RSC, PCC, and to a lesser extent cIPL directly connect to nearly all areas within the MTL. This pathway also directly connects to many thalamic nuclei that in turn project to the MTL. While little is known about the neural activity in RSC and PCC of primates, PCC contains eye movement-related information, and therefore this pathway is a plausible route for eye movement signals to reach the MTL. The anatomical connections of RSC support the idea that eye movement-related activity could be found in RSC as well. Lastly, the same pathway is also present in rodents and supports spatial representations based on physical location.

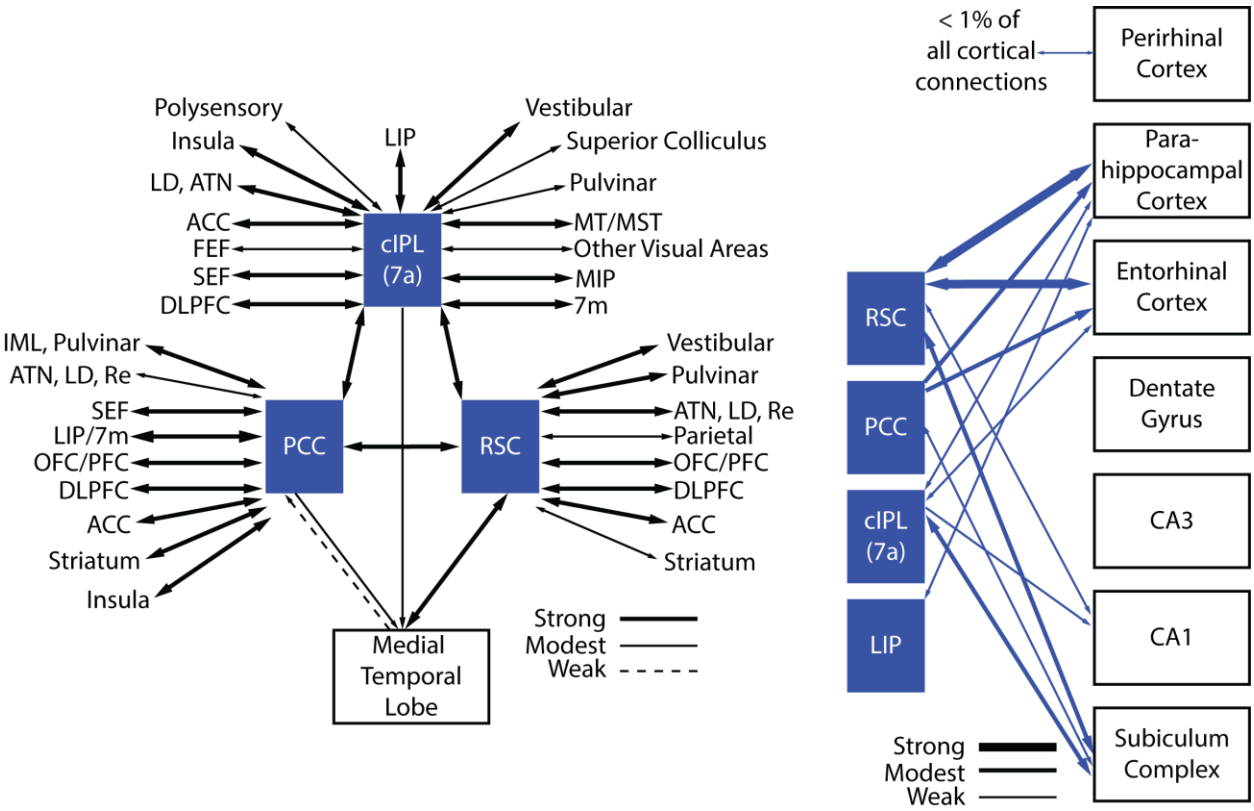

Figure 5-4 Direct Pathway #1-Parieto-Medial Temporal Pathway

The main pathway by which the MTL receives spatial information arises from the caudal intraparietal lobule (cIPL: PG & Opt) and passes through the posterior cingulate (PCC) and retrosplenial cortices (RSC). The RSC has stronger connections to the MTL than PCC. Furthermore, RSC's feedforward connections to the MTL are weaker than its feedback from the MTL. PCC on the other hand only receives weak feedback from the MTL. The anatomical connections of cIPL suggest that cIPL integrates a variety of signals including signal from visual (e.g. MT/MST), eye movement (e.g. SEF), cognitive (e.g. ACC), and body movements areas (e.g. MIP). PCC has strong connections to areas involved in the production and regulation of eye and body movements. On the other hand, RSC has some connections to areas involved in eye and body movements but has stronger connections to limbic areas (e.g. OFC). Overall, this pathway connects to most structures within the MTL involved in spatial processing except the Dentate Gyrus and CA3; less than 1% of cortical inputs into the perirhinal cortex arise from this pathway.

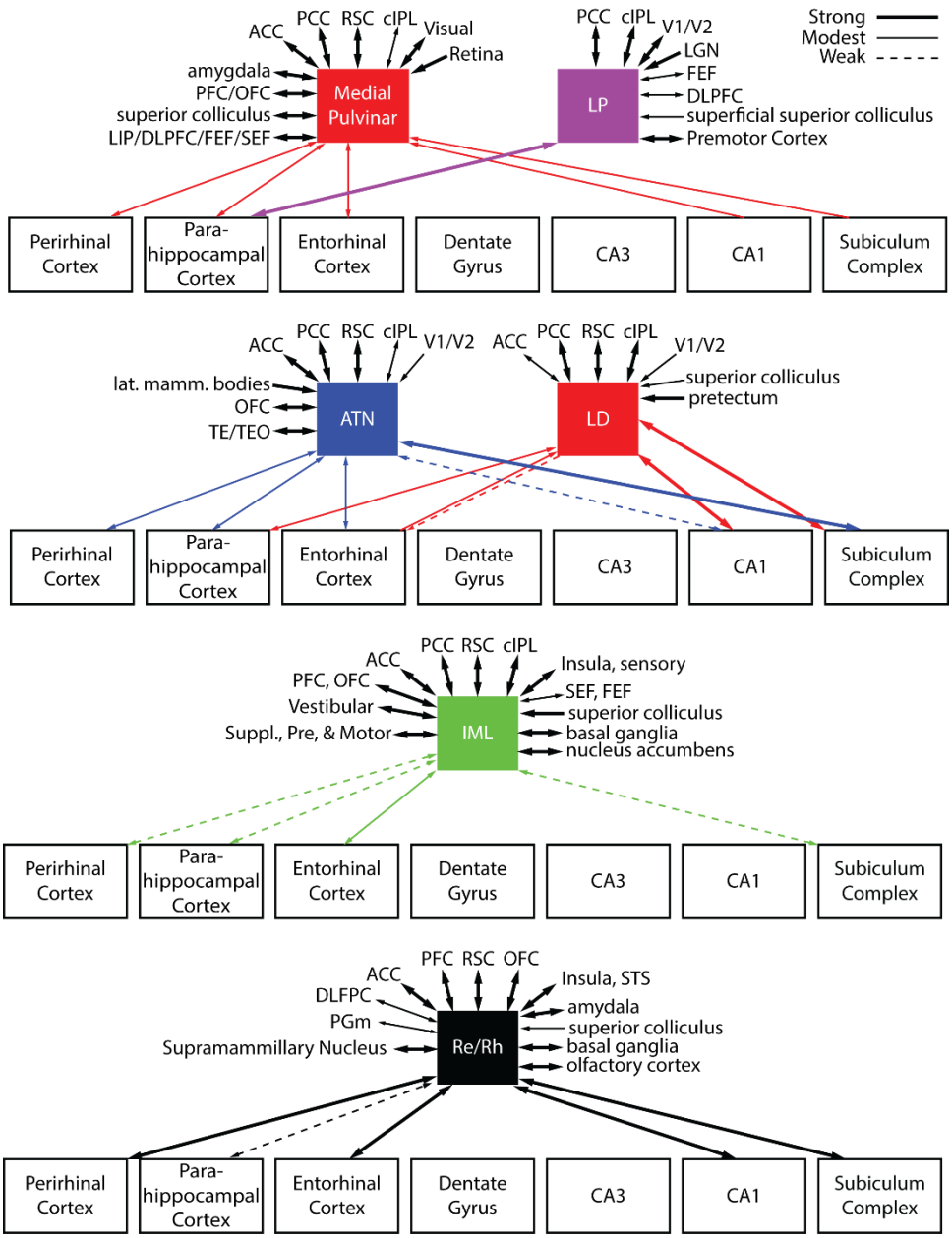

Figure 5-5 Direct Pathway #2-Thalamo-Medial Temporal Pathway

The MTL has strong connections to several thalamic nuclei that are known to or may carry eye movement-related signals. The connection patterns of each nucleus are quite different. Despite their anatomical and functional differences, the role of the various thalamic nuclei in memory may be similar. The thalamus may provide important timing signals and help gate information transfer to and from the MTL. Alternatively, the thalamus may provide a corollary discharge signal allowing the MTL to update spatial representations in real time. Further, the thalamus (e.g. ATN) may also directly provide spatial inputs to the MTL. MD is not shown since the lateral portions of MD are involved in eye movements—mediated by strong connections with the superior colliculus— and are not connected with the MTL. SEF and DLFPC *may* have reciprocal connections with MDpc and MDmc which are connected with the MTL (not shown). The Dentate Gyrus and CA3 do not receive appreciable thalamic input.

5.4.2 *Direct Pathway #2: Thalamo-Medial Temporal Pathway*

The higher-order thalamic nuclei are well connected to the oculomotor and memory networks. It is, therefore, not surprising that the thalamus is another direct pathway by which eye movement-related information may reach the hippocampus (**Figure 5.5**). Thalamic inputs into the MTL have been described before but not in the context of eye movements (Aggleton et al., 2011). As with the Parieto-Medial Temporal pathway, the Thalamo-Medial Temporal Pathway also has access to nearly every subregions of the MTL. However, individual nuclei have distinct but somewhat overlapping connection patterns. Unfortunately, unlike the Parieto-Medial Temporal pathway, the anatomy and function of Thalamo-Medial Temporal Pathway are poorly understood; however, the basic anatomy appears conserved across species. Here, I will focus on the LD, IML, Re/Rh, ATN, and medial pulvinar. The medial pulvinar and ATN, in particular, will provide exemplars for the role of the higher-order thalamus in providing the MTL with eye movement-related signals.

LD projects to several subregions in the MTL including CA1, the Postsubiculum and Presubiculum, and to a much lesser extent the entorhinal cortex (Saunders et al., 2005; Jones, 2007; Aggleton et al., 2011; Varela et al., 2014). In turn, LD also receives strong inputs from these areas including the entorhinal cortex. LD also has strong connections with the RSC, PCC, cIPL, and to a lesser extent ACC (Thompson and Robertson, 1987b); note these areas seem to synapse onto anatomically separate populations of neurons. Unlike MD, LD receives only weak inputs from the superior colliculus and V1/V2 (Harting et al., 1980; Thompson and Robertson, 1987b, a). LD also receives inputs from several pretectal nuclei which are involved in motor control, smooth pursuit eye movements, pupillary reflex, and vergence (Berman, 1977; Thompson and Robertson, 1987b; Rees and Roberts, 1993; ButtnerEnnever et al., 1996; Morin and Studholme, 2014).

Electrophysiological recordings from LD in primates show eye-position, direction, and eye movement sensitive neurons (Schlag-Rey and Schlag, 1984; Tanaka, 2007). LD in rodents encodes head-direction (Mizumori and Williams, 1993). LD lesions in rodents impair spatial memory and disrupt place cells (Mizumori et al., 1994). In an apparent contradiction, lesions to LD do not abolish head-direction tuning in the Postsubiclum suggesting that the ATN, not, LD is the source of head-direction information (Golob et al., 1998). Furthermore, animals with LD lesions were impaired on a spatial working memory task. Overall, these findings indicate that the LD may have a stronger functional association with the hippocampal place cells than with head-direction cells.

The IML are thought to play a role in controlling cortical excitability, attention, arousal, and synchrony particularly in the frontal, motor, prefrontal, and parietal cortices (Akert and Hartmannvonmonakow, 1980; Sadikot et al., 1990; Berendse and Groenewegen, 1991; Sadikot et al., 1992; Van der Werf et al., 2002; Hsu and Price, 2007; Saalmann and Kastner, 2011; Saalmann, 2014; Wijesinghe et al., 2015). Both the anterior and posterior groups share many connections, but the anterior group is well connected with the frontal and parietal cortices, and the posterior group is well connected to the prefrontal, premotor, supplementary motor, motor cortices, and striatum. The IML also have strong connections with vestibular nuclei, reticular formation, cerebellum, and superior colliculus as well as many neuromodulatory areas, amygdala, and nucleus accumbens. Other cortical connections are quite diffuse and include ACC, OFC, PCC, RSC, the insula, posterior parietal cortex, and sensory cortex; light connections to FEF are observed, and SEF connections are probable given the strong IML connections to various motor areas. Both the anterior and posterior IML are connected with the MTL, but the specific connection patterns are largely unknown. The IML project to the perirhinal, parahippocampal, and entorhinal cortices as well as the Prosubiculum and Subiculum proper. The entorhinal cortex seems to have the strongest

connections. IML's connections to MTL are lighter than other thalamic nuclei, but the IML appear to play a strong role in regulating the activity of areas directly connected to the MTL (e.g. RSC).

The anterior IML contain saccade direction modulated neurons like LD (Schlag-Rey and Schlag, 1984; Wyder et al., 2003; Tanaka, 2007). Interestingly, these neurons respond before, during, and after the saccade allowing them to be involved in the generation of eye movements as well as monitoring eye position after the saccade. These neurons also appear contextually modulated (Wyder et al., 2004). Lesions to the anterior IML produces deficits in consciousness and attention (Schiff, 2008; Saalmann, 2014). Posterior IML show multimodal sensory response to auditory, visual, and somatosensory information (Matsumoto et al., 2001; Saalmann, 2014). Lesions to the posterior IML produce deficits in task shifting (Liebermann et al., 2013)

Overall, the largest thalamic input to MTL comes from Re and Rh. Re and Rh are often described together as the function and anatomy of the Rh nuclei are similar to that of the Re; however, the Rh shows additional connections to the motor, somatosensory, and posterior parietal cortices (Vertes et al., 2006; Saalmann, 2014). In rodents, Re is reciprocally connected with mPFC, ACC, RSC, perirhinal cortex, entorhinal cortex, CA1, Parasubiculum, and Subiculum proper (Vertes et al., 2006; Ding, 2013; Saalmann, 2014; Vertes, 2015). Re also has connections to the supramammillary nucleus, basal forebrain, amygdala, hypothalamus, and brainstem, OFC, insula, claustrum, LGN, and VTA (Vertes, 2015). Re also receives a light projection from the superior colliculus (Harting et al., 1980; Thompson and Robertson, 1987b). Importantly, there are no direct connections from mPFC back to the hippocampus, but the mPFC has strong connections to Re which in turn provide the hippocampus with information from the mPFC. Unfortunately, very little appears to be known about Re in primates. Many of the connections described above appear to be present in primates (Yeterian and Pandya, 1989; Nakano et al., 1990; Barbas et al., 1991; Morecraft

et al., 1992; Dermon and Barbas, 1994). In primates, Re appears to have relatively strong connections with ACC, basal ganglia, OFC, and olfactory cortex but also receives a light projection from the superior colliculus, the posterior parietal cortex (e.g. PGm), and DLPFC (Harting et al., 1980; Schmahmann and Pandya, 1990).

Single unit recordings in rodents supporting the function of Re are limited, but Re seems to play an important role in regulating the excitability of CA1 and ACC (Saalmann, 2014). Single unit recordings also suggest Re plays a role in spatial working memory and processing of contextual information (Xu and Sudhof, 2013; Duan et al., 2015; Ito et al., 2015). Inactivation and lesions of Re impair performance on spatial working memory and task shifting similar to damage to the mPFC and hippocampus suggesting Re is important for interactions between the hippocampus and mPFC (Saalmann, 2014; Layfield et al., 2015). Almost nothing is known about the function of Re in primates, but the anatomical connections of Re suggest it is possible for Re to contain eye movement-related information.

In rodents, the [dorsal] ATN are an important node in the head-direction network (Vogt and Miller, 1983; Taube, 1995, 2007; Yoder et al., 2011a). ATN is connected to many of the same areas as LD. ATN receives inputs from CA1, V1/V2, and lateral mammillary nucleus. ATN is also reciprocally connected with the RSC, ACC, MEC, OFC, perirhinal cortex, parahippocampus, and subiculum complex with the strongest connections to Presubiculum and Postsubiculum (Ding, 2013). Note that the Postsubiculum comprises the dorsal portion of the Presubiculum. Primate connections to the ATN are less understood but thought to be conserved across species. The ATN in primates may have additional connections that include IT, DLPFC, and posterior parietal cortex including cIPL (Vogt and Pandya, 1987; Schmahmann and Pandya, 1990; Cavada et al., 2000).

Head-direction cells are commonly found in the ATN (Yoder et al., 2011b; Clark and Taube, 2012). Lesions to the ATN completely abolishes head-direction tuning in the subiculum and produce spatial memory impairments. Similarly, lesions of the ATN in monkeys results in impairments in object-place memory (Parker and Gaffan, 1997). Lesions limited to the ATN in humans are rare but suggest that the ATN in humans also plays a role in relational memory (Daum and Ackermann, 1994; Schnider et al., 1996; Harding et al., 2000; Tanaka et al., 2012). Other lesion studies suggest that ATN inputs into the MTL create an independent pathway separate from RSC and PCC (Golob and Taube, 1997). Interestingly, head-direction tuning in the PostSubiculum is delayed ~30 ms relative to the ATN suggesting the subiculum receives an efference copy from the ATN as ATN signals anticipate upcoming head-direction (Taube and Muller, 1998). I could not identify any paper focusing on single unit recordings in the primate ATN. However, Tanaka found some neurons in the anteroventral ATN that were sensitive to eye position (Tanaka, 2007).

The pulvinar is widely involved in a variety of functions representing its connections to a wide distribution of brain areas. Of particular interest is the medial portion as the medial pulvinar is involved in vision, attention, and multisensory integration (Grieve et al., 2000). The medial pulvinar has reciprocal connections with the striate cortex, extrastriate cortex, posterior parietal cortex (including LIP and cIPL), temporal cortex, PFC, ACC, OFC, amygdala, and superior colliculus (Romanski et al., 1997; Grieve et al., 2000); the medial pulvinar also receives direct input from the retina. The FEF, LIP, DLPFC, and SEF are all connected to the medial pulvinar, but some areas like FEF may have stronger connections to the central/lateral pulvinar than the medial pulvinar (Barbas et al., 1991; Romanski et al., 1997). While medial pulvinar receives inputs from most of the MTL, medial pulvinar only projects to the perirhinal, parahippocampus, and entorhinal cortices (Baleydier and Mauguiere, 1985; Kondo et al., 2005; Aggleton et al., 2011).

The MTL, RSC, PCC, cIPL, STS, and PFC appear to connect to the same regions within the medial pulvinar.

Single unit recordings in the pulvinar show complex behavioral responses to eye movements, eye position, and stimulus parameters (e.g. shape and color) earlier than some cortical areas (Robinson et al., 1990; Benevento and Port, 1995; Zhou et al., 2016). Inactivation of pulvinar can cause spatial neglect and visuomotor deficits (Wilke et al., 2010). Other studies have found the pulvinar to be important for other cognitive processes such as goal-directed behavior and decision-making (Acuna et al., 1990; Komura et al., 2013). Reversible inactivation of the pulvinar leads to spatial neglect and visuomotor deficits such as deficits in hand-eye coordination in goal-directed behavior (Wilke et al., 2010). Further, human lesions studies suggest the pulvinar is important for spatial and temporal attention (Arend et al., 2008b; Arend et al., 2008a; Snow et al., 2009). Unfortunately, not all lesion studies and single unit recordings are localized to the medial pulvinar, but the pulvinar appears important for integrating multimodal information in service of goal-directed behavior particularly in visuospatial attention during eye and body movements.

In many species, the lateral posterior (LP) nucleus of the thalamus is considered an extension of the pulvinar though in primates it is more distinct. Like the pulvinar, LP has been implicated in integrating and coordinate information across the cortex, but LP's connections appear more visual and motor-oriented than those of the pulvinar. Very little is known about the function of LP. What is known is that LP has strong connections with the parahippocampus, premotor cortex, cIPL, PCC, early visual areas, LGN, and reticular thalamic nucleus. LP also has light connections with the FEF, superficial layers of the superior colliculus, and DLPFC (Jones and Powell, 1971; Mason and Groos, 1981; Symonds et al., 1981; Rodrigoangulo and Reinososuarez, 1988; Yeterian and Pandya, 1988; Romanski et al., 1997). Both pulvinar and LP

have reach-modulated neurons in monkeys (Acuna et al., 1990). LP seems ideal for rapid visual input into the MTL and may contain eye movement-related activity due to its strong visual inputs as well as connections to cIPL and PCC.

In summary, there are many direct pathways from the higher-order thalamus to most regions within the MTL. LD and pulvinar contain strong connections to the MTL and are known to contain both eye movement and body movement related information. While LD has stronger connections to CA1 and the subiculum, the pulvinar has stronger connections to the perirhinal, parahippocampal, and entorhinal cortices. The strongest thalamic inputs, however, to the MTL are from the ATN and Re/Rh. Unfortunately, strong evidence for eye movement-related signals in the ATN and Re/Rh is missing because few primate studies have recorded neurons in these areas. However, it would not be surprising if eye movement-related signals exist as these nuclei are well connected to PCC and cIPL which do contain eye movement-related signals. Other thalamic nuclei like the IML only have weak connections to the MTL but do contain eye movement-related signals. Rather, these nuclei have strong connections to areas directly connected with the MTL like RSC, PCC, and PFC. Therefore, the IML likely regulate the input and output of the MTL.

5.4.3 *Indirect Pathway: Visuo-Medial Temporal Pathway*

There may exist several indirect pathways by which eye movement-related activity may reach the MTL. In particular areas like DLPFC, FEF, and LIP exert top-down control over visual areas that are major inputs into the MTL (Noudoost et al., 2010). The thalamus also likely plays a similar role in modulating the activity of visual areas. As an example, below I will detail the role of FEF in top-down modulation of V4, but similar processes likely apply to other pathways that regulate MTL inputs. These pathways directly regulate the ebb and flow of visual information

around the time of the saccade which in turn regulates the ebb and flow of visual activity entering the MTL.

There is strong evidence that FEF exerts top-down control over V4, which provides the major input into the parahippocampal cortex. FEF also has connections to IT which provides input to the perirhinal cortex. FEF has strong direct connections to V4 as well as indirect connections through the pulvinar (Gattass et al., 2014). The portion of V4 connected to the parahippocampus is mainly concerned with peripheral vision, and unlike the rest of the V4, these peripheral areas are heavily connected with the posterior parietal cortex suggesting that peripheral V4 is involved in visuospatial attention (Ungerleider et al., 2008). Interestingly, FEF projects to all regions of V4.

Spatial attention modulates single unit responses in V4 (Pasupathy and Connor, 1999; Roe et al., 2012; Steinmetz and Moore, 2014). Interestingly, receptive fields in V4 show presaccadic shifts towards the upcoming saccade target (Tolias et al., 2001). Microstimulation of FEF causes similar changes in V4 receptive field suggesting that presaccadic changes in V4 receptive fields may be mediated by FEF (Armstrong et al., 2006). These presaccadic shifts may lead to a perceptual enhancement observed just before the saccade (Hoffman and Subramaniam, 1995; Kowler et al., 1995; Rolfs and Carrasco, 2012). V4 also shows saccadic suppressions for non-preferred targets (Han et al., 2009; Burrows et al., 2014).

In summary, V4 responses for preferred targets at certain retinotopic locations are selectively enhanced. These enhancements occur before the saccade while suppression occurs immediately before, during, and into the beginning of the fixation period. Enhancement and suppression likely affect the ebb and flow of visual information into the MTL specifically through the perirhinal and parahippocampal cortices. FEF and V4 are great examples of an indirect

pathway, but other indirect pathways also exist that likely exhibit similar changes in activity around the time of a saccade.

5.4.4 *Anatomical and Functional Bridges*

Several areas are well-connected to both the oculomotor and memory networks but are not necessarily part of either. In particular, ACC and the insula form strong connections with both networks. ACC and the insula have been implicated in integrating a wide variety of information in service of various cognitive functions. Both areas appear to integrate cognitive, motor, and sensory signals. Regarding eye movements and memory, these areas could effectively send and receive information across both networks. Further, these areas are well positioned to modulate arousal and other motor functions. Given their diverse functions and anatomical connections, I suggest these areas act as additional bridges between the oculomotor and memory networks.

ACC is a large and diverse area, but all subregions of ACC are well interconnected with each other. ACC has been implicated in a variety of higher-order functions including attention, conflict monitoring, emotion, eye and body movements, learning, and reward/action-outcome evaluation (Bush et al., 2000; Paus, 2001; Ito et al., 2003; Botvinick et al., 2004). ACC has extensive connections that share many parallels to that of PCC. Interestingly, theta activity in ACC is linked to attention and error-correction indicating that ACC is part of a frontal network interconnected with the MTL involved in learning and memory (Tsujimoto et al., 2006; Young and McNaughton, 2009; Tsujimoto et al., 2010; Womelsdorf et al., 2010a; Womelsdorf et al., 2010b). Lesions to ACC cause a variety of impairments including deficits in the spontaneous initialization of movements and speech, inability to suppress inappropriate motor actions, as well as perform complex motor behaviors. Lesions to certain areas of ACC can lead to impairments of reflexive saccades and changes in other saccade statistics (Gaymard et al., 1998). ACC lesions also

cause deficits in reward-related learning (Shima and Tanji, 1998; Parkinson et al., 2000; Rushworth et al., 2003; Kennerley et al., 2006). "ACC seems to come into play when rehearsed actions are not sufficient to guide behavior" (Paus, 2001); thus ACC seems to play a role in learning new behaviors. Most single unit activity in ACC is post-saccadic and is modulated by reward expectation, prediction errors, and anticipation (Niki and Watanabe, 1979; Schall et al., 2002; Quilodran et al., 2008; Hayden et al., 2011). Further, neurons in ACC motor areas also play a role in voluntary, reward-based motor selection (Shima and Tanji, 1998). Electrical stimulation of cingulate motor areas (i.e. "cingulate eye fields") produces body and eye movements (Mitz and Godschalk, 1989; Luppino et al., 1991; Paus, 2001).

ACC's role in learning is not entirely surprising since the ACC is a major output of the hippocampus, entorhinal cortex, and parahippocampus (Vogt and Pandya, 1987). ACC also has strong connections to DLPFC, OFC, amygdala, ventral striatum, VTA, other neuromodulatory areas, MDmc, ATN, and midline thalamic nuclei (e.g. Re) (Vogt et al., 1979; Vogt and Pandya, 1987; Bates and Goldman-Rakic, 1993). Other notable connections include STS, STG, cIPL, PGm, and the insula. ACC's connections to cIPL and ATN are weaker than those of PCC. Motor areas within ACC project directly to the primary motor cortex, premotor cortex, supplementary motor areas (including SEF), DLPFC, and spinal cord. Interestingly, limbic connections (e.g. MTL) also reach the motor regions in ACC (Paus, 2001). Despite being functionally connected, FEF receives only light projects from ACC (Huerta et al., 1987; Wang et al., 2004; Lynch and Tian, 2006b; Babapoor-Farrokhran et al., 2017); most information in ACC travels through the SEF to reach the FEF (Schall et al., 2002).

As mentioned before, the function of the insula may be similar to that of ACC. Specifically, insular cortex is implicated in higher-order functions such as cognition, emotion, memory,

attention, sensorimotor integration, and reward expectation (Augustine, 1996; Nieuwenhuys, 2012). A similar role between the insula and ACC suggests similar connectivity patterns. However, while they share common connections and connections with each other, the insula seems to have stronger connections to sensory areas.

Insular cortex receives widespread connections from a variety of areas including areas that encode auditory, vestibular, somatosensory, gustatory, and visual information. In general, the insula is well connected to the amygdala, striatum, OFC, PFC, ACC, and pulvinar, cIPL, premotor and supplementary motor cortices, and perirhinal and parahippocampal cortices (Augustine, 1996); the insula is also sparsely connected to PCC and IT cortex. Most connections are reciprocal, but the three subdivision of the insula (Ig, Id, and Ia) have different connectivity patterns (Augustine, 1996; Flynn et al., 1999); the posterior portion (Ig, Id) appears to contain more visual activity. Ig is strongly connected to somatosensory areas and supplementary/premotor areas. Ig receives few inputs from the entorhinal cortex and amygdala. Ig has no apparent connections to FEF, but there are a few connections to SEF (Huerta and Kaas, 1990). Id has widespread connections illustrating its role in multisensory integration. Ia is particularly well connected with ACC, cIPL, STS, claustrum, PFC including DLPFC, perirhinal cortex, and entorhinal cortex.

Insular activity appears unrelated to saccades though the activity of many neurons appears to increase after fixation onset (Mesulam and Mufson, 1982a, b; Mufson and Mesulam, 1982; Asahi et al., 2006); perhaps the responses of insular neurons are gated by attention. Other insular neurons respond to reward expectation, visual stimuli, motor actions, sound, somatosensation, and vestibular inputs (Grusser et al., 1990; Zhang et al., 1999; Asahi et al., 2006; Mizuhiki et al., 2012). Interestingly, stimulation of the insula can cause motor movements suggesting that the insula may be important for complex sensory-motor responses (Showers and Lauer, 1961; Afif et al., 2010).

In humans, functional imaging implicates the insula in relational memory retrieval and is often co-activated with cingulate, prefrontal, and MTL networks (Fink et al., 1996; Ghaem et al., 1997; Young et al., 2012).

5.4.5 *FEF and MTL Connections*

Schall et al. suggested that a very small number of TF neurons may project to the most lateral and ventral parts of FEF (BA 45) (Schall et al., 1995). However, retrograde tracers injected into TF suggests that FEF connections to TF are almost nonexistent (Suzuki and Amaral, 1994a). Functionally speaking, the lateral parts of FEF appear to control smaller amplitude eye movements and thus are more involved with foveal vision. The more medial parts of FEF are associated with larger amplitude eye movements and are thus more involved in peripheral vision (Lynch and Tian, 2006a). Thus, FEF (BA 45) labeled in Schall et. al. would be unlikely to project to TF as TF process peripheral vision more so than foveal vision. Pandya and colleagues have shown non-FEF portions of BA 45 are connected with the parahippocampus (TF/TL) suggesting that the connections found by Schall et al. may be due to diffusion traces into non-FEF BA 45 (Yeterian et al., 2012).

Several other studies have proposed that the parahippocampal cortex (TH/TF) has monosynaptic connections with FEF (Pierrot-Deseilligny et al., 2004; Shen et al., 2016). The data used in these study comes from the CoCoMac database (Stephan et al., 2001; Kotter, 2004; Bakker et al., 2012). CoCoMac references several papers (Felleman and Van Essen, 1991; Young, 1993), but surprisingly these connection are not shown. I dug further, but no concrete connection between FEF and MTL was found. Therefore it is unlikely that the MTL has monosynaptic connections with FEF. However, there is likely functional connection between the MTL and FEF.

5.4.6 *The Medial Septum and Other Neuromodulatory Inputs*

The neuromodulatory systems are well connected to the oculomotor and memory networks, but do these areas have anything to do with eye movements? The short answer appears to be no. There is no clear evidence of eye movement-related activity within any of neuromodulatory nuclei, but current findings suggest an indirect link between eye movements and neural activity. Nearly all neuromodulators play a role in arousal, attention, motivation, and synaptic plasticity which can modulate eye movements in the context of learning and memory. Below, I wish to briefly mention a few relevant points that may have been missed in the sections above.

Neuromodulator inputs are extremely important for shaping neural activity in both networks. The subiculum receives a large amount of input from the "locus coeruleus, median raphe nucleus, nucleus of diagonal band, and ventral tegmental area, which are the origins of noradrenergic, serotonergic, cholinergic, and dopaminergic projections to the hippocampal formation, respectively" (Ding, 2013). The hippocampus proper also receives some neuromodulatory inputs but not as much as the subiculum. Various PFC areas, thalamic nuclei, and the basal ganglia are also reciprocally connected with these neuromodulatory systems (Sara, 2009). ACC has relatively strong connections to nearly all neuromodulatory centers suggesting that ACC may exert top-down control over the excitability of much of the brain.

The locus coeruleus (LC) and the medial septum are the two most relevant areas for linking eye movements and memory. For example, LC activity is correlated with pupil diameter (Aston-Jones and Cohen, 2005), but there is "no consistent relationship between LC activity and simple eye position or direction of eye movement" (Aston-Jones et al., 1999). Interestingly, LC neurons stop firing during REM sleep but only show diminished activity during slow wave sleep (Astonjones and Bloom, 1981).

The medial septum in rodents plays an important role in regulating hippocampal theta. The medial septum innervates the hippocampus, subiculum, entorhinal cortex, and RSC with GABAergic and cholinergic fibers (Mesulam et al., 1983; Gulyas et al., 1991; Unal et al., 2015). Medial septal neurons in primates also appear to fire rhythmically in theta range (Lamour et al., 1984). Further, local field potentials in the medial septum are modulated by eye movements though single unit neurons modulated by eye movements have not been found (Sobotka and Ringo, 1997).

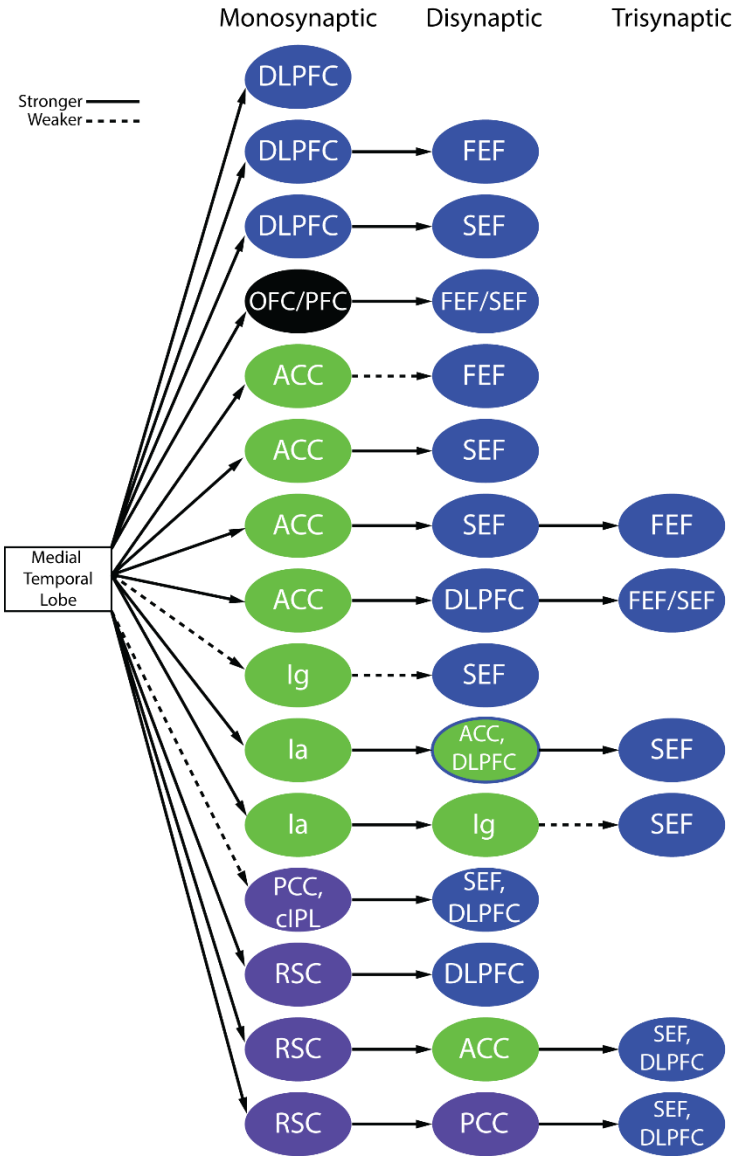

Figure 5-6 Cortical Output Pathways from the MTL to the Oculomotor Network
There exist a large number of pathways by which memory-related activity in the MTL could affect eye movements. Here, I show 15 potential cortical pathways, but many other cortical and thalamic pathways are also possible. Most pathways terminate at DLPFC or SEF, but many also terminate onto FEF. Pathways through DLPFC and ACC are relatively strong and short. A monosynaptic pathway to DLPFC may be important for inhibiting eye movements but insufficient for the generation of all types of eye movements. Pathways terminating on SEF and DLPFC by extension reach FEF by an additional synapse. Several disynaptic and trisynaptic pathways exist to LIP. For example, a weak disynaptic pathway exists through cIPL to LIP. Other potential pathways to LIP exist through ACC. However, LIPs role in the top-down regulation of eye movements seems substantially weaker than those in the PFC. Lastly, the insula (Ia and Ig) create several additional pathways by which memory signals could influence eye movements, but the strongest pathways are from Ia to ACC or DLFPC.

5.4.7 *Output Pathways*

There are several potential pathways by which memory influences eye movements (**Figure 5.6**). First and foremost the same pathways that provide the MTL with eye movement-related signals also receive strong feedback from the MTL. Thus reciprocal connections between the MTL, the thalamus, and RSC allow eye movement-related and memory information to flow in both directions. These pathways form disynaptic and trisynaptic connections between the MTL and oculomotor regions. The total number of plausible pathways is rather large as all these areas are strongly interconnected. Below, I briefly describe the pathways that I found most promising based on the inferred strength of connections and function of each area. I focus on cortical pathways as the thalamic pathways are more numerous, and I strongly believe the thalamic pathways perform a different function (see section below).

DLPFC and ACC receive modest to strong input from the MTL. DLPFC is strongly involved in the cognitive control of eye movements though DLPFC is likely involved in the inhibition and modulation rather than the generation of saccades. Thus the DLFPC forms a monosynaptic pathway by which memory can influence eye movements; however, DLPFC alone may be insufficient for generating eye movements. Instead, DLPFC can relay memory-related signals to FEF and SEF, which are involved in the generation of saccades. Similarly, ACC projects strongly to SEF and weakly to FEF. Additionally, OFC and other PFC areas receive strong inputs from the MTL, and these areas in turn project directly to DLFPC, FEF, and SEF.

Briefly, the insula provides another pathway by which memory signals may influence eye movements, but there are no direct pathways from the insula to FEF. Instead, weak pathways exist from Ig to SEF and other supplementary motor areas; however, Ig only weakly connects with entorhinal cortex. Instead, Ia is strongly connected with the MTL. Ia is interconnected with Ig

which can project to SEF or other supplementary motor areas. However, the strongest pathways through Ia are mediated by ACC or DLPFC and their respective connections. Thus, the MTL has several strong trisynaptic pathways through the insula that could influence eye movements.

Finally, as mentioned before the Parieto-Medial Temporal pathway has many reciprocal connections with the MTL. RSC, in particular, has the strongest connections with the MTL. cIPL and to a lesser extent PCC also receive some direct feedback from the MTL. Given the connectivity patterns of these areas, there are many potential routes by which memory-related signals could influence eye movements. The shortest and strongest pathway is from RSC to DLFPC. Alternatively, both cIPL and PCC project directly to SEF and DLPFC. cIPL also has light connections to FEF and strong connections to LIP. RSC projections to ACC, which in turn projects to DLPFC and SEF, also provide an additional, and meaningful pathway. Lastly, as noted before PCC has stronger connections to motor areas than RSC. Thus, strong memory signals from RSC could travel to PCC which in turn could influence multiple motor areas including SEF as well as LIP.

In summary, there exist a large number of pathways to and from the oculomotor and memory networks. Many of these pathways allow information to flow back and forth. The shortest connection between these networks is from the MTL to DLPFC, but this pathway may be insufficient for generating eye movements. Instead, interconnections within PFC, as a whole, create an ideal network which by multiple pathways into and out of it can influence eye movement and memories. Particularly important nodes include ACC, DLPFC, FEF, and SEF. The functional implications of these pathways are considered in the discussion below.

5.5 DISCUSSION

5.5.1 *The Supplementary Eye Fields and Subiculum Complex as Special Nodes for both Networks*

Of all the areas described so far, I believe SEF and the subiculum have a special role in integrating memory and eye movement-related signals. ACC, DLPFC, and the FEF also play important roles (Shen et al., 2016). While ACC may not be important for generating eye movements, ACC appears to monitor the activity of many cortical areas and creates an ideal relay for the oculomotor and memory networks. DLFPC receives modest outputs from the subiculum and through Re sends information back to the MTL. Further, FEF has many potential disynaptic and trisynaptic routes to and from the MTL. Nonetheless, from a functional standpoint, SEF and DLFPC seem to be more interconnected with the MTL than FEF. Further, in the context of memory, SEF and DLPFC are functionally more interesting. Below, I describe my thoughts in relation to those of Shen and colleagues who suggest FEF and DLFPC are the most important nodes.

Shen and colleagues suggest that FEF and DLPFC are particularly well-suited for communicating information between the memory and oculomotor networks. Further, these areas are well connected with premotor neurons in the reticular formation, and thus they have direct influence over the generation of the eye movements. DLPFC receives modest input from the subiculum creating a shorter pathway than FEF which receives memory-related activity from the MTL through disynaptic connections only. They also found high communicability between memory and oculomotor networks via many other areas including the pulvinar, V2/V4, cIPL, perirhinal and parahippocampal cortices, insula (Ig), ACC, DLPFC, OFC, and other PFC area.

They suggested these areas, through CA1 and the subiculum, form disynaptic connections with FEF. In their analysis LIP was only marginally communicable with both networks.

In general, I agree with their findings that several areas are highly communicable across the memory and oculomotor networks, but further scrutiny of their results is needed. In particular, I believe they need to rethink some of their connective patterns. First, the hippocampal output to V2/V4 is minimal; while V4 has strong connections to the parahippocampal and perirhinal cortices, there are no apparent connections with CA1, subiculum, or entorhinal cortex (Ninomiya et al., 2012). Second, as mentioned above the parahippocampal and perirhinal cortices are not connected to FEF. Third, ACC is weakly connected to FEF. Fourth, insular cortex (Ig) only receives light connections from entorhinal cortex and other MTL areas; it is Ia that is strongly connected to the MTL and PFC; and Ig does not have connections with FEF but weak connections with SEF. In summary, the only meaningful disynaptic connections to the FEF are through DLPFC, other PFC structures, OFC, and [medial] pulvinar. PCC and RSC are also potential candidates but PCC only receives minor feedback from the MTL and RSC has weaker connections to motor areas.

The results from Shen and colleagues are still meaningful but need to be accepted only after careful consideration. Some of the issues arise from the CoCoMac database others arise for the strength of the connections that were not considered. After these considerations, disynaptic connections from the MTL to FEF may not be as impactful as once considered. Rather, other connection schemes are more reasonable. Instead, the SEF and DLPFC have stronger and more meaningful connections between the oculomotor and memory networks. These areas in turn project directly to FEF but focusing on these nodes have different implications. In their analysis, SEF and DLPFC have high communicability with both networks with DLPFC have stronger

communicability than even FEF (Shen et al., 2016). Higher communicability with SEF than FEF may be plausible if we take into account the considerations above. I will not further discuss DLFPC, but DLPFC may play a similar role to SEF.

Why would SEF be more important than FEF? SEF has been implicated in learning and the production of motor sequences (Chen and Wise, 1997; Histed and Miller, 2006). Further, low threshold stimulation of SEF evokes neck, forelimb, and eye movements to fixed points in space rather than retinotopic coordinates (Abzug and Sommer, 2017). Thus, SEF may code information in allocentric coordinates (Olson and Gettner, 1995). In contrast, FEF encodes eye movements in retinotopic coordinates with some degree of head-centered bias (Caruso et al., 2017).

These functional characteristics make SEF an ideal target for the interaction between eye movements and memory. Navigation requires the coordination of several movements (e.g. walk 10 ft. then turn left) in sequence rather than say a single movement (e.g. take 1 step). Efficient navigation in familiar environments requires the MTL, but for spatial information in the MTL to influence behavior, this information must be sent elsewhere. Spatial information in the MTL is likely sent to PFC, ACC, DLPFC, posterior parietal cortex, RSC, and PCC (indirectly). These areas can combine the memory information in the MTL with visual, postural, motivational, and other forms of information that define the current physical and cognitive state of the animal. SEF can then integrate the combined information across these areas through its direct connections to them. Within SEF, this information could be used to form a motor plan to produce a sequence of eye and body movements. Individual eye movements are then produced by sending the motor plan to FEF and superior colliculus.

Anatomically speaking, DLPFC and the SEF are also good targets for the interaction between the oculomotor and various memory systems outside of the MTL. In particular, the

networks formed by DLPFC and the SEF are strongly connected to the basal ganglia (caudate), cerebellum (through the pons), and various thalamic nuclei involved in other forms of learning and memory (Shook et al., 1988; Huerta and Kaas, 1990; Shook et al., 1990, 1991; Cavada et al., 2000; Schall et al., 2002; Lynch and Tian, 2006a). Thalamic connections include *all* subdivisions of MD, area X, and the ventralanterior nuclei; area X and the ventralanteior nuclei are strongly connected with the cerebellum and basal ganglia, respectively. Thus, DLFPC and the SEF form an ideal node by which various learning and memory systems can interact to influence behavior.

The canonical model that information in the MTL is processed in a serial and hierarchical fashion is vastly oversimplified. Inputs into the MTL occur within almost all subregions to a varying degree. Of particular interest is the subiculum complex which has approximately equal amounts of input and output. In rodents, certain subicular subdivisions (Pre-, Para-, and PostSubiculum) are the main sources of head-directions signals from the ATN to the MTL. Head-direction signals in the ATN are predictive of head movements while subiculum activity reflects head movements in real time. In other words, the ATN sends a corollary discharge signal to the MTL through the subiculum. The subiculum also has strong connections to other thalamic nuclei include the midline nuclei (Re/Rh), IML, and LD. Also, these subicular subdivisions also have direct, reciprocal connections with the MEC, LEC, cIPL, DLPFC, and RSC, PCC, ACC, V1/V2, parahippocampus, perirhinal, TEO, claustrum, and OFC.

Direct inputs into the MTL that bypasses the classical circuitry may be important for integrating cognitive and spatial information in real time. It's unclear whether these direct inputs give rise to spatial representations throughout the MTL. Instead, direct connections may carry corollary discharge signals required to update spatial representations in real-time. Alternatively, these connections may be important for timing signals that are necessary for communicating with

various cortical and subcortical areas involved in encoding, retrieval, and consolidation of memories. Regardless of their specific function, these direct inputs likely play an important role in shaping the output of the MTL.

5.5.2 *Functional Implications of the Anatomy*

The anatomical connections to and from the MTL that give rise to spatial representations have many functional implications. In particular, the same pathways appear to exist in both rodents and primates. However, there exist major differences in the quantitative distribution of certain connections. For one, in primates, there is an abundance of visual and visuospatial inputs into the MTL whereas in rodents visual inputs are balanced by olfaction, somatosensation, and audition. These anatomical differences suggest that the hippocampus in primates should carry more visual information than in rodents. While little is known about the connections in humans, visual processing also occupies a disproportionate amount of neocortex in comparison to other sensory modalities. Despite differences in the inputs to the MTL the connection patterns with the MTL are mostly conserved across species. The conservation of the connections within the MTL suggests that the MTL is processing information in a fundamentally similar way across species.

In primates, the same areas that process visuospatial representations that feed into the MTL also process body movements in conjunction with eye movements. This implies that eye movement information should also reach the MTL. Not surprisingly, there are several primate studies that find gaze-based representations in the MTL that encode eye position and eye movements (Ringo et al., 1994; Rolls, 1999; Nowicka and Ringo, 2000; Killian et al., 2012; Killian et al., 2015; Wirth et al., 2017). It is very important to understand that the same pathways that carry eye movement information are also the same pathways that provide information about physical

movements to the MTL in rodents. Additional pathways are not necessary to explain the differences between rodents and primates.

The differences between spatial representations identified in rodents and primates suggest that the sensorimotor processes used in each species to actively explore their environments inevitably influence the type of spatial representations that develop in the MTL. Rodents use sniffing and whisking to explore their environments up close while primates use eye movements to efficiently explore space from afar. In both species, other sensory modalities still play important roles in shaping spatial representations within the MTL. It is entirely plausible that spatial representations in primates could encode the physical position of the monkey in space, but gaze-related information should not be ignored. Lastly, recent evidence from bats suggests that the hippocampal place code is different for different sensory modalities (Geva-Sagiv et al., 2016). These findings highlight the importance of active sensing in shaping spatial representations in the MTL.

The relative amount of neocortex in primates devoted to visual processing also may influence the organization of inputs into the MTL. In particular, RSC, PCC, ACC, PFC, perirhinal cortex, parahippocampal cortex, and entorhinal cortex are relatively expanded in comparison to these areas in rodents (Andersen, 2007). The implications of these expansions are unknown but could have several effects. One, the expansion of these cortical areas could signify that the hippocampus and other MTL structures are less important for certain types of spatial memory such as spatial working memory. Lesions to the hippocampus in rodents produce deficits in many spatial working memory tasks, but lesions to the hippocampus in primates produce less consistent results (Sapiurka et al., 2016). Second, expansion of these areas may simply imply that secondary visual processing occurs outside unimodal visual areas thus more processed visual information enters the

MTL in primates. Third, the computational demands of representing space at a distance (i.e. gaze-modulated representations) may require more cortical processing power than representing the physical position of an animal in space.

There are many convergent and divergent pathways into and out of the MTL, but why are there so many pathways? One plausible reason is that the multiple loops formed across the cortex, thalamus, and striatum may be important for learning. These loops could provide both positive and negative feedback signals which are important for learning. Alternatively, various loops could be involved in different cognitive processes, and by having many converging and diverging connections, the MTL can flexibly engage in different cognitive tasks. Thalamic connections to a wide variety of areas could help with interareal communication. Lastly, another possibility is that different loops are important for different types of learning and memory. For example, connections to the ventral stream may be engaged during perceptual learning while connections to the PFC may be involved in spatial working memory. Overall, the widespread connections of the MTL and functions ascribed to it suggest that the MTL is flexibly engaged in a variety of processes and that these loops likely aid in the diverse cognitive functions of the MTL. The diverse loops also allow the MTL to interact with nondeclarative learning systems and potentially facilitate nondeclarative learning at its earliest stages, though the MTL is not necessary for nondeclarative learning (Squire, 1992).

Several stages of processing are necessary to transform egocentric representations into allocentric representations. If the MTL in primates truly encodes spatial information in an allocentric reference frame, then direct connections to the oculomotor network would never make sense. Allocentric spatial information must first be transformed into egocentric representations. This transformation could occur in a variety of brain regions including RSC. Once in an egocentric

reference frame, information must then be transformed into retinotopic coordinates. Gain fields allow for single-step transformations once in information is represented in an egocentric reference outside of the MTL (Smith and Crawford, 2005; Blohm et al., 2009), but additional steps may also be required. On the other hand, areas like SEF already appears to code information in allocentric coordinates negating the need for several transformations; however, eventually, the information must be transformed into retinotopic coordinates. Essentially, the need to transform information back into retinotopic coordinates from allocentric coordinates requires several processing stages likely mediated by several brain areas. The number of areas necessary for this transformation depends on the pathway of interest.This strongly implies at least disynaptic if not trisynaptic pathways between the MTL and oculomotor regions. However, full transformations may not be necessary as learning may occur optimally in certain reference frames.

5.5.3 *Future Directions*

More anatomical and functional studies are needed to elucidate the connections between the memory and oculomotor networks. Many questions still remain unanswered. Are there more anatomical pathways into and out of the MTL than described here? What specific role do the thalamic nuclei play? Do certain pathways provide greater spatial information than others? Is the spatial information that each pathway carries similar? Do different neurons within each brain region connect to different brain regions or do they send collaterals to multiple regions? Lastly, do SEF, DLPFC, and the MTL truly project to the same subdivisions of MD?

A large amount anatomy was done in the 1980's and 1990's, but critically much more work still needs to be done. In particularly, double and triple labeling studies would be particularly useful to determine if the same neurons in, for example, DLPFC receive input from the subiculum, ACC, and SEF or are these distinct subpopulations? Improved viral vectors can begin to target specific

genetic subpopulations to understand at the very least whether connections are onto inhibitory or excitatory neurons. Targeting of specific subregions within each area could also be plausible. Transgenic primates would also be useful for mapping anatomical and functional connections between areas.

In addition to understanding the anatomy better, a greater understanding the function of areas within the primate MTL is necessary. Many primate physiologists have focused on trying to replicate rodent findings, but the primate contains a different type of spatiotemporal information. Instead, unique experiments directly aimed at understating the MTL in primates is necessary. Further, many of the ongoing MTL experiments are overly complex and undermine our ability to create a mechanistic understanding of the function of the MTL. The oculomotor network is only as well understood as it is today because researchers have built their understating from the ground up first using extremely simplistic experiments. Now that a basic mechanistic understanding exists, researchers can assess the role of these areas in more complex and naturalistic behaviors. Truly understanding the MTL in primates is going to require a similar approach. Part of this approach will require creating a better understanding the direct and indirect pathways.

Chapter 6. DISCUSSION

6.1 Future Directions: Viewing Behavior as Foraging Strategy

We can think of viewing behavior as a foraging strategy where monkeys gather visual information (e.g. *Chapter 3*). Two types of behaviors define foraging strategy: exploration and exploitation. Explorative behaviors are optimized for gathering new information as quickly as possible. Exploitative behaviors are optimized by previously obtained information and used to gain a better and more detailed understanding one's environment. I hypothesize that viewing behavior during novel image presentations is characterized by exploration while memory for a stimulus shifts behavior towards exploitation. Further, I hypothesize that the hippocampus and other MTL structures are the sources of this stimulus memory.

In addition to my work, previous studies have shown that long-term stimulus memory (i.e. relational memory) correlates with changes in viewing behavior (Kaspar and Konig, 2011; Gameiro et al., 2017). Specifically, long-term stimulus memory correlates with increases in fixation durations and decreases in saccade amplitudes (e.g. **Figure 4.5**). Shorter fixation durations and larger amplitude saccades have been associated with exploration while longer fixation durations and shorter amplitude saccades have been associated with exploitation (Kaspar and Konig, 2011; Gameiro et al., 2017). Long-term memory also changes the distribution of fixation locations, potentially biasing observers towards new fixation locations during repeated image presentations (Kaspar and Konig, 2011; Gameiro et al., 2017). Combined, these results suggest that memory exerts control over the spatial and temporal patterns of eye movements.

Measures of fixation durations, saccade amplitudes, and fixation locations only assess individual spatial and temporal components of behavior, but we must assess behavior as a whole

to test the foraging hypothesis. Eye movements do not occur in isolation. Instead, consecutive eye movements interact with each other in space and time. Thus we must find measures that explain the spatiotemporal pattern of eye movements for a *whole* scan path. There are many methods for doing this (Coutrot et al., 2017). However, many are convoluted, computationally expensive, or difficult to relate to cognition. Below, I focus on recurrence quantification analysis which meets the above requirements necessary to test the foraging hypothesis.

Scientists first developed recurrence analysis to understand complex, nonlinear systems (Webber Jr and Zbilut, 2005), but researchers have recently applied recurrence analysis to scan paths (Anderson et al., 2013). Recurrence analysis is akin to calculating the autocorrelation of the states of a system. When analyzing viewing behavior, fixation locations are the discrete states of the scan path. Unfortunately, recurrence does not include measures such as fixation durations but instead analyzes ordinal fixation patterns. Recurrence analysis can also be used to quantify the similarity between two scan paths (Anderson et al., 2015); this type of recurrence analysis is called cross-recurrence and is analogous to cross-correlation.

Two fixations are recurrent if their locations are similar within a certain distance; I use a threshold of two degrees of visual angle, as this is consistent with the literature (Anderson et al., 2015). **Figure 6.1** shows a recurrence plot for a single, hypothetical scan path. The recurrence plots are symmetrical, and the line of incidence (i.e. the central diagonal) is always one as in autocorrelation plots. The x- and y-axes are ordinal fixation number. Ones (yellow squares) represent recurrent fixations while zeros (blue) represent non-recurrent fixations.

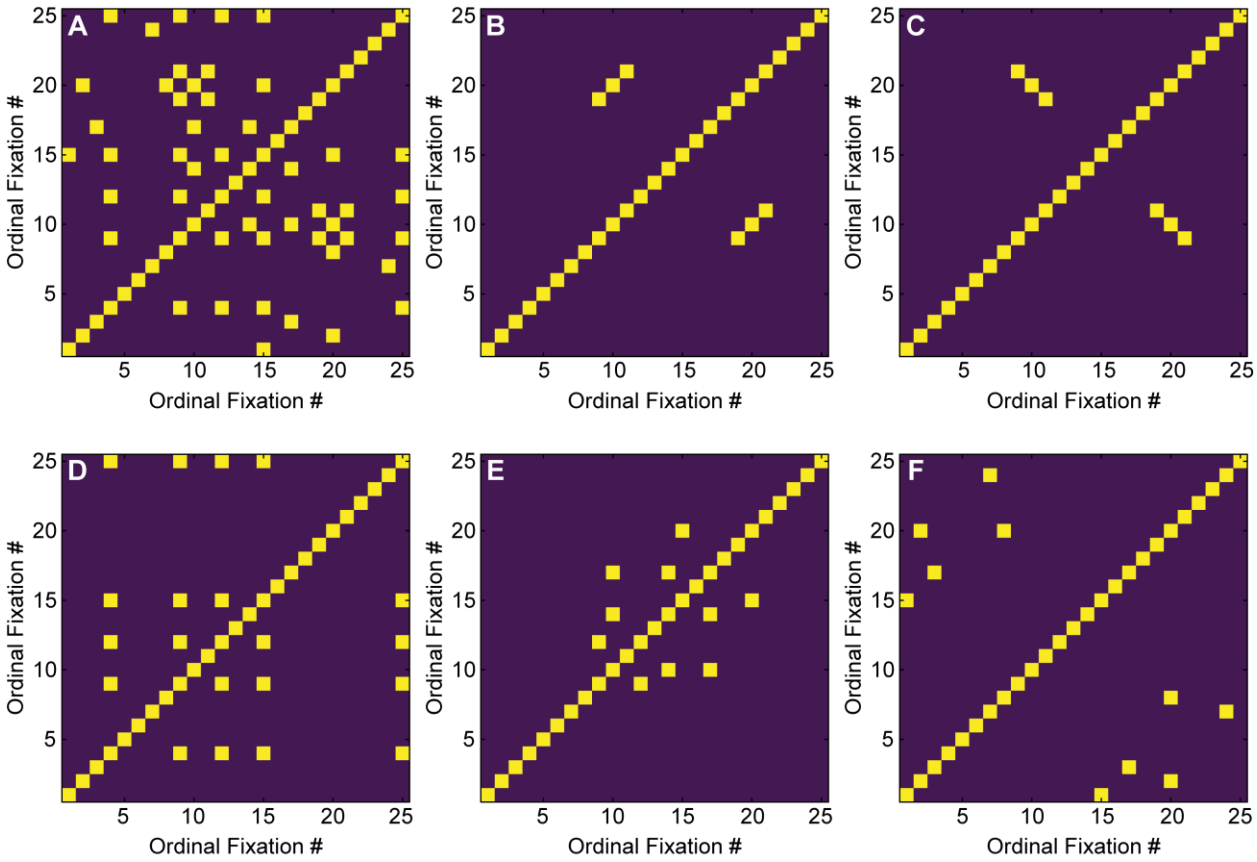

Figure 6-1: Recurrence Plots

A) A hypothetical recurrence plot illustrating recurrent fixations as yellow squares. Like an autocorrelation, the central diagonal (line of incidence) is always one. **B)** Diagonal patterns parallel to the line of incidence represent forward retraces. **C)** Diagonal patterns perpendicular to the line of incidence represent reverse retraces. **D)** Horizontal and vertical patterns represent laminar fixations. **E)** Recurrent fixations close to the line of incidence represent locally-oriented behavior (i.e. exploitation). **F)** Recurrent fixations far from the line of incidence represent globally-oriented (i.e. exploration) behavior.

Recurrence analysis is both a graphical and quantitative method. Visual inspection of a recurrence plot readily depicts several spatiotemporal patterns. The pattern of 1's and 0's in recurrence plot can also be quantified using several measures. The four most common measures are recurrence rate, determinism, laminarity, and center of recurrence mass.

The recurrence rate measures the number of observed recurrent fixations divided by the total number of possible recurrent fixations. In other words, the recurrence rate represents the percent of fixations that occur at previously fixated locations. Recurrence rates are typically around 5% and occur approximately two times more likely than chance (data not shown).

Determinism measures sequences of recurring fixations. Determinism is represented by diagonals in the recurrence plots (**Figures 6.1B & 6.1C**), which are sequences typically composed of three fixations (data not shown). Diagonals parallel to the line of incidence illustrate forward retraces in which observers scan the same fixation locations in the same order (**Figure 6.1B**). Conversely, diagonals perpendicular to the line of incidence illustrate reverse retraces in which observers scan the same fixation locations in the reverse order (**Figure 6.1C**). Retraces may be particularly useful for encoding information as they grant observers additional opportunities to strengthen previously encoded information. Further, reverse retraces may also demonstrate a behavioral correlate of retrieval. Consequently, I expect reverse retraces to be more prevalent during repeated presentations.

Laminarity represents fixation locations that are fixated multiple times. Laminar fixations are represented by horizontal and vertical patterns in the recurrence plots (**Figure 6.1D**). Laminarity is unlikely to be correlated with memory in the free viewing of images. Instead, particularly interesting image locations (e.g. salient locations) likely draw observers to the same location multiple times.

The center of recurrence mass, or CORM, measures the spatiotemporal distribution of fixation locations. Recurrent fixations close to the line of incidence produce smaller CORM values and represent locally-oriented behavior (i.e. exploitation) (**Figure 6.1E**). Conversely, recurrent fixations far from the line of incidence produce larger CORM values and represent globally-oriented behavior (i.e. exploration) (**Figure 6.1F**).

The four recurrence measures above describe eye movement patterns in individual scan paths, but recurrence plots averaged over many scan paths can illustrate additional factors that influence behavior across many scan paths. Below, I use data from ~2,000 scan paths collected from 4 monkeys during the free viewing of novel and repeated images. This task is nearly identical to the task described in *Chapter 4*. The average recurrence plot across these 2,000 scan paths reveals several additional patterns of eye movements (**Figure 6.2**). The four recurrence measures do not explicitly quantify these emergent patterns.

First, during both novel and repeat image presentations, I observe a large number of recurrent fixations parallel to the line of incidence but offset by one fixation. These recurrent fixations represent what are called 1-backs. In essence, an observer fixates location X, then fixates location Y, and then returns to fixation location X on the following fixation. Not surprising, 1-backs and other *n*-backs are common in free viewing paradigms (Wilming et al., 2013). Overall, 1-backs occur on approximately 11% of fixations. I did not observe a large number of 2-backs or 3-backs in this task, but some of our other data sets contain a larger number of *n*-backs (data not shown). The 1-back rate is similar (*ks-test*, $p > 0.5$) for novel and repeat image presentations (data not shown). Regarding memory formation, 1-backs may be useful for building and examining spatial relationships between viewed items.

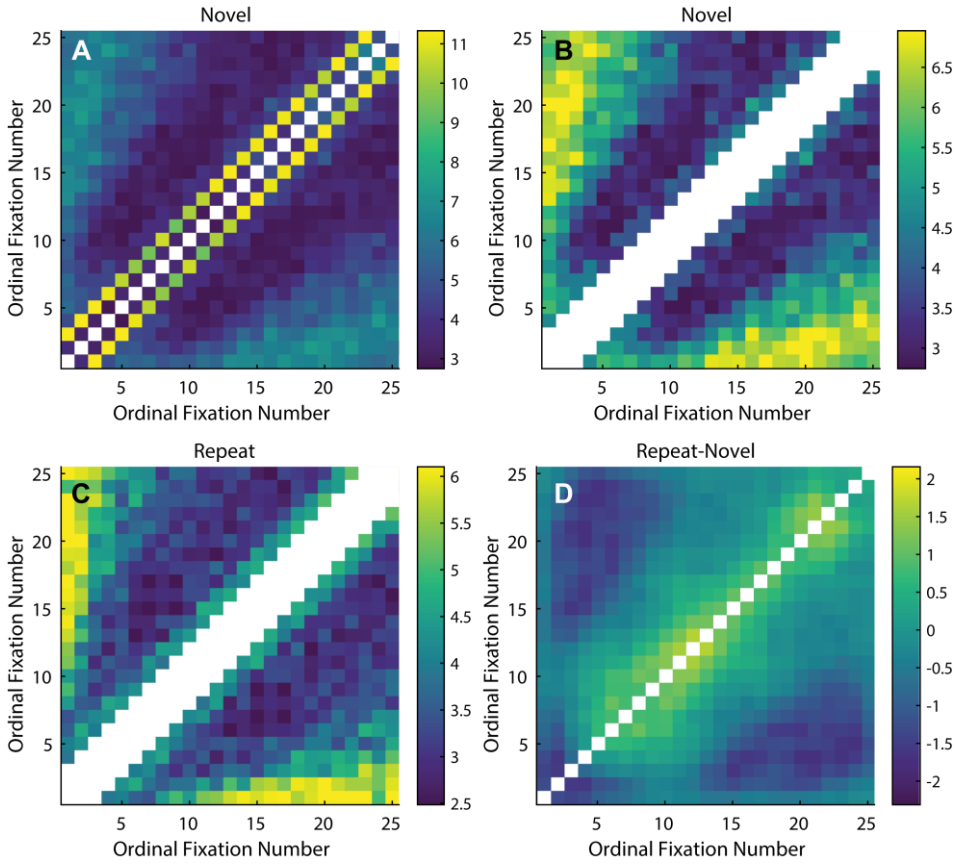

Figure 6-2: Average Recurrence Plots Across Many Scan Paths

The average recurrence plots show additional factors that influence behavior across many scan paths. The color bar represents the percent of fixations that are recurrent. Note I replaced the line of incidence with white pixels, which are neutral. **A)** The average recurrence plot for novel image presentations contains a large number (~11%) of recurrent fixations parallel to the line of incidence that represents 1-backs. **B)** A second recurrence pattern is clear after I replace the *n*-backs with white pixels. These recurrent fixations are just as strong as the 1-backs but more diffuse. These recurrences far from the line of incidence represent long-range returns similar to the inhibition of return modeled in *Chapter 3*. **C)** During repeat presentations, the rate of long-range returns decreases, but there are a small number of long-range returns for the first few fixations which occur at highly salient locations. Repeat presentations contained a similar pattern of *n*-backs (not shown). **D)** To further illustrate the influence of long-term stimulus memory, I subtracted the average recurrence plot for scan paths during novel image presentations from the average recurrence plot for scan paths during repeat presentations. Compared to novel image presentations, repeat presentations contain more local recurrences close to the line of incidence and a decrease in the number of long-range recurrences.

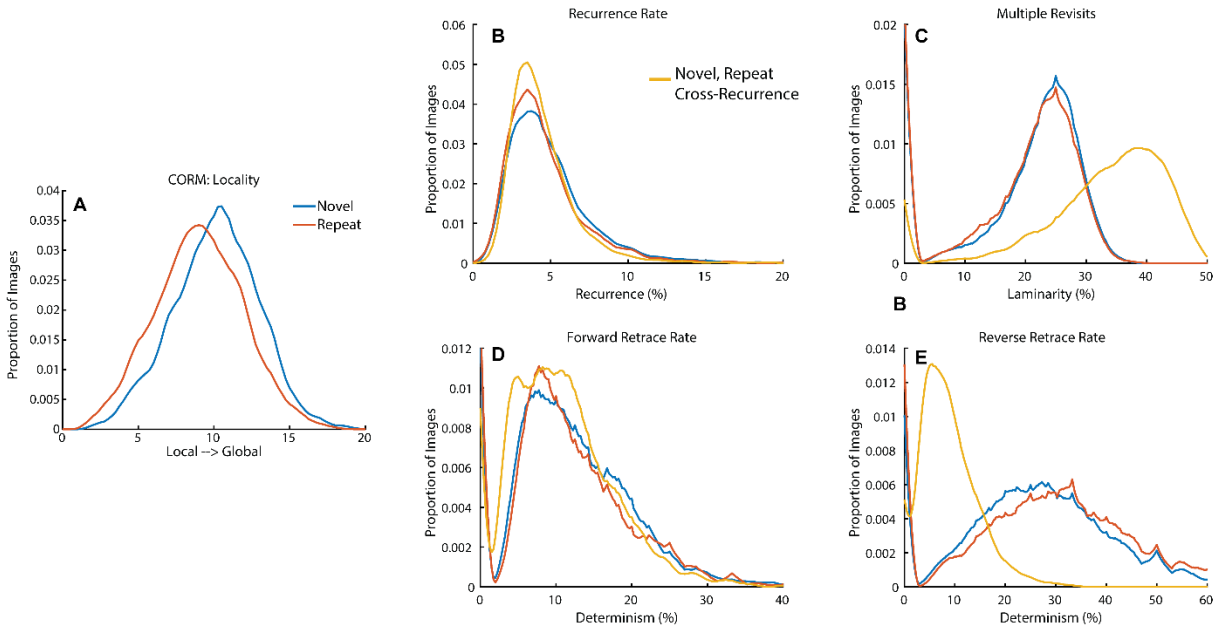

Figure 6-3: Recurrence Measures for Novel and Repeat Scan Paths
The four common recurrence measures show differences in eye movement patterns between novel and repeat presentations. **A)** Scan paths during novel image presentations are significantly (*paired t-test, $p < 0.05$*) more globally oriented than during repeat presentations. **B)** The recurrence rate and **(C)** laminarity do not change with stimulus novelty. The cross-recurrence for laminarity suggest that monkeys fixate many of the same fixation locations across presentation type. **D)** Forward retraces are more prevalent during novel image presentations (*ks-test*, $p < 0.05$), but reverse retraces **(E)** are more common during repeat presentations (*ks-test*, $p < 0.05$). The cross-recurrence analysis suggests that during repeat presentations, monkeys retrace previous scan paths only in the forward direction.

A second pattern emerges when I remove the *n*-back pattern (**Figure 6.2B**). The second pattern represents long-range returns similar to the inhibition of return modeled in *Chapter 3*. This pattern of long-range returns is not weaker than the 1-backs but simply more diffuse; long-range returns do not occur for fixed pairs of ordinal fixations. Long-range returns represent recurrent fixations separated by approximately 15 fixations or 4 seconds. Essentially, the monkey spends the first 3.5 seconds exploring new parts of the image, and then the monkey returns to locations that they fixated at the beginning of the trial. During repeat presentations, the rate of long-range returns decreases (**Figure 6.2C**); there are a small number of long-range returns for the first few fixations which occur at highly salient locations. To illustrate the difference between novel and repeat scan paths, I subtracted the average recurrence plots for the novel scan paths from the repeat scan paths. Scan paths during repeat presentations contain more recurrent fixations close to the line of incidence and fewer long-range recurrences (**Figure 6.2D**).

These results suggest that globally oriented behavior (i.e. exploration) describes scan paths during novel presentations while locally oriented behavior (i.e. exploitation) describes scan paths during repeat presentations. Indeed, using CORM, scan paths during novel image presentations are significantly (*paired t-test*, $p < 0.05$) more globally oriented than scan paths during repeat image presentations (**Figure 6.3A**). Other recurrence measures show only weak effects of stimulus novelty (**Figure 6.3**). Specifically, stimulus novelty affects the forward and reverse retrace rates (*ks-test, $p < 0.05$*): forward retraces are more prevalent during novel image presentations (**Figure 6.3D**) while reverse retraces are more prevalent repeat presentations (**Figure 6.3E**).

A cross-recurrence analysis shows that repeat scan paths rapidly diverge from novel scan paths: only the first few fixations are similar in location and order (**Figure 6.4**). There is also an

elevated recurrence rate along the line of incidence. From the four common recurrence measures, the line of incidence likely represents forward retraces (**Figure 6.4D**). Reverse retraces are uncommon. Furthermore, the laminarity measure suggests that many of the same locations are being revisited.

It is interesting that I find sequences of eye movements in the behavior and sequences of neural activity aligned to eye movements in the hippocampus, but is there a link between the two? Do eye movement patterns correlate in any manner with memory or hippocampal neural activity? For a preliminary analysis, I took data from the same four monkeys who performed a scene manipulation task (Smith et al., 2006b; Smith and Squire, 2008b) and asked whether certain spatiotemporal patterns of eye movements subsequently predict memory (**Figure 6.5A**). I used the scene manipulation task because we have a good measure of hippocampal-dependent memory in this task. In the scene manipulation task, a novel image presentation is followed by the presentation of a repeated image in which nothing has changed, an image in which one object was replaced with another object, or an image in which one object was moved to a different part of the image. In agreement with human behavior (Smith et al., 2006b; Smith and Squire, 2008b), monkeys spend significantly (*t-test, $p < 0.05$*) more time looking at the replaced and moved objects compared to objects that were not manipulated (**Figure 6.5A**). Here, the object and immediate area around the object is termed the region of interest (ROI).

First, I took the four recurrence measures, fixation durations, and saccade amplitudes, for ~2200 novel scan paths (n = ~700 for each presentation type). I then projected these 6D values into a 1D space using PCA because I hypothesize that memory is only changing one variable, foraging strategy. Then, I split the novel scan paths into "good" and "bad" mnemonic behaviors by taking the top and bottom 33% of the 1D space, respectively. "Good" mnemonic behaviors

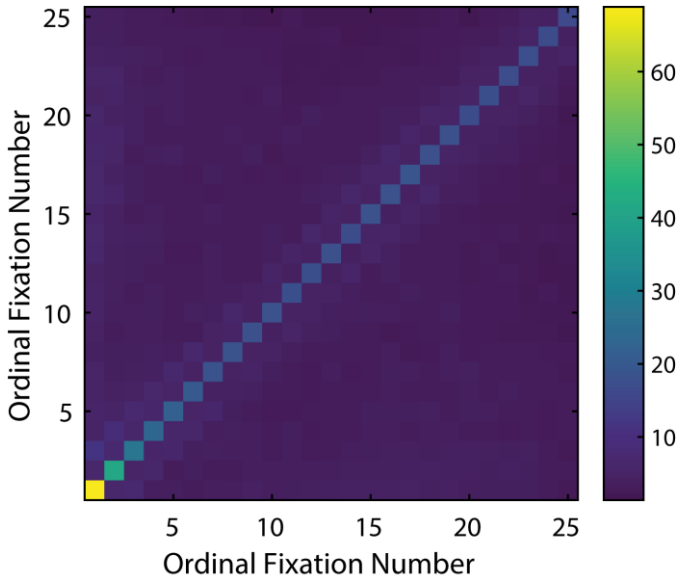

Figure 6-4 Cross-Recurrence between Novel and Repeat Scan Paths
Analysis of the average cross-recurrence plot between novel and repeat scan paths suggests that only the first few fixations are similar in location and order across presentation type. The first few fixations are also often at the most salient locations suggesting that the first few fixations are similar due to the influence of bottom-up salience. Note the diagonal in cross-recurrence is meaningful and suggests there is an abundance of forward retraces throughout the image presentation. The scale bar represents the percentage of fixations that are cross-recurrent.

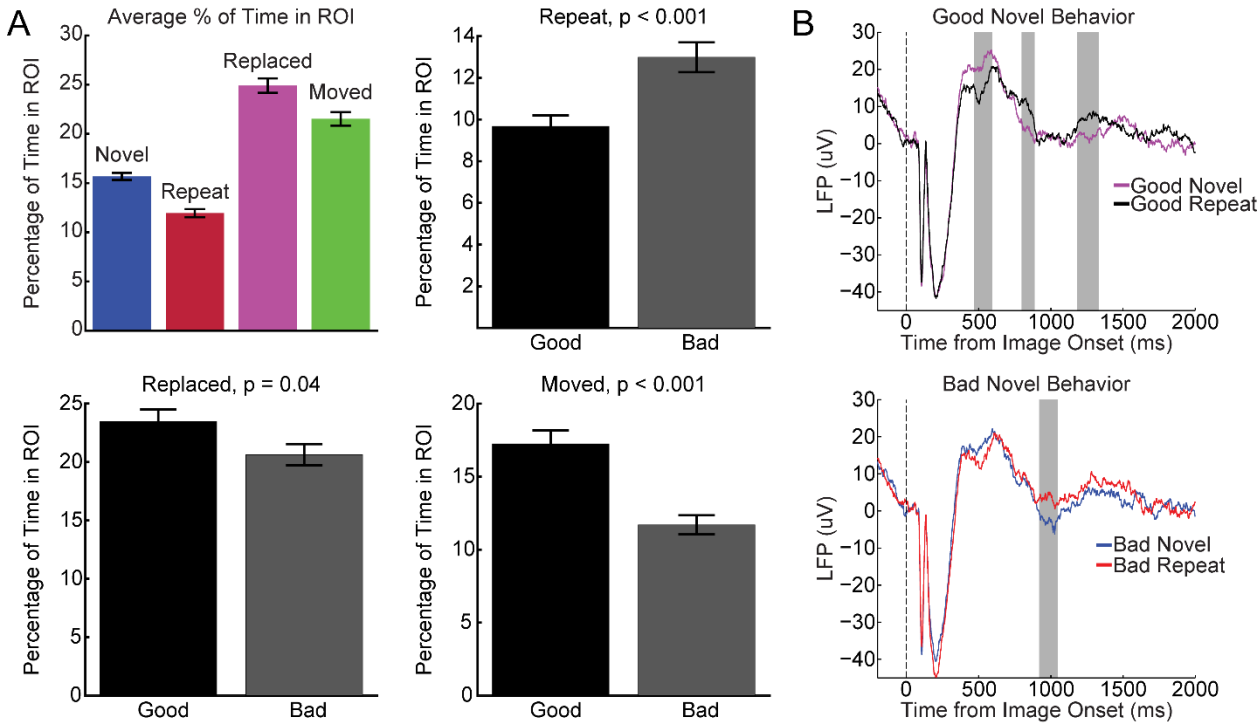

Figure 6-5: Recurrence and Subsequently Memory

Using the four common recurrence measures, fixation durations, and saccade amplitudes, I divided novel image presentations into trials with "good" and "bad" mnemonic behavior. I then asked if "good" behavior during novel image presentations subsequently predicted memory better than "bad" behavior. **A)** In a scene manipulation task, "good" mnemonic behavior lead to an increase in looking time in the manipulated region of interest (ROI) compared to "bad" mnemonic behavior (t-test, $p < 0.05$). Similarly, "good" mnemonic behavior lead to a decrease in looking time in the ROI during repeated presentations. **B)** I also applied this analysis to LFPs recorded in the hippocampus during a free viewing task with novel and repeat image presentations (see *Chapter 4*). "Good" mnemonic behavior was associated with a greater separation in the LFPs for novel vs. repeat presentations. Conversely, there was a smaller and later difference in the LFPs for novel vs. repeat presentations in trials with "bad" mnemonic behavior. Shaded regions represent significant time points calculated using bootstrapping and corrected for multiple comparisons, $p < 0.05$.

are behaviors that are useful for encoding information into memory, while "bad" mnemonic behaviors are behaviors that are bad for encoding information into memory.

Surprisingly, certain spatiotemporal patterns of eye movements during novel image presentations correlate with a decrease in looking time in the region of interest during repeat presentations and an increase in looking time in the region of interest during manipulated presentations (**Figure 6.5A**). The direction of these effects strongly supports the hypothesis that certain spatiotemporal patterns of eye movements are important for encoding information into memory. It has yet to be determined which components of this 6D space subsequently predict memory. However, fixation durations and the locality of the recurrent fixations, as measured by CORM, appear to play a substantial role in predicting subsequent memory.

Finally, I performed the same analysis on the neural data from *Chapter 4*. Unfortunately, there was not enough statistical power to perform this analysis on individual neurons, so instead, I performed this analysis on LFPs (**Figure 6.5B**). For each recording session (n = 84), I determined whether novel trials contained "good" or "bad" mnemonic behavior by taking the top and bottom 33% of the 1D space. Then, I calculated the average stimulus-evoked LFPs across all the "good" novel trials; similarly, I calculated the average stimulus-evoked LFPs for the repeated image presentations of these "good" novel trials. I then performed a bootstrapping analysis to determine if the evoked LFPs were significantly different across novel and repeat image presentations. The same analysis was performed for "bad" image trials separately. For "good" mnemonic behavior trials, there was a large separation in the LFPs, but for "bad" mnemonic behavior trials, there was a smaller and later separation in LFPs. These results suggest that the recurrence analysis can accurately measure the behavioral effects of long-term stimulus memory reflected in the

hippocampal LFPs. Future work is necessary to determine if these memory signals are only present in the hippocampus or whether they simply reach the hippocampus through its connections.

In conclusion, recurrence analysis simply and beautifully summarizes all of our previous findings in one analysis. In particular, recurrence analysis supports our hypothesis that foraging strategy explains free viewing behavior as a search for visual information. Further, recurrence analysis has the potential for measuring the influences of hippocampal-dependent memory on viewing behavior. Likewise, recurrence analysis could be useful for understanding neural data collected during free viewing tasks. The neural data in *Chapter 4* suggests that the hippocampus may encode spatiotemporal sequences reflecting the sequences of eye movements observed in the behavior. The final recurrence analysis (**Figure 6.5**) suggests that certain patterns of eye movements are important for encoding information in the hippocampus. Thus, I ultimately hypothesize that the spatiotemporal patterns of activity I observe in the hippocampus are essential for the formation of relational memories and that certain patterns of eye movements help the hippocampus build a spatial representation of the visual environment. Additionally, these patterns of eye movements could be used by several other brain regions for perception and other cognitive processes.

6.2 CONCLUSION

My results suggest that viewing behavior is a dynamic process driven by multiple factors including bottom-up salience, oculomotor constraints, working memory in the form of inhibition of return, and long-term stimulus memory (i.e. relational memory). At first, viewing behavior during novel image presentations can be explained by globally-oriented behavior (i.e. exploration), but then long-term stimulus memory shifts behavior towards a locally-oriented state (i.e.

exploitation). Further, eye movements subsequently affect memory and modulate neural activity in the hippocampus. These results demonstrate a reciprocal relationship between eye movements and memory. As illustrated in *Chapter 5,* there are a sufficient number of pathways by which information could flow between the oculomotor and memory networks to explain these results. Future work will have to determine whether the hippocampus is causally involved in the behavioral signatures of memory observed in this thesis.

My results highlight the importance of active sensing in organizing neural activity in the hippocampus. Rodents primarily use sniffing and whisking to explore their environments up-close; not surprisingly, sniffing and whisking play an important role in organizing hippocampal activity during active olfactory-based exploration (Grion et al., 2016; Kleinfeld et al., 2016). On the other hand, primates use eye movements and vision to explore their environment from afar. Therefore, one would hypothesize that spatial representations in primates would be different from those in rodents and include some dependence on eye movements. Indeed, I show that the hippocampus contains gaze modulated spatial and contextual representations. Moreover, eye movements temporally organize these spatial and contextual representations. Many other studies have also shown that eye movements play an important role in organizing neural activity in the primate hippocampus (Ringo et al., 1994; Hoffman et al., 2013a; Jutras et al., 2013a). Further support for the active sensing hypothesis also comes from hippocampal recordings in bats (Ulanovsky and Moss, 2007; Finkelstein et al., 2015; Geva-Sagiv et al., 2016). First, spatial representations in flying bats represent the 3D position of the bat. Second, bats have different place codes for visual exploration and exploration using echolocation.

Despite the differences in how the hippocampus represents space in each species, there are many similarities across species including how individual neurons conjunctively code space with

non-spatial information (e.g. time and context). This combination of spatial, temporal, and contextual information is necessary to formation relational memories. These functional similarities suggest that the neural mechanisms of memory are conserved across species. Consistent with this interpretation, the anatomy of the hippocampus and MTL are largely conserved across species. However, the inputs to the hippocampus and MTL are much more visual in primates than in rodents. The large proportion of neocortex devoted to visual processing in primates corresponds with how primates primarily use eye movements and vision to explore their environments. Therefore, we should expect to find different types of spatiotemporal information in the hippocampus of every species, yet we should expect the hippocampus to perform a similar function in every species.

Modeling work may aid in understanding these differences across species, but models of spatial representations in the primate hippocampus are scarce. At the very least these primate models need to include eye movements. Further, the work presented in the *Future Directions* section suggests that these models need to include realistic patterns of movements as visual exploration is structured, and the structure of these patterns influences memory encoding. At least one modeling paper emphasizes that the brain may even build spatial representations governed by the structure of the animal's movements (Franzius et al., 2007).

In conclusion, the hippocampus encodes the information necessary to build a mental representation of one's environment in service of creating memories. The hippocampus of each species contains ethologically relevant spatiotemporal information reflecting how each species actively explores their environment. Thus future work in primates should focus on understanding the hippocampus as it relates to ethologically relevant behaviors in primates. In essence, primates

are not simply large rodents. Nonetheless, we can use rodents to understand the neural mechanism of memory because the structure and function of the MTL are conserved across species.

Chapter 7. REFERENCES

Abzug Z, Sommer MA (2017) Supplementary Eye Fields. Reference Module in Neuroscience and Biobehavioral Psychology.

Acuna C, Cudeiro J, Gonzalez F, Alonso JM, Perez R (1990) Lateral-Posterior and Pulvinar Reaching Cells - Comparison with Parietal Area-5a - a Study in Behaving Macaca-Nemestrina Monkeys. Exp Brain Res 82:158-166.

Afif A, Minotti L, Kahane P, Hoffmann D (2010) Anatomofunctional organization of the insular cortex: A study using intracerebral electrical stimulation in epileptic patients. Epilepsia 51:2305-2315.

Aggleton JP, Dumont JR, Warburton EC (2011) Unraveling the contributions of the diencephalon to recognition memory: A review. Learn Memory 18:384-400.

Aghajan ZM, Schuette P, Fields T, Tran M, Siddiqui S, Hasulak N, Tcheng TK, Eliashiv D, Stern J, Fried I (2016) Theta Oscillations in the Human Medial Temporal Lobe during Real World Ambulatory Movement. bioRxiv:078055.

Agster KL, Burwell RD (2013) Hippocampal and subicular efferents and afferents of the perirhinal, postrhinal, and entorhinal cortices of the rat. Behavioural Brain Research 254:50-64.

Agster KL, Pereira IT, Saddoris MP, Burwell RD (2016) Subcortical connections of the perirhinal, postrhinal, and entorhinal cortices of the rat. II. efferents. Hippocampus 26:1213-1230.

Aguirre GK, D'Esposito M (1999) Topographical disorientation: a synthesis and taxonomy. Brain 122:1613-1628.

Akert K, Hartmannvonmonakow K (1980) Relationships of Precentral, Premotor and Prefrontal Cortex to the Mediodorsal and Intralaminar Nuclei of the Monkey Thalamus. Acta Neurobiol Exp 40:7-&.

Alexander AS, Nitz DA (2015) Retrosplenial cortex maps the conjunction of internal and external spaces. Nat Neurosci 18:1143-+.

Amaral DG, Price JL (1984) Amygdalo-cortical projections in the monkey (Macaca fascicularis). J Comp Neurol 230:465-496.

Amaral DG, Witter MP (1989) The three-dimensional organization of the hippocampal formation: a review of anatomical data. Neuroscience 31:571-591.

Andersen P (2007) The hippocampus book: Oxford University Press.

Andersen RA (1989) Visual and Eye-Movement Functions of the Posterior Parietal Cortex. Annu Rev Neurosci 12:377-403.

Andersen RA, Asanuma C, Essick G, Siegel RM (1990) Corticocortical Connections of Anatomically and Physiologically Defined Subdivisions within the Inferior Parietal Lobule. Journal of Comparative Neurology 296:65-113.

Andersen RA, Snyder LH, Li C-S, Stricanne B (1993) Coordinate transformations in the representation of spatial information. Current opinion in neurobiology 3:171-176.

Anderson NC, Anderson F, Kingstone A, Bischof WF (2015) A comparison of scanpath comparison methods. Behav Res Methods 47:1377-1392.

Anderson NC, Bischof WF, Laidlaw KE, Risko EF, Kingstone A (2013) Recurrence quantification analysis of eye movements. Behav Res Methods 45:842-856.

Andrews TJ, Coppola DM (1999) Idiosyncratic characteristics of saccadic eye movements when viewing different visual environments. Vision Research 39:2947-2953.

Annese J, Schenker-Ahmed NM, Bartsch H, Maechler P, Sheh C, Thomas N, Kayano J, Ghatan A, Bresler N, Frosch MP (2014) Postmortem examination of patient HM's brain based on histological sectioning and digital 3D reconstruction. Nature communications 5:3122.

Arend I, Rafal R, Ward R (2008a) Spatial and temporal deficits are regionally dissociable in patients with pulvinar lesions. Brain 131:2140-2152.

Arend I, Machado L, Ward R, McGrath M, Ro T, Rafal RD (2008b) The role of the human pulvinar in visual attention and action: evidence from temporal-order judgment, saccade decision, and antisaccade tasks. Prog Brain Res 171:475-483.

Arleo A, Gerstner W (2000) Spatial cognition and neuro-mimetic navigation: a model of hippocampal place cell activity. Biol Cybern 83:287-299.

Armstrong KM, Fitzgerald JK, Moore T (2006) Changes in visual receptive fields with microstimulation of frontal cortex. Neuron 50:791-798.

Asahi T, Uwano T, Eifuku S, Tamura R, Endo S, Ono T, Nishijo H (2006) Neuronal responses to a delayed-response delayed-reward go/nogo task in the monkey posterior insular cortex. Neuroscience 143:627-639.
Aston-Jones G, Cohen JD (2005) An integrative theory of locus coeruleus-norepinephrine function: Adaptive gain and optimal performance. Annu Rev Neurosci 28:403-450.
Aston-Jones G, Rajkowski J, Cohen J (1999) Role of locus coeruleus in attention and behavioral flexibility. Biol Psychiat 46:1309-1320.
Astonjones G, Bloom FE (1981) Activity of Norepinephrine-Containing Locus Coeruleus Neurons in Behaving Rats Anticipates Fluctuations in the Sleep-Waking Cycle. J Neurosci 1:876-886.
Augustine JR (1996) Circuitry and functional aspects of the insular lobe in primates including humans. Brain Res Rev 22:229-244.
Averbeck BB, Lee D (2007) Prefrontal neural correlates of memory for sequences. J Neurosci 27:2204-2211.
Babapoor-Farrokhran S, Vinck M, Womelsdorf T, Everling S (2017) Theta and beta synchrony coordinate frontal eye fields and anterior cingulate cortex during sensorimotor mapping. Nature Communications 8.
Bakker R, Wachtler T, Diesmann M (2012) CoCoMac 2.0 and the future of tract-tracing databases. Front Neuroinform 6:30.
Baleydier C, Mauguiere F (1985) Anatomical Evidence for Medial Pulvinar Connections with the Posterior Cingulate Cortex, the Retrosplenial Area, and the Posterior Parahippocampal Gyrus in Monkeys. Journal of Comparative Neurology 232:219-228.
Barbas H, Blatt GJ (1995) Topographically specific hippocampal projections target functionally distinct prefrontal areas in the rhesus monkey. Hippocampus 5:511-533.
Barbas H, Henion THH, Dermon CR (1991) Diverse Thalamic Projections to the Prefrontal Cortex in the Rhesus-Monkey. Journal of Comparative Neurology 313:65-94.
Bartesaghi R, Gessi T (2004) Parallel activation of field CA2 and dentate gyrus by synaptically elicited perforant path volleys. Hippocampus 14:948-963.
Barthelmé S, Trukenbrod H, Engbert R, Wichmann F (2012) Modelling fixation locations using spatial point processes. arXiv preprint arXiv:12072370.
Bates JF, Goldman-Rakic PS (1993) Prefrontal connections of medial motor areas in the rhesus monkey. J Comp Neurol 336:211-228.
Batista AP, Buneo CA, Snyder LH, Andersen RA (1999) Reach plans in eye-centered coordinates. Science 285:257-260.
Bellistri E, Aguilar J, Brotons-Mas JR, Foffani G, de la Prida LM (2013) Basic properties of somatosensory-evoked responses in the dorsal hippocampus of the rat. J Physiol-London 591:2667-2686.
Ben-Hur A, Elisseeff A, Guyon I (2002) A stability based method for discovering structure in clustered data. Pac Symp Biocomput:6-17.
Benevento LA, Port JD (1995) Single Neurons with Both Form Color Differential Responses and Saccade-Related Responses in the Nonretinotopic Pulvinar of the Behaving Macaque Monkey. Visual Neurosci 12:523-544.
Berendse HW, Groenewegen HJ (1991) Restricted Cortical Termination Fields of the Midline and Intralaminar Thalamic Nuclei in the Rat. Neuroscience 42:73-102.
Berg DJ, Boehnke SE, Marino RA, Munoz DP, Itti L (2009) Free viewing of dynamic stimuli by humans and monkeys. J Vis 9:19 11-15.
Berman N (1977) Connections of the pretectum in the cat. J Comp Neurol 174:227-254.
Berman RA, Wurtz RH (2010) Functional Identification of a Pulvinar Path from Superior Colliculus to Cortical Area MT. J Neurosci 30:6342-6354.
Bindemann M (2010) Scene and screen center bias early eye movements in scene viewing. Vision Res 50:2577-2587.
Bird CM, Burgess N (2008) The hippocampus and memory: insights from spatial processing. Nat Rev Neurosci 9:182-194.
Bjerknes TL, Moser EI, Moser MB (2014) Representation of Geometric Borders in the Developing Rat. Neuron 82:71-78.
Blair HT, Cho J, Sharp PE (1998) Role of the lateral mammillary nucleus in the rat head direction circuit: a combined single unit recording and lesion study. Neuron 21:1387-1397.
Blatt GJ, Rosene DL (1998) Organization of direct hippocampal efferent projections to the cerebral cortex of the rhesus monkey: Projections from CA1, prosubiculum, and subiculum to the temporal lobe. Journal of Comparative Neurology 392:92-114.
Bledowski C, Rahm B, Rowe JB (2009) What "works" in working memory? Separate systems for selection and updating of critical information. J Neurosci 29:13735-13741.

Blohm G, Keith GP, Crawford JD (2009) Decoding the Cortical Transformations for Visually Guided Reaching in 3D Space. Cerebral Cortex 19:1372-1393.
Boccara CN, Sargolini F, Thoresen VH, Solstad T, Witter MP, Moser EI, Moser MB (2010) Grid cells in pre- and parasubiculum. Nat Neurosci 13:987-U112.
Boccignone G, Ferraro M (2004) Modelling gaze shift as a constrained random walk. Physica A 331:207-218.
Boccignone G, Ferraro M (2013) Ecological Sampling of Gaze Shifts. IEEE Trans Cybern.
Bohbot VD, Allen JJ, Nadel L (2000) Memory deficits characterized by patterns of lesions to the hippocampus and parahippocampal cortex. Ann N Y Acad Sci 911:355-368.
Bohbot VD, Copara MS, Gotman J, Ekstrom AD (2017) Low-frequency theta oscillations in the human hippocampus during real-world and virtual navigation. Nature Communications 8.
Bohbot VD, Kalina M, Stepankova K, Spackova N, Petrides M, Nadel L (1998) Spatial memory deficits in patients with lesions to the right hippocampus and to the right parahippocampal cortex. Neuropsychologia 36:1217-1238.
Bonnevie T, Dunn B, Fyhn M, Hafting T, Derdikman D, Kubie JL, Roudi Y, Moser EI, Moser MB (2013) Grid cells require excitatory drive from the hippocampus. Nat Neurosci 16:309-317.
Botvinick MM, Cohen JD, Carter CS (2004) Conflict monitoring and anterior cingulate cortex: an update. Trends Cogn Sci 8:539-546.
Brandon MP, Koenig J, Leutgeb JK, Leutgeb S (2014) New and distinct hippocampal place codes are generated in a new environment during septal inactivation. Neuron 82:789-796.
Brandon MP, Bogaard AR, Libby CP, Connerney MA, Gupta K, Hasselmo ME (2011) Reduction of theta rhythm dissociates grid cell spatial periodicity from directional tuning. Science 332:595-599.
Brown MW, Aggleton JP (2001) Recognition memory: What are the roles of the perirhinal cortex and hippocampus? Nat Rev Neurosci 2:51-61.
Bruce N, Tsotsos J (2005) Saliency based on information maximization. In: Advances in neural information processing systems, pp 155-162.
Buckmaster CA, Eichenbaum H, Amaral DG, Suzuki WA, Rapp PR (2004) Entorhinal cortex lesions disrupt the relational organization of memory in monkeys. J Neurosci 24:9811-9825.
Buffalo EA, Bellgowan PSF, Martin A (2006) Distinct roles for medial temporal lobe structures in memory for objects and their locations. Learn Memory 13:638-643.
Buffalo EA, Ramus SJ, Squire LR, Zola SM (2000) Perception and recognition memory in monkeys following lesions of area TE and perirhinal cortex. Learn Memory 7:375-382.
Buffalo EA, Bertini G, Ungerleider LG, Desimone R (2005) Impaired filtering of distracter stimuli by TE neurons following V4 and TEO lesions in macaques. Cerebral Cortex 15:141-151.
Buffalo EA, Ramus SJ, Clark RE, Teng E, Squire LR, Zola SM (1999) Dissociation between the effects of damage to perirhinal cortex and area TE. Learn Memory 6:572-599.
Burgess N (2006) Spatial memory: how egocentric and allocentric combine. Trends Cogn Sci 10:551-557.
Burgess N (2008) Spatial cognition and the brain. Year in Cognitive Neuroscience 2008 1124:77-97.
Burgess N, Barry C, O'Keefe J (2007) An oscillatory interference model of grid cell firing. Hippocampus 17:801-812.
Burrows BE, Zirnsak M, Akhlaghpour H, Wang M, Moore T (2014) Global Selection of Saccadic Target Features by Neurons in Area V4. J Neurosci 34:6700-6706.
Burwell (1996) The perirhinal and postrhinal cortices of the rat: A review of neuroanatomical literature and comparison with findings from the monkey brain (vol 5, pg 390, 1995). Hippocampus 6:340-340.
Burwell RD (2000) The parahippocampal region: Corticocortical connectivity. Ann Ny Acad Sci 911:25-42.
Burwell RD, Amaral DG (1998a) Perirhinal and postrhinal cortices of the rat: interconnectivity and connections with the entorhinal cortex. J Comp Neurol 391:293-321.
Burwell RD, Amaral DG (1998b) Cortical afferents of the perirhinal, postrhinal, and entorhinal cortices of the rat. Journal of Comparative Neurology 398:179-205.
Burwell RD, Witter MP, Amaral DG (1995) Perirhinal and postrhinal cortices of the rat: A review of the neuroanatomical literature and comparison with findings from the monkey brain. Hippocampus 5:390-408.
Buschman TJ, Miller EK (2007) Top-down versus bottom-up control of attention in the prefrontal and posterior parietal cortices. Science 315:1860-1862.
Bush D, Barry C, Burgess N (2014) What do grid cells contribute to place cell firing? Trends Neurosci 37:136-145.
Bush G, Luu P, Posner MI (2000) Cognitive and emotional influences in anterior cingulate cortex. Trends Cogn Sci 4:215-222.

Bussey TJ, Muir JL, Aggleton JP (1999) Functionally dissociating aspects of event memory: the effects of combined perirhinal and postrhinal cortex lesions on object and place memory in the rat. J Neurosci 19:495-502.
ButtnerEnnever JA, Cohen B, Horn AKE, Reisine H (1996) Pretectal projections to the oculomotor complex of the monkey and their role in eye movements. Journal of Comparative Neurology 366:348-359.
Buzsaki G, Moser EI (2013) Memory, navigation and theta rhythm in the hippocampal-entorhinal system. Nat Neurosci 16:130-138.
Bylinskii Z, DeGennaro EM, Rajalingham R, Ruda H, Zhang J, Tsotsos JK (2015) Towards the quantitative evaluation of visual attention models. Vision Res 116:258-268.
Byrne P, Becker S, Burgess N (2007) Remembering the past and imagining the future: A neural model of spatial memory and imagery. Psychol Rev 114:340-375.
Carr MF, Jadhav SP, Frank LM (2011) Hippocampal replay in the awake state: a potential substrate for memory consolidation and retrieval. Nat Neurosci 14:147-153.
Caruso VC, Pages DS, Sommer M, Groh JM (2017) Beyond the labeled line: variation in visual reference frames from intraparietal cortex to frontal eye fields and the superior colliculus. bioRxiv.
Cavada C, Goldman-Rakic PS (1989) Posterior parietal cortex in rhesus monkey: I. Parcellation of areas based on distinctive limbic and sensory corticocortical connections. J Comp Neurol 287:393-421.
Cavada C, Company T, Tejedor J, Cruz-Rizzolo RJ, Reinoso-Suarez F (2000) The anatomical connections of the macaque monkey orbitofrontal cortex. A review. Cereb Cortex 10:220-242.
Chafee MV, Crowe DA, Averbeck BB, Georgopoulos AP (2005) Neural, correlates of spatial judgement during object construction in parietal cortex. Cerebral Cortex 15:1393-1413.
Chawarska K, Shic F (2009) Looking but not seeing: Atypical visual scanning and recognition of faces in 2 and 4-year-old children with autism spectrum disorder. Journal of Autism and Developmental Disorders 39:1663.
Chawarska K, Macari S, Shic F (2013) Decreased Spontaneous Attention to Social Scenes in 6-Month-Old Infants Later Diagnosed with Autism Spectrum Disorders. Biol Psychiat 74:195-203.
Chen LL, Wise SP (1997) Conditional oculomotor learning: population vectors in the supplementary eye field. J Neurophysiol 78:1166-1169.
Clark BJ, Taube JS (2012) Vestibular and attractor network basis of the head direction cell signal in subcortical circuits. Front Neural Circuit 6.
Clark BJ, Bassett JP, Wang SS, Taube JS (2010) Impaired Head Direction Cell Representation in the Anterodorsal Thalamus after Lesions of the Retrosplenial Cortex. J Neurosci 30:5289-5302.
Clark KL, Armstrong KM, Moore T (2011) Probing neural circuitry and function with electrical microstimulation. P Roy Soc B-Biol Sci 278:1121-1130.
Clower DM, West RA, Lynch JC, Strick PL (2001) The inferior parietal lobule is the target of output from the superior colliculus, hippocampus, and cerebellum. J Neurosci 21:6283-6291.
Colby CL, Goldberg ME (1999) Space and attention in parietal cortex. Annu Rev Neurosci 22:319-349.
Colgin LL, Moser EI, Moser MB (2008) Understanding memory through hippocampal remapping. Trends Neurosci 31:469-477.
Colgin LL, Leutgeb S, Jezek K, Leutgeb JK, Moser EI, McNaughton BL, Moser MB (2010) Attractor-Map Versus Autoassociation Based Attractor Dynamics in the Hippocampal Network. Journal of Neurophysiology 104:35-50.
Corkin S (2002) What's new with the amnesic patient H.M.? Nat Rev Neurosci 3:153-160.
Coutrot A, Hsiao JH, Chan AB (2017) Scanpath modeling and classification with hidden Markov models. Behav Res Methods.
Crapse TB, Sommer MA (2012) Frontal eye field neurons assess visual stability across saccades. J Neurosci 32:2835-2845.
Crawford JD, Henriques DYP, Medendorp WP (2011) Three-Dimensional Transformations for Goal-Directed Action. Annual Review of Neuroscience, Vol 34 34:309-331.
Crone EE, Schultz CB (2008) Old models explain new observations of butterfly movement at patch edges. Ecology 89:2061-2067.
Crowe DA, Averbeck BB, Chafee MV (2008) Neural ensemble decoding reveals a correlate of viewer- to object-centered spatial transformation in monkey parietal cortex. J Neurosci 28:5218-5228.
Crowe DA, Chafee MV, Averbeck BB, Georgopoulos AP (2004) Neural activity in primate parietal area 7a related to spatial analysis of visual mazes. Cerebral Cortex 14:23-34.
Crutcher MD, Calhoun-Haney R, Manzanares CM, Lah JJ, Levey AI, Zola SM (2009) Eye Tracking During a Visual Paired Comparison Task as a Predictor of Early Dementia. Am J Alzheimers Dis 24:258-266.

Crutcher MD C-HR, Manzanares CM, Lah JJ, Levey AI, Zola SM. (2009) Eye tracking during a visual paired comparison task as a predictor of early dementia. Am J Alzheimers Dis Other Demen 24:258-266.
Curtis CE, D'Esposito M (2003) Persistent activity in the prefrontal cortex during working memory. Trends Cogn Sci 7:415-423.
Daum I, Ackermann H (1994) Frontal-Type Memory Impairment Associated with Thalamic Damage. Int J Neurosci 77:187-198.
de Araujo IET, Rolls ET, STringer SM (2001) A view model which accounts for the spatial fields of hippocampal primate spatial view cells and rat place cells. Hippocampus 11:699-706.
de la Vega A, Yarkoni T, Wager TD, Banich MT (2016) Large-scale meta-analysis suggests low regional modularity in lateral frontal cortex. bioRxiv:083352.
De Weerd P, Desimone R, Ungerleider LG (2003) Generalized deficits in visual selective attention after V4 and TEO lesions in macaques. Eur J Neurosci 18:1671-1691.
Dean HL, Platt ML (2006) Allocentric spatial referencing of neuronal activity in macaque posterior cingulate cortex. J Neurosci 26:1117-1127.
Dean HL, Crowley JC, Platt ML (2004) Visual and saccade-related activity in macaque posterior cingulate cortex. J Neurophysiol 92:3056-3068.
Dermon CR, Barbas H (1994) Contralateral Thalamic Projections Predominantly Reach Transitional Cortices in the Rhesus-Monkey. Journal of Comparative Neurology 344:508-531.
Deshmukh SS, Knierim JJ (2011) Representation of non-spatial and spatial information in the lateral entorhinal cortex. Front Behav Neurosci 5.
Desimone R, Duncan J (1995) Neural mechanisms of selective visual attention. Annu Rev Neurosci 18:193-222.
Dewhurst R NM, Jarodzka H, Foulsham T, Johansson R, Holmqvist K. (2012) It Depends on How You Look at It: Scanpath Comparison in Multiple Dimensions with MultiMatch, a Vector-based Approach. Behavior research methods 44:1079-1100.
Dias R, Robbins TW, Roberts AC (1997) Dissociable forms of inhibitory control within prefrontal cortex with an analog of the Wisconsin Card Sort Test: Restriction to novel situations and independence from "on-line" processing. J Neurosci 17:9285-9297.
Ding SL (2013) Comparative Anatomy of the Prosubiculum, Subiculum, Presubiculum, Postsubiculum, and Parasubiculum in Human, Monkey, and Rodent. Journal of Comparative Neurology 521:4145-4162.
Ding SL, Van Hoesen G, Rockland KS (2000) Inferior parietal lobule projections to the presubiculum and neighboring ventromedial temporal cortical areas. Journal of Comparative Neurology 425:510-530.
Dolleman-Van Der Weel MJ, Witter MP (1996) Projections from the nucleus reuniens thalami to the entorhinal cortex, hippocampal field CA1, and the subiculum in the rat arise from different populations of neurons. J Comp Neurol 364:637-650.
DollemanVanderWeel MJ, Witter MP (1996) Projections from the nucleus reuniens thalami to the entorhinal cortex, hippocampal field CA1, and the subiculum in the rat arise from different populations of neurons. Journal of Comparative Neurology 364:637-650.
Donahue CH, Lee D (2015) Dynamic routing of task-relevant signals for decision making in dorsolateral prefrontal cortex. Nat Neurosci 18:295-301.
Dragoi G, Buzsaki G (2006) Temporal encoding of place sequences by hippocampal cell assemblies. Neuron 50:145-157.
Duan AR, Varela C, Zhang Y, Shen Y, Xiong L, Wilson MA, Lisman J (2015) Delta frequency optogenetic stimulation of the thalamic nucleus reuniens is sufficient to produce working memory deficits: relevance to schizophrenia. Biol Psychiat 77:1098-1107.
Duchowski AT (2002) A breadth-first survey of eye-tracking applications. Behav Res Meth Ins C 34:455-470.
Duchowski AT (2007) Eye Tracking Methodology: Theory and Practice. In, 2nd Edition: Springer.
Dudoit S, Fridlyand J (2002) A prediction-based resampling method for estimating the number of clusters in a dataset. Genome Biol 3.
Eacott MJ, Gaffan D, Murray EA (1994) Preserved Recognition Memory for Small Sets, and Impaired Stimulus Identification for Large Sets, Following Rhinal Cortex Ablations in Monkeys. Eur J Neurosci 6:1466-1478.
Ebitz RB, Moore T (2017) Selective Modulation of the Pupil Light Reflex by Microstimulation of Prefrontal Cortex. J Neurosci 37:5008-5018.
Edwards SB, Ginsburgh CL, Henkel CK, Stein BE (1979) Sources of subcortical projections to the superior colliculus in the cat. J Comp Neurol 184:309-329.
Eichenbaum H (2000) A cortical-hippocampal system for declarative memory. Nat Rev Neurosci 1:41-50.

Eichenbaum H (2014) Time cells in the hippocampus: a new dimension for mapping memories. Nat Rev Neurosci 15:732-744.
Eichenbaum H, Dudchenko P, Wood E, Shapiro M, Tanila H (1999) The hippocampus, memory, and place cells: Is it spatial memory or a memory space? Neuron 23:209-226.
Einhauser W, Kruse W, Hoffmann KP, Konig P (2006) Differences of monkey and human overt attention under natural conditions. Vision Res 46:1194-1209.
Ekstrom AD, Ranganath C (2017) Space, Time and Episodic Memory: the Hippocampus is all over the Cognitive Map. Hippocampus.
Ekstrom AD, Caplan JB, Ho E, Shattuck K, Fried I, Kahana MJ (2005) Human hippocampal theta activity during virtual navigation. Hippocampus 15:881-889.
Ekstrom AD, Kahana MJ, Caplan JB, Fields TA, Isham EA, Newman EL, Fried I (2003) Cellular networks underlying human spatial navigation. Nature 425:184-188.
Elazary L, Itti L (2008) Interesting objects are visually salient. J Vis 8:3 1-15.
Engbert R, Kliegl R (2003) Microsaccades uncover the orientation of covert attention. Vision Res 43:1035-1045.
Everling S, Munoz DP (2000) Neuronal correlates for preparatory set associated with pro-saccades and anti-saccades in the primate frontal eye field. J Neurosci 20:387-400.
Felleman DJ, Van Essen DC (1991) Distributed hierarchical processing in the primate cerebral cortex. Cereb Cortex 1:1-47.
Felsen G, Dan Y (2005) A natural approach to studying vision. Nat Neurosci 8:1643-1646.
Filimon F (2015) Are All Spatial Reference Frames Egocentric? Reinterpreting Evidence for Allocentric, Object-Centered, or World-Centered Reference Frames. Front Hum Neurosci 9.
Fink GR, Markowitsch HJ, Reinkemeier M, Bruckbauer T, Kessler J, Heiss WD (1996) Cerebral representation of one's own past: Neural networks involved in autobiographical memory. J Neurosci 16:4275-4282.
Finkelstein A, Derdikman D, Rubin A, Foerster JN, Las L, Ulanovsky N (2015) Three-dimensional head-direction coding in the bat brain. Nature 517:159-164.
Flynn FG, Benson DF, Ardila A (1999) Anatomy of the insula - functional and clinical correlates. Aphasiology 13:55-78.
Franzius M, Sprekeler H, Wiskott L (2007) Slowness and sparseness lead to place, head-direction, and spatial-view cells. Plos Comput Biol 3:1605-1622.
Frisoni GB, Fox NC, Jack CR, Scheltens P, Thompson PM (2010) The clinical use of structural MRI in Alzheimer disease. Nat Rev Neurol 6:67-77.
Fujisawa S, Amarasingham A, Harrison MT, Buzsaki G (2008) Behavior-dependent short-term assembly dynamics in the medial prefrontal cortex. Nat Neurosci 11:823-833.
Funahashi S, Bruce CJ, Goldman-Rakic PS (1989) Mnemonic coding of visual space in the monkey's dorsolateral prefrontal cortex. J Neurophysiol 61:331-349.
Funahashi S, Bruce CJ, Goldman-Rakic PS (1991) Neuronal activity related to saccadic eye movements in the monkey's dorsolateral prefrontal cortex. J Neurophysiol 65:1464-1483.
Funahashi S, Bruce CJ, Goldman-Rakic PS (1993) Dorsolateral prefrontal lesions and oculomotor delayed-response performance: evidence for mnemonic "scotomas". J Neurosci 13:1479-1497.
Funahashi S, Takeda K, Watanabe Y (2004) Neural mechanisms of spatial working memory: contributions of the dorsolateral prefrontal cortex and the thalamic mediodorsal nucleus. Cogn Affect Behav Neurosci 4:409-420.
Furuya Y, Matsumoto J, Hori E, Boas CV, Tran AH, Shimada Y, Ono T, Nishijo H (2014) Place-related neuronal activity in the monkey parahippocampal gyrus and hippocampal formation during virtual navigation. Hippocampus 24:113-130.
Gameiro RR, Kaspar K, Konig SU, Nordholt S, Konig P (2017) Exploration and Exploitation in Natural Viewing Behavior. Sci Rep-Uk 7.
Gattass R, Galkin TW, Desimone R, Ungerleider LG (2014) Subcortical Connections of Area V4 in the Macaque. Journal of Comparative Neurology 522:1941-1965.
Gaymard B, Rivaud S, Cassarini JF, Dubard T, Rancurel G, Agid Y, Pierrot-Deseilligny C (1998) Effects of anterior cingulate cortex lesions on ocular saccades in humans. Exp Brain Res 120:173-183.
Gener T, Perez-Mendez L, Sanchez-Vives MV (2013) Tactile Modulation of Hippocampal Place Fields. Hippocampus 23:1453-1462.
George PJ, Horel JA, Cirillo RA (1989) Reversible cold lesions of the parahippocampal gyrus in monkeys result in deficits on the delayed match-to-sample and other visual tasks. Behav Brain Res 34:163-178.

Geva-Sagiv M, Romani S, Las L, Ulanovsky N (2016) Hippocampal global remapping for different sensory modalities in flying bats. Nat Neurosci 19:952-958.
Ghaem O, Mellet E, Crivello F, Tzourio N, Mazoyer B, Berthoz A, Denis M (1997) Mental navigation along memorized routes activates the hippocampus, precuneus, and insula. Neuroreport 8:739-744.
Giocomo LM, Moser MB, Moser EI (2011) Computational models of grid cells. Neuron 71:589-603.
Girard B, Berthoz A (2005) From brainstem to cortex: Computational models of saccade generation circuitry. Prog Neurobiol 77:215-251.
Gluck MA, Meeter M, Myers CE (2003) Computational models of the hippocampal region: linking incremental learning and episodic memory. Trends Cogn Sci 7:269-276.
Golob EJ, Taube JS (1997) Head direction cells and episodic spatial information in rats without a hippocampus. P Natl Acad Sci USA 94:7645-7650.
Golob EJ, Wolk DA, Taube JS (1998) Recordings of postsubiculum head direction cells following lesions of the laterodorsal thalamic nucleus. Brain Research 780:9-19.
Gottlieb J, Goldberg ME (1999) Activity of neurons in the lateral intraparietal area of the monkey during an antisaccade task. Nat Neurosci 2:906-912.
Grieve KL, Acuna C, Cudeiro J (2000) The primate pulvinar nuclei: vision and action. Trends Neurosci 23:35-39.
Grion N, Akrami A, Zuo YF, Stella F, Diamond ME (2016) Coherence between Rat Sensorimotor System and Hippocampus Is Enhanced during Tactile Discrimination. Plos Biol 14.
Grusser OJ, Pause M, Schreiter U (1990) Localization and responses of neurones in the parieto-insular vestibular cortex of awake monkeys (Macaca fascicularis). J Physiol 430:537-557.
Gulyas AI, Seress L, Toth K, Acsady L, Antal M, Freund TF (1991) Septal GABAergic neurons innervate inhibitory interneurons in the hippocampus of the macaque monkey. Neuroscience 41:381-390.
Hafting T, Fyhn M, Molden S, Moser MB, Moser EI (2005) Microstructure of a spatial map in the entorhinal cortex. Nature 436:801-806.
Hafting T, Fyhn M, Bonnevie T, Moser MB, Moser EI (2008) Hippocampus-independent phase precession in entorhinal grid cells. Nature 453:1248-U1250.
Hales JB, Schlesiger MI, Leutgeb JK, Squire LR, Leutgeb S, Clark RE (2014) Medial entorhinal cortex lesions only partially disrupt hippocampal place cells and hippocampus-dependent place memory. Cell Rep 9:893-901.
Han X, Xian SX, Moore T (2009) Dynamic sensitivity of area V4 neurons during saccade preparation. P Natl Acad Sci USA 106:13046-13051.
Hanes DP, Wurtz RH (2001) Interaction of the frontal eye field and superior colliculus for saccade generation. Journal of Neurophysiology 85:804-815.
Hannula DE, Ranganath C (2009) The Eyes Have It: Hippocampal Activity Predicts Expression of Memory in Eye Movements. Neuron 63:592-599.
Hannula DE, Baym CL, Warren DE, Cohen NJ (2012) The Eyes Know: Eye Movements as a Veridical Index of Memory. Psychol Sci 23:278-287.
Hannula DE, Althoff RR, Warren DE, Riggs L, Cohen NJ, Ryan JD (2010) Worth a glance: using eye movements to investigate the cognitive neuroscience of memory. Front Hum Neurosci 4.
Harding A, Halliday G, Caine D, Kril J (2000) Degeneration of anterior thalamic nuclei differentiates alcoholics with amnesia. Brain 123 (Pt 1):141-154.
Harel J, Koch C, Perona P (2006) Graph-based visual saliency. In: Advances in neural information processing systems, pp 545-552.
Harting JK, Huerta MF, Frankfurter AJ, Strominger NL, Royce GJ (1980) Ascending Pathways from the Monkey Superior Colliculus - an Autoradiographic Analysis. Journal of Comparative Neurology 192:853-882.
Hayden BY, Heilbronner SR, Pearson JM, Platt ML (2011) Surprise signals in anterior cingulate cortex: neuronal encoding of unsigned reward prediction errors driving adjustment in behavior. J Neurosci 31:4178-4187.
Hayhoe M, Ballard D (2005a) Eye movements in natural behavior. Trends Cogn Sci 9:188-194.
Hayhoe M, Ballard D (2005b) Eye movements in natural behavior. Trends Cogn Sci 9:188-194.
Heekeren HR, Marrett S, Ruff DA, Bandettini PA, Ungerleider LG (2006) Involvement of human left dorsolateral prefrontal cortex in perceptual decision making is independent of response modality. P Natl Acad Sci USA 103:10023-10028.
Henderson JM, Brockmole JR, Castelhano MS, Mack ML (2007) Visual saliency does not account for eye movements during visual search in real-world scenes. In: Eye Movement Research: Insights into Mind and Brain (Gompel Rv, Fischer M, Murray W, Hill R, eds), pp 537-562. Oxford: Elsevier.
Herkenham M (1978) The connections of the nucleus reuniens thalami: evidence for a direct thalamo-hippocampal pathway in the rat. J Comp Neurol 177:589-610.

Hetherington PA, Shapiro ML (1997) Hippocampal place fields are altered by the removal of single visual cues in a distance-dependent manner. Behav Neurosci 111:20-34.
Hikosaka O, Takikawa Y, Kawagoe R (2000) Role of the basal ganglia in the control of purposive saccadic eye movements. Physiol Rev 80:953-978.
Histed MH, Miller EK (2006) Microstimulation of frontal cortex can reorder a remembered spatial sequence. Plos Biol 4:826-835.
Hitier M, Besnard S, Smith PF (2014) Vestibular pathways involved in cognition. Front Integr Neurosci 8:59.
Hoffman JE, Subramaniam B (1995) The Role of Visual-Attention in Saccadic Eye-Movements. Percept Psychophys 57:787-795.
Hoffman KL, Dragan MC, Leonard TK, Micheli C, Montefusco-Siegmund R, Valiante TA (2013a) Saccades during visual exploration align hippocampal 3-8 Hz rhythms in human and non-human primates. Front Syst Neurosci 7:43.
Hoffman KL, Dragan MC, Leonard TK, Micheli C, Montefusco-Siegmund R, Valiante TA (2013b) Saccades during visual exploration align hippocampal 3-8 Hz rhythms in human and non-human primates. Frontiers in Systems Neuroscience 7.
Hopfield JJ (1982) Neural Networks and Physical Systems with Emergent Collective Computational Abilities. P Natl Acad Sci-Biol 79:2554-2558.
Hori E, Nishio Y, Kazui K, Umeno K, Tabuchi E, Sasaki K, Endo S, Ono T, Nishijo H (2005) Place-related neural responses in the monkey hippocampal formation in a virtual space. Hippocampus 15:991-996.
Howard MW, Eichenbaum H (2015) Time and space in the hippocampus. Brain Research 1621:345-354.
Hsu DT, Price JL (2007) Midline and intralaminar thalamic connections with the orbital and medial prefrontal networks in macaque monkeys. Journal of Comparative Neurology 504:89-111.
Huerta MF, Kaas JH (1990) Supplementary Eye Field as Defined by Intracortical Microstimulation - Connections in Macaques. Journal of Comparative Neurology 293:299-330.
Huerta MF, Krubitzer LA, Kaas JH (1986) Frontal Eye Field as Defined by Intracortical Microstimulation in Squirrel-Monkeys, Owl Monkeys, and Macaque Monkeys .1. Subcortical Connections. Journal of Comparative Neurology 253:415-439.
Huerta MF, Krubitzer LA, Kaas JH (1987) Frontal Eye Field as Defined by Intracortical Microstimulation in Squirrel-Monkeys, Owl Monkeys, and Macaque Monkeys .2. Cortical Connections. Journal of Comparative Neurology 265:332-361.
Huxlin KR, Saunders RC, Marchionini D, Pham HA, Merigan WH (2000) Perceptual deficits after lesions of inferotemporal cortex in macaques. Cereb Cortex 10:671-683.
Insausti R, Munoz M (2001) Cortical projections of the non-entorhinal hippocampal formation in the cynomolgus monkey (Macaca fascicularis). Eur J Neurosci 14:435-451.
Insausti R, Amaral DG (2008) Entorhinal cortex of the monkey: IV. Topographical and laminar organization of cortical afferents. Journal of Comparative Neurology 509:608-641.
Ishizuka N, Weber J, Amaral DG (1990) Organization of intrahippocampal projections originating from CA3 pyramidal cells in the rat. J Comp Neurol 295:580-623.
Ito HT, Zhang SJ, Witter MP, Moser EI, Moser MB (2015) A prefrontal-thalamo-hippocampal circuit for goal-directed spatial navigation. Nature 522:50-U82.
Ito J, Maldonado P, Singer W, Grun S (2011) Saccade-related modulations of neuronal excitability support synchrony of visually elicited spikes. Cereb Cortex 21:2482-2497.
Ito S, Stuphorn V, Brown JW, Schall JD (2003) Performance monitoring by the anterior cingulate cortex during saccade countermanding. Science 302:120-122.
Itti L, Koch C, Niebur E (1998) A model of saliency-based visual attention for rapid scene analysis. Ieee T Pattern Anal 20:1254-1259.
Jacobs J, Kahana MJ, Ekstrom AD, Mollison MV, Fried I (2010) A sense of direction in human entorhinal cortex. Proc Natl Acad Sci U S A 107:6487-6492.
Jacobs J, Weidemann CT, Miller JF, Solway A, Burke JF, Wei XX, Suthana N, Sperling MR, Sharan AD, Fried I, Kahana MJ (2013) Direct recordings of grid-like neuronal activity in human spatial navigation. Nat Neurosci 16:1188-1190.
Jay MF, Sparks DL (1984) Auditory receptive fields in primate superior colliculus shift with changes in eye position. Nature 309:345-347.
Jones E (2007) The thalamus 2 volume set. In: Cambridge University Press Cambridge, UK.
Jones EG, Powell TP (1971) An analysis of the posterior group of thalamic nuclei on the basis of its afferent connections. J Comp Neurol 143:185-216.

Judd T, Durand F, Torralba A (2011) Fixations on low-resolution images. J Vis 11:1-20.
Jutras MJ, Buffalo EA (2010a) Recognition memory signals in the macaque hippocampus. Proc Natl Acad Sci U S A 107:401-406.
Jutras MJ, Buffalo EA (2010b) Recognition memory signals in the macaque hippocampus. Proceedings of the National Academy of Sciences 107:401-406.
Jutras MJ, Buffalo EA (2013) Oscillatory correlates of memory in non-human primates. Neuroimage.
Jutras MJ, Fries P, Buffalo EA (2009) Gamma-band synchronization in the macaque hippocampus and memory formation. J Neurosci 29:12521-12531.
Jutras MJ, Fries P, Buffalo EA (2013a) Oscillatory activity in the monkey hippocampus during visual exploration and memory formation. Proc Natl Acad Sci U S A 110:13144-13149.
Jutras MJ, Fries P, Buffalo EA (2013b) Oscillatory activity in the monkey hippocampus during visual exploration and memory formation. Proc Natl Acad Sci 110:13144-13149.
Kafkas A, Montaldi D (2011) Recognition memory strength is predicted by pupillary responses at encoding while fixation patterns distinguish recollection from familiarity. Q J Exp Psychol 64:1971-1989.
Kaspar K, Konig P (2011) Overt Attention and Context Factors: The Impact of Repeated Presentations, Image Type, and Individual Motivation. Plos One 6.
Katsuki F, Constantinidis C (2012) Early involvement of prefrontal cortex in visual bottom-up attention. Nat Neurosci 15:1160-1166.
Kennerley SW, Walton ME, Behrens TEJ, Buckley MJ, Rushworth MFS (2006) Optimal decision making and the anterior cingulate cortex. Nat Neurosci 9:940-947.
Killian NJ, Jutras MJ, Buffalo EA (2012) A map of visual space in the primate entorhinal cortex. Nature 491:761-764.
Killian NJ, Potter SM, Buffalo EA (2015) Saccade direction encoding in the primate entorhinal cortex during visual exploration. Proc Natl Acad Sci U S A 112:15743-15748.
Kim S, Sapiurka M, Clark RE, Squire LR (2013) Contrasting effects on path integration after hippocampal damage in humans and rats. P Natl Acad Sci USA 110:4732-4737.
Kimmel DL, Mammo D, Newsome WT (2012) Tracking the eye non-invasively: simultaneous comparison of the scleral search coil and optical tracking techniques in the macaque monkey. Front Behav Neurosci 6:49.
Kimura A, Yonetani R, Hirayama T (2013) Computational Models of Human Visual Attention and Their Implementations: A Survey. Ieice T Inf Syst E96d:562-578.
Kleinfeld D, Deschenes M, Ulanovsky N (2016) Whisking, Sniffing, and the Hippocampal theta-Rhythm: A Tale of Two Oscillators. Plos Biol 14.
Knierim JJ, Kudrimoti HS, McNaughton BL (1998) Interactions between idiothetic cues and external landmarks in the control of place cells and head direction cells. Journal of Neurophysiology 80:425-446.
Kobayashi Y, Amaral DG (2003) Macaque monkey retrosplenial cortex: II. Cortical afferents. Journal of Comparative Neurology 466:48-79.
Kobayashi Y, Amaral DG (2007) Macaque monkey retrosplenial cortex: III. Cortical efferents. Journal of Comparative Neurology 502:810-833.
Koenig J, Linder AN, Leutgeb JK, Leutgeb S (2011) The spatial periodicity of grid cells is not sustained during reduced theta oscillations. Science 332:592-595.
Kohler C (1985) Intrinsic projections of the retrohippocampal region in the rat brain. I. The subicular complex. J Comp Neurol 236:504-522.
Kollmorgen S, Nortmann N, Schroder S, Konig P (2010) Influence of Low-Level Stimulus Features, Task Dependent Factors, and Spatial Biases on Overt Visual Attention. Plos Comput Biol 6.
Komogortsev OV, Karpov A (2013) Automated classification and scoring of smooth pursuit eye movements in the presence of fixations and saccades. Behavior research methods 45:203-215.
Komogortsev OV, Gobert DV, Jayarathna S, Koh DH, Gowda SM (2010) Standardization of Automated Analyses of Oculomotor Fixation and Saccadic Behaviors. Ieee T Bio-Med Eng 57:2635-2645.
Komura Y, Nikkuni A, Hirashima N, Uetake T, Miyamoto A (2013) Responses of pulvinar neurons reflect a subject's confidence in visual categorization. Nat Neurosci 16:749-+.
Kondo H, Saleem KS, Price JL (2005) Differential connections of the perirhinal and parahippocampal cortex with the orbital and medial prefrontal networks in macaque monkeys. Journal of Comparative Neurology 493:479-509.
Konig SD, Buffalo EA (2014) A nonparametric method for detecting fixations and saccades using cluster analysis: Removing the need for arbitrary thresholds. J Neurosci Meth 227:121-131.

König SD, Buffalo EA (2014) A nonparametric method for detecting fixations and saccades using cluster analysis: Removing the need for arbitrary thresholds. Journal of neuroscience methods 227:121-131.
Konkel A, Cohen NJ (2009) Relational memory and the hippocampus: representations and methods. Front Neurosci 3:166-174.
Kosel KC, Vanhoesen GW, Rosene DL (1983) A Direct Projection from the Perirhinal Cortex (Area-35) to the Subiculum in the Rat. Brain Research 269:347-351.
Kotter R (2004) Online retrieval, processing, and visualization of primate connectivity data from the CoCoMac database. Neuroinformatics 2:127-144.
Kowler E, Anderson E, Dosher B, Blaser E (1995) The Role of Attention in the Programming of Saccades. Vision Res 35:1897-1916.
Kravitz DJ, Saleem KS, Baker CI, Mishkin M (2011) A new neural framework for visuospatial processing. Nat Rev Neurosci 12:217-230.
Krekelberg B, Kubischik M, Hoffmann KP, Bremmer F (2003) Neural correlates of visual localization and perisaccadic mislocalization. Neuron 37:537-545.
Krubitzer L (2007) The magnificent compromise: cortical field evolution in mammals. Neuron 56:201-208.
Krupic J, Bauza M, Burton S, Barry C, O'Keefe J (2015) Grid cell symmetry is shaped by environmental geometry. Nature 518:232-U199.
Kurylo DD, Skavenski AA (1991) Eye-Movements Elicited by Electrical-Stimulation of Area Pg in the Monkey. Journal of Neurophysiology 65:1243-1253.
Lagun D, Manzanares C, Zola SM, Buffalo EA, Agichtein E (2011) Detecting cognitive impairment by eye movement analysis using automatic classification algorithms. J Neurosci Meth 201:196-203.
Lakatos P, Chen CM, O'Connell MN, Mills A, Schroeder CE (2007) Neuronal oscillations and multisensory interaction in primary auditory cortex. Neuron 53:279-292.
Lamour Y, Dutar P, Jobert A (1984) Septo-Hippocampal and Other Medial Septum-Diagonal Band Neurons - Electrophysiological and Pharmacological Properties. Brain Research 309:227-239.
Land MF (2012) The Operation of the Visual System in Relation to Action. Curr Biol 22:R811-R817.
Langston RF, Ainge JA, Couey JJ, Canto CB, Bjerknes TL, Witter MP, Moser EI, Moser MB (2010) Development of the Spatial Representation System in the Rat. Science 328:1576-1580.
Lavenex P, Suzuki WA, Amaral DG (2002) Perirhinal and parahippocampal cortices of the macaque monkey: Projections to the neocortex. Journal of Comparative Neurology 447:394-420.
Layfield DM, Patel M, Hallock H, Griffin AL (2015) Inactivation of the nucleus reuniens/rhomboid causes a delay-dependent impairment of spatial working memory. Neurobiol Learn Mem 125:163-167.
Lee B, Pesaran B, Andersen RA (2011) Area MSTd neurons encode visual stimuli in eye coordinates during fixation and pursuit. J Neurophysiol 105:60-68.
Lee I, Yoganarasimha D, Rao G, Knierim JJ (2004) Comparison of population coherence of place cells in hippocampal subfields CA1 and CA3. Nature 430:456-459.
Lee K, Buxton H, Feng HF (2005) Cue-guided search: A computational model of selective attention. Ieee T Neural Networ 16:910-924.
Leech R, Sharp DJ (2014) The role of the posterior cingulate cortex in cognition and disease. Brain 137:12-32.
Lehmann SJ, Corneil BD (2016) Transient Pupil Dilation after Subsaccadic Microstimulation of Primate Frontal Eye Fields. J Neurosci 36:3765-3776.
Lengyel M, Szatmary Z, Erdi P (2003) Dynamically detuned oscillations account for the coupled rate and temporal code of place cell firing. Hippocampus 13:700-714.
Leutgeb JK, Leutgeb S, Moser MB, Moser EI (2007) Pattern separation in the dentate gyrus and CA3 of the hippocampus. Science 315:961-966.
Lever C, Burton S, Jeewajee A, O'Keefe J, Burgess N (2009) Boundary Vector Cells in the Subiculum of the Hippocampal Formation. J Neurosci 29:9771-9777.
Liebermann D, Ploner CJ, Kraft A, Kopp UA, Ostendorf F (2013) A dysexecutive syndrome of the medial thalamus. Cortex 49:40-49.
Lisman JE (1999a) Relating hippocampal circuitry to function: Recall of memory sequences by reciprocal dentate-CA3 interactions. Neuron 22:233-242.
Lisman JE (1999b) Relating hippocampal circuitry to function: recall of memory sequences by reciprocal dentate-CA3 interactions. Neuron 22:233-242.
Liston DB, Krukowski AE, Stone LS (2012) Saccade detection during smooth tracking. Displays.
Liu P, Bilkey DK (1996) Direct connection between perirhinal cortex and hippocampus is a major constituent of the lateral perforant path. Hippocampus 6:125-135.

Liu ZX, Shen K, Olsen RK, Ryan JD (2017) Visual Sampling Predicts Hippocampal Activity. J Neurosci 37:599-609.
Luppino G, Matelli M, Camarda RM, Gallese V, Rizzolatti G (1991) Multiple representations of body movements in mesial area 6 and the adjacent cingulate cortex: an intracortical microstimulation study in the macaque monkey. J Comp Neurol 311:463-482.
Lynch JC, Tian JR (2006a) Cortico-cortical networks and cortico-subcortical loops for the higher control of eye movements. Neuroanatomy of the Oculomotor System 151:461-501.
Lynch JC, Tian JR (2006b) Cortico-cortical networks and cortico-subcortical loops for the higher control of eye movements. Prog Brain Res 151:461-501.
Lyon DC, Nassi JJ, Callaway EM (2010) A Disynaptic Relay from Superior Colliculus to Dorsal Stream Visual Cortex in Macaque Monkey. Neuron 65:270-279.
MacDonald CJ, Lepage KQ, Eden UT, Eichenbaum H (2011) Hippocampal "Time Cells" Bridge the Gap in Memory for Discontiguous Events. Neuron 71:737-749.
Malkova L, Mishkin M (2003) One-trial memory for object-place associations after separate lesions of hippocampus and posterior parahippocampal region in the monkey. J Neurosci 23:1956-1965.
Mannan SK, Kennard C, Husain M (2009) The role of visual salience in directing eye movements in visual object agnosia. Curr Biol 19:R247-248.
Maris E, Oostenveld R (2007) Nonparametric statistical testing of EEG- and MEG-data. J Neurosci Methods 164:177-190.
Martinez-Conde S, Macknik SL (2015) From Exploration to Fixation: An Integrative View of Yarbus's Vision. Perception 44:884-899.
Martinez-Conde S, Otero-Millan J, Macknik SL (2013) The impact of microsaccades on vision: towards a unified theory of saccadic function. Nat Rev Neurosci 14:83-96.
Martinez-Conde S, Macknik SL, Troncoso XG, Hubel DH (2009) Microsaccades: a neurophysiological analysis. Trends Neurosci 32:463-475.
Mason R, Groos GA (1981) Cortico-recipient and tecto-recipient visual zones in the rat's lateral posterior (pulvinar) nucleus: an anatomical study. Neurosci Lett 25:107-112.
Matsumoto N, Minamimoto T, Graybiel AM, Kimura M (2001) Neurons in the thalamic CM-Pf complex supply striatal neurons with information about behaviorally significant sensory events. Journal of Neurophysiology 85:960-976.
McAlonan K, Cavanaugh J, Wurtz RH (2008) Guarding the gateway to cortex with attention in visual thalamus. Nature 456:391-394.
McCoy AN, Crowley JC, Haghighian G, Dean HL, Platt ML (2003) Saccade reward signals in posterior cingulate cortex. Neuron 40:1031-1040.
McKenzie S, Frank AJ, Kinsky NR, Porter B, Riviere PD, Eichenbaum H (2014) Hippocampal Representation of Related and Opposing Memories Develop within Distinct, Hierarchically Organized Neural Schemas. Neuron 83:202-215.
McNaughton BL, Battaglia FP, Jensen O, Moser EI, Moser MB (2006) Path integration and the neural basis of the 'cognitive map'. Nat Rev Neurosci 7:663-678.
Meister ML, Buffalo EA (2015) Getting directions from the hippocampus: The neural connection between looking and memory. Neurobiol Learn Mem.
Meister ML, Buffalo EA (2016) Getting directions from the hippocampus: the neural connection between looking and memory. Neurobiol Learn Mem 134:135-144.
Mendoza-Halliday D, Torres S, Martinez-Trujillo JC (2014) Sharp emergence of feature-selective sustained activity along the dorsal visual pathway. Nat Neurosci 17:1255-1262.
Mesulam MM, Mufson EJ (1982a) Insula of the Old-World Monkey .1. Architectonics in the Insulo-Orbito-Temporal Component of the Paralimbic Brain. Journal of Comparative Neurology 212:1-22.
Mesulam MM, Mufson EJ (1982b) Insula of the Old-World Monkey .3. Efferent Cortical Output and Comments on Function. Journal of Comparative Neurology 212:38-52.
Mesulam MM, Mufson EJ, Levey AI, Wainer BH (1983) Cholinergic Innervation of Cortex by the Basal Forebrain - Cyto-Chemistry and Cortical Connections of the Septal Area, Diagonal Band Nuclei, Nucleus Basalis (Substantia Innominata), and Hypothalamus in the Rhesus-Monkey. Journal of Comparative Neurology 214:170-197.
Meunier M, Bachevalier J, Mishkin M, Murray EA (1993) Effects on visual recognition of combined and separate ablations of the entorhinal and perirhinal cortex in rhesus monkeys. J Neurosci 13:5418-5432.

Miao CL, Cao QC, Ito HT, Yamahachi H, Witter MP, Moser MB, Moser EI (2015) Hippocampal Remapping after Partial Inactivation of the Medial Entorhinal Cortex. Neuron 88:590-603.
Miller EK, Buschman TJ (2013) Cortical circuits for the control of attention. Curr Opin Neurobiol 23:216-222.
Miller JF, Neufang M, Solway A, Brandt A, Trippel M, Mader I, Hefft S, Merkow M, Polyn SM, Jacobs J, Kahana MJ, Schulze-Bonhage A (2013) Neural activity in human hippocampal formation reveals the spatial context of retrieved memories. Science 342:1111-1114.
Mitchell A, Chakraborty S (2013) What does the mediodorsal thalamus do? Frontiers in Systems Neuroscience 7.
Mitz AR, Godschalk M (1989) Eye-movement representation in the frontal lobe of rhesus monkeys. Neurosci Lett 106:157-162.
Mizuhiki T, Richmond BJ, Shidara M (2012) Encoding of reward expectation by monkey anterior insular neurons. J Neurophysiol 107:2996-3007.
Mizumori SJ, Williams JD (1993) Directionally selective mnemonic properties of neurons in the lateral dorsal nucleus of the thalamus of rats. J Neurosci 13:4015-4028.
Mizumori SJ, Ragozzino KE, Cooper BG, Leutgeb S (1999) Hippocampal representational organization and spatial context. Hippocampus 9:444-451.
Mizumori SJY, Miya DY, Ward KE (1994) Reversible Inactivation of the Lateral Dorsal Thalamus Disrupts Hippocampal Place Representation and Impairs Spatial-Learning. Brain Research 644:168-174.
Morecraft RJ, Geula C, Mesulam MM (1992) Cytoarchitecture and Neural Afferents of Orbitofrontal Cortex in the Brain of the Monkey. Journal of Comparative Neurology 323:341-358.
Morin LP, Studholme KM (2014) Retinofugal Projections in the Mouse. Journal of Comparative Neurology 522:3733-3753.
Morris R, Petrides M, Pandya DN (1999) Architecture and connections of retrosplenial area 30 in the rhesus monkey (macaca mulatta). Eur J Neurosci 11:2506-2518.
Moser EI, Kropff E, Moser MB (2008a) Place cells, grid cells, and the brain's spatial representation system. Annu Rev Neurosci 31:69-89.
Moser EI, Kropff E, Moser MB (2008b) Place cells, grid cells, and the brain's spatial representation system. Annu Rev Neurosci 31:69-89.
Moser EI, Roudi Y, Witter MP, Kentros C, Bonhoeffer T, Moser MB (2014) Grid cells and cortical representation. Nat Rev Neurosci 15:466-481.
Moser MB, Rowland DC, Moser EI (2015) Place cells, grid cells, and memory. Cold Spring Harb Perspect Biol 7:a021808.
Mueller A, Hong DS, Shepard S, Moore T (2017) Linking ADHD to the Neural Circuitry of Attention. Trends Cogn Sci 21:474-488.
Mufson EJ, Mesulam MM (1982) Insula of the Old-World Monkey .2. Afferent Cortical Input and Comments on the Claustrum. Journal of Comparative Neurology 212:23-37.
Munoz DP, Everling S (2004) Look away: the anti-saccade task and the voluntary control of eye movement. Nat Rev Neurosci 5:218-228.
Najemnik J, Geisler WS (2005) Optimal eye movement strategies in visual search. Nature 434:387-391.
Nakano K, Kayahara T, Tsutsumi T, Ushiro H (2000) Neural circuits and functional organization of the striatum. J Neurol 247:1-15.
Nakano K, Hasegawa Y, Tokushige A, Nakagawa S, Kayahara T, Mizuno N (1990) Topographical Projections from the Thalamus, Subthalamic Nucleus and Pedunculopontine Tegmental Nucleus to the Striatum in the Japanese Monkey, Macaca-Fuscata. Brain Research 537:54-68.
Naya Y, Suzuki WA (2011) Integrating What and When Across the Primate Medial Temporal Lobe. Science 333:773-776.
Nemanic S, Alvarado MC, Bachevalier J (2004) The hippocampal/parahippocampal regions and recognition memory: insights from visual paired comparison versus object-delayed nonmatching in monkeys. J Neurosci 24:2013-2026.
Nieuwenhuys R (2012) The insular cortex: A review. Evolution of the Primate Brain: From Neuron to Behavior 195:123-163.
Niki H, Watanabe M (1979) Prefrontal and cingulate unit activity during timing behavior in the monkey. Brain Res 171:213-224.
Ninomiya T, Sawamura H, Inoue K, Takada M (2012) Multisynaptic Inputs from the Medial Temporal Lobe to V4 in Macaques. Plos One 7.
Nishijo H, Ono T, Eifuku S, Tamura R (1997) The relationship between monkey hippocampus place-related neural activity and action in space. Neuroscience Letters 226:57-60.

Nordfang M, Dyrholm M, Bundesen C (2013) Identifying Bottom-Up and Top-Down Components of Attentional Weight by Experimental Analysis and Computational Modeling. J Exp Psychol Gen 142:510-535.
Norman G, Eacott MJ (2005) Dissociable effects of lesions to the perirhinal cortex and the postrhinal cortex on memory for context and objects in rats. Behav Neurosci 119:557-566.
Noudoost B, Chang MH, Steinmetz NA, Moore T (2010) Top-down control of visual attention. Current Opinion in Neurobiology 20:183-190.
Nowicka A, Ringo JL (2000) Eye position-sensitive units in hippocampal formation and in inferotemporal cortex of the Macaque monkey. Eur J Neurosci 12:751-759.
Nystrom M, Holmqvist K (2010) An adaptive algorithm for fixation, saccade, and glissade detection in eyetracking data. Behav Res Methods 42:188-204.
O'Keefe J (1976) Place units in the hippocampus of the freely moving rat. Exp Neurol 51:78-109.
O'Keefe J, Dostrovsky J (1971) The hippocampus as a spatial map. Preliminary evidence from unit activity in the freely-moving rat. Brain Res 34:171-175.
Okeefe J, Nadel L (1979) The Cognitive Map as a Hippocampus. Behav Brain Sci 2:520-528.
Okeefe J, Recce ML (1993) Phase Relationship between Hippocampal Place Units and the Eeg Theta-Rhythm. Hippocampus 3:317-330.
Olsen RK, Sebanayagam V, Lee Y, Moscovitch M, Grady CL, Rosenbaum RS, Ryan JD (2016) The relationship between eye movements and subsequent recognition: Evidence from individual differences and amnesia. Cortex 85:182-193.
Olson CR, Musil SY (1992) Topographic organization of cortical and subcortical projections to posterior cingulate cortex in the cat: evidence for somatic, ocular, and complex subregions. J Comp Neurol 324:237-260.
Olson CR, Gettner SN (1995) Object-Centered Direction Selectivity in the Macaque Supplementary Eye Field. Science 269:985-988.
Olson CR, Musil SY, Goldberg ME (1996) Single neurons in posterior cingulate cortex of behaving macaque: eye movement signals. J Neurophysiol 76:3285-3300.
Otero-Millan J, Troncoso XG, Macknik SL, Serrano-Pedraza I, Martinez-Conde S (2008) Saccades and microsaccades during visual fixation, exploration, and search: foundations for a common saccadic generator. J Vis 8:21 21-18.
Parker A, Gaffan D (1997) The effect of anterior thalamic and cingulate cortex lesions on object-in-place memory in monkeys. Neuropsychologia 35:1093-1102.
Parkhurst D, Law K, Niebur E (2002) Modeling the role of salience in the allocation of overt visual attention. Vision Res 42:107-123.
Parkinson JA, Willoughby PJ, Robbins TW, Everitt BJ (2000) Disconnection of the anterior cingulate cortex and nucleus accumbens core impairs Pavlovian approach behavior: Further evidence for limbic cortical-ventral striatopallidal systems. Behav Neurosci 114:42-63.
Pastalkova E, Itskov V, Amarasingham A, Buzsaki G (2008) Internally generated cell assembly sequences in the rat hippocampus. Science 321:1322-1327.
Pasupathy A, Connor CE (1999) Responses to contour features in macaque area V4. Journal of Neurophysiology 82:2490-2502.
Patel VR, Zee DS (2015) The cerebellum in eye movement control: nystagmus, coordinate frames and disconjugacy. Eye (Lond) 29:191-195.
Paus T (2001) Primate anterior cingulate cortex: Where motor control, drive and cognition interface. Nat Rev Neurosci 2:417-424.
Pereira A, Ribeiro S, Wiest M, Moore LC, Pantoja J, Lin SC, Nicolelis MAL (2007) Processing of tactile information by the hippocampus. P Natl Acad Sci USA 104:18286-18291.
Pergola G, Suchan B (2013) Associative learning beyond the medial temporal lobe: many actors on the memory stage. Front Behav Neurosci 7.
Pesaran B, Nelson MJ, Andersen RA (2006) Dorsal premotor neurons encode the relative position of the hand, eye, and goal during reach planning. Neuron 51:125-134.
Petrides M (1985) Deficits in Non-Spatial Conditional Associative Learning after Periarcuate Lesions in the Monkey. Behavioural Brain Research 16:95-101.
Petrides M, Pandya DN (1999) Dorsolateral prefrontal cortex: comparative cytoarchitectonic analysis in the human and the macaque brain and corticocortical connection patterns. Eur J Neurosci 11:1011-1036.
Pham DT, Dimov SS, Nguyen CD (2005) Selection of K in K-means clustering. P I Mech Eng C-J Mec 219:103-119.

Phinney RE, Siegel RM (2000) Speed selectivity for optic flow in area 7a of the behaving macaque. Cerebral Cortex 10:413-421.
Pierrot-Deseilligny C, Milea D, Muri RM (2004) Eye movement control by the cerebral cortex. Curr Opin Neurol 17:17-25.
Pierrot-Deseilligny C, Muri RM, Ploner CJ, Gaymard B, Demeret S, Rivaud-Pechoux S (2003) Decisional role of the dorsolateral prefrontal cortex in ocular motor behaviour. Brain 126:1460-1473.
Ploner CJ, Gaymard BM, Rivaud-Pechoux S, Baulac M, Clemenceau S, Samson S, Pierrot-Deseilligny C (2000) Lesions affecting the parahippocampal cortex yield spatial memory deficits in humans. Cereb Cortex 10:1211-1216.
Prerau MJ, Lipton PA, Eichenbaum HB, Eden UT (2014) Characterizing context-dependent differential firing activity in the hippocampus and entorhinal cortex. Hippocampus 24:476-492.
Quilodran R, Rothe M, Procyk E (2008) Behavioral shifts and action valuation in the anterior cingulate cortex. Neuron 57:314-325.
Quirk GJ, Muller RU, Kubie JL (1990) The firing of hippocampal place cells in the dark depends on the rat's recent experience. J Neurosci 10:2008-2017.
Rajkai C, Lakatos P, Chen CM, Pincze Z, Karmos G, Schroeder CE (2008) Transient cortical excitation at the onset of visual fixation. Cerebral Cortex 18:200-209.
Ray JP, Price JL (1993) The Organization of Projections from the Mediodorsal Nucleus of the Thalamus to Orbital and Medial Prefrontal Cortex in Macaque Monkeys. Journal of Comparative Neurology 337:1-31.
Rayner K (2009) Eye movements and attention in reading, scene perception, and visual search. Q J Exp Psychol 62:1457-1506.
Redish AD (1999) Beyond the cognitive map: from place cells to episodic memory: MIT Press.
Redish AD, Touretzky DS (1998) The role of the hippocampus in solving the Morris water maze. Neural Comput 10:73-111.
Rees H, Roberts MHT (1993) The Anterior Pretectal Nucleus - a Proposed Role in Sensory Processing. Pain 53:121-135.
Remme MWH, Lengyel M, Gutkin BS (2010) Democracy-Independence Trade-Off in Oscillating Dendrites and Its Implications for Grid Cells. Neuron 66:429-437.
Richmond J, Nelson CA (2009) Relational memory during infancy: evidence from eye tracking. Dev Sci 12:549-556.
Rigotti M, Barak O, Warden MR, Wang XJ, Daw ND, Miller EK, Fusi S (2013) The importance of mixed selectivity in complex cognitive tasks. Nature 497:585-590.
Ringo JL, Sobotka S, Diltz MD, Bunce CM (1994) Eye-Movements Modulate Activity in Hippocampal, Parahippocampal, and Inferotemporal Neurons. Journal of Neurophysiology 71:1285-1288.
Robinson DL, Mcclurkin JW, Kertzman C (1990) Orbital Position and Eye-Movement Influences on Visual Responses in the Pulvinar Nuclei of the Behaving Macaque. Exp Brain Res 82:235-246.
Robinson FR, Fuchs AF (2001) The role of the cerebellum in voluntary eye movements. Annu Rev Neurosci 24:981-1004.
Robinson NTM, Priestley JB, Rueckemann JW, Garcia AD, Smeglin VA, Marino FA, Eichenbaum H (2017) Medial Entorhinal Cortex Selectively Supports Temporal Coding by Hippocampal Neurons. Neuron 94:677-+.
Rockland KS, Van Hoesen GW (1999) Some temporal and parietal cortical connections converge in CA1 of the primate hippocampus. Cerebral Cortex 9:232-237.
Rodrigoangulo ML, Reinososuarez F (1988) Connections to the Lateral Posterior Pulvinar Thalamic Complex from the Reticular and Ventral Lateral Geniculate Thalamic Nuclei - a Topographical Study in the Cat. Neuroscience 26:449-459.
Roe AW, Chelazzi L, Connor CE, Conway BR, Fujita I, Gallant JL, Lu HD, Vanduffel W (2012) Toward a Unified Theory of Visual Area V4. Neuron 74:12-29.
Rolfs M, Carrasco M (2012) Rapid Simultaneous Enhancement of Visual Sensitivity and Perceived Contrast during Saccade Preparation. J Neurosci 32:13744-13753.
Rolls ET (1999) Spatial view cells and the representation of place in the primate hippocampus. Hippocampus 9:467-480.
Rolls ET, Stringer SM, Elliot T (2006) Entorhinal cortex grid cells can map to hippocampal place cells by competitive learning. Network-Comp Neural 17:447-465.
Romanski LM, Giguere M, Bates JF, GoldmanRakic PS (1997) Topographic organization of medial pulvinar connections with the prefrontal cortex in the rhesus monkey. Journal of Comparative Neurology 379:313-332.

Ross J, Morrone MC, Goldberg ME, Burr DC (2001) Changes in visual perception at the time of saccades. Trends in Neurosciences 24:113-121.
Rothblat LA, Vnek N, Gleason TC, Kromer LF (1993) Role of the parahippocampal region in spatial and non-spatial memory: effects of parahippocampal lesions on rewarded alternation and concurrent object discrimination learning in the rat. Behav Brain Res 55:93-100.
Rozzi S, Ferrari PF, Bonini L, Rizzolatti G, Fogassi L (2008) Functional organization of inferior parietal lobule convexity in the macaque monkey: electrophysiological characterization of motor, sensory and mirror responses and their correlation with cytoarchitectonic areas. Eur J Neurosci 28:1569-1588.
Rubin A, Yartsev MM, Ulanovsky N (2014a) Encoding of Head Direction by Hippocampal Place Cells in Bats. J Neurosci 34:1067-1080.
Rubin RD, Watson PD, Duff MC, Cohen NJ (2014b) The role of the hippocampus in flexible cognition and social behavior. Front Hum Neurosci 8.
Rueckemann JW, DiMauro AJ, Rangel LM, Han X, Boyden ES, Eichenbaum H (2016) Transient optogenetic inactivation of the medial entorhinal cortex biases the active population of hippocampal neurons. Hippocampus 26:246-260.
Rushworth MF, Hadland KA, Gaffan D, Passingham RE (2003) The effect of cingulate cortex lesions on task switching and working memory. J Cogn Neurosci 15:338-353.
Russchen FT, Amaral DG, Price JL (1987) The Afferent Input to the Magnocellular Division of the Mediodorsal Thalamic Nucleus in the Monkey, Macaca-Fascicularis. Journal of Comparative Neurology 256:175-210.
Rutishauser U, Koch C (2007) Probabilistic modeling of eye movement data during conjunction search via feature-based attention. J Vis 7:5.
Rutishauser U, Mamelak AN, Schuman EM (2006) Single-trial learning of novel stimuli by individual neurons of the human hippocampus-amygdala complex. Neuron 49:805-813.
Ryan L, Cox C, Hayes SM, Nadel L (2008) Hippocampal activation during episodic and semantic memory retrieval: comparing category production and category cued recall. Neuropsychologia 46:2109-2121.
Saalmann YB (2014) Intralaminar and medial thalamic influence on cortical synchrony, information transmission and cognition. Front Syst Neurosci 8:83.
Saalmann YB, Kastner S (2011) Cognitive and Perceptual Functions of the Visual Thalamus. Neuron 71:209-223.
Sadikot AF, Parent A, Francois C (1990) The centre median and parafascicular thalamic nuclei project respectively to the sensorimotor and associative-limbic striatal territories in the squirrel monkey. Brain Res 510:161-165.
Sadikot AF, Parent A, Smith Y, Bolam JP (1992) Efferent Connections of the Centromedian and Parafascicular Thalamic Nuclei in the Squirrel-Monkey - a Light and Electron-Microscopic Study of the Thalamostriatal Projection in Relation to Striatal Heterogeneity. Journal of Comparative Neurology 320:228-242.
Sakon JJ, Naya Y, Wirth S, Suzuki WA (2014) Context-dependent incremental timing cells in the primate hippocampus. P Natl Acad Sci USA 111:18351-18356.
Salvucci DD, Goldberg JH (2000) Identifying fixations and saccades in eye-tracking protocols. In: Proceedings of the 2000 symposium on Eye tracking research & applications, pp 71-78. Palm Beach Gardens, Florida, USA: ACM.
Sapiurka M, Squire LR, Clark RE (2016) Distinct roles of hippocampus and medial prefrontal cortex in spatial and nonspatial memory. Hippocampus 26:1515-1524.
Sara SJ (2009) The locus coeruleus and noradrenergic modulation of cognition. Nat Rev Neurosci 10:211-223.
Sarel A, Finkelstein A, Las L, Ulanovsky N (2017) Vectorial representation of spatial goals in the hippocampus of bats. Science 355:176-180.
Sato N, Sakata H, Tanaka YL, Taira M (2006) Navigation-associated medial parietal neurons in monkeys. Proc Natl Acad Sci U S A 103:17001-17006.
Sato N, Sakata H, Tanaka YL, Taira M (2010) Context-dependent place-selective responses of the neurons in the medial parietal region of macaque monkeys. Cereb Cortex 20:846-858.
Saunders RC, Rosene DL, Van Hoesen GW (1988) Comparison of the efferents of the amygdala and the hippocampal formation in the rhesus monkey: II. Reciprocal and non-reciprocal connections. J Comp Neurol 271:185-207.
Saunders RC, Mishkin M, Aggleton JP (2005) Projections from the entorhinal cortex, perirhinal cortex, presubiculum, and parasubiculum to the medial thalamus in macaque monkeys: identifying different pathways using disconnection techniques. Exp Brain Res 167:1-16.
Save E, Nerad L, Poucet B (2000) Contribution of multiple sensory information to place field stability in hippocampal place cells. Hippocampus 10:64-76.

Schall JD, Stuphorn V, Brown JW (2002) Monitoring and control of action by the frontal lobes. Neuron 36:309-322.
Schall JD, Morel A, King DJ, Bullier J (1995) Topography of Visual-Cortex Connections with Frontal Eye Field in Macaque - Convergence and Segregation of Processing Streams. J Neurosci 15:4464-4487.
Schapiro AC, Turk-Browne NB, Botvinick MM, Norman KA (2017) Complementary learning systems within the hippocampus: a neural network modelling approach to reconciling episodic memory with statistical learning. Phil Trans R Soc B 372:20160049.
Schiff ND (2008) Central thalamic contributions to arousal regulation and neurological disorders of consciousness. Molecular and Biophysical Mechanisms of Arousal, Alertness, and Attention 1129:105-118.
Schlag-Rey M, Schlag J (1984) Visuomotor functions of central thalamus in monkey. I. Unit activity related to spontaneous eye movements. J Neurophysiol 51:1149-1174.
Schlag-Rey M, Amador N, Sanchez H, Schlag J (1997) Antisaccade performance predicted by neuronal activity in the supplementary eye field. Nature 390:398-401.
Schmahmann JD, Pandya DN (1990) Anatomical Investigation of Projections from Thalamus to Posterior Parietal Cortex in the Rhesus-Monkey - a Wga-Hrp and Fluorescent Tracer Study. Journal of Comparative Neurology 295:299-326.
Schnider A, Gutbrod K, Hess CW, Schroth G (1996) Memory without context: Amnesia with confabulations after infarction of the right capsular genu. J Neurol Neurosur Ps 61:186-193.
Schroeder CE, Wilson DA, Radman T, Scharfman H, Lakatos P (2010) Dynamics of Active Sensing and perceptual selection. Curr Opin Neurobiol 20:172-176.
Scoville WB, Milner B (1957) Loss of recent memory after bilateral hippocampal lesions. J Neurol Neurosurg Psychiatry 20:11-21.
Selemon LD, Goldmanrakic PS (1988) Common Cortical and Subcortical Targets of the Dorsolateral Prefrontal and Posterior Parietal Cortices in the Rhesus-Monkey - Evidence for a Distributed Neural Network Subserving Spatially Guided Behavior. J Neurosci 8:4049-4068.
Shen K, Bezgin G, Selvam R, McIntosh AR, Ryan JD (2016) An Anatomical Interface between Memory and Oculomotor Systems. J Cognitive Neurosci 28:1772-1783.
Shic F, Scassellati B (2007) A behavioral analysis of computational models of visual attention. Int J Comput Vision 73:159-177.
Shic F, Scassellati B, Chawarska K (2008) The incomplete fixation measure. In: Proceedings of the 2008 symposium on Eye tracking research & applications, pp 111-114. Savannah, Georgia: ACM.
Shima K, Tanji J (1998) Role for cingulate motor area cells in voluntary movement selection based on reward. Science 282:1335-1338.
Shimozaki SS, Hayhoe MM, Zelinsky GJ, Weinstein A, Merigan WH, Ballard DH (2003) Effect of parietal lobe lesions on saccade targeting and spatial memory in a naturalistic visual search task. Neuropsychologia 41:1365-1386.
Shook BL, Schlag-Rey M, Schlag J (1988) Direct projection from the supplementary eye field to the nucleus raphe interpositus. Exp Brain Res 73:215-218.
Shook BL, Schlag-Rey M, Schlag J (1990) Primate supplementary eye field: I. Comparative aspects of mesencephalic and pontine connections. J Comp Neurol 301:618-642.
Shook BL, Schlag-Rey M, Schlag J (1991) Primate supplementary eye field. II. Comparative aspects of connections with the thalamus, corpus striatum, and related forebrain nuclei. J Comp Neurol 307:562-583.
Showers MJ, Lauer EW (1961) Somatovisceral motor patterns in the insula. J Comp Neurol 117:107-115.
Skaggs WE, McNaughton BL, Gothard KM, Markus EJ (1993) An information-theoretic approach to deciphering the hippocampal code. In: In: Citeseer.
Skaggs WE, McNaughton BL, Wilson MA, Barnes CA (1996) Theta phase precession in hippocampal neuronal populations and the compression of temporal sequences. Hippocampus 6:149-172.
Small DM, Gitelman DR, Gregory MD, Nobre AC, Parrish TB, Mesulam MM (2003) The posterior cingulate and medial prefrontal cortex mediate the anticipatory allocation of spatial attention. Neuroimage 18:633-641.
Smith CN, Squire LR (2008a) Experience-dependent eye movements reflect hippocampus-dependent (aware) memory. J Neurosci 28:12825-12833.
Smith CN, Squire LR (2008b) Experience-Dependent Eye Movements Reflect Hippocampus-Dependent (Aware) Memory. J Neurosci 28:12825-12833.
Smith CN, Hopkins RO, Squire LR (2006a) Experience-dependent eye movements, awareness, and hippocampus-dependent memory. J Neurosci 26:11304-11312.
Smith CN, Hopkins RO, Squire LR (2006b) Experience-dependent eye movements, awareness, and hippocampus-dependent memory. J Neurosci 26:11304-11312.

Smith DM, Mizumori SJY (2006a) Hippocampal place cells, context, and episodic memory. Hippocampus 16:716-729.
Smith DM, Mizumori SJY (2006b) Learning-related development of context-specific neuronal responses to places and events The hippocampal role in context processing. J Neurosci 26:3154-3163.
Smith DM, Barredo J, Mizumori SJY (2012) Complimentary roles of the hippocampus and retrosplenial cortex in behavioral context discrimination. Hippocampus 22:1121-1133.
Smith MA, Crawford JD (2005) Distributed population mechanism for the 3-D oculomotor reference frame transformation. Journal of neurophysiology 93:1742-1761.
Snow JC, Allen HA, Rafal RD, Humphreys GW (2009) Impaired attentional selection following lesions to human pulvinar: Evidence for homology between human and monkey. P Natl Acad Sci USA 106:4054-4059.
Sober SJ, Wohlgemuth MJ, Brainard MS (2008) Central contributions to acoustic variation in birdsong. J Neurosci 28:10370-10379.
Sobotka S, Ringo JL (1997) Saccadic eye movements, even in darkness, generate event-related potentials recorded in medial sputum and medial temporal cortex. Brain Res 756:168-173.
Solstad T, Moser EI, Einevoll GT (2006) From grid cells to place cells: A mathematical model. Hippocampus 16:1026-1031.
Sommer MA, Wurtz RH (2002) A pathway in primate brain for internal monitoring of movements. Science 296:1480-1482.
Sommer MA, Wurtz RH (2004) What the brain stem tells the frontal cortex. II. Role of the SC-MD-FEF pathway in corollary discharge. Journal of Neurophysiology 91:1403-1423.
Sprague JM, Meikle TH, Jr. (1965) The Role of the Superior Colliculus in Visually Guided Behavior. Exp Neurol 11:115-146.
Squire LR (1992) Memory and the Hippocampus - a Synthesis from Findings with Rats, Monkeys, and Humans. Psychol Rev 99:195-231.
Sreenivasan S, Fiete I (2011) Grid cells generate an analog error-correcting code for singularly precise neural computation. Nat Neurosci 14:1330-U1154.
Steinmetz NA, Moore T (2014) Eye Movement Preparation Modulates Neuronal Responses in Area V4 When Dissociated from Attentional Demands. Neuron 83:496-506.
Stephan KE, Kamper L, Bozkurt A, Burns GA, Young MP, Kotter R (2001) Advanced database methodology for the Collation of Connectivity data on the Macaque brain (CoCoMac). Philos Trans R Soc Lond B Biol Sci 356:1159-1186.
Strange BA, Witter MP, Lein ES, Moser EI (2014) Functional organization of the hippocampal longitudinal axis. Nat Rev Neurosci 15:655-669.
Su HS, Bentivoglio M (1990) Thalamic midline cell populations projecting to the nucleus accumbens, amygdala, and hippocampus in the rat. J Comp Neurol 297:582-593.
Suzuki M, Gottlieb J (2013) Distinct neural mechanisms of distractor suppression in the frontal and parietal lobe. Nat Neurosci 16:98-104.
Suzuki WA, Amaral DG (1990) Cortical inputs to the CA1 field of the monkey hippocampus originate from the perirhinal and parahippocampal cortex but not from area TE. Neuroscience letters 115:43-48.
Suzuki WA, Amaral DG (1994a) Perirhinal and parahippocampal cortices of the macaque monkey: cortical afferents. J Comp Neurol 350:497-533.
Suzuki WA, Amaral DG (1994b) Topographic Organization of the Reciprocal Connections between the Monkey Entorhinal Cortex and the Perirhinal and Parahippocampal Cortices. J Neurosci 14:1856-1877.
Swanson LW, Sawchenko PE, Cowan WM (1981) Evidence for collateral projections by neurons in Ammon's horn, the dentate gyrus, and the subiculum: a multiple retrograde labeling study in the rat. J Neurosci 1:548-559.
Symonds LL, Rosenquist AC, Edwards SB, Palmer LA (1981) Projections of the Pulvinar-Lateral Posterior Complex to Visual Cortical Areas in the Cat. Neuroscience 6:1995-2020.
Tan HM, Bassett JP, O'Keefe J, Cacucci F, Wills TJ (2015) The Development of the Head Direction System before Eye Opening in the Rat. Curr Biol 25:479-483.
Tanaka H, Hoshino Y, Watanabe Y, Sakurai K, Takekawa H, Hirata K (2012) A Case of Strategic-infarct Mild Cognitive Impairment. Neurologist 18:211-213.
Tanaka M (2007) Spatiotemporal properties of eye position signals in the primate central thalamus. Cereb Cortex 17:1504-1515.
Tatler BW (2007) The central fixation bias in scene viewing: selecting an optimal viewing position independently of motor biases and image feature distributions. J Vis 7:4 1-17.
Tatler BW, Vincent BT (2008) Systematic tendencies in scene viewing. Journal of Eye Movement Research 2:1-18.

Tatler BW BR, and Gilchrist ID (2005) Visual correlates of fixation selection: effects of scale and time. Vision Research 45:643-659.
Taube JS (1995) Head direction cells recorded in the anterior thalamic nuclei of freely moving rats. J Neurosci 15:70-86.
Taube JS (2007) The head direction signal: Origins and sensory-motor integration. Annu Rev Neurosci 30:181-207.
Taube JS, Muller RU (1998) Comparisons of head direction cell activity in the postsubiculum and anterior thalamus of freely moving rats. Hippocampus 8:87-108.
Taylor AM, Jeffery G, Lieberman AR (1986) Subcortical Afferent and Efferent Connections of the Superior Colliculus in the Rat and Comparisons between Albino and Pigmented Strains. Exp Brain Res 62:131-142.
Teng E, Squire LR (1999) Memory for places learned long ago is intact after hippocampal damage. Nature 400:675-677.
Thier P, Andersen RA (1998) Electrical microstimulation distinguishes distinct saccade-related areas in the posterior parietal cortex. Journal of Neurophysiology 80:1713-1735.
Thompson SM, Robertson RT (1987a) Organisation of subcortical pathways for sensory projections to the limbic cortex. II. Afferent projections to the thalamic lateral dorsal nucleus in the rat. Journal of Comparative Neurology 265:189-202.
Thompson SM, Robertson RT (1987b) Organisation of subcortical pathways for sensory projections to the limbic cortex. I. Subcortical projections to the medial limbic cortex in the rat. Journal of Comparative Neurology 265:175-188.
Tolias AS, Moore T, Smirnakis SM, Tehovnik EJ, Siapas AG, Schiller PH (2001) Eye movements modulate visual receptive fields of V4 neurons. Neuron 29:757-767.
Tseng PH, Carmi R, Cameron IGM, Munoz DP, Itti L (2009) Quantifying center bias of observers in free viewing of dynamic natural scenes. J Vision 9.
Tseng PH, Cameron IGM, Pari G, Reynolds JN, Munoz DP, Itti L (2013a) High-throughput classification of clinical populations from natural viewing eye movements. J Neurol 260:275-284.
Tseng PH, Cameron IG, Pari G, Reynolds JN, Munoz DP, Itti L (2013b) High-throughput classification of clinical populations from natural viewing eye movements. J Neurol 260:275-284.
Tsodyks M (1999) Attractor neural network models of spatial maps in hippocampus. Hippocampus 9:481-489.
Tsujimoto T, Shimazu H, Isomura Y (2006) Direct recording of theta oscillations in primate prefrontal and anterior cingulate cortices. Journal of Neurophysiology 95:2987-3000.
Tsujimoto T, Shimazu H, Isomura Y, Sasaki K (2010) Theta Oscillations in Primate Prefrontal and Anterior Cingulate Cortices in Forewarned Reaction Time Tasks. Journal of Neurophysiology 103:827-843.
Turano KA, Geruschat DR, Baker FH (2003) Oculomotor strategies for the direction of gaze tested with a real-world activity. Vision Res 43:333-346.
Ulanovsky N, Moss CF (2007) Hippocampal cellular and network activity in freely moving echolocating bats. Nat Neurosci 10:224-233.
Ulanovsky N, Yartsev M (2013) Representation of three-dimensional space in the hippocampus of freely flying bats. J Mol Neurosci 51:S125-S126.
Unal G, Joshi A, Viney TJ, Kis V, Somogyi P (2015) Synaptic Targets of Medial Septal Projections in the Hippocampus and Extrahippocampal Cortices of the Mouse. J Neurosci 35:15812-15826.
Ungerleider LG, Galkin TW, Desimone R, Gattass R (2008) Cortical connections of area V4 in the macaque. Cerebral Cortex 18:477-499.
Urgolites ZJ, Kim S, Hopkins RO, Squire LR (2016) Map reading, navigating from maps, and the medial temporal lobe. P Natl Acad Sci USA 113:14289-14293.
Urruty T, Lew S, Ihadaddene N, Simovici DA (2007) Detecting eye fixations by projection clustering. ACM Trans Multimedia Comput Commun Appl 3:1-20.
Van der Werf YD, Witter MP, Groenewegen HJ (2002) The intralaminar and midline nuclei of the thalamus. Anatomical and functional evidence for participation in processes of arousal and awareness. Brain Res Rev 39:107-140.
Van Essen D, Drury H (1997) Structural and functional analyses of human cerebral cortex using a surface-based atlas. J Neurosci 17:7079-7102.
Van Essen DC (2004) Organization of visual areas in macaque and human cerebral cortex. The visual neurosciences 1:507-521.
van Groen T, Miettinen P, Kadish I (2003) The entorhinal cortex of the mouse: organization of the projection to the hippocampal formation. Hippocampus 13:133-149.

van Strien NM, Cappaert NLM, Witter MP (2009) The anatomy of memory: an interactive overview of the parahippocampal-hippocampal network. Nat Rev Neurosci 10:272-282.
Vangroen T, Wyss JM (1992) Connections of the Retrosplenial Dysgranular Cortex in the Rat. Journal of Comparative Neurology 315:200-216.
Vann SD, Aggleton JP, Maguire EA (2009) What does the retrosplenial cortex do? Nat Rev Neurosci 10:792-U750.
Varela C, Kumar S, Yang JY, Wilson MA (2014) Anatomical substrates for direct interactions between hippocampus, medial prefrontal cortex, and the thalamic nucleus reuniens. Brain Structure & Function 219:911-929.
Ventre-Dominey J (2014) Vestibular function in the temporal and parietal cortex: distinct velocity and inertial processing pathways. Front Integr Neurosci 8:53.
Ventre J, Faugier-Grimaud S (1988) Projections of the temporo-parietal cortex on vestibular complex in the macaque monkey (Macaca fascicularis). Exp Brain Res 72:653-658.
Verghese P (2001) Visual search and attention: A signal detection theory approach. Neuron 31:523-535.
Vertes RP (2015) Major diencephalic inputs to the hippocampus: supramammillary nucleus and nucleus reuniens. Circuitry and function. Prog Brain Res 219:121-144.
Vertes RP, Hoover WB, Do Valle AC, Sherman A, Rodriguez JJ (2006) Efferent projections of reuniens and rhomboid nuclei of the thalamus in the rat. Journal of Comparative Neurology 499:768-796.
Vogt BA, Miller MW (1983) Cortical Connections between Rat Cingulate Cortex and Visual, Motor, and Postsubicular Cortices. Journal of Comparative Neurology 216:192-210.
Vogt BA, Pandya DN (1987) Cingulate cortex of the rhesus monkey: II. Cortical afferents. J Comp Neurol 262:271-289.
Vogt BA, Rosene DL, Pandya DN (1979) Thalamic and Cortical Afferents Differentiate Anterior from Posterior Cingulate Cortex in the Monkey. Science 204:205-207.
Vogt BA, Finch DM, Olson CR (1992) Functional heterogeneity in cingulate cortex: the anterior executive and posterior evaluative regions. Cereb Cortex 2:435-443.
Voss JL, Bridge DJ, Cohen NJ, Walker JA (2017) A Closer Look at the Hippocampus and Memory. Trends Cogn Sci 21:577-588.
Wagman IH, Krieger HP, Papatheodorou CA, Bender MB (1961) Eye movements elicited by surface and depth stimulation of the frontal lobe of Macaque mulatta. J Comp Neurol 117:179-188.
Walther D, Koch C (2006) Modeling attention to salient proto-objects. Neural Networks 19:1395-1407.
Wang CA, Boehnke SE, White BJ, Munoz DP (2012) Microstimulation of the Monkey Superior Colliculus Induces Pupil Dilation Without Evoking Saccades. J Neurosci 32:3629-3636.
Wang L, Sarnaik R, Rangarajan K, Liu X, Cang J (2010) Visual receptive field properties of neurons in the superficial superior colliculus of the mouse. J Neurosci 30:16573-16584.
Wang S, Jiang M, Duchesne XM, Laugeson EA, Kennedy DP, Adolphs R, Zhao Q (2015a) Atypical Visual Saliency in Autism Spectrum Disorder Quantified through Model-Based Eye Tracking. Neuron 88:604-616.
Wang Y, Matsuzaka Y, Shima K, Tanji J (2004) Cingulate cortical cells projecting to monkey frontal eye field and primary motor cortex. Neuroreport 15:1559-1563.
Wang Y, Romani S, Lustig B, Leonardo A, Pastalkova E (2015b) Theta sequences are essential for internally generated hippocampal firing fields. Nat Neurosci 18:282-288.
Wass SV, Smith TJ, Johnson MH (2013) Parsing eye-tracking data of variable quality to provide accurate fixation duration estimates in infants and adults. Behav Res Methods 45:229-250.
Watanabe Y, Funahashi S (2012) Thalamic mediodorsal nucleus and working memory. Neurosci Biobehav Rev 36:134-142.
Webber Jr CL, Zbilut JP (2005) Recurrence quantification analysis of nonlinear dynamical systems. Tutorials in contemporary nonlinear methods for the behavioral sciences:26-94.
Whishaw IQ, Maaswinkel H, Gonzalez CL, Kolb B (2001) Deficits in allothetic and idiothetic spatial behavior in rats with posterior cingulate cortex lesions. Behav Brain Res 118:67-76.
White BJ, Berg DJ, Kan JY, Marino RA, Itti L, Munoz DP (2017) Superior colliculus neurons encode a visual saliency map during free viewing of natural dynamic video. Nat Commun 8:14263.
Widloski J, Fiete I (2014) How does the brain solve the computational problems of spatial navigation? In: Space, Time and Memory in the Hippocampal Formation, pp 373-407: Springer.
Wiener SI, Paul CA, Eichenbaum H (1989) Spatial and Behavioral-Correlates of Hippocampal Neuronal-Activity. J Neurosci 9:2737-2763.
Wijesinghe R, Protti DA, Camp AJ (2015) Vestibular Interactions in the Thalamus. Front Neural Circuit 9.

Wilke M, Turchi J, Smith K, Mishkin M, Leopold DA (2010) Pulvinar Inactivation Disrupts Selection of Movement Plans. J Neurosci 30:8650-8659.
Wills TJ, Cacucci F, Burgess N, O'Keefe J (2010) Development of the Hippocampal Cognitive Map in Preweanling Rats. Science 328:1573-1576.
Wills TJ, Lever C, Cacucci F, Burgess N, O'Keefe J (2005) Attractor dynamics in the hippocampal representation of the local environment. Science 308:873-876.
Wilming N, Betz T, Kietzmann TC, Konig P (2011) Measures and limits of models of fixation selection. Plos One 6:e24038.
Wilming N, Harst S, Schmidt N, Konig P (2013) Saccadic momentum and facilitation of return saccades contribute to an optimal foraging strategy. Plos Comput Biol 9:e1002871.
Winson J (1978) Loss of hippocampal theta rhythm results in spatial memory deficit in the rat. Science 201:160-163.
Winter SS, Clark BJ, Taube JS (2015) Disruption of the head direction cell network impairs the parahippocampal grid cell signal. Science 347:870-874.
Winters BD, Forwood SE, Cowell RA, Saksida LM, Bussey TJ (2004) Double dissociation between the effects of peri-postrhinal cortex and hippocampal lesions on tests of object recognition and spatial memory: Heterogeneity of function within the temporal lobe. J Neurosci 24:5901-5908.
Wirth S, Baraduc P, Plante A, Pinede S, Duhamel JR (2017) Gaze-informed, task-situated representation of space in primate hippocampus during virtual navigation. PLoS Biol 15:e2001045.
Wirth S, Yanike M, Frank LM, Smith AC, Brown EN, Suzuki WA (2003) Single neurons in the monkey hippocampus and learning of new associations. Science 300:1578-1581.
Witter MP (2007) Intrinsic and extrinsic wiring of CA3: Indications for connectional heterogeneity. Learn Memory 14:705-713.
Witter MP, Amaral DG (1991) Entorhinal cortex of the monkey: V. Projections to the dentate gyrus, hippocampus, and subicular complex. J Comp Neurol 307:437-459.
Witter MP, Naber PA, van Haeften T, Machielsen WCM, Rombouts SARB, Barkhof F, Scheltens P, da Silva FHL (2000) Cortico-hippocampal communication by way of parallel parahippocampal-subicular pathways. Hippocampus 10:398-410.
Wittner L, Henze DA, Zaborszky L, Buzsaki G (2007) Three-dimensional reconstruction of the axon arbor of a CA3 pyramidal cell recorded and filled in vivo. Brain Struct Funct 212:75-83.
Wolfe JM (1994) Guided Search 2.0 - a Revised Model of Visual-Search. Psychon B Rev 1:202-238.
Womelsdorf T, Johnston K, Vinck M, Everling S (2010a) Theta-activity in anterior cingulate cortex predicts task rules and their adjustments following errors. P Natl Acad Sci USA 107:5248-5253.
Womelsdorf T, Vinck M, Leung LS, Everling S (2010b) Selective theta-synchronization of choice-relevant information subserves goal-directed behavior. Front Hum Neurosci 4.
Wood ER, Dudchenko PA, Robitsek RJ, Eichenbaum H (2000) Hippocampal neurons encode information about different types of memory episodes occurring in the same location. Neuron 27:623-633.
Wurtz RH, Goldberg ME (1972a) Activity of Superior Colliculus in Behaving Monkey .4. Effects of Lesions on Eye-Movements. Journal of Neurophysiology 35:587-&.
Wurtz RH, Goldberg ME (1972b) Activity of superior colliculus in behaving monkey. 3. Cells discharging before eye movements. J Neurophysiol 35:575-586.
Wyder MT, Massoglia DP, Stanford TR (2003) Quantitative assessment of the timing and tuning of visual-related, saccade-related, and delay period activity in primate central thalamus. Journal of Neurophysiology 90:2029-2052.
Wyder MT, Massoglia DP, Stanford TR (2004) Contextual modulation of central thalamic delay-period activity: representation of visual and saccadic goals. J Neurophysiol 91:2628-2648.
Wyss JM, Vangroen T (1992) Connections between the Retrosplenial Cortex and the Hippocampal-Formation in the Rat - a Review. Hippocampus 2:1-12.
Wyss JM, Swanson LW, Cowan WM (1979) A study of subcortical afferents to the hippocampal formation in the rat. Neuroscience 4:463-476.
Xu W, Sudhof TC (2013) A Neural Circuit for Memory Specificity and Generalization. Science 339:1290-1295.
Yamawaki N, Radulovic J, Shepherd GM (2016) A Corticocortical Circuit Directly Links Retrosplenial Cortex to M2 in the Mouse. J Neurosci 36:9365-9374.
Yarbus A (1967) Eye movements and vision. 1967. New York.
Yartsev MM, Ulanovsky N (2013) Representation of three-dimensional space in the hippocampus of flying bats. Science 340:367-372.

Yartsev MM, Witter MP, Ulanovsky N (2011) Grid cells without theta oscillations in the entorhinal cortex of bats. Nature 479:103-107.
Yassa MA, Stark CEL (2011) Pattern separation in the hippocampus. Trends Neurosci 34:515-525.
Yeterian EH, Pandya DN (1988) Corticothalamic connections of paralimbic regions in the rhesus monkey. J Comp Neurol 269:130-146.
Yeterian EH, Pandya DN (1989) Thalamic Connections of the Cortex of the Superior Temporal Sulcus in the Rhesus-Monkey. Journal of Comparative Neurology 282:80-97.
Yeterian EH, Pandya DN, Tomaiuolo F, Petrides M (2012) The cortical connectivity of the prefrontal cortex in the monkey brain. Cortex 48:58-81.
Yoder RM, Clark BJ, Taube JS (2011a) Origins of landmark encoding in the brain. Trends Neurosci 34:561-571.
Yoder RM, Clark BJ, Brown JE, Lamia MV, Valerio S, Shinder ME, Taube JS (2011b) Both visual and idiothetic cues contribute to head direction cell stability during navigation along complex routes. Journal of Neurophysiology 105:2989-3001.
Yoshida K, Oka H (1995) Topographical projections from the medial septum-diagonal band complex to the hippocampus: a retrograde tracing study with multiple fluorescent dyes in rats. Neurosci Res 21:199-209.
Young CK, McNaughton N (2009) Coupling of Theta Oscillations between Anterior and Posterior Midline Cortex and with the Hippocampus in Freely Behaving Rats. Cerebral Cortex 19:24-40.
Young KD, Erickson K, Nugent AC, Fromm SJ, Mallinger AG, Furey ML, Drevets WC (2012) Functional anatomy of autobiographical memory recall deficits in depression. Psychol Med 42:345-357.
Young MP (1993) The organization of neural systems in the primate cerebral cortex. Proc Biol Sci 252:13-18.
Yttri EA, Liu YQ, Snyder LH (2013) Lesions of cortical area LIP affect reach onset only when the reach is accompanied by a saccade, revealing an active eye-hand coordination circuit. P Natl Acad Sci USA 110:2371-2376.
Yukie M (2000) Connections between the medial temporal cortex and the CA1 subfield of the hippocampal formation in the Japanese monkey (Macaca fuscata). Journal of Comparative Neurology 423:282-298.
Zehetleitner M, Koch AI, Goschy H, Muller HJ (2013) Salience-Based Selection: Attentional Capture by Distractors Less Salient Than the Target. Plos One 8.
Zhang LY, Tong MH, Marks TK, Shan HH, Cottrell GW (2008) SUN: A Bayesian framework for saliency using natural statistics. J Vision 8.
Zhang ZH, Dougherty PM, Oppenheimer SM (1999) Monkey insular cortex neurons respond to baroreceptive and somatosensory convergent inputs. Neuroscience 94:351-360.
Zhao Q, Koch C (2011) Learning a saliency map using fixated locations in natural scenes. J Vision 11.
Zhong YM, Rockland KS (2004) Connections between the anterior inferotemporal cortex (area TE) and CA1 of the hippocampus in monkey. Exp Brain Res 155:311-319.
Zhou H, Schafer RJ, Desimone R (2016) Pulvinar-Cortex Interactions in Vision and Attention. Neuron 89:209-220.
Zilli EA (2012) Models of grid cell spatial firing published 2005-2011. Front Neural Circuit 6.
Zola SM, Manzanares CM, Clopton P, Lah JJ, Levey AI (2013) A behavioral task predicts conversion to mild cognitive impairment and Alzheimer's disease. Am J Alzheimers Dis Other Demen 28:179-184.
Zola SM, Squire LR, Teng E, Stefanacci L, Buffalo EA, Clark RE (2000) Impaired recognition memory in monkeys after damage limited to the hippocampal region. J Neurosci 20:451-463.

Chapter 8. VITA

Seth Koenig was born in Hoffman Estates, Illinois, on November 9, 1988. He studied at the Georgia Institute of Technology where he received a B.S. in Biomedical Engineering in 2011. He then entered a joint Ph.D. program in Biomedical Engineering at the Georgia Institute of Technology and Emory University. He started his dissertation research in Elizabeth Buffalo's lab. He followed the lab to the University of Washington to finish his dissertation research in the Neuroscience Ph.D. program.